Measuring isolated prompt γ production in small & large collision systems with ALICE

- ➡ Differential p_T cross section
  - ✱ pp at $\sqrt{s}$ = 13 TeV arXiv:2407.01165 New
  - ✱ pp at $\sqrt{s}$ = 8 TeV & p–Pb at $\sqrt{s_{NN}}$ = 8.16 TeV preliminary
  - ✱ pp & Pb–Pb at $\sqrt{s_{NN}}$ = 5.02 TeV arXiv:2409.12641, ALICE-PUBLIC-2024-003 New
- ➡ Isolated γ-hadron correlation
  - ✱ Pb–Pb at $\sqrt{s_{NN}}$ = 5.02 TeV preliminary

Gustavo CONESA BALBASTRE
LPSC Grenoble — IN2P3-CNRS-UGA
for the ALICE Collaboration

Hard Probes | Nagasaki, Japan | 25/09/2024

Motivation

- γ are **color neutral: not affected** by *"quark-gluon plasma" (QGP)* presence in *heavy-ion collisions* unlike **partons** that **lose energy**
- Direct γ, *not originating from hadronic deca*

$$R_{AA} = \frac{1}{\langle N_{coll} \rangle} \frac{d^2\sigma_{AA} / (dp_T\, d\eta)}{d^2\sigma_{pp} / (dp_T\, d\eta)}$$

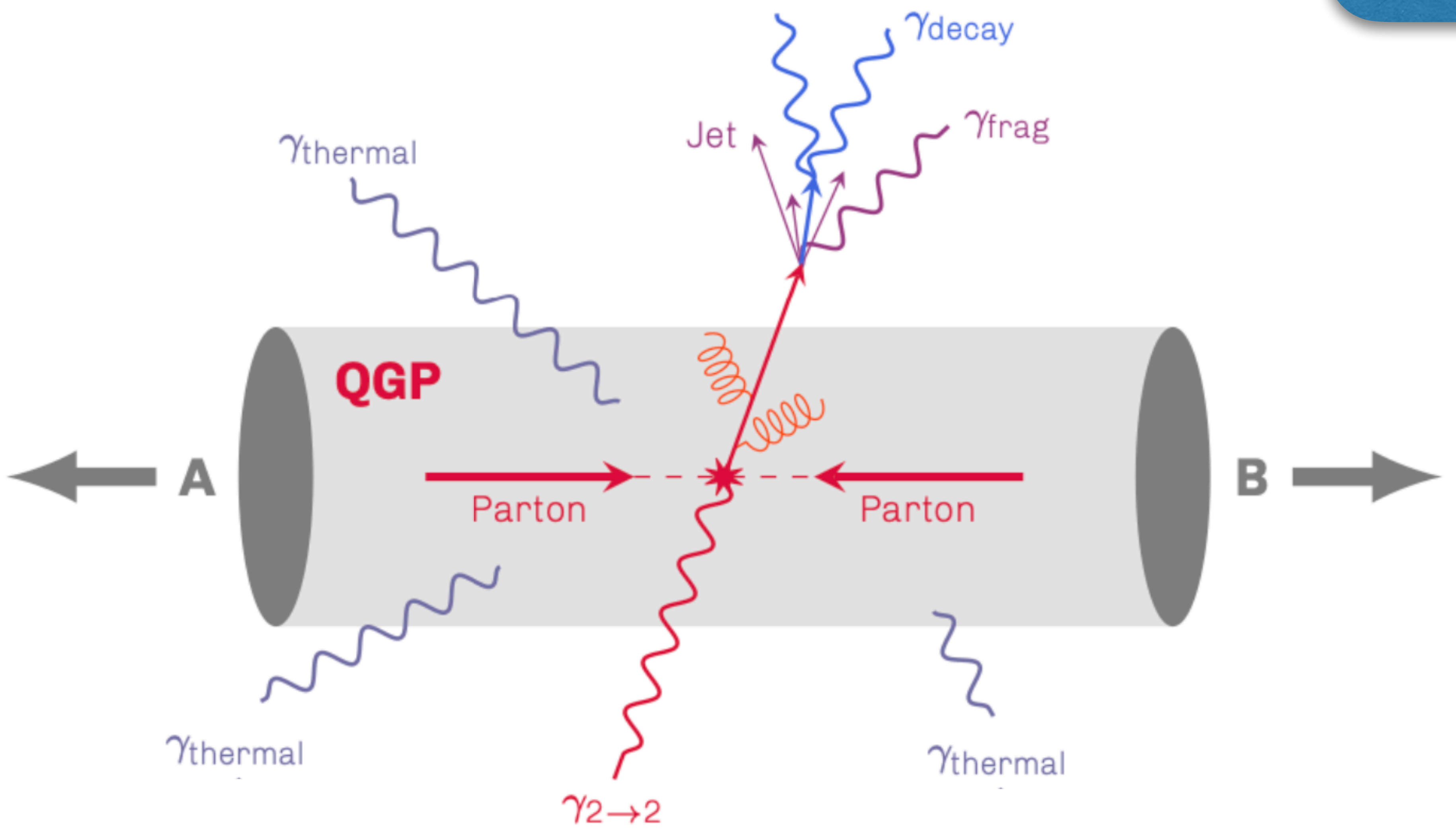

Motivation

- γ are **color neutral: not affected** by *"quark-gluon plasma" (QGP)* presence in *heavy-ion collisions* unlike **partons** that **lose energy**
- Direct γ, *not originating from hadronic decays*

$$R_{AA} = \frac{1}{\langle N_{coll} \rangle} \frac{d^2\sigma_{AA} / (dp_T\, d\eta)}{d^2\sigma_{pp} / (dp_T\, d\eta)}$$

➡ **Direct thermal γ: R_{AA} >> 1**
– QGP thermal radiation
– Measure ***T* & time/size evolution**

- EM Talk D. Peressounko Tuesday 10:20
- EM Talk J. Jung Tuesday 12:10

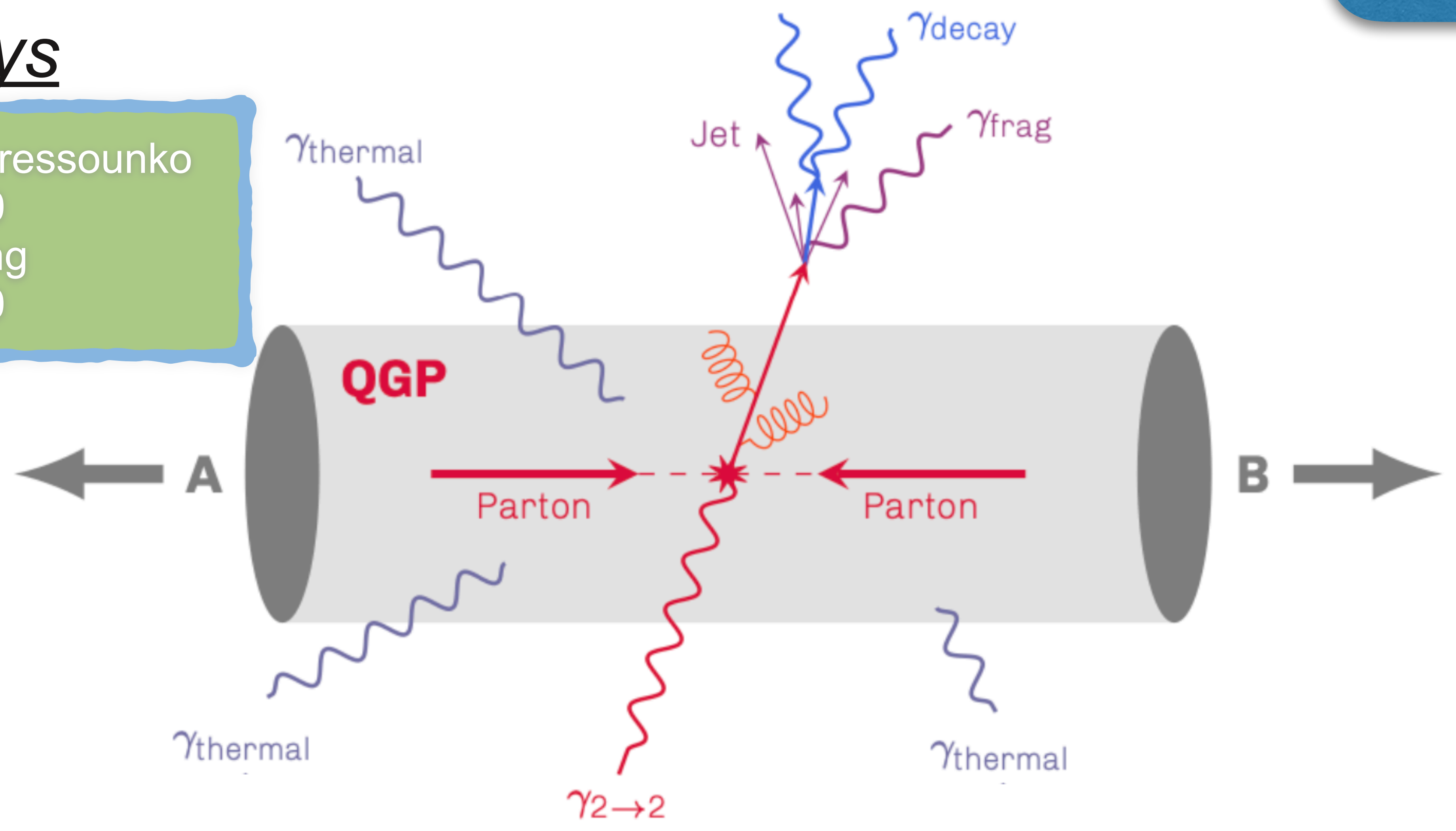

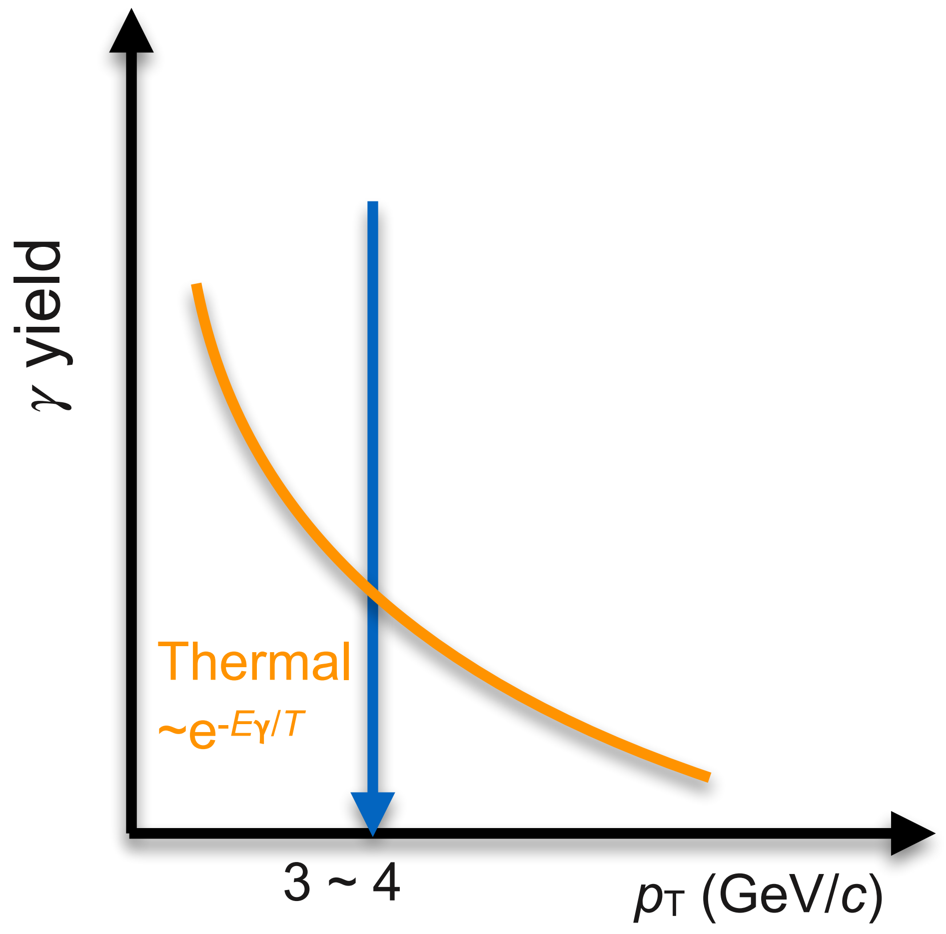

Motivation

$$R_{AA} = \frac{1}{\langle N_{coll} \rangle} \frac{d^2\sigma_{AA} / (dp_T\, d\eta)}{d^2\sigma_{pp} / (dp_T\, d\eta)}$$

- γ are **color neutral: not affected** by *"quark-gluon plasma" (QGP)* presence in *heavy-ion collisions* unlike **partons** that **lose energy**
- Direct γ, *not originating from hadronic decays*

➡ **Direct thermal γ: R_{AA} >> 1**
- QGP thermal radiation
- Measure ***T* & time/size evolution**

➡ **Direct prompt γ: $R_{AA} \approx 1$**
- Initial hard scattering, processes at LO:

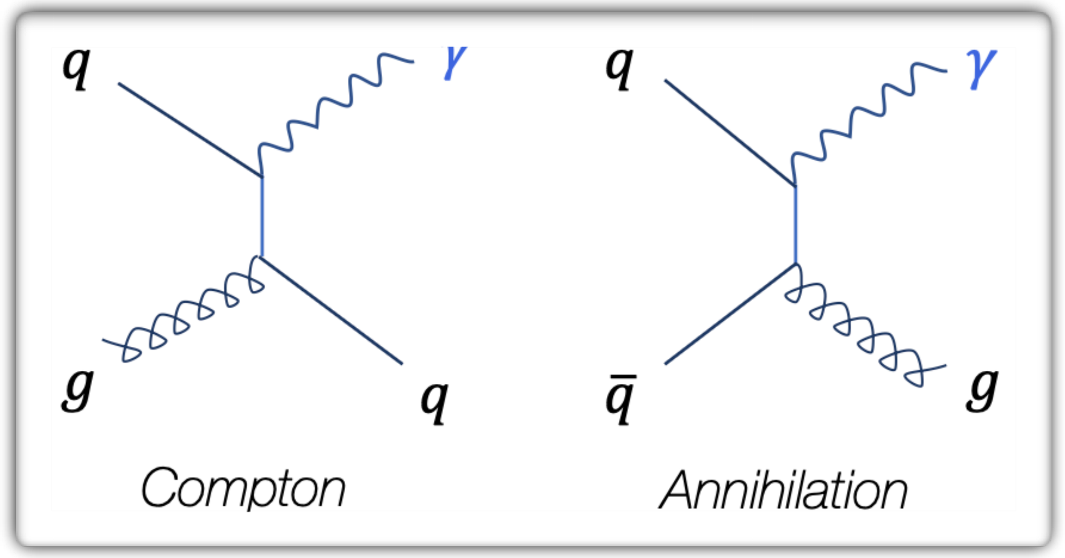

- **Test pQCD** predictions, **constrain (n)PDFs & FF**
  - Cold nuclear matter (nPDF) effects can lead to $R_{AA} \neq 1$
- $p_T^{\gamma} \simeq p_T^{\text{parton}}$, before parton loses Δ*E* in QGP
- Measure **FF modifications**, where is the Δ*E* radiated?

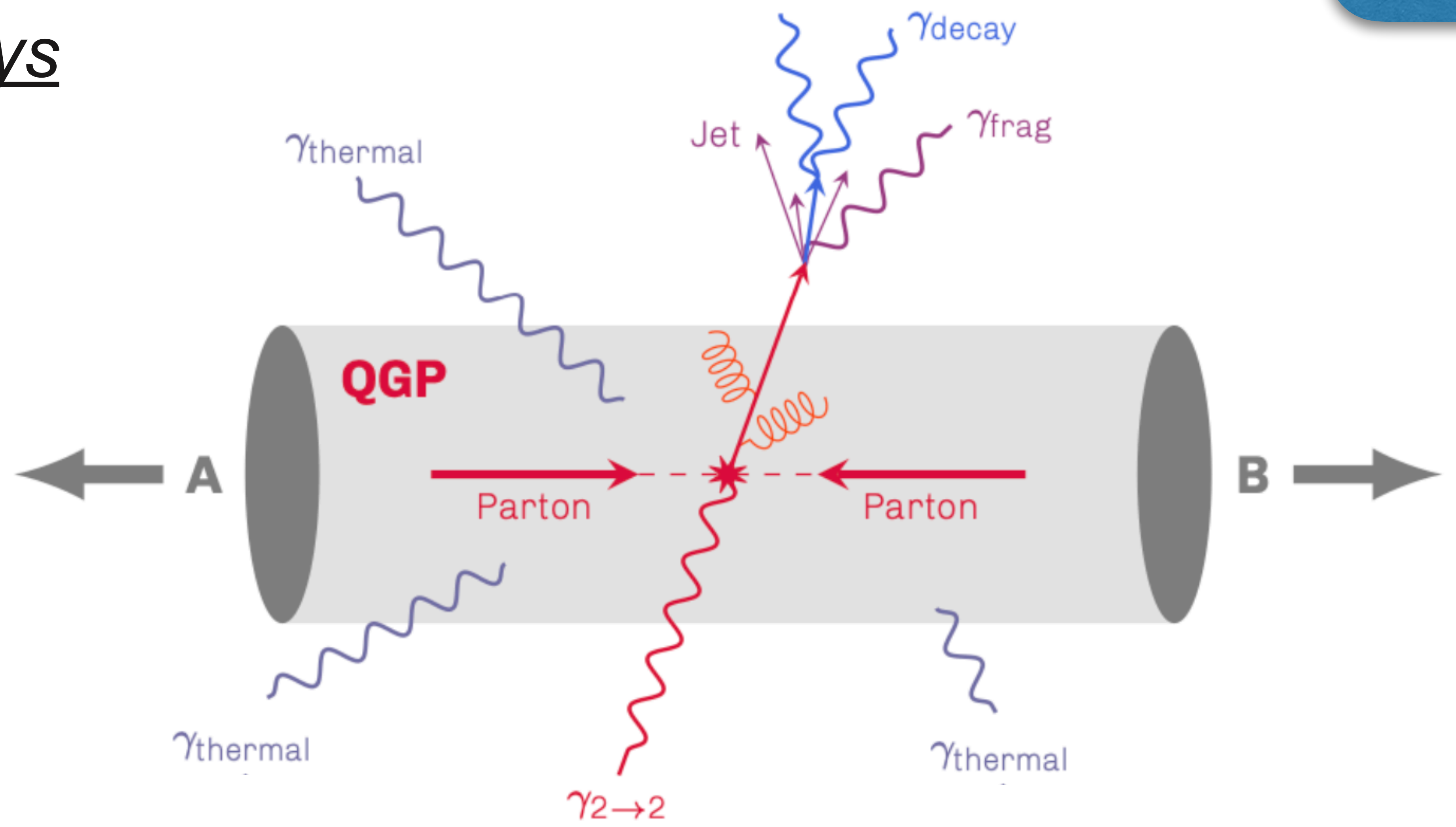

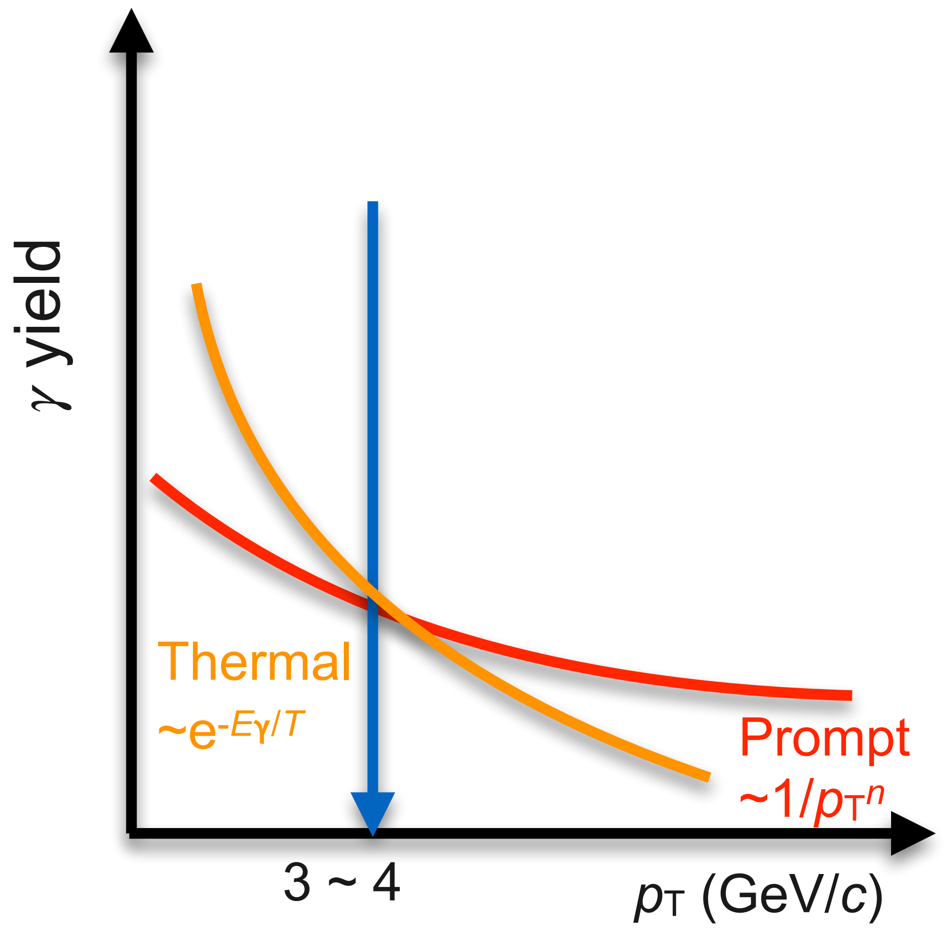

$$d\sigma^{hard}_{AB\to h} = f_{a/A}(x_1, Q^2) \otimes f_{b/B}(x_2, Q^2) \otimes d\sigma^{hard}_{ab\to c}(x_1, x_2, Q^2) \otimes D_{c\to h}(z, Q^2)$$

PDFs — *Hard scattering (pQCD)* — *Fragmentation function* (FF)

Motivation

- γ are **color neutral: not affected** by *"quark-gluon plasma" (QGP)* presence in *heavy-ion collisions* unlike **partons** that **lose energy**
- Direct γ, *not originating from hadronic decays*

$$R_{AA} = \frac{1}{\langle N_{coll} \rangle} \frac{d^2\sigma_{AA} / (dp_T\, d\eta)}{d^2\sigma_{pp} / (dp_T\, d\eta)}$$

➡ **Direct thermal γ: R_{AA} >> 1**
- QGP thermal radiation
- Measure ***T* & time/size evolution**

➡ **Direct prompt γ: $R_{AA} \approx 1$**
- Initial hard scattering, processes at LO:

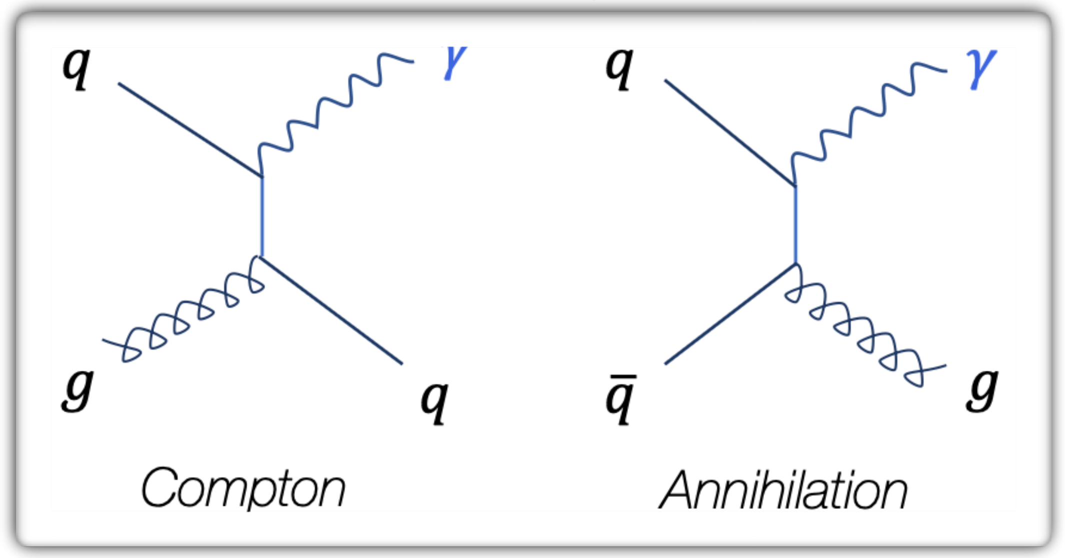

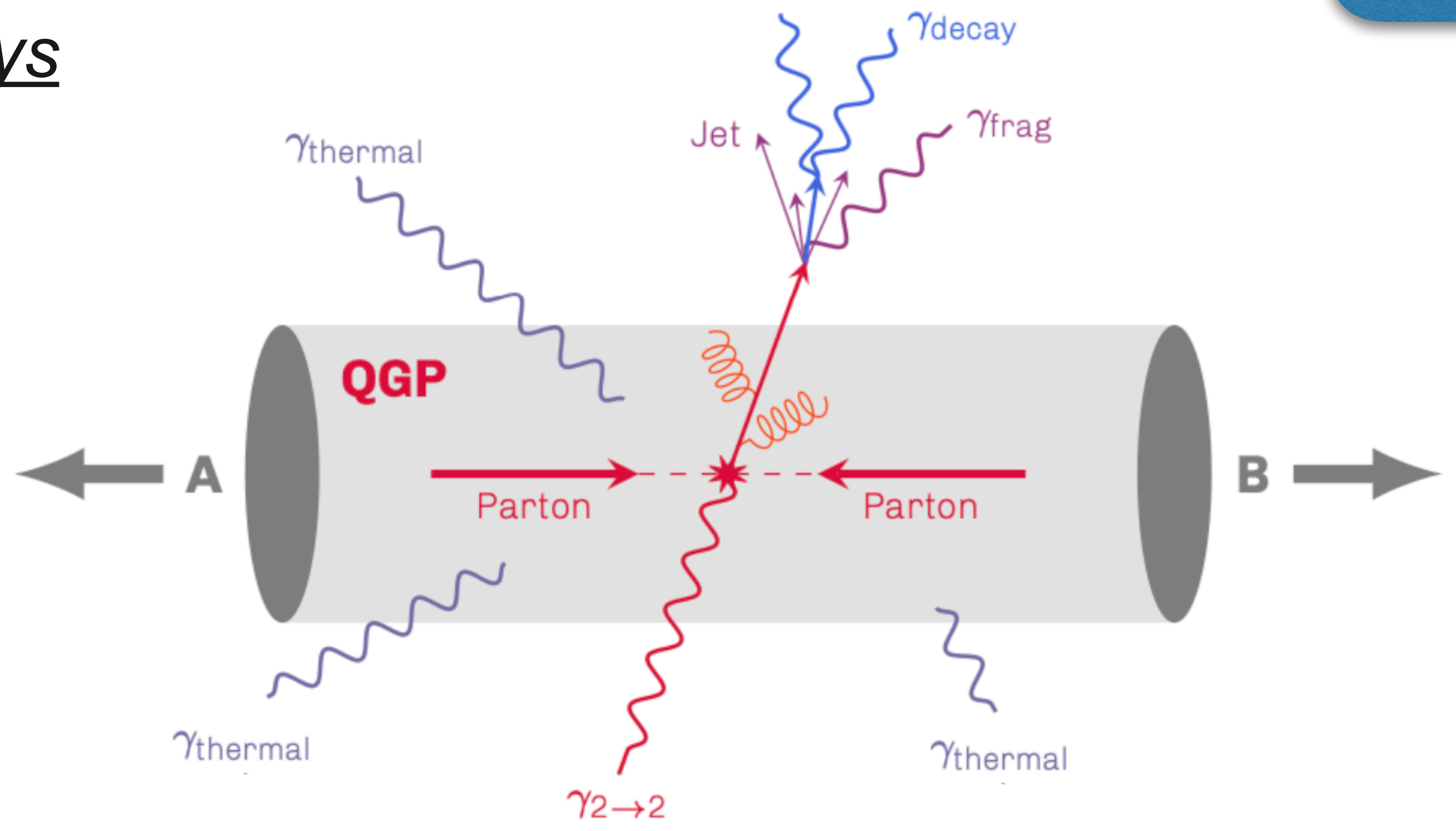

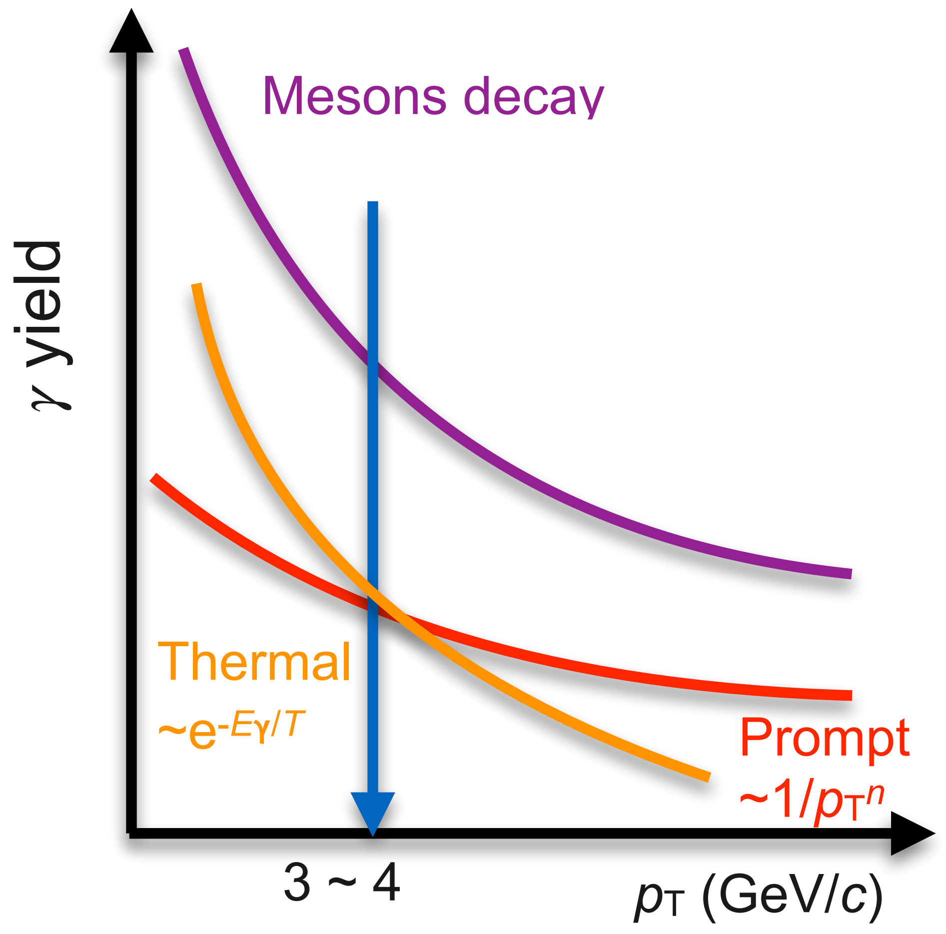

$$d\sigma^{hard}_{AB\to h} = f_{a/A}(x_1, Q^2) \otimes f_{b/B}(x_2, Q^2) \otimes d\sigma^{hard}_{ab\to c}(x_1, x_2, Q^2) \otimes D_{c\to h}(z, Q^2)$$

PDFs — *Hard scattering (pQCD)* — *Fragmentation function* (FF)

- **Test pQCD** predictions, **constrain (n)PDFs & FF**
  - Cold nuclear matter (nPDF) effects can lead to $R_{AA} \neq 1$
- $p_T^{\gamma} \simeq p_T^{\mathrm{parton}}$, before parton loses ΔE in QGP
- Measure **FF modifications**, where is the ΔE radiated?

➡ **Decay γ (π^0 & η): R_{AA} << 1**
- **Main background for direct γ measurements**

Motivation

$$R_{AA} = \frac{1}{\langle N_{coll} \rangle} \frac{d^2\sigma_{AA} \,/\, (dp_T \, d\eta)}{d^2\sigma_{pp} \,/\, (dp_T \, d\eta)}$$

- **γ** are **color neutral: not affected** by *"quark-gluon plasma" (QGP)* presence in *heavy-ion collisions* unlike **partons** that **lose energy**
- Direct **γ**, *not originating from hadronic decays*

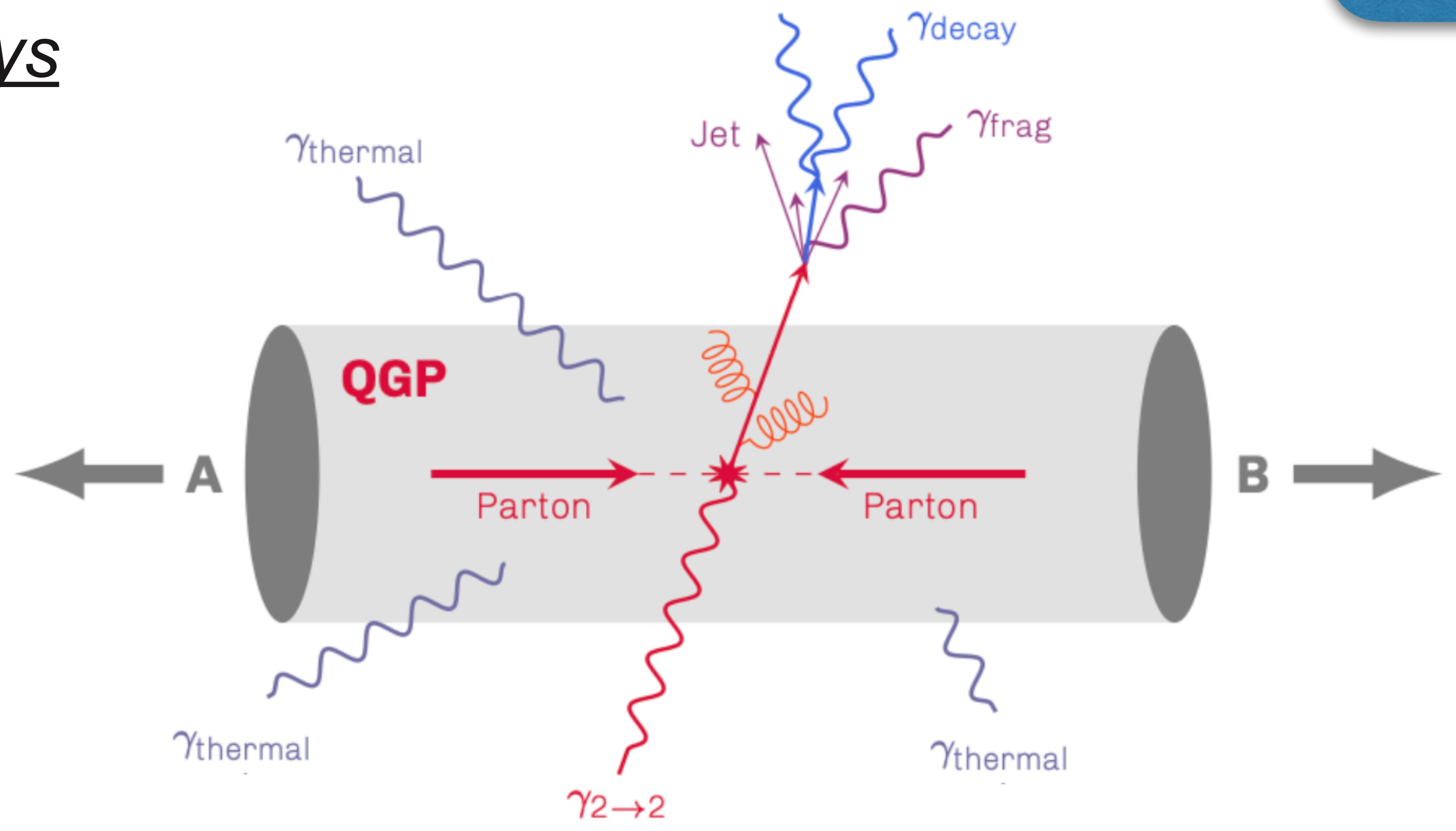

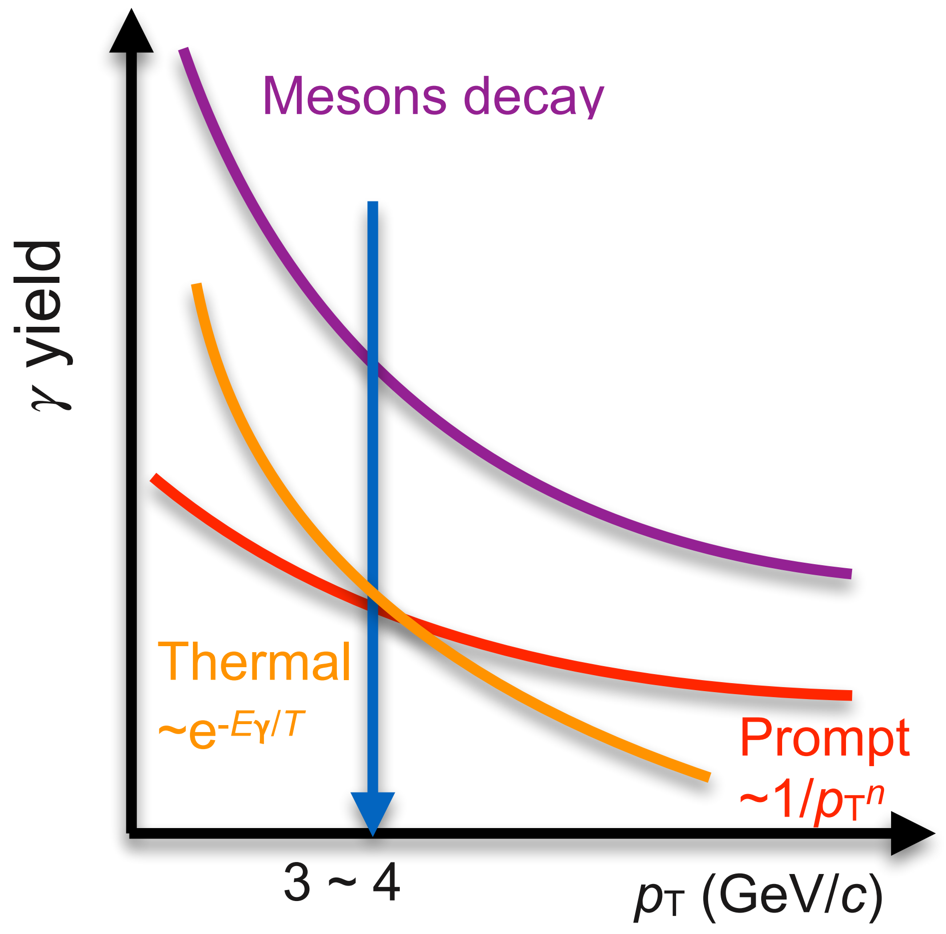

➡ **Direct thermal γ:** $R_{AA} >> 1$
- QGP thermal radiation
- Measure ***T* & time/size evolution**

➡ **Direct prompt γ:** $R_{AA} \approx 1$
- Initial hard scattering, processes at LO:

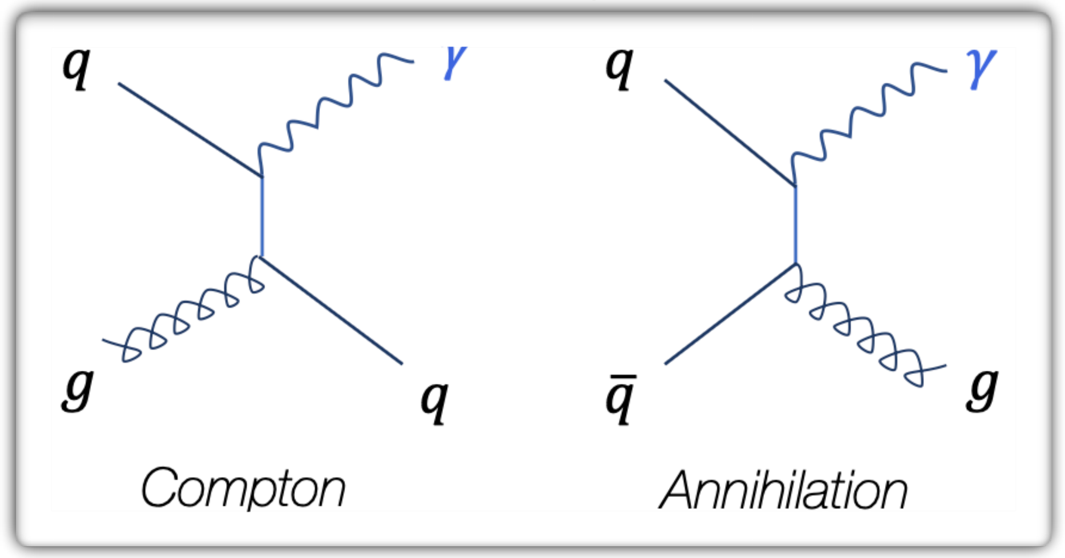

$$d\sigma^{hard}_{AB\to h} = f_{a/A}(x_1, Q^2) \otimes f_{b/B}(x_2, Q^2) \otimes d\sigma^{hard}_{ab\to c}(x_1, x_2, Q^2) \otimes D_{c\to h}(z, Q^2)$$

PDFs — *Hard scattering (pQCD)* — *Fragmentation function* (FF)

- **Test pQCD** predictions, **constrain (n)PDFs & FF**
  - Cold nuclear matter (nPDF) effects can lead to $R_{AA} \neq 1$
- $p_T^{\gamma} \simeq p_T^{\text{parton}}$, before parton loses Δ*E* in QGP
- Measure **FF modifications**, where is the Δ*E* radiated?

➡ **Decay γ** (π^0 & η): $R_{AA} << 1$
- **Main background for direct γ measurements**

➡ **Other direct γ sources:**
- Fragmentation γ: $R_{AA} < 1$ comparable yield to direct prompt γ
- QGP pre-equilibrium γ? $R_{AA} >> 1$ (glasma phase)
- Jet-QGP interaction γ? $R_{AA} >> 1$ (hard partons scattering)

Signal selection & purity

- Selection:
  - ➡ Isolation: $p_{\mathrm{T,\,min}}^{\mathrm{iso,\,ch}} < \sum p_{\mathrm{T}}^{\mathrm{tracks\ in\ cone}} - \rho_{\mathrm{UE}} \cdot \pi \cdot R^2$ in cone radius R
  - ➡ Shower elongation: σ^2_{long} for "narrow" clusters
- Purity, ABCD method: Phase space of calorimeter clusters divided in 4 regions: $\mathbb{A}$, signal dominated & $\mathbb{B}$-$\mathbb{C}$-$\mathbb{D}$, background dominated

$$P = 1 - \underbrace{\left(\frac{N_n^{\overline{\mathrm{iso}}}/N_n^{\mathrm{iso}}}{N_w^{\overline{\mathrm{iso}}}/N_w^{\mathrm{iso}}}\right)_{\mathrm{data}}}_{\text{Data driven}} \times \underbrace{\left(\frac{B_n^{\mathrm{iso}}/N_n^{\overline{\mathrm{iso}}}}{N_w^{\mathrm{iso}}/N_w^{\overline{\mathrm{iso}}}}\right)_{\mathrm{MC}}}_{\text{PYTHIA}}$$

$N_{n,w}^{\mathrm{iso},\overline{\mathrm{iso}}}$ = jet-jet ($B_{n,w}^{\mathrm{iso},\overline{\mathrm{iso}}}$) + γ-jet ($S_{n,w}^{\mathrm{iso},\overline{\mathrm{iso}}}$)

- ➡ Semi data-driven approach, simulation used to correct correlations between $p_{\mathrm{T}}^{\mathrm{iso,\,ch}}$ and σ^2_{long}

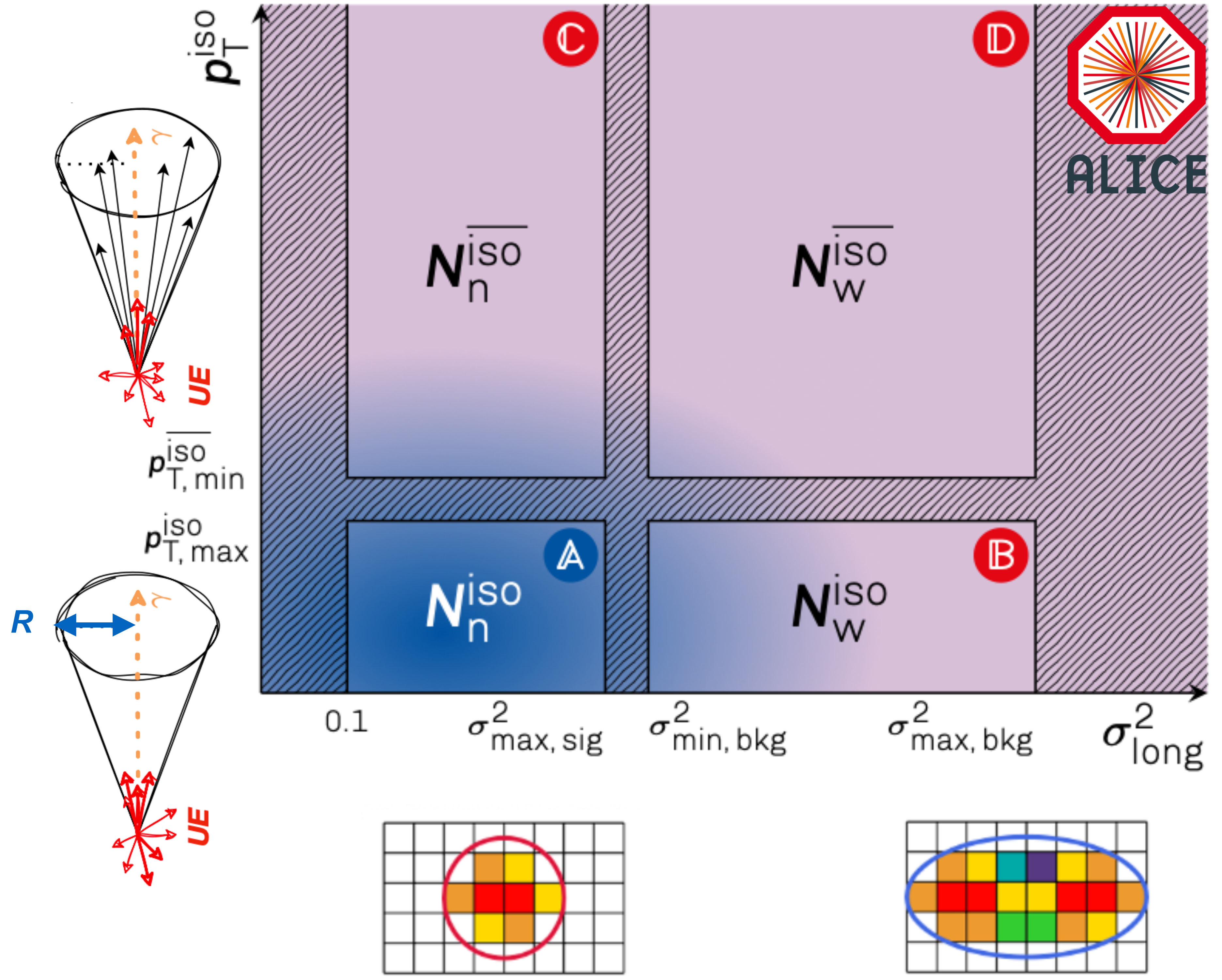

- Selection details in back-up

Signal selection & purity, pp $\sqrt{s}$ = 13 TeV

- Selection:
  - ➡ Isolation: $p_{\mathrm{T,\,min}}^{\mathrm{iso,\,ch}} < \sum p_{\mathrm{T}}^{\mathrm{tracks\ in\ cone}} - \rho_{\mathrm{UE}} \cdot \pi \cdot R^2$ in cone radius R
  - ➡ Shower elongation: σ_{long}^2 for "narrow" clusters
- Purity, ABCD method: Phase space of calorimeter clusters divided in 4 regions: 𝔸, signal dominated & 𝔹-ℂ-𝔻, background dominated

Data driven — PYTHIA

$$P = 1 - \left(\frac{N_n^{\overline{\mathrm{iso}}}/N_n^{\mathrm{iso}}}{N_w^{\overline{\mathrm{iso}}}/N_w^{\mathrm{iso}}}\right)_{\mathrm{data}} \times \left(\frac{B_n^{\mathrm{iso}}/N_n^{\overline{\mathrm{iso}}}}{N_w^{\mathrm{iso}}/N_w^{\overline{\mathrm{iso}}}}\right)_{\mathrm{MC}}$$

$N_{n,w}^{\mathrm{iso},\overline{\mathrm{iso}}}$ = jet-jet ($B_{n,w}^{\mathrm{iso},\overline{\mathrm{iso}}}$) + γ-jet ($S_{n,w}^{\mathrm{iso},\overline{\mathrm{iso}}}$)

- ➡ Semi data-driven approach, simulation used to correct correlations between $p_{\mathrm{T}}^{\mathrm{iso,\,ch}}$ and σ_{long}^2

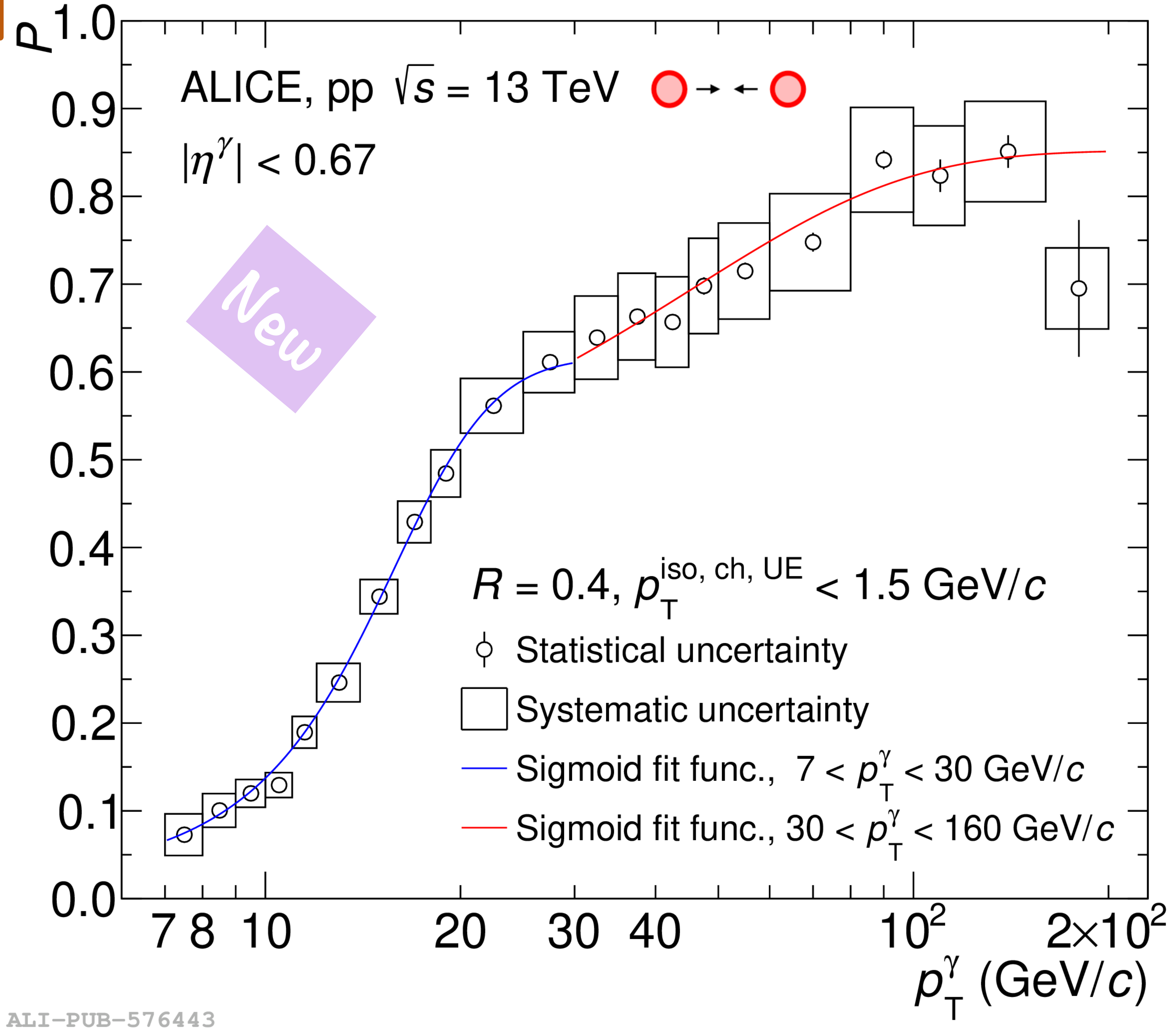

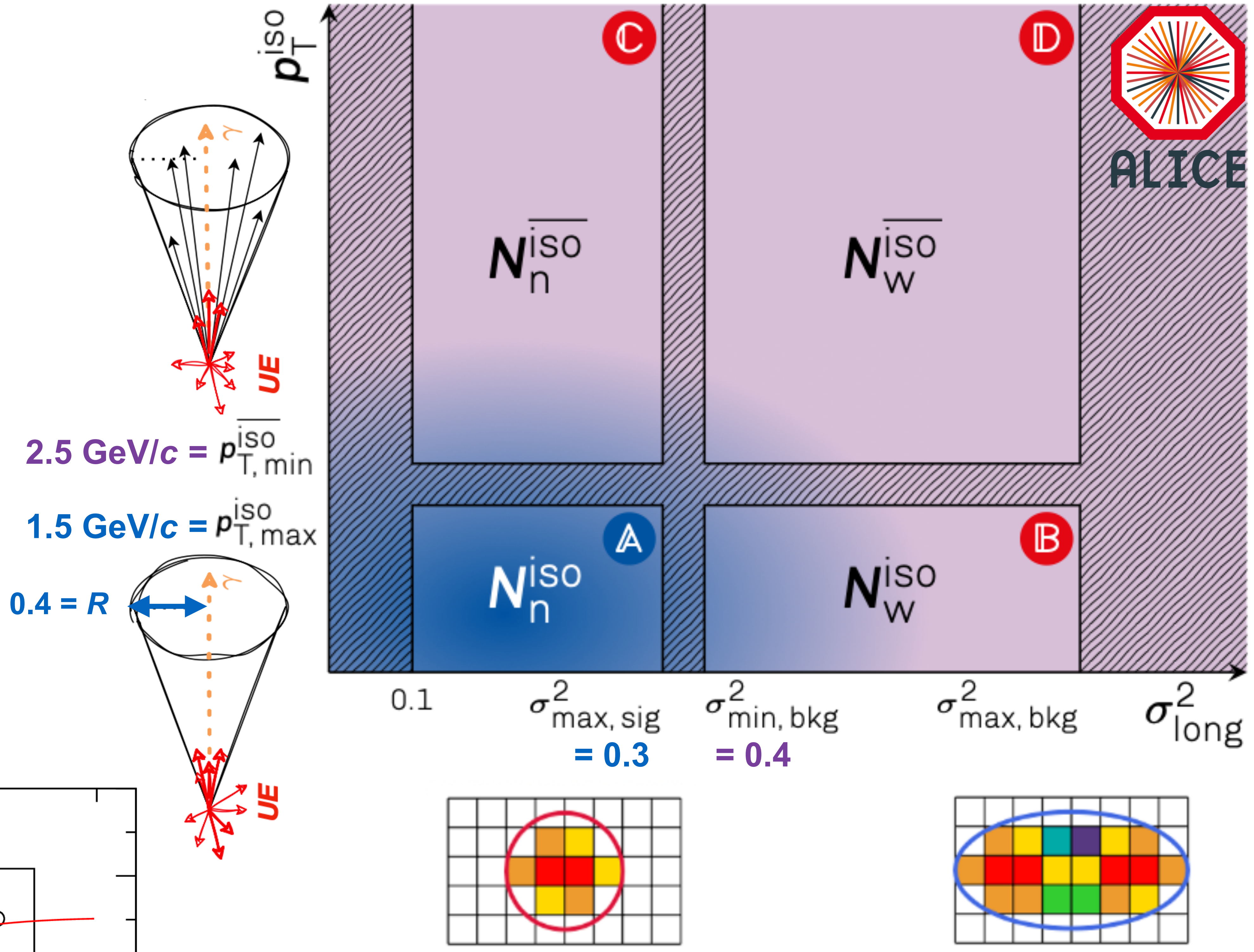

- Selection details in back-up
- Reduce the influence of statistical fluctuations with sigmoid function fits

ALI-PUB-576443

Signal selection & purity, Pb–Pb $\sqrt{s_{NN}}$ = 5.02 TeV

- Selection:
  - ➡ Isolation: $p_{T,\,min}^{iso,\,ch} < \sum p_{T}^{tracks\ in\ cone} - \rho_{UE} \cdot \pi \cdot R^2$ in cone radius R
  - ➡ Shower elongation: σ_{long}^2 for "narrow" clusters
- Purity, ABCD method: Phase space of calorimeter clusters divided in 4 regions: 𝔸, signal dominated & 𝔹-ℂ-𝔻, background dominated

$$P = 1 - \underbrace{\left(\frac{N_n^{\overline{iso}}/N_n^{iso}}{N_w^{\overline{iso}}/N_w^{iso}}\right)_{data}}_{\text{Data driven}} \times \underbrace{\left(\frac{B_n^{iso}/N_n^{\overline{iso}}}{N_w^{iso}/N_w^{\overline{iso}}}\right)_{MC}}_{\text{PYTHIA}}$$

$N_{n,w}^{iso,\overline{iso}}$= jet-jet ($B_{n,w}^{iso,\overline{iso}}$) + γ-jet ($S_{n,w}^{iso,\overline{iso}}$)

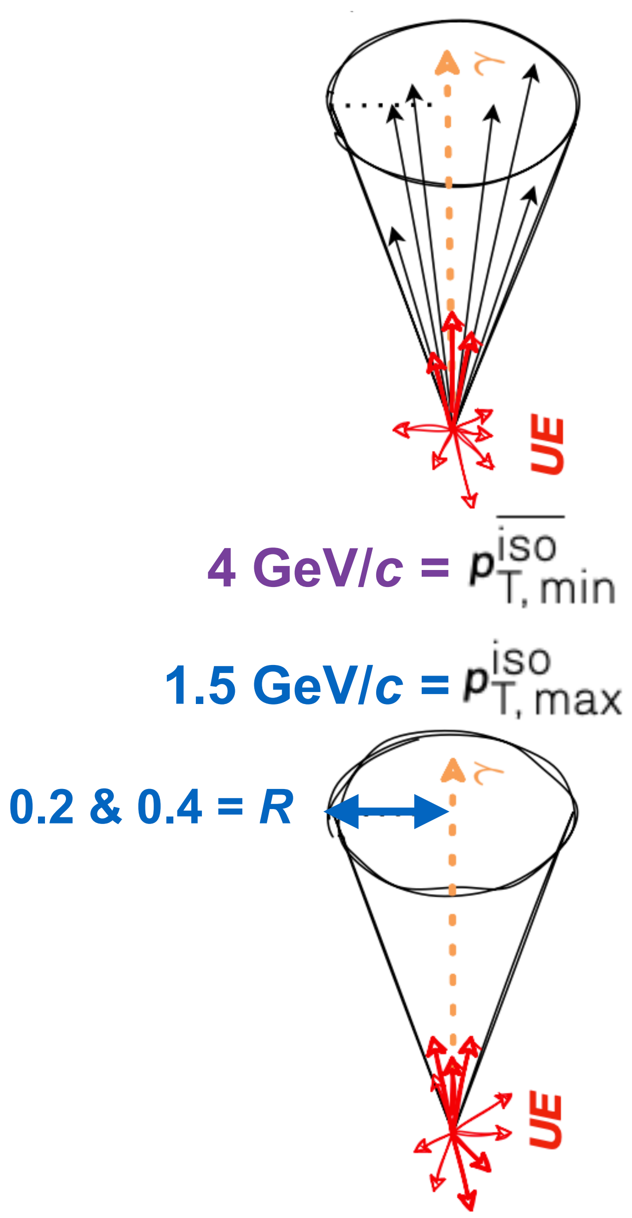

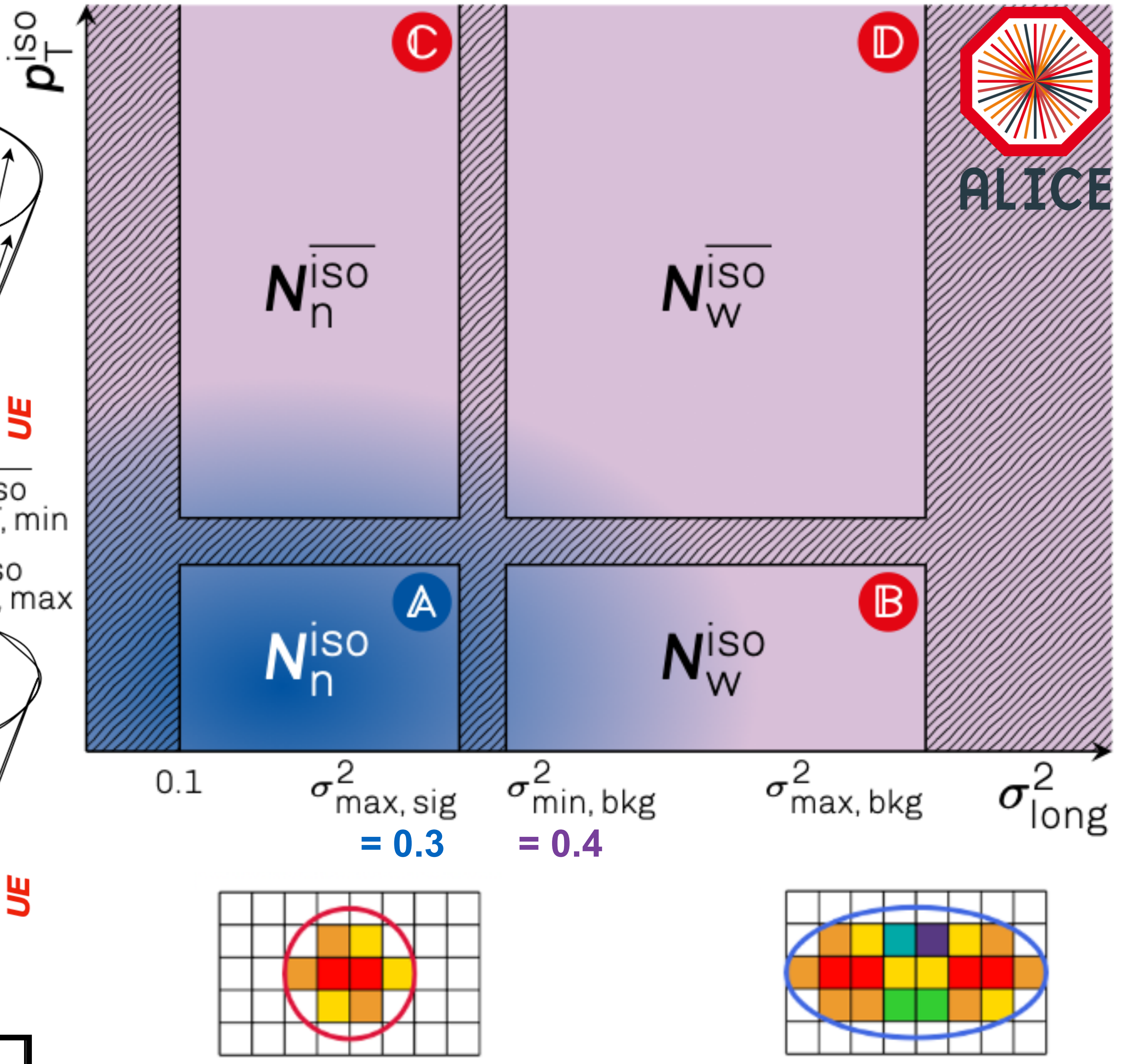

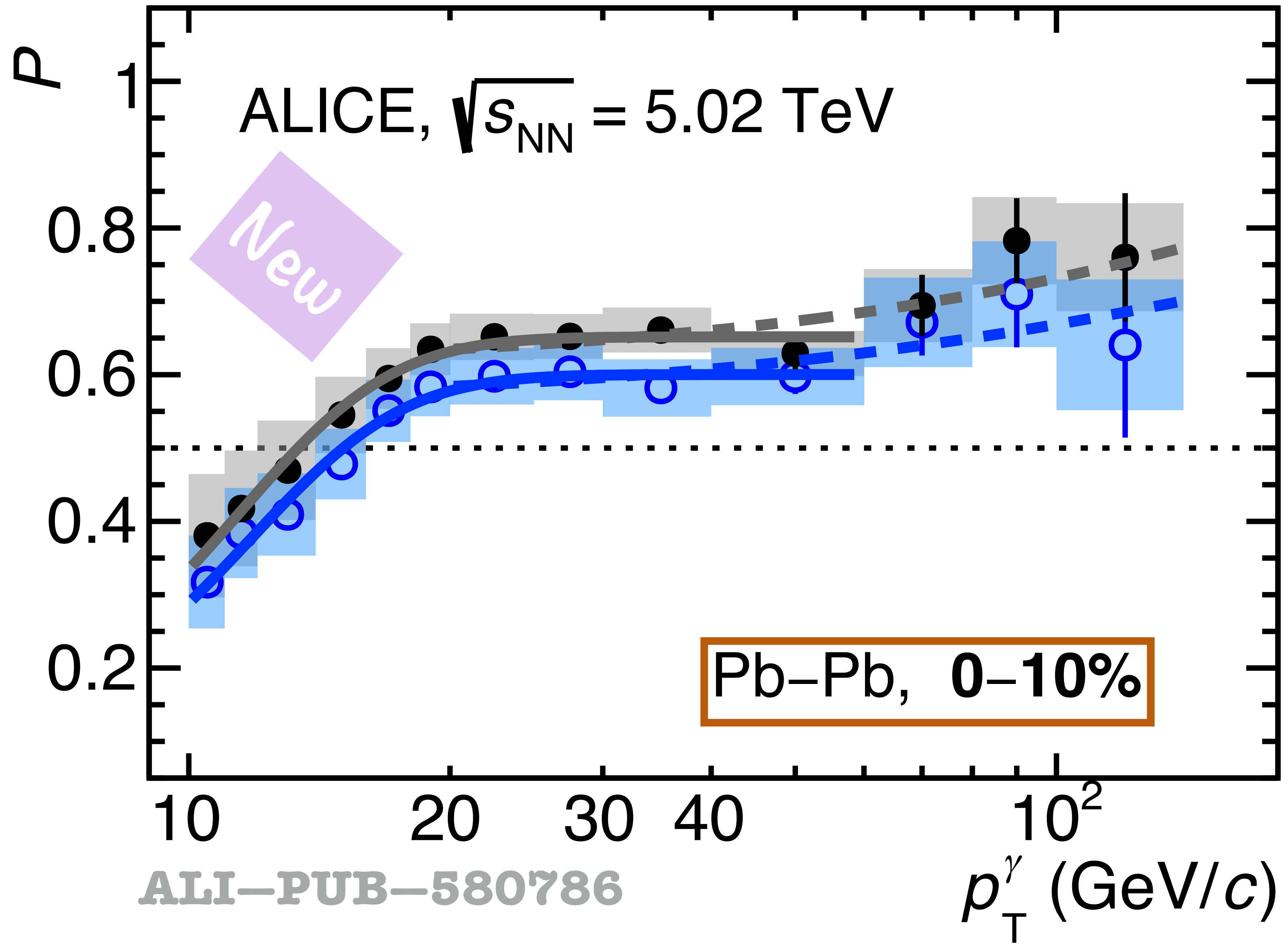

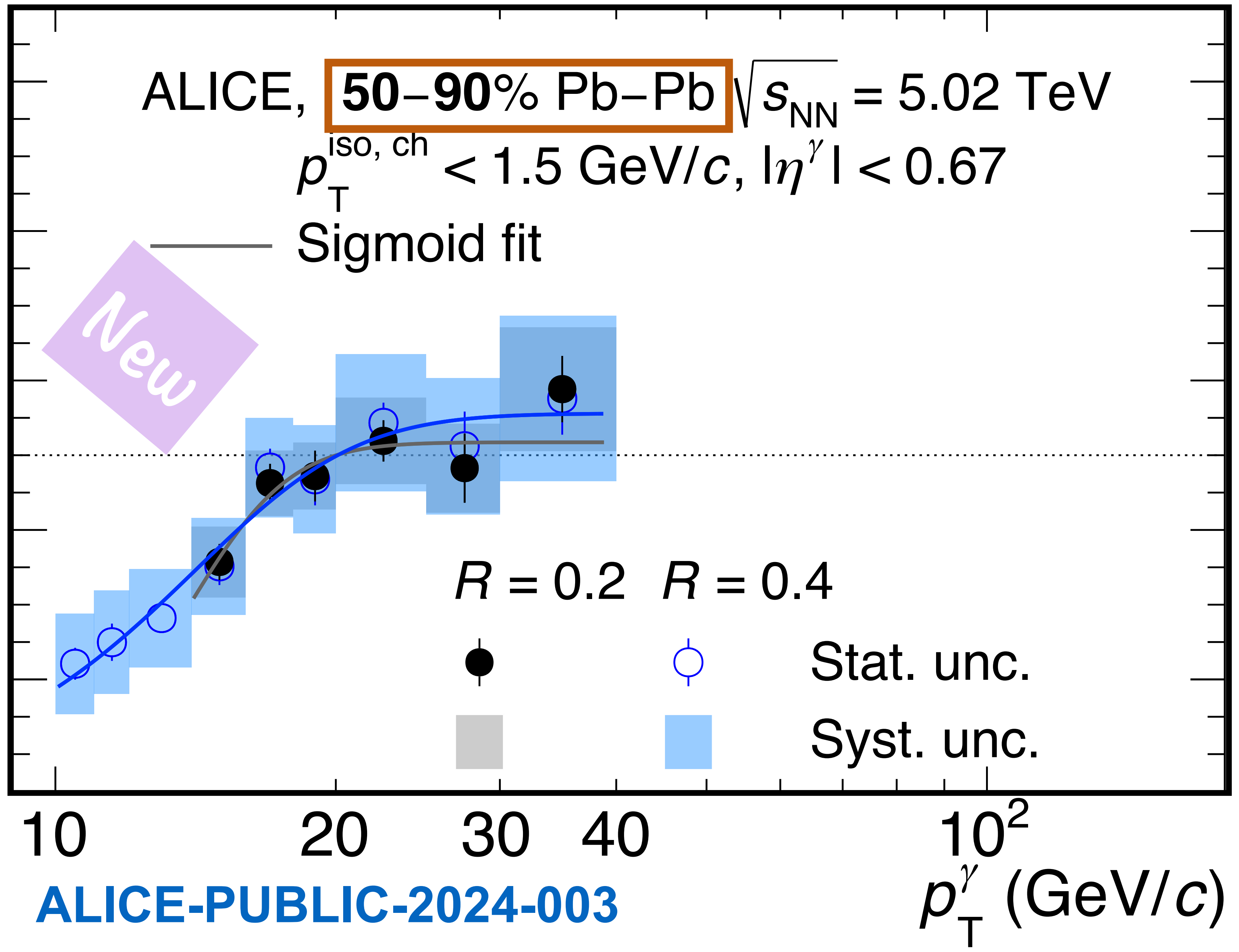

ALICE-PUBLIC-2024-003

- Selection details in back-up
- Reduce the influence of statistical fluctuations with sigmoid function fits

Cross section, pp $\sqrt{s}$ = 13 TeV

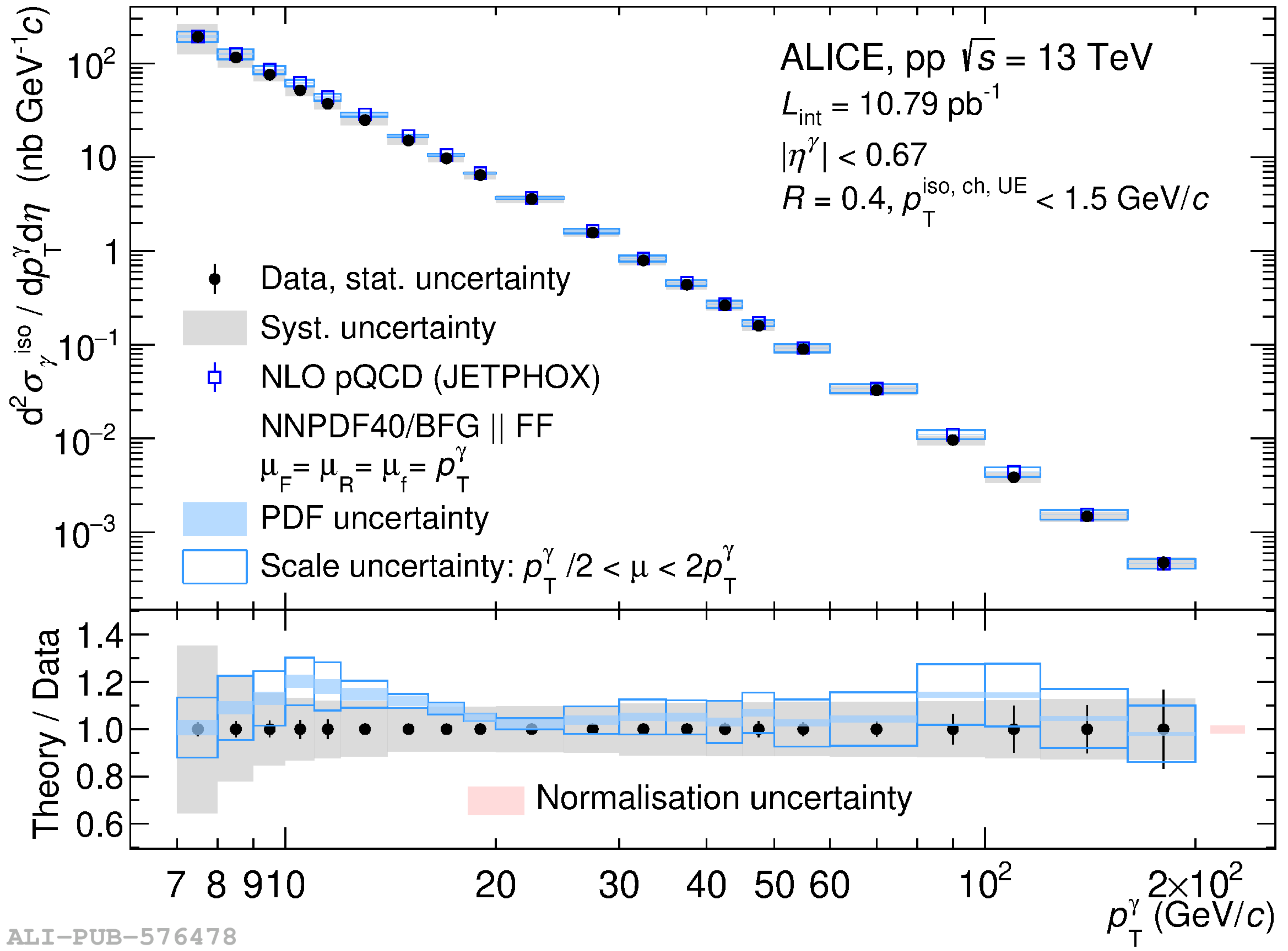

- NLO pQCD predictions (JETPHOX) and data agree
- Significantly lower p_T than CMS and ATLAS at $\sqrt{s}$ = 13 TeV
- Lowest x_T at mid-rapidity

Cross section, pp $\sqrt{s}$ = 13 TeV

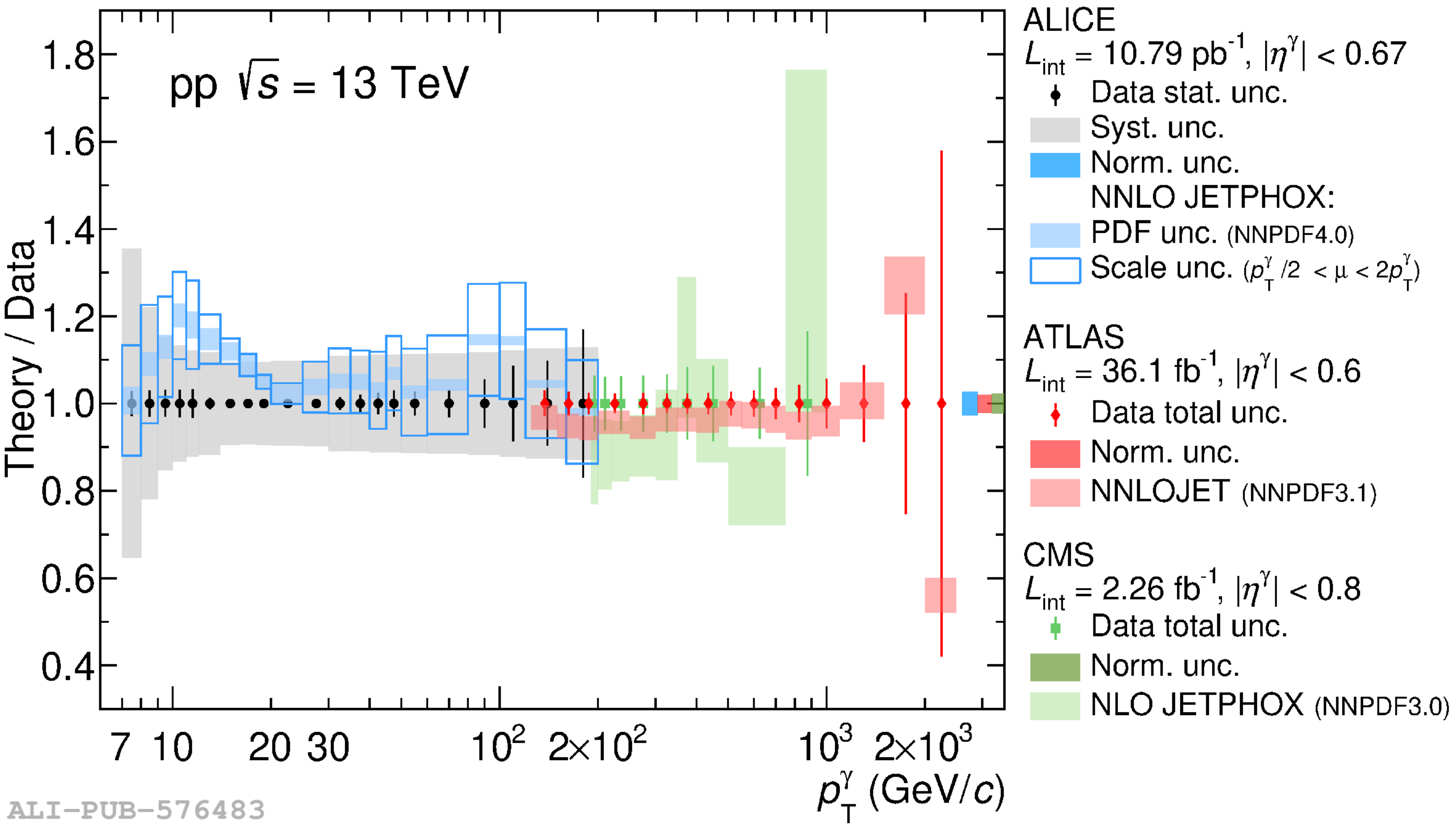

ATLAS JHEP 2019 (2019) 203
arXiv:1908.02746 [hep-ex]

CMS Eur. Phys. J. C 79 (2019) 20
arXiv:1807.00782 [hep-ex]

- NLO pQCD predictions (JETPHOX) and data agree
- Significantly lower p_T than CMS and ATLAS at $\sqrt{s}$ = 13 TeV
- Lowest x_T at mid-rapidity

Cross section, pp $\sqrt{s}$ = 13 TeV

New

ALICE

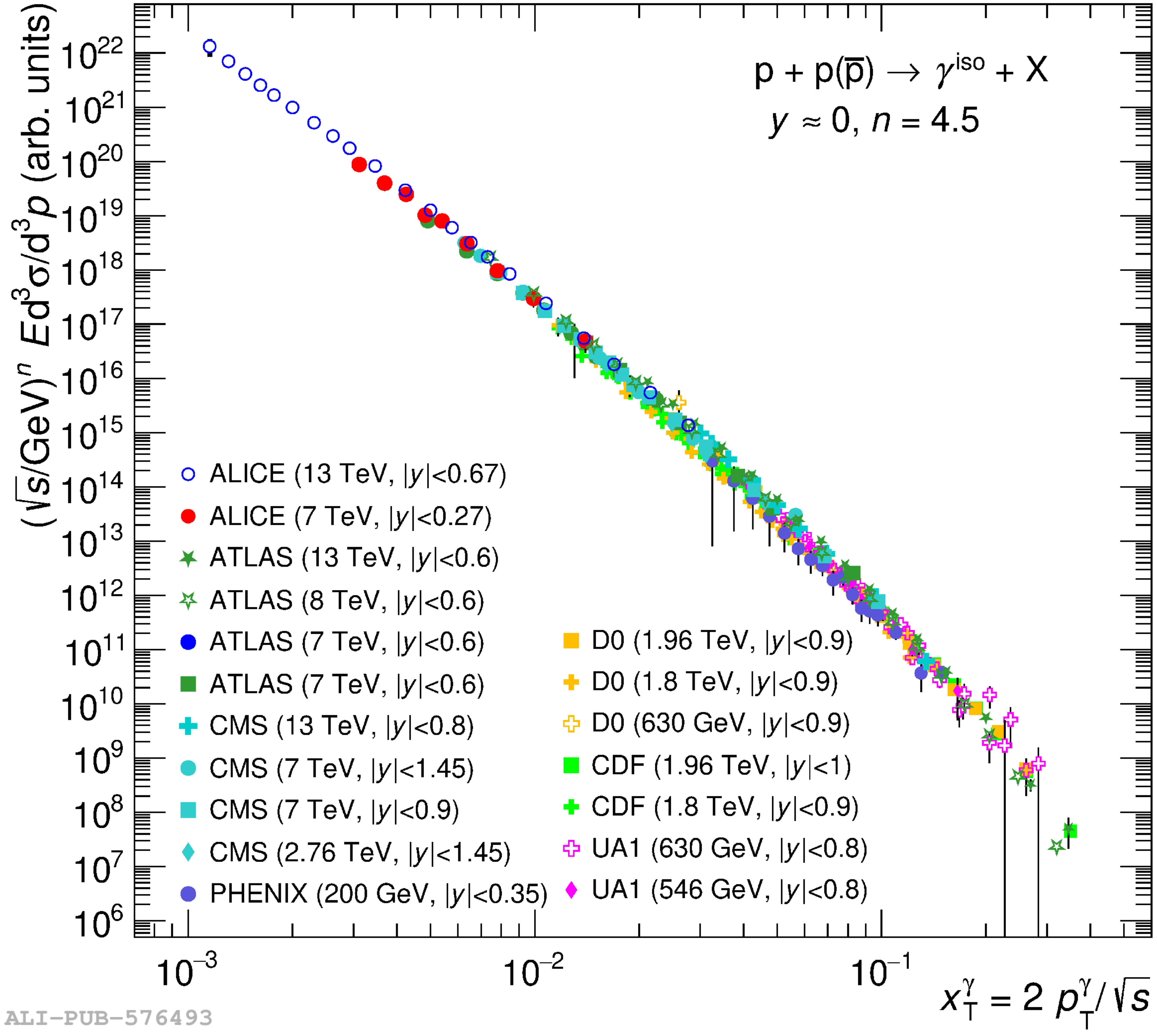

- NLO pQCD predictions (JETPHOX) and data agree
- Significantly lower p_T than CMS and ATLAS at $\sqrt{s}$ = 13 TeV
- Lowest x_T at mid-rapidity

$\left(\sqrt{s}\right)^{4.5}$ scale from x_T ~10^{-3} to 10^{-1}

Full list of older results compiled in D. D'Enterria & J. Rojo Nucl. Phys. B 860 (2012), arXiv:1202.1762 [hep-ph]

Cross section, p–Pb $\sqrt{s_{NN}}$ = 8.16 TeV

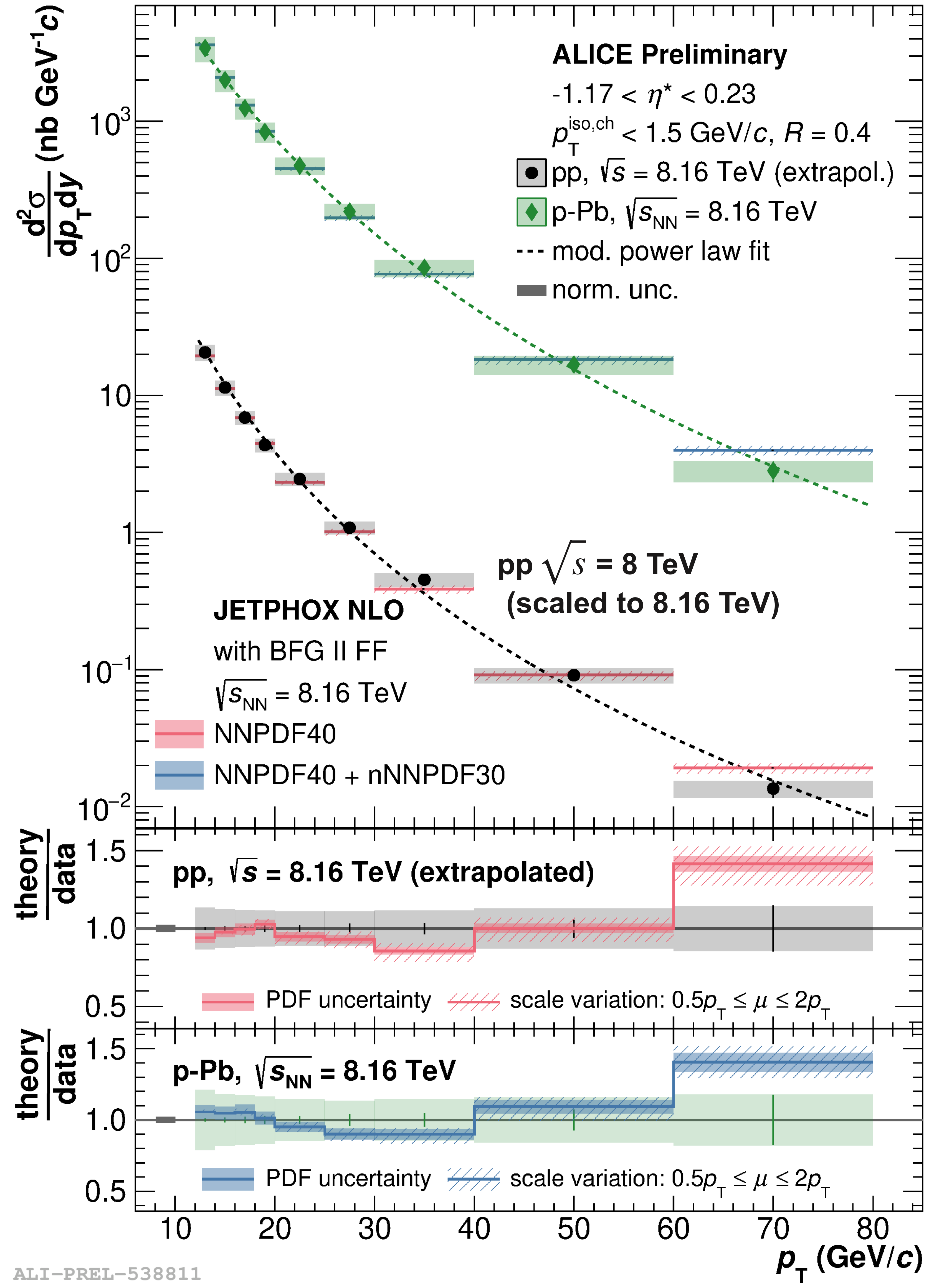

- NLO pQCD predictions (JETPHOX) and data agree

$$R_{pA} = \frac{d^2\sigma^{\gamma}_{pA}/dp_T\,dy^*}{A_{Pb}\times d^2\sigma^{\gamma}_{pp}/dp_T\,dy^*}$$

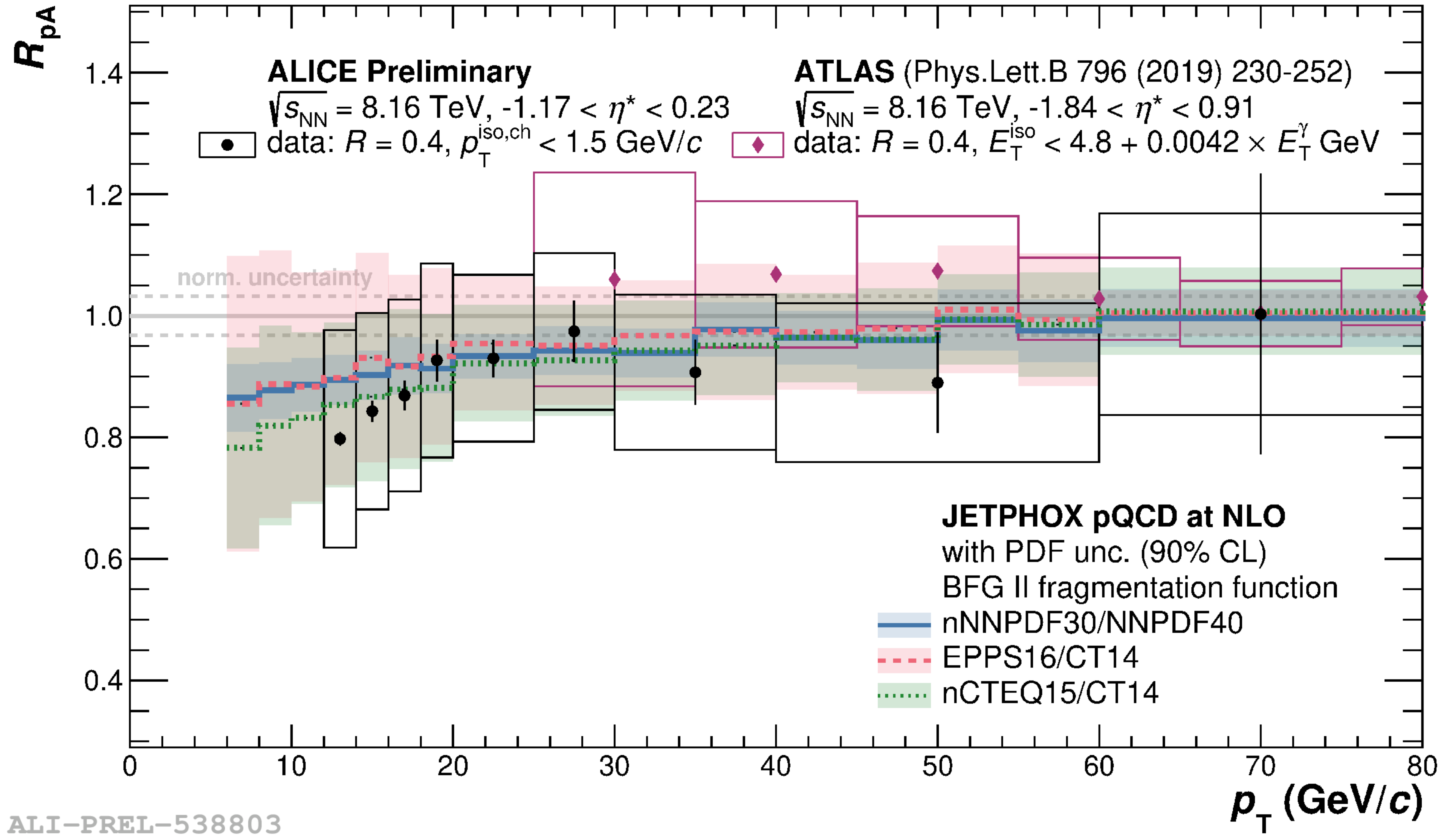

- R_{pA} in agreement with unity
  - Hints of lower than unity for p_T < 20 GeV/c, expected in theory, cold nuclear matter effects, shadowing
  - No suppression at high p_T, agreement with ATLAS

Cross section, pp & Pb–Pb at $\sqrt{s_{\rm NN}}$ = 5.02 TeV

$$\frac{\mathrm{d}^2\sigma^{\gamma\ \rm iso}}{\mathrm{d}p_{\rm T}\,\mathrm{d}\eta} = \frac{\sigma_{\rm NN}^{\rm INEL}}{N_{\rm events}\times {\rm RF}_{\varepsilon_{\rm trig}}} \times \frac{\mathrm{d}^2 N}{\mathrm{d}p_{\rm T}\,\mathrm{d}\eta} \times \frac{P}{{\rm Acc}\times\varepsilon_{\gamma}^{\rm iso}\times\varepsilon_{\rm trig}}$$

New

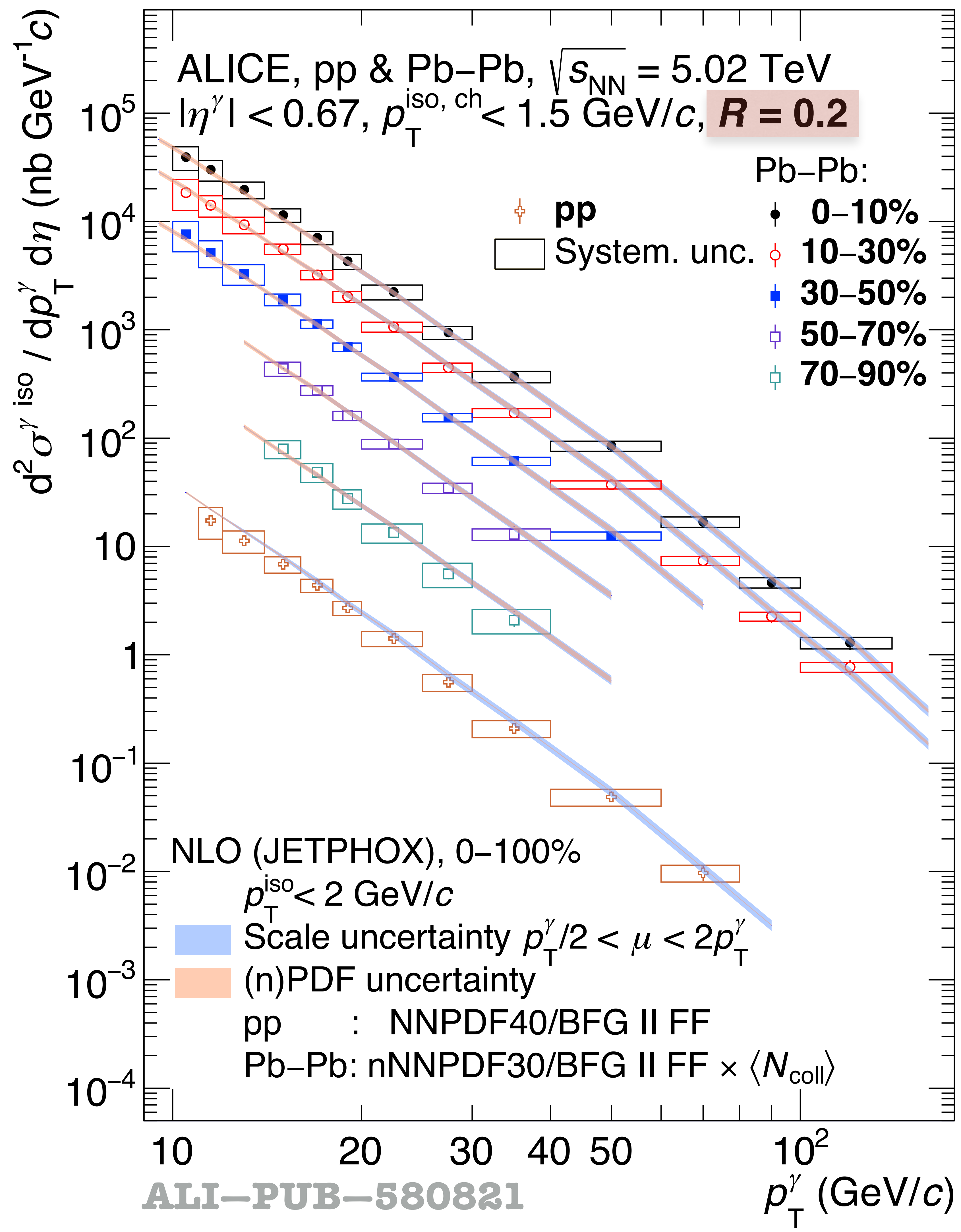

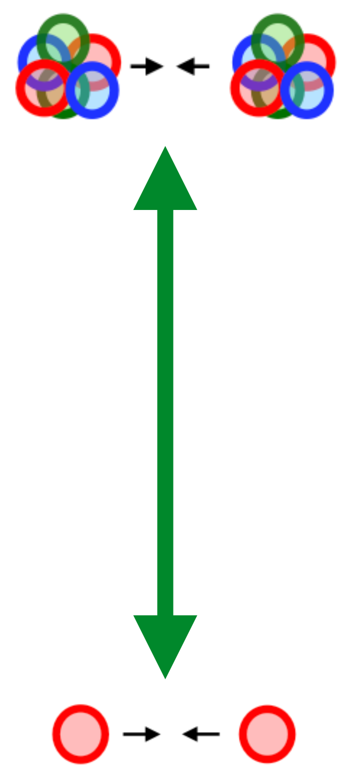

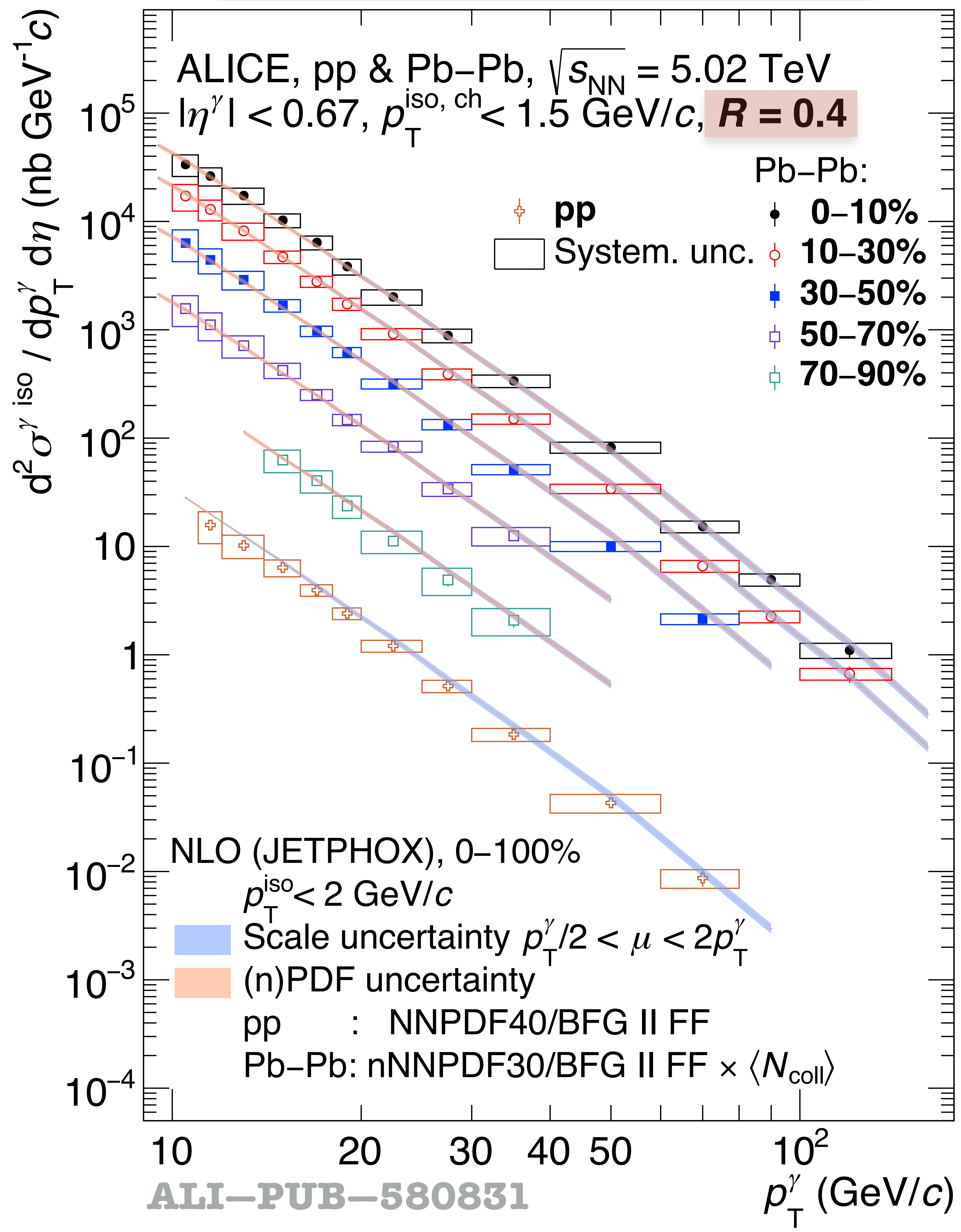

- Wide range: 10 < $p_{\rm T}$ < 140 GeV/c in Pb–Pb 0-30% & 11 < $p_{\rm T}$ < 80 GeV/c in pp
- NLO pQCD predictions (JETPHOX)
  - ➡ Note: Theory calculated for 0–100%, **PDF (pp) & nPDF** $\times N_{\rm coll}$ **(Pb–Pb)**

Cross section, pp & Pb–Pb at $\sqrt{s_{NN}}$ = 5.02 TeV

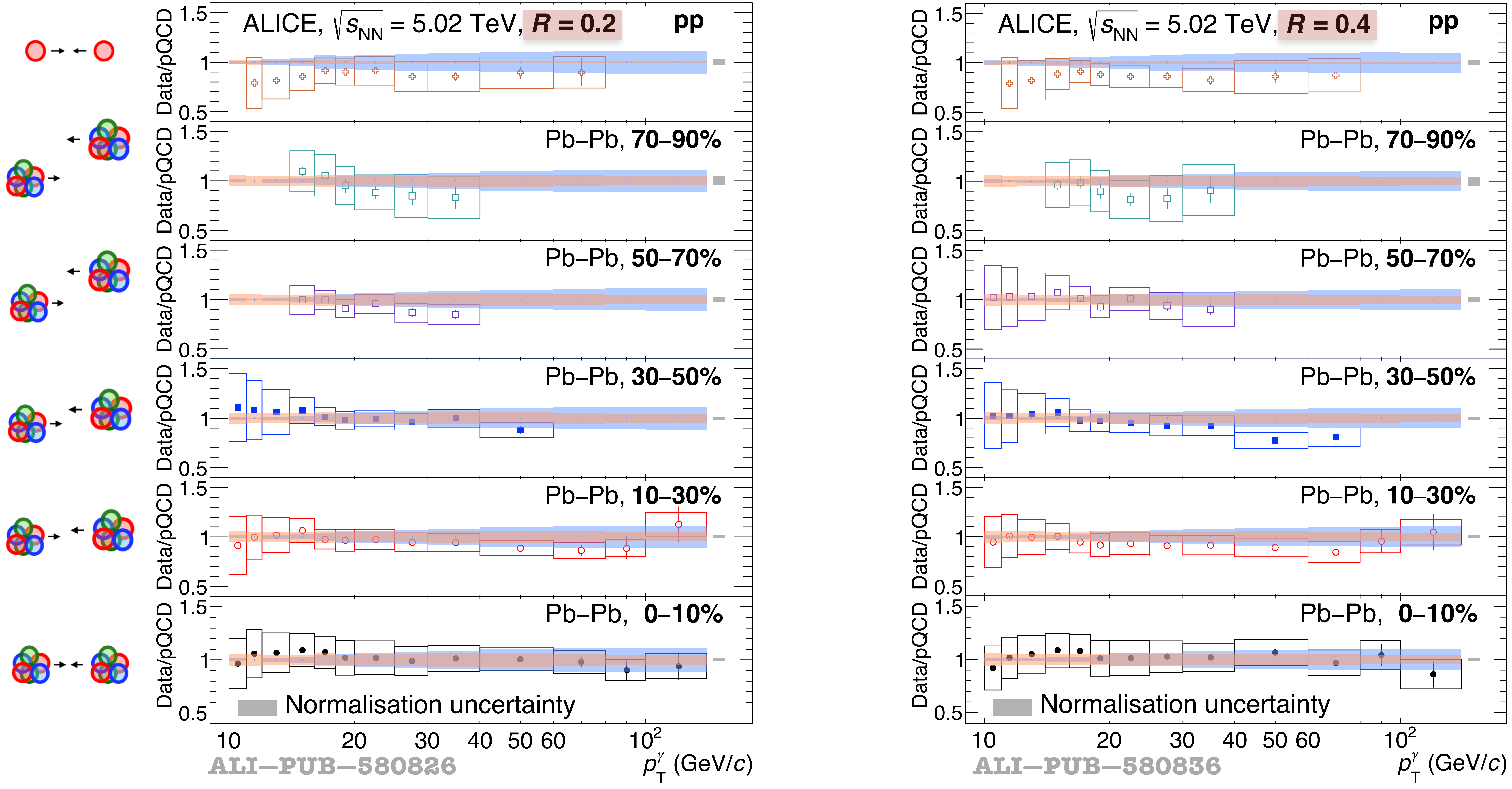

- NLO pQCD predictions (JETPHOX)
  - ➡ Note: Theory calculated for 0–100%, **PDF (pp) & nPDF** $\times N_{coll}$ **(Pb–Pb)**
- Theory & data agreement for both *R* and collision system

Cross section *R* ratio, pp & Pb–Pb at $\sqrt{s_{NN}}$ = 5.02 TeV

$$f_{R(0.4/0.2)} = \left.\frac{d^2\sigma}{dp_T\, d\eta}\right|_{(R=0.4)} \Big/ \left.\frac{d^2\sigma}{dp_T\, d\eta}\right|_{(R=0.2)}$$

- Sensitive to fraction of fragmentation γ surviving the isolation selection
  ➡ Interesting for theory models

- Agreement with theory and between collision systems
  ➡ Theory (NLO): controls the isolation mechanism, fragmentation γ & prompt γ production even in Pb–Pb

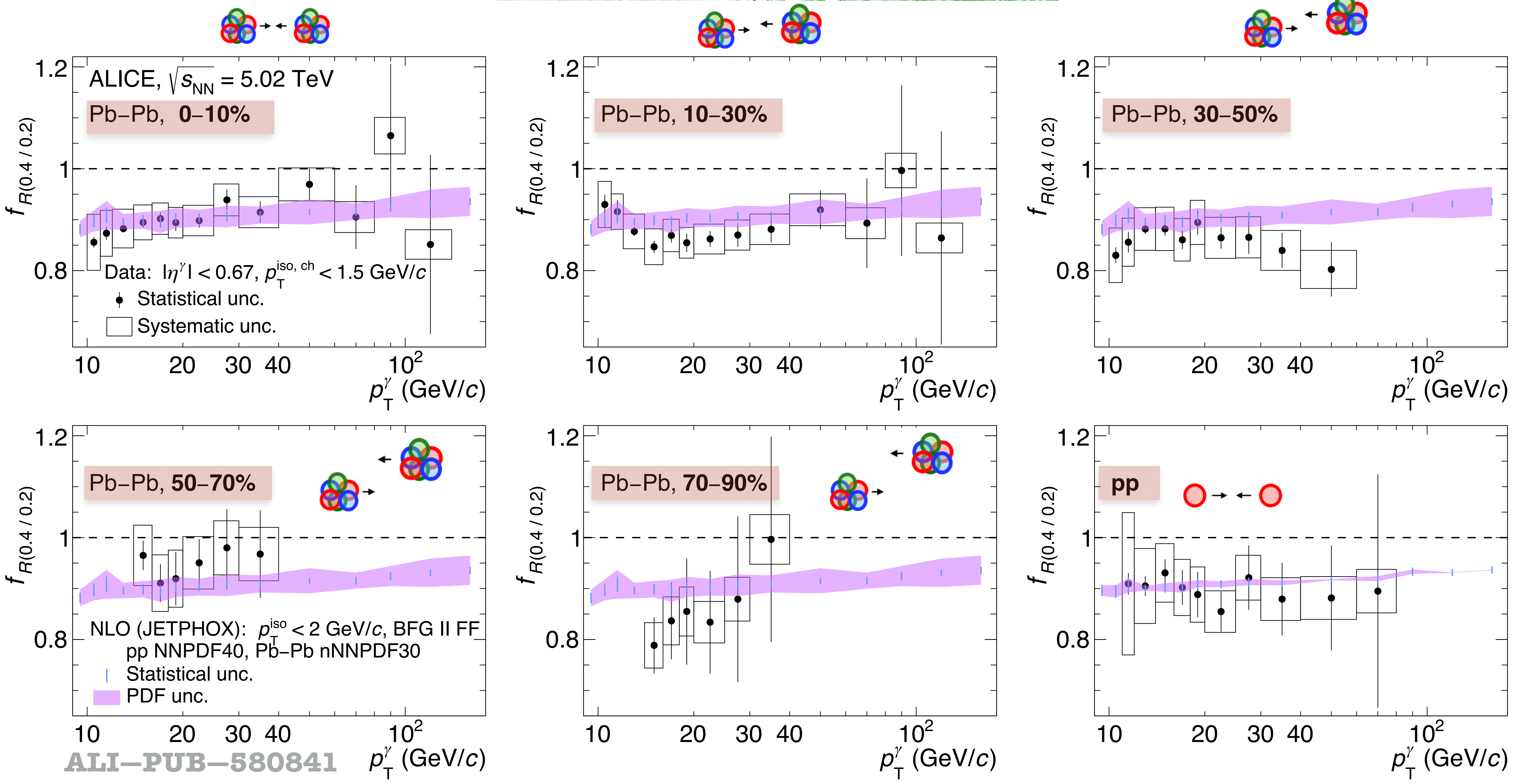

✳ Not shown (back-up): ATLAS pp $\sqrt{s}$ =13 TeV, for p_T > 250 GeV/c
JHEP 07 (2023) 86 arXiv:2302.00510

Nuclear modification factor R_{AA}, pp & Pb–Pb at $\sqrt{s_{NN}}$ = 5.02 TeV

$$R_{AA} = \frac{1}{\langle N_{coll} \rangle} \frac{d^2\sigma_{AA} / (dp_T\, d\eta)}{d^2\sigma_{pp} / (dp_T\, d\eta)}$$

- 0-70%
  - ➡ Consistent with unity within the unc. for both R
    - ✤ No modification of the prompt γ yield due to the QGP as expected
  - ➡ Agreement with NLO pQCD incorporating cold matter nuclear effects: PDF vs nPDF

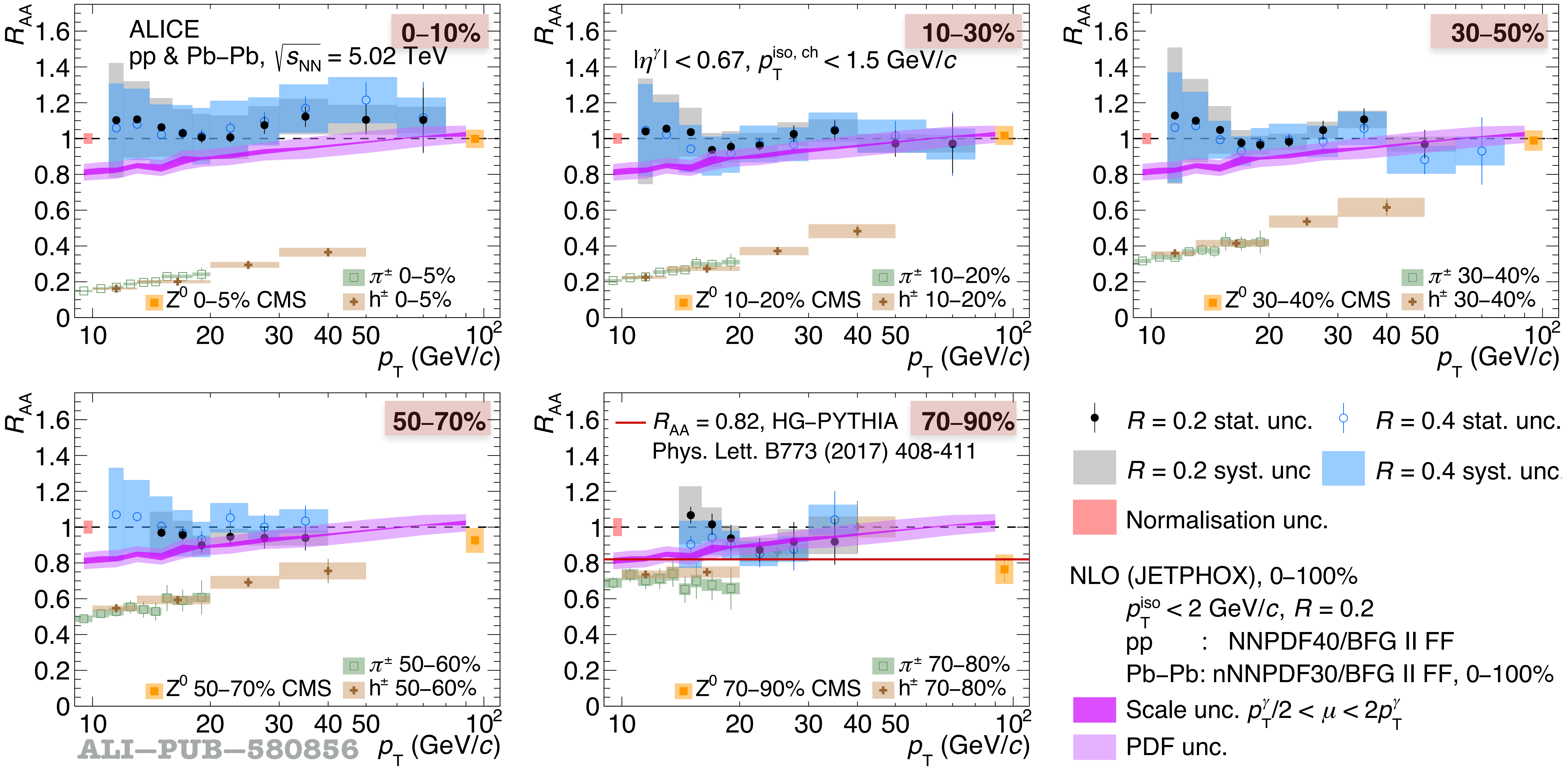

Nuclear modification factor R_{AA}, pp & Pb–Pb at $\sqrt{s_{NN}}$ = 5.02 TeV

$$R_{AA} = \frac{1}{\langle N_{coll} \rangle} \frac{d^2\sigma_{AA} / (dp_T\, d\eta)}{d^2\sigma_{pp} / (dp_T\, d\eta)}$$

- 0-70%
  - ➡ Consistent with unity within the unc. for both R
    - ✤ No modification of the prompt γ yield due to the QGP as expected
  - ➡ Agreement with NLO pQCD incorporating cold matter nuclear effects: PDF vs nPDF
- 70-90%
  - ➡ Closer to 0.9 than 1 for both R likely due to centrality selection bias of Glauber model
  - ➡ Model by C. Loizides & A. Morsch (Phys. Lett. B773 (2017) 408-411) yields a value at 0.82
    - ✤ In agreement within the uncertainties
  - ➡ Seen by CMS with Z^0 bosons

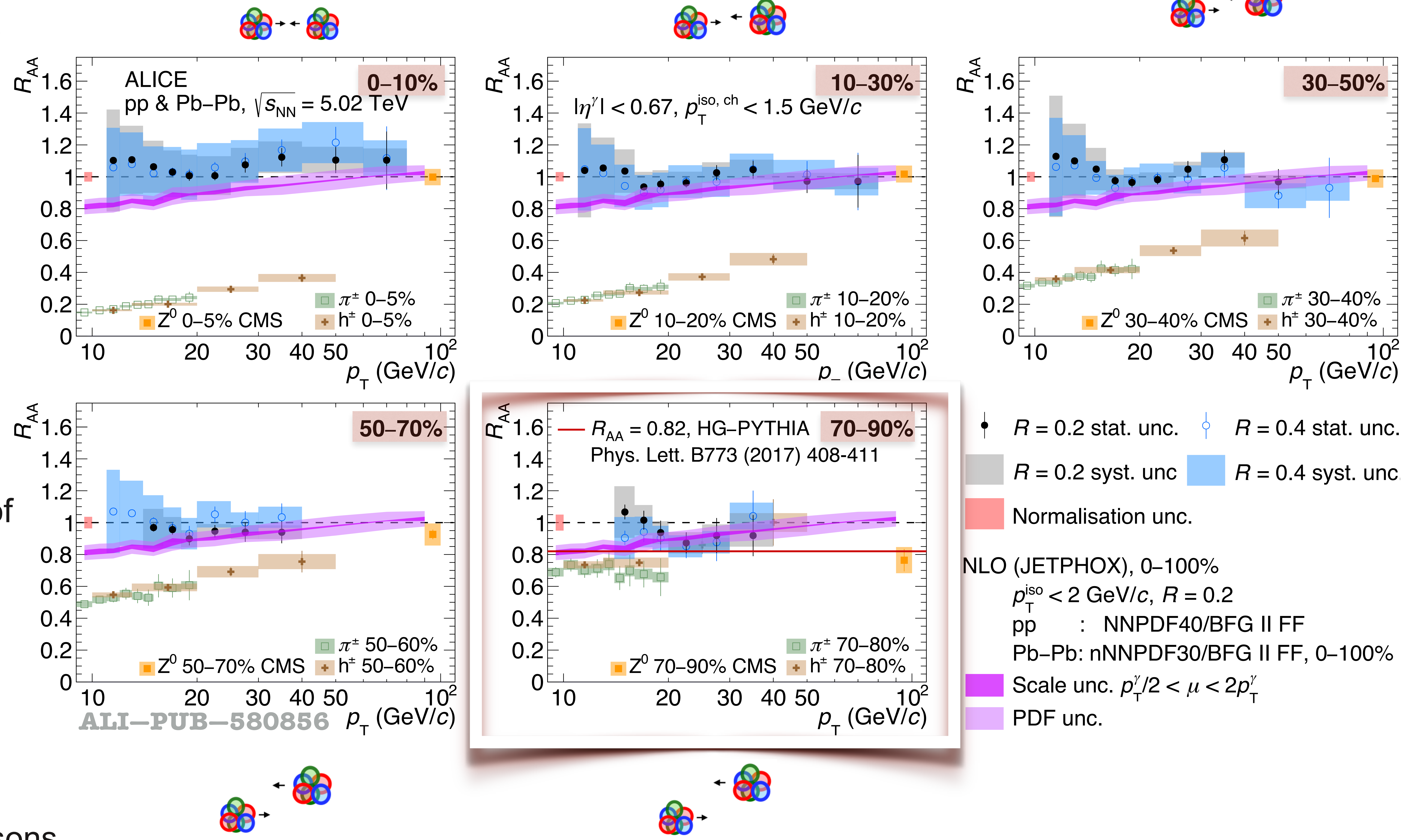

Nuclear modification factor R_{AA}, pp & Pb–Pb at $\sqrt{s_{NN}}$ = 5.02 TeV

$$R_{AA} = \frac{1}{\langle N_{coll} \rangle} \frac{d^2\sigma_{AA} / (dp_T\, d\eta)}{d^2\sigma_{pp} / (dp_T\, d\eta)}$$

- **ALICE** & **CMS**: good agreement in the overlapping region 25 < p_T < 40–80 GeV/c

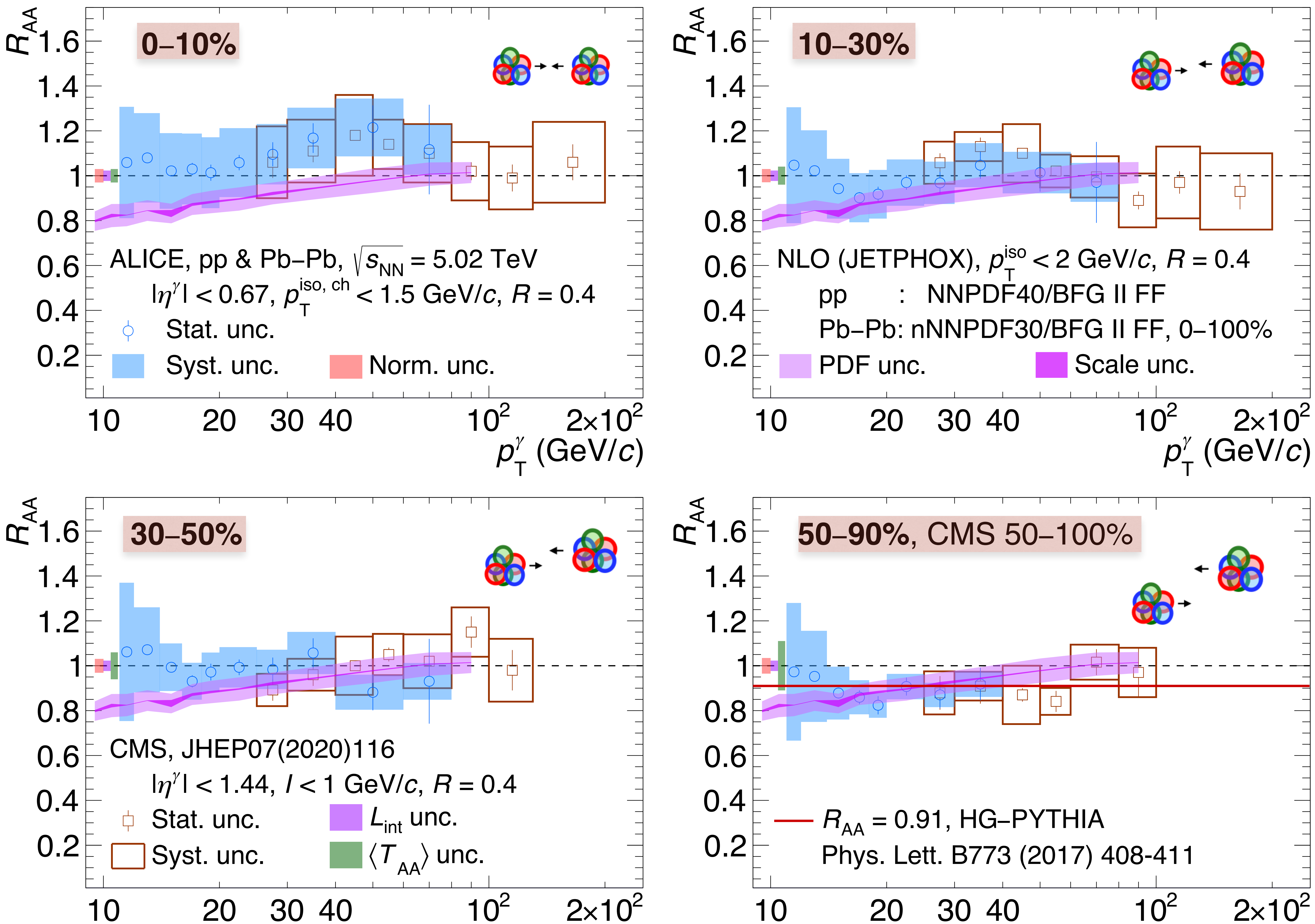

ALICE-PUBLIC-2024-003

Nuclear modification factor R_{AA}, pp & Pb–Pb at $\sqrt{s_{NN}}$ = 5.02 TeV

New

ALICE

$$R_{AA} = \frac{1}{\langle N_{coll} \rangle} \frac{d^2\sigma_{AA} / (dp_T\, d\eta)}{d^2\sigma_{pp} / (dp_T\, d\eta)}$$

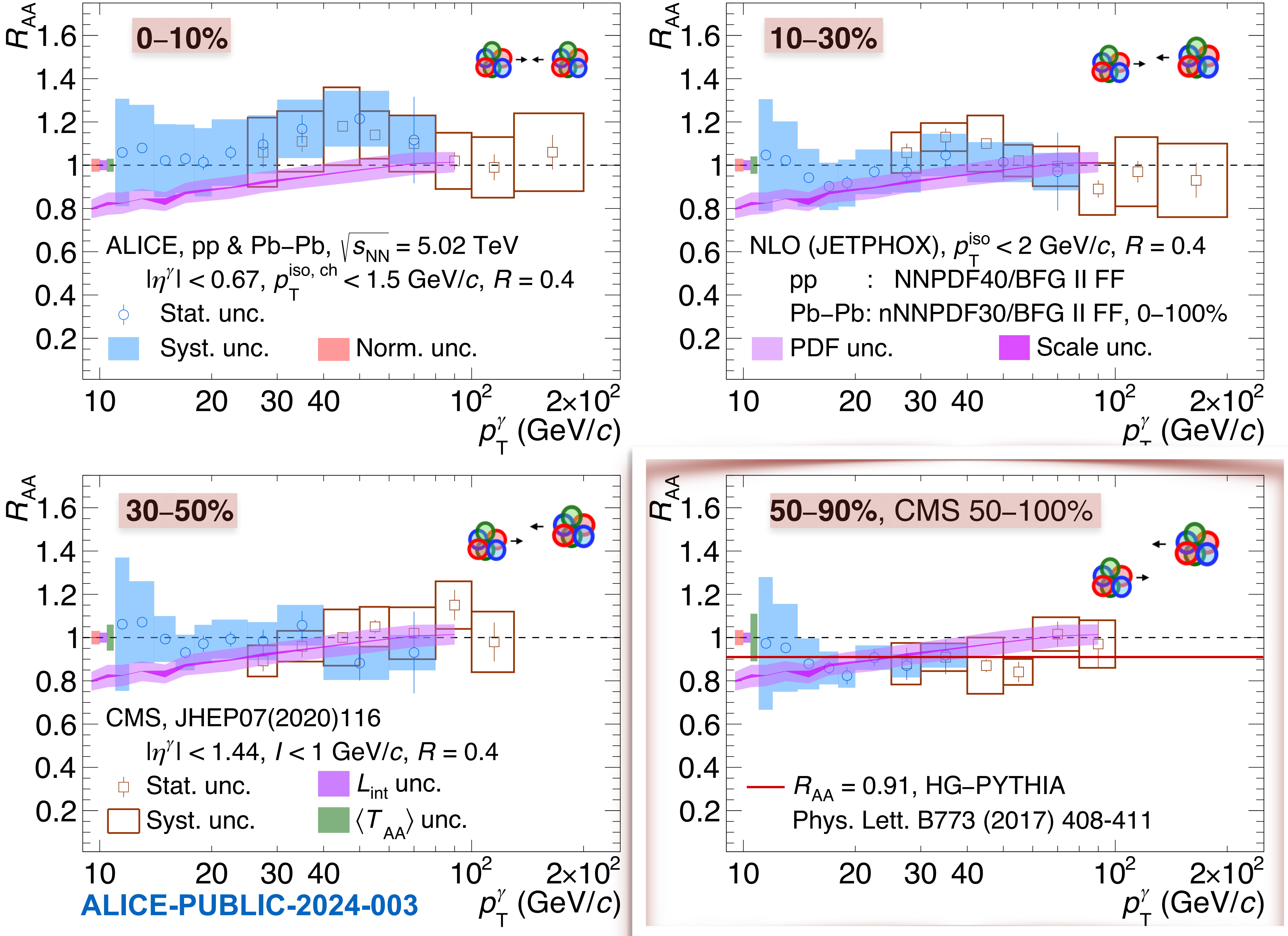

ALICE-PUBLIC-2024-003

- **ALICE & CMS**: good agreement in the overlapping region 25 < p_T < 40–80 GeV/c

- 50-90%
  - ➡ Closer to 0.9 than 1 for both R likely due to centrality selection bias of Glauber model
  - ➡ Model by C. Loizides & A. Morsch (Phys. Lett. B773 (2017) 408-411) yields a value at 0.91
    - ✤ In agreement within the uncertainties

Isolated γ-hadron correlations in Pb–Pb at $\sqrt{s_{\rm NN}}$ = 5.02 TeV, R = 0.2

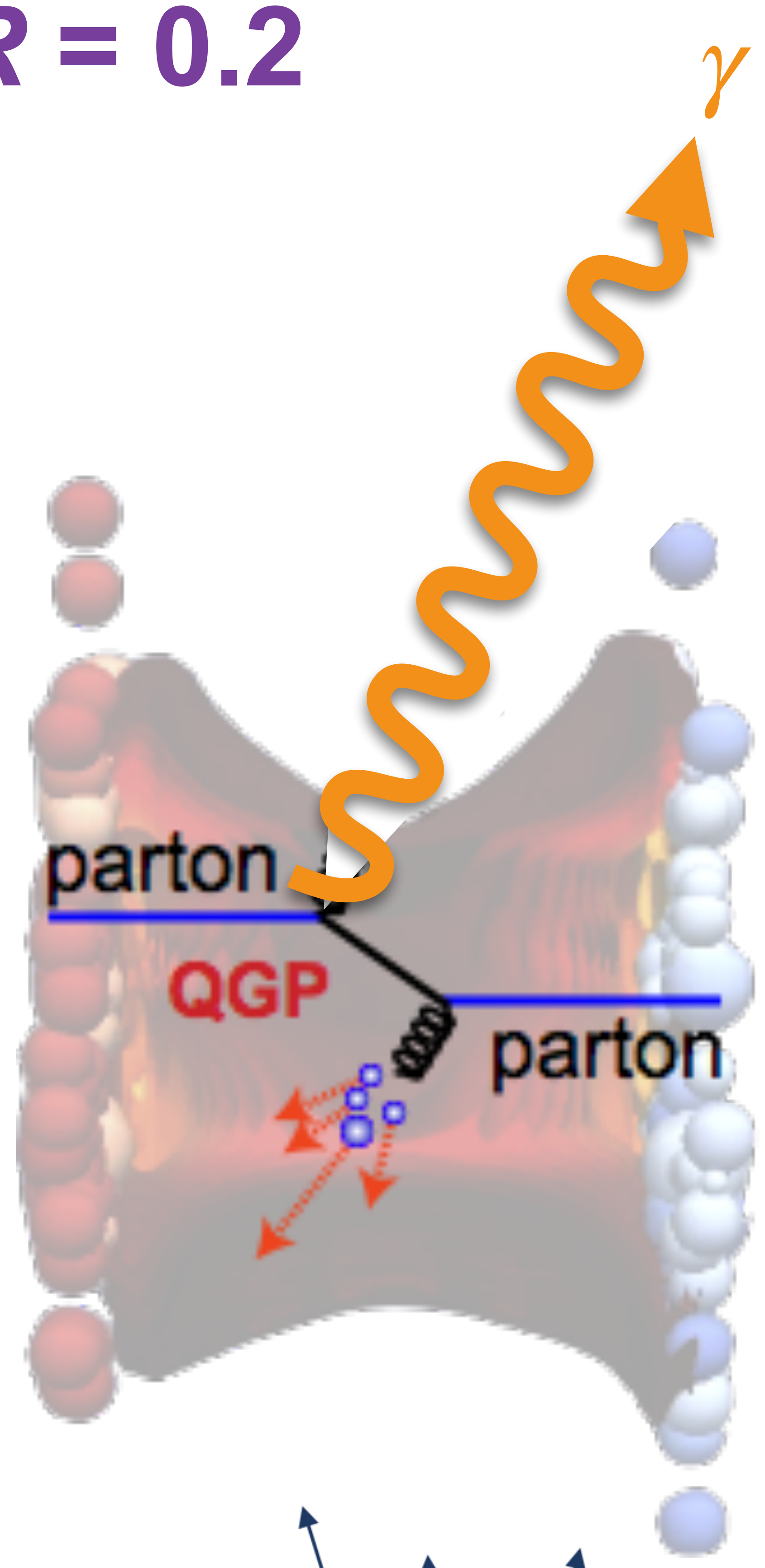

- Prompt γ associated to a parton emitted in opposite side
- **Tags the parton initial energy** $p_{\rm T}^{\gamma} \simeq p_{\rm T}^{\rm parton}$, before losing Δ*E* in QGP
  - ➡ Aim: Measure FF modifications, where is the Δ*E* radiated?

- Observables:
  - ➡ Trigger: isolated narrow or wide clusters, R = 0.2 & $p_{\rm T}^{\rm iso\ ch}$ < 1.5 GeV/*c*
  - ➡ Azimuthal correlation: $\Delta\varphi = \varphi^{\rm trigger} - \varphi^{\rm track}$ with
  - ➡ $z_{\rm T} = \frac{p_{\rm T}^{\rm track}}{p_T^{\rm trigger}}$ and $\mathrm{D}(z_{\rm T}) = \frac{1}{N^{\rm trigger}} \frac{{\rm d}\ N^{\rm track}}{{\rm d}\ z_{\rm T}}$ for tracks in $|\Delta\varphi| > 3/5\pi$ rad (mirrored)
  - ➡ **When trigger = prompt γ, $\mathrm{D}(z_{\rm T})$ is a proxy for FF**
  - ➡ Measurement: 18 < $p_T^{\rm trigger}$< 40 GeV/*c* & $p_T^{\rm track}$ > 0.5 GeV/*c*
    - Details in back-up

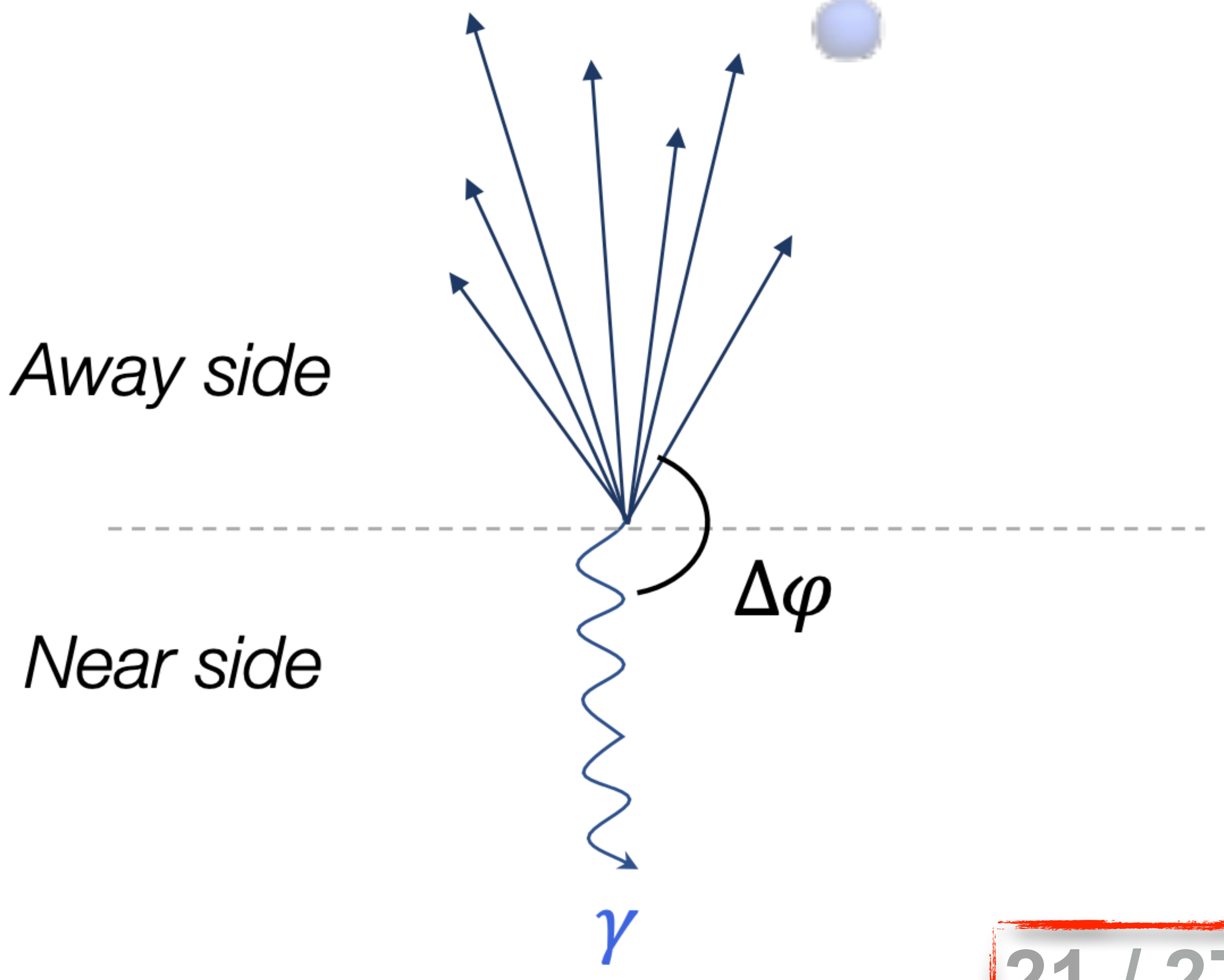

Isolated γ-hadron correlations in p–Pb & pp, R = 0.4: $D(z_T)$

ALICE

- Previous published results in p–Pb and pp collisions
  - ➡ Agreement between systems and with PYTHIA
  - ➡ Note: Pb–Pb collisions measurement (next slides) done in <u>different p_T ranges</u> and is compared directly to pQCD predictions

Phys Rev C 102 (2020) 044908

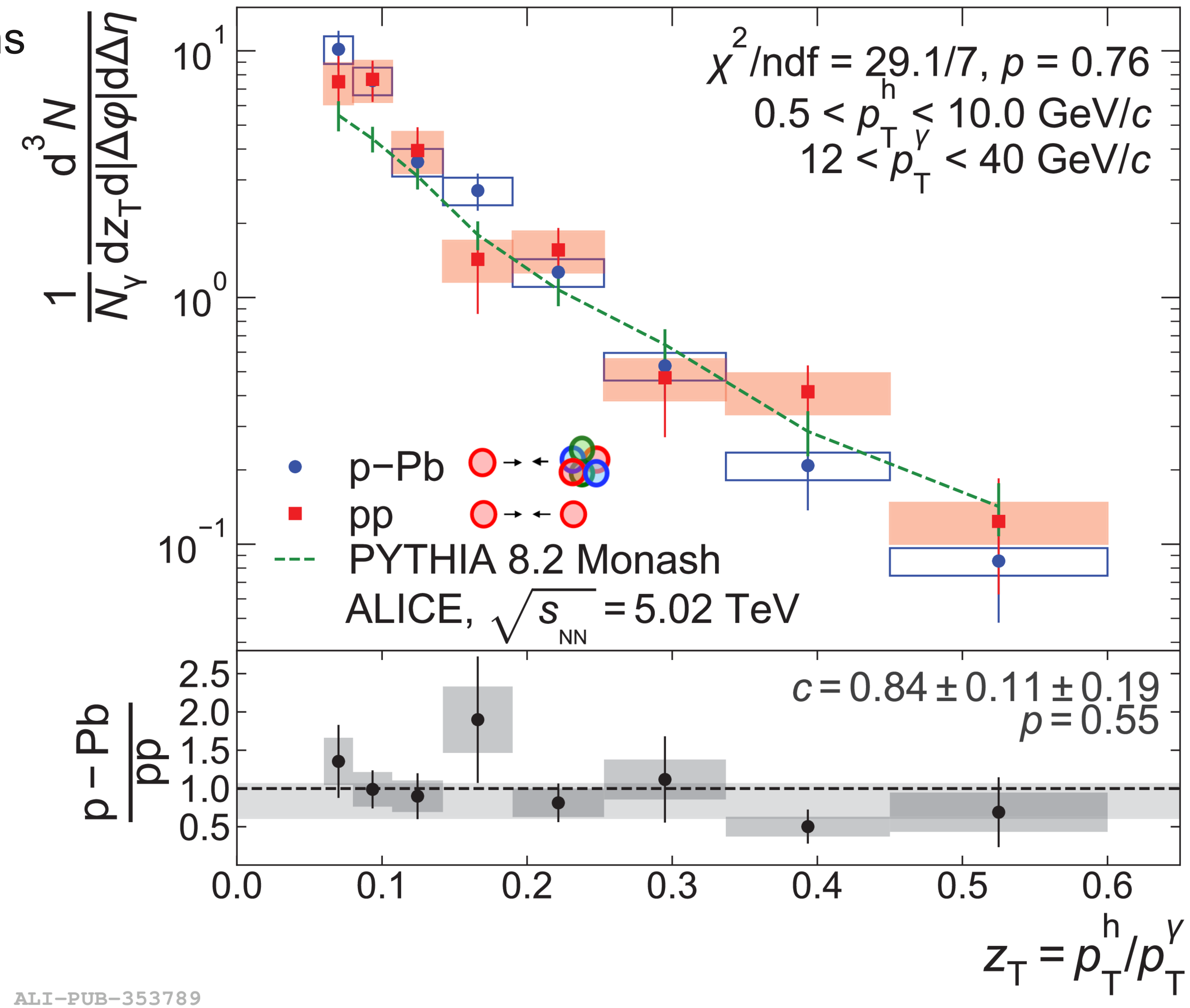

Isolated γ-hadron correlations in Pb–Pb: $D(z_T)$

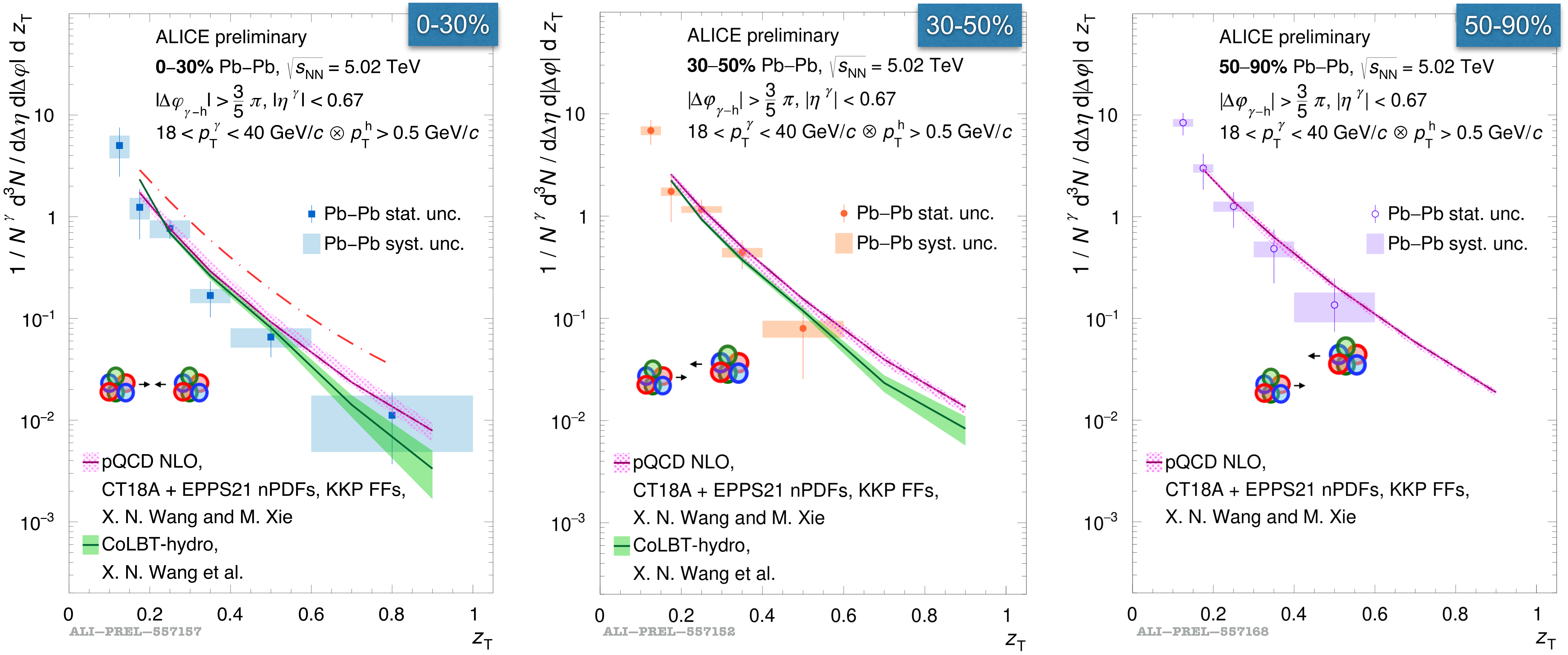

- Pb–Pb data compared with theory: *NLO pQCD* and *CoLBT* (0-50% only)
  - ➡ In agreement with both models
  - ➡ Discrimination not possible yet

- *Phys. Rev. C 103, 034911, Xie, Wang and Zhang,*
- *Phys. Rev. Lett. 103, 032302, Xie, Wang and Zhang*
- *Phys.Lett.B 777 (2018) 86-90 , Chen et al.*

Isolated γ-hadron correlations in Pb–Pb: $D(z_T)$

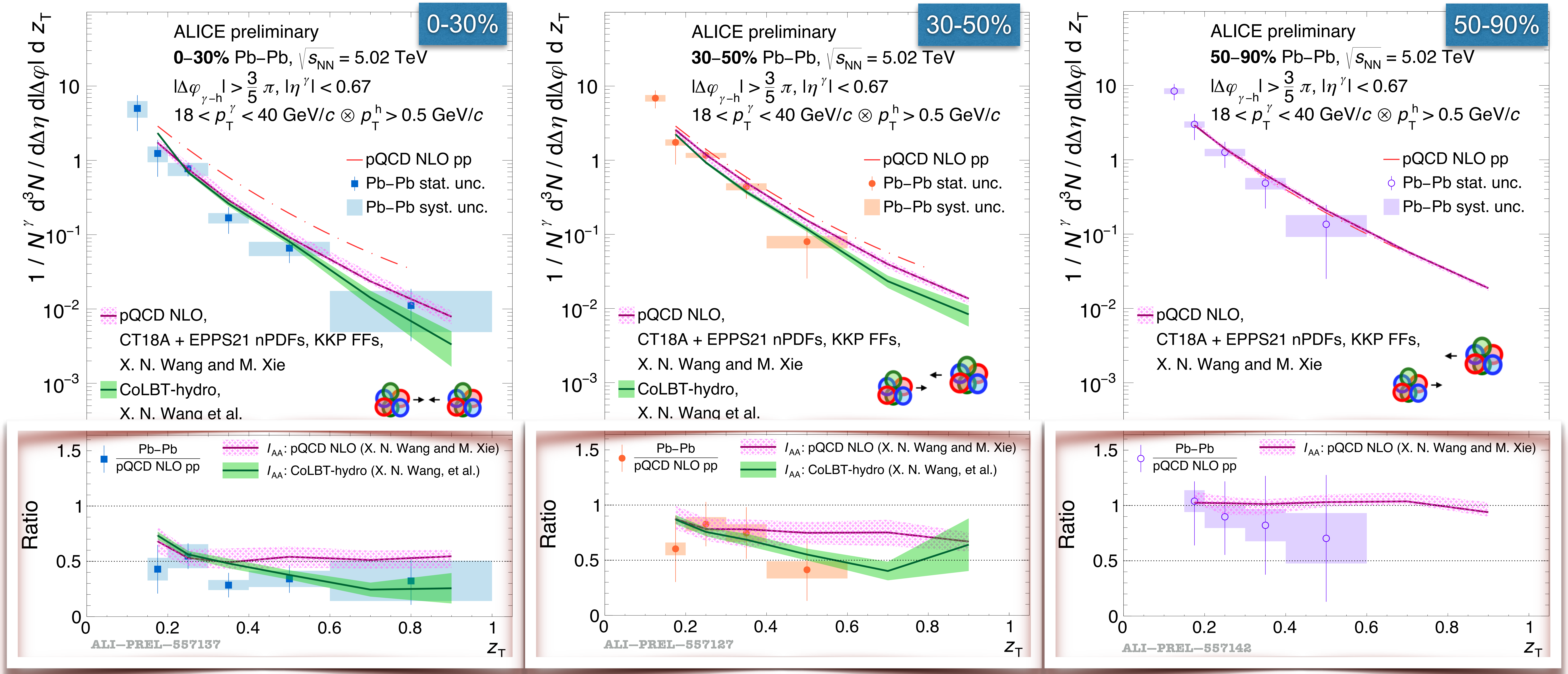

- Ratio with respect to NLO pQCD pp collision simulation → A proxy for $I_{AA} = \frac{D(z_T)_{\text{Pb–Pb}}}{D(z_T)_{\text{pp}}}$
- Clear modifications in data with respect to NLO pQCD pp simulation
- Comparison with I_{AA} from NLO pQCD and CoLBT models → agreement

Summary

➡ Cross section

- Data in agreement with NLO pQCD in multiple collision systems & $\sqrt{s_{NN}}$
- Lowest measured x_T at mid-rapidity in pp collisions at $\sqrt{s}$ = 13 TeV
- Ratio of cross sections for different R in agreement with theory and within the different collision systems

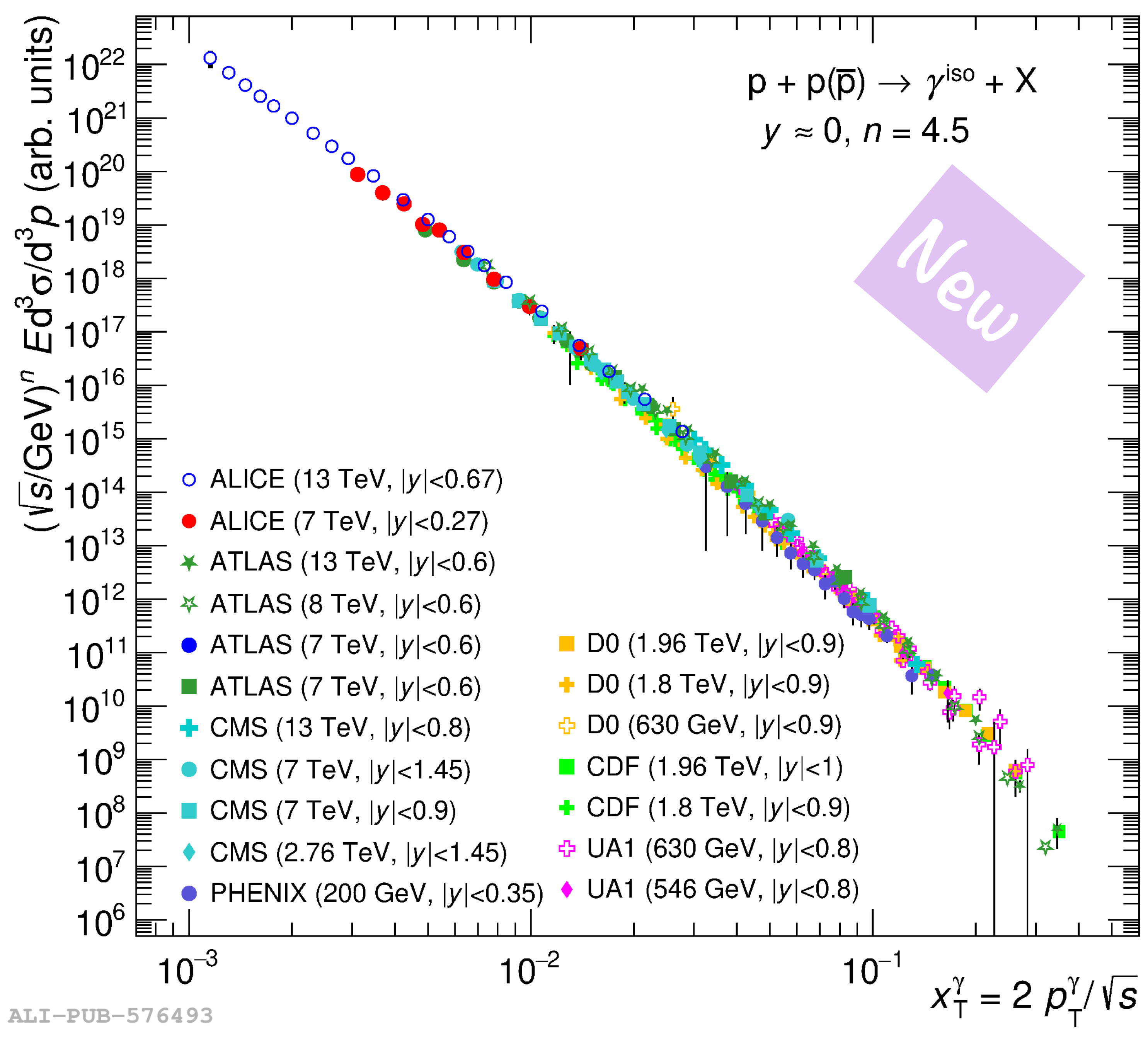

Summary

➡ Cross section

- Data in agreement with NLO pQCD in multiple collision systems & $\sqrt{s_{\rm NN}}$
- Lowest measured $x_{\rm T}$ at mid-rapidity in pp collisions at $\sqrt{s}$ = 13 TeV
- Ratio of cross sections for different R in agreement with theory and within the different collision systems

- Pb–Pb: $R_{\rm AA} \simeq 1$, no $\boldsymbol{\gamma}$ production modification by QGP
  - but for 50–90% & 70–90%: $R_{\rm AA} \simeq 0.9$, agreement (1$\boldsymbol{\sigma}$) with HG-PYTHIA, model of the centrality selection bias
  - Pb-Pb col. agree with nPDF prediction
- p–Pb: $R_{\rm pA} \simeq 1$, no $\boldsymbol{\gamma}$ production modification
  - Hints of suppression for $p_{\rm T}$ < 20 GeV/c in p–Pb, in agreement with pQCD nPDF / PDF at low $p_{\rm T}$

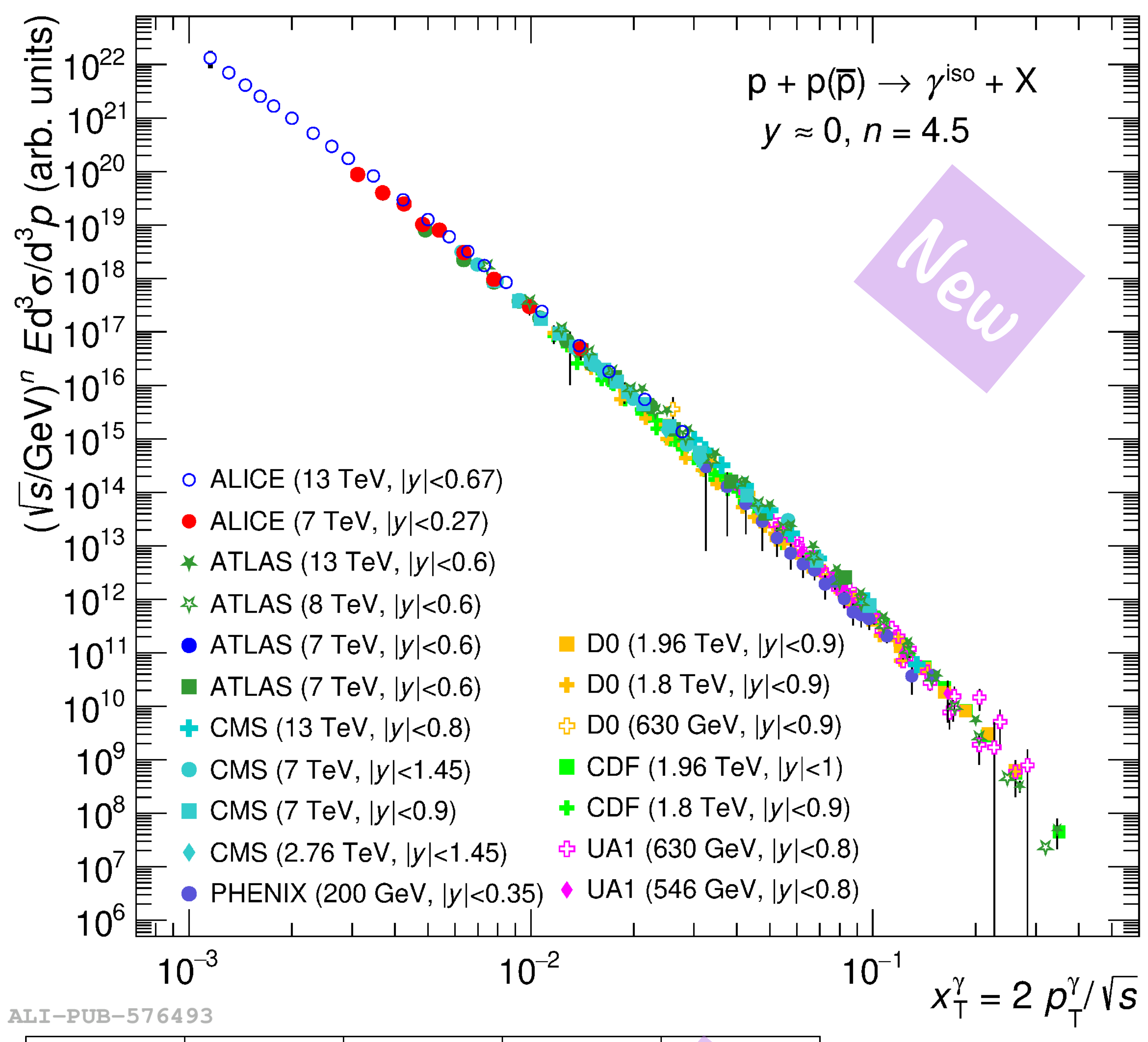

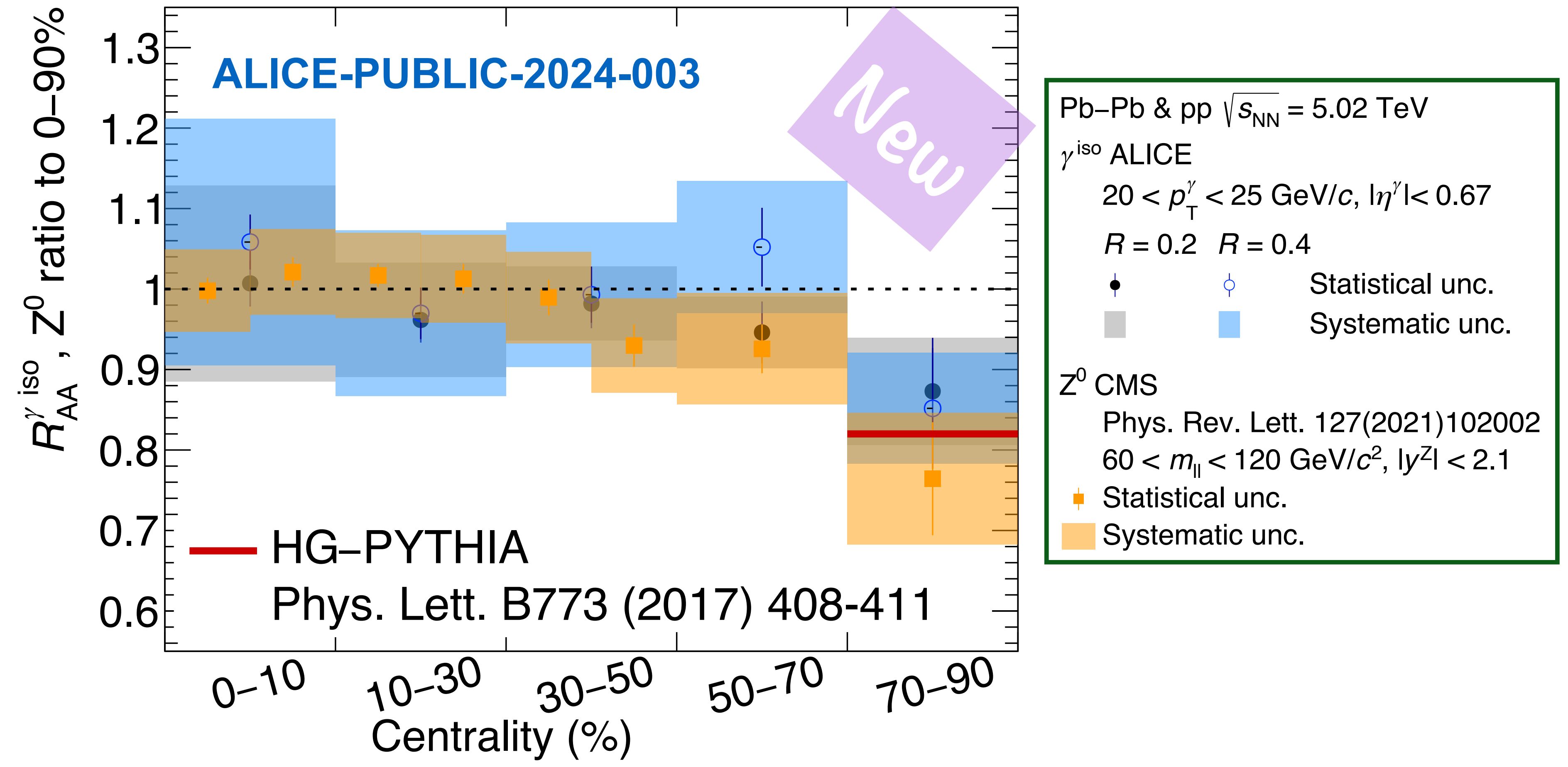

Summary

➡ **Cross section**

- Data in agreement with NLO pQCD in multiple collision systems & $\sqrt{s_{\rm NN}}$
- Lowest measured $x_{\rm T}$ at mid-rapidity in pp collisions at $\sqrt{s}$ = 13 TeV
- Ratio of cross sections for different R in agreement with theory and within the different collision systems

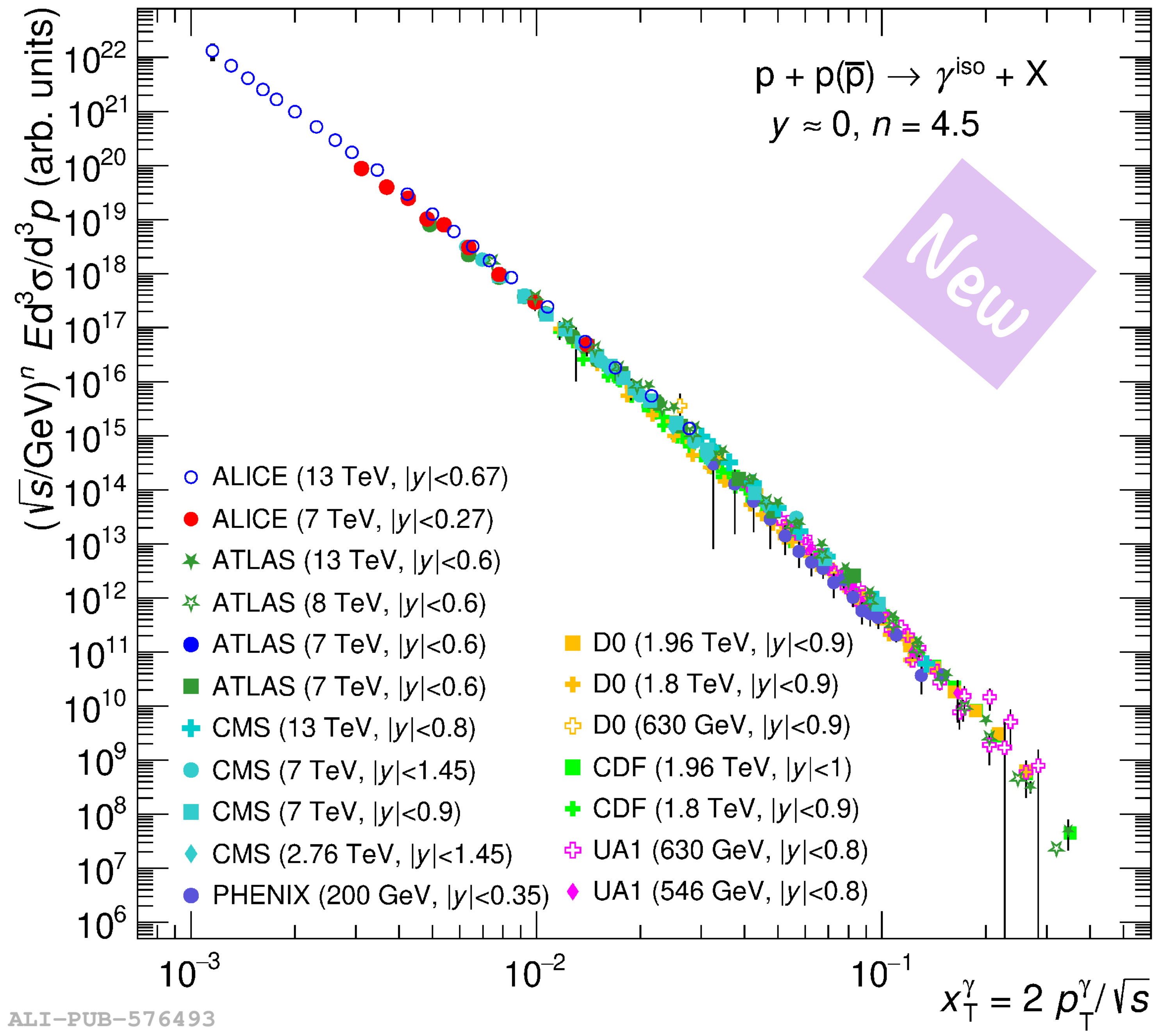

- Pb–Pb: $R_{\rm AA} \simeq 1$, no γ production modification by QGP
  - but for 50–90% & 70–90%: $R_{\rm AA} \simeq 0.9$, agreement (1σ) with HG-PYTHIA, model of the centrality selection bias
  - Pb-Pb col. agree with nPDF prediction
- p–Pb: $R_{\rm pA} \simeq 1$, no γ production modification
  - Hints of suppression for $p_{\rm T}$ < 20 GeV/c in p–Pb, in agreement with pQCD nPDF / PDF at low $p_{\rm T}$

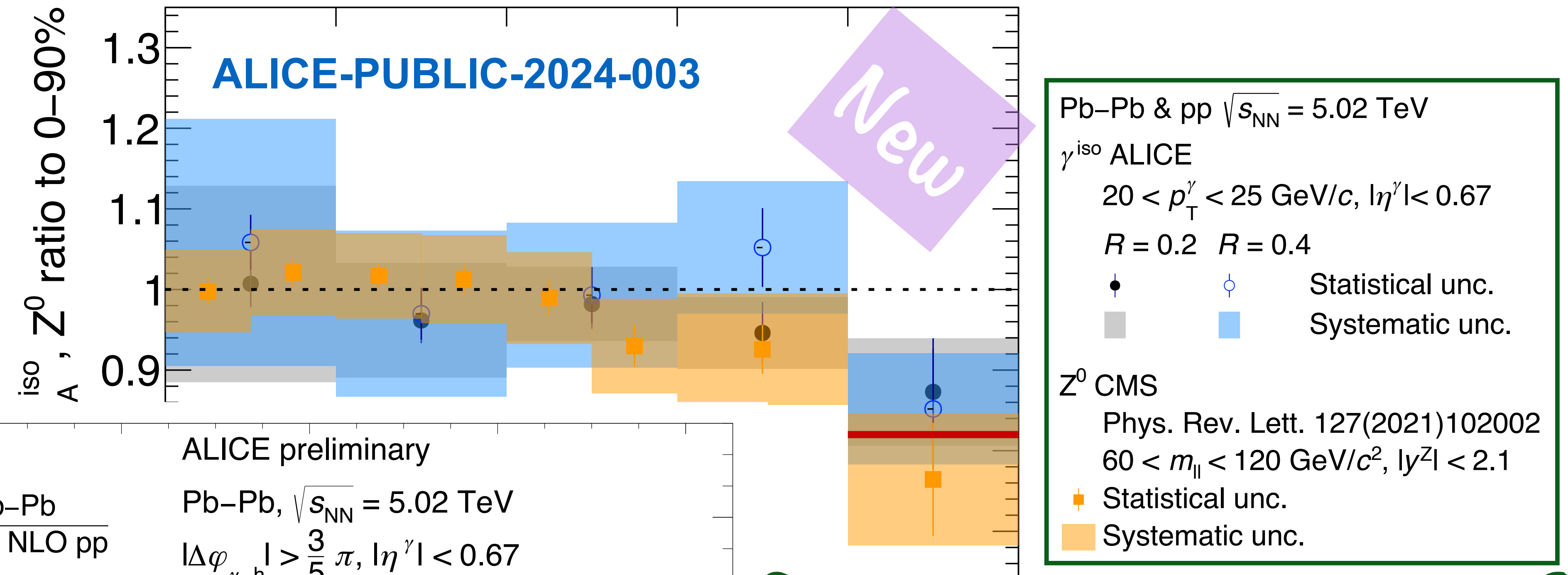

➡ **γ–hadron corr. in Pb–Pb at $\sqrt{s_{\rm NN}}$ = 5.02 TeV**

- **Very statistically limited, challenging!**
- $z_{\rm T}$ distribution significantly lower than pp NLO pQCD in central
  - FF modification: stronger for central compared to peripheral
- Results described by two models, model discrimination not possible

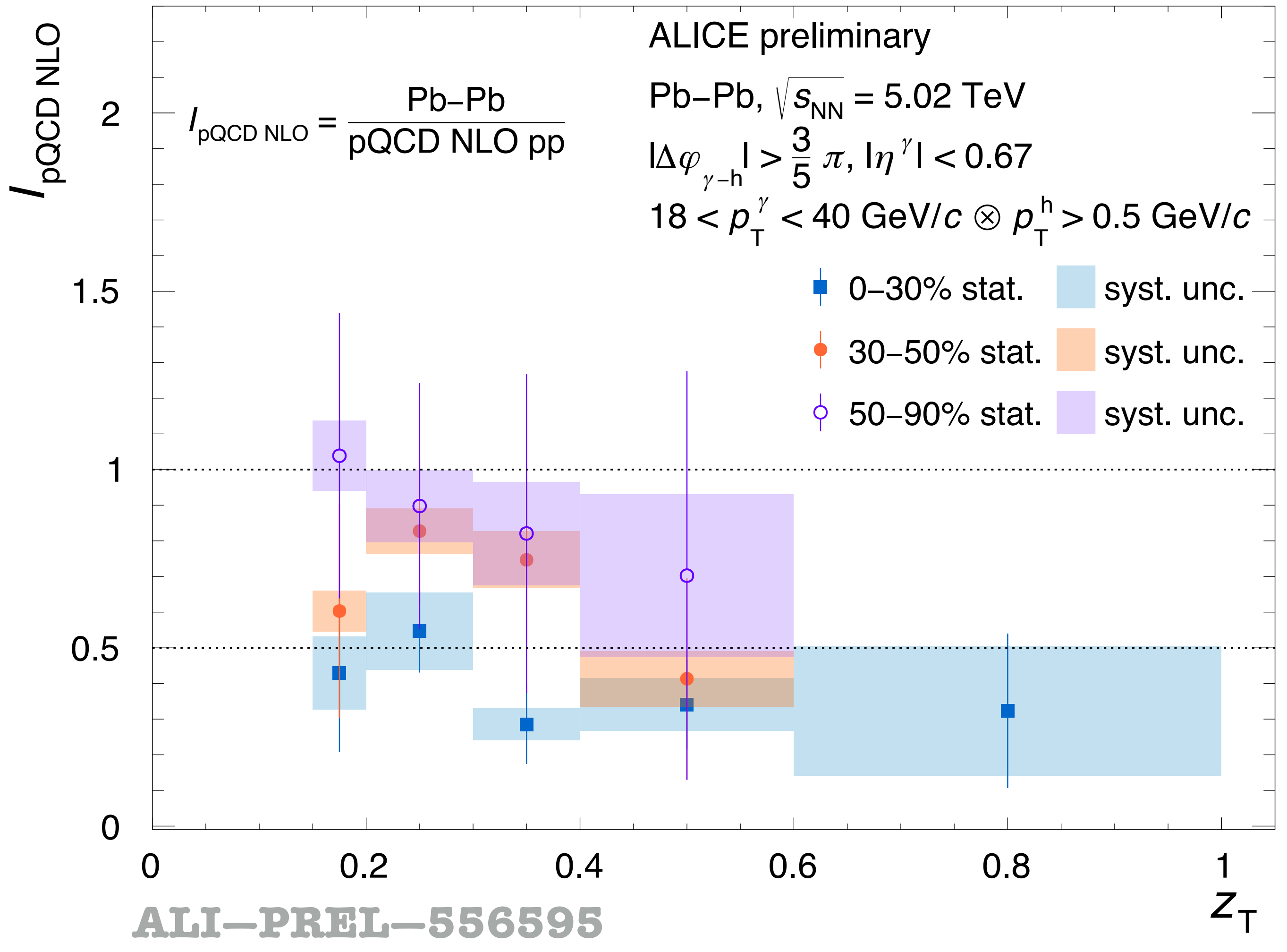

Expected improvement with Run 3 + Run 4 data samples, in particular γ-hadron correlations

BACK-UP

Pb–Pb 50-90%: cross section and ratios

ALICE-PUBLIC-2024-003

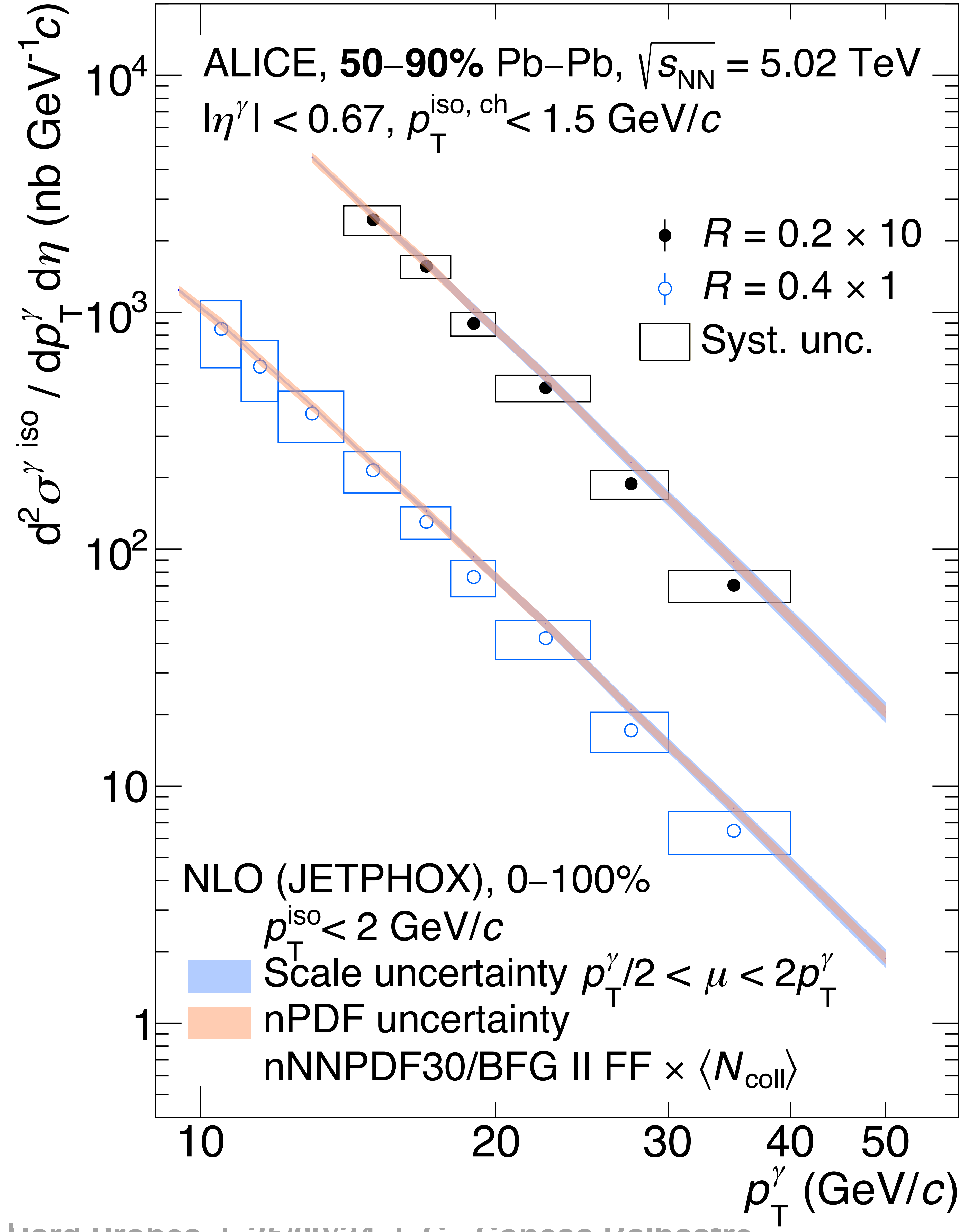

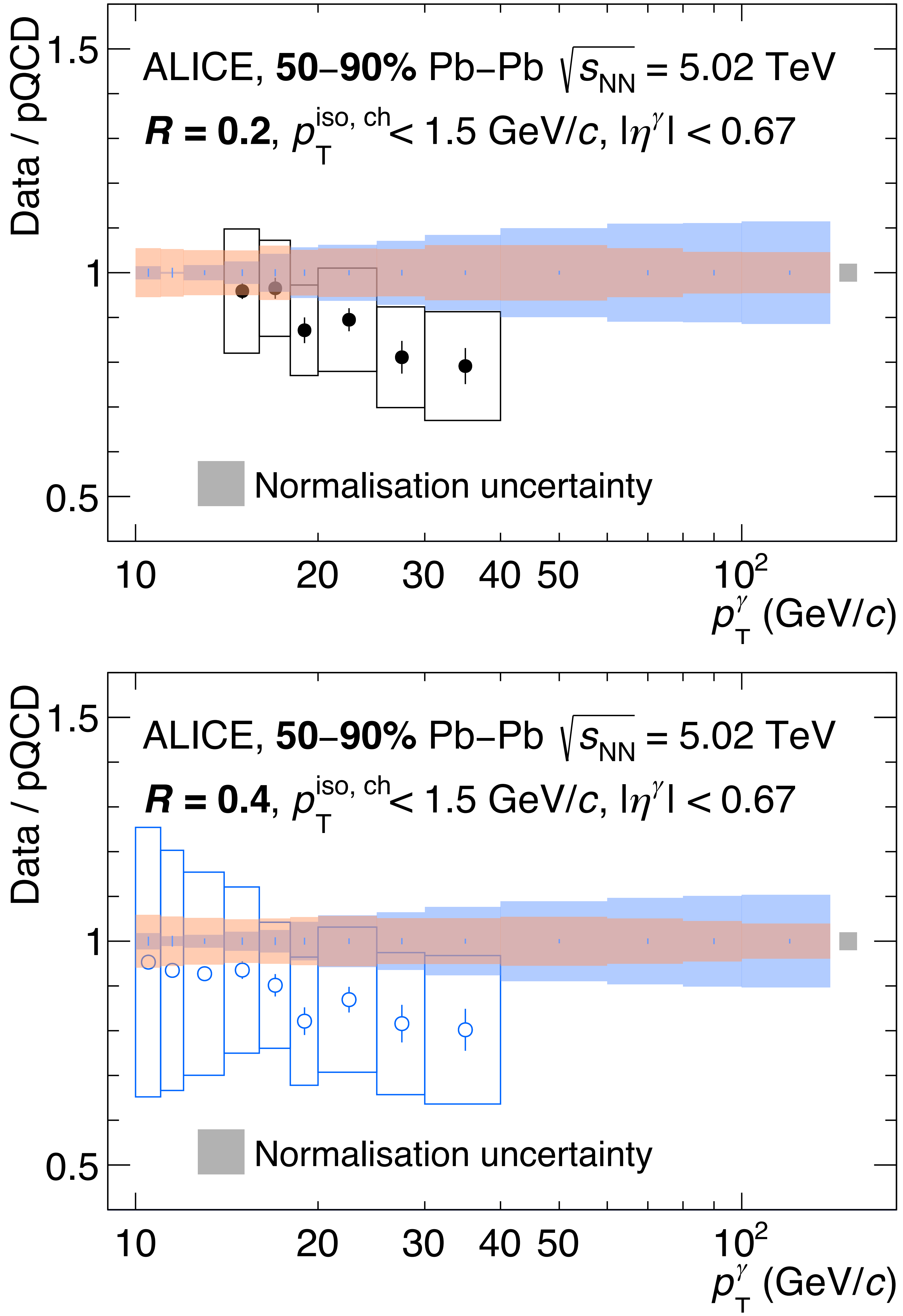

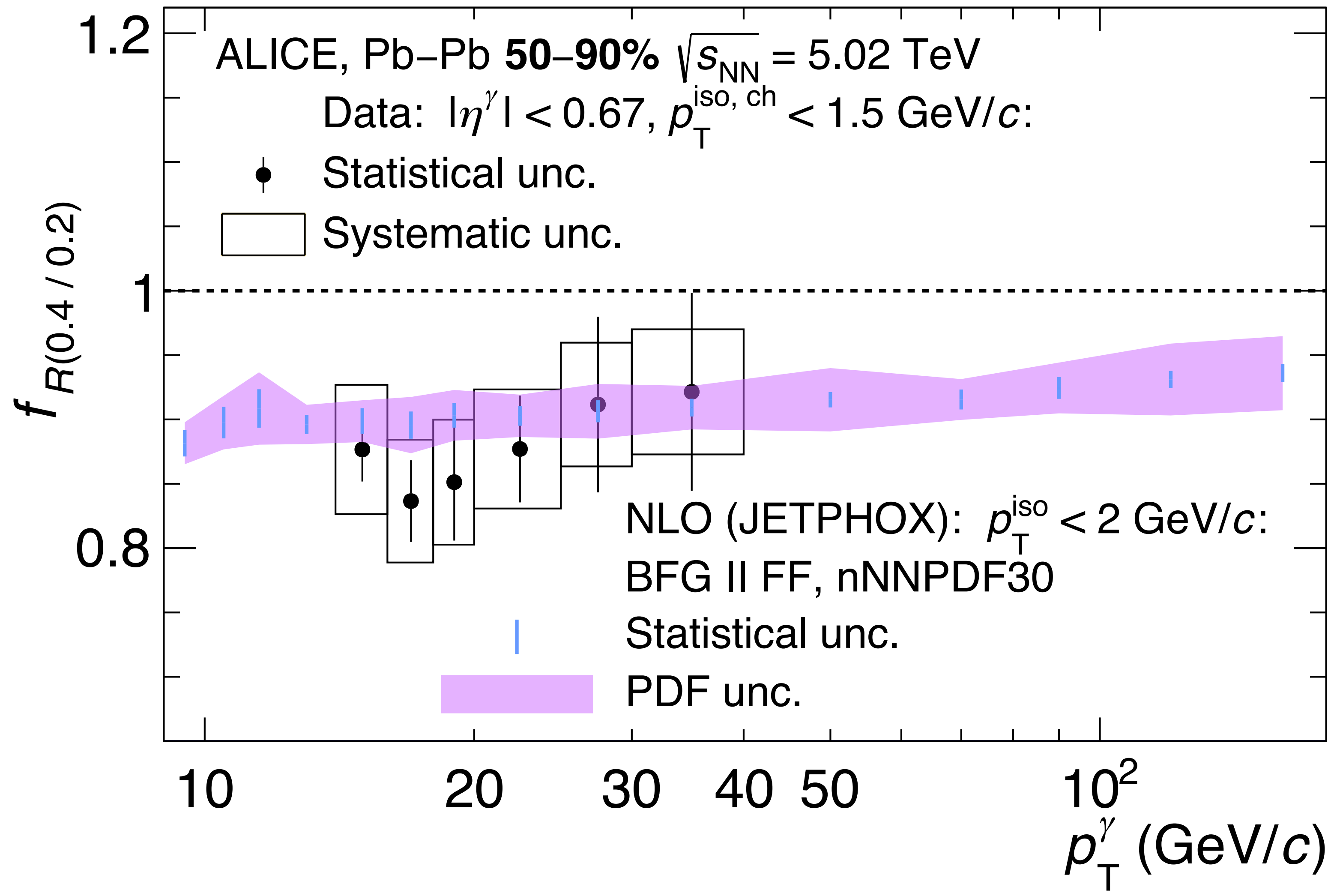

Nuclear modification factor R_{AA}, pp & Pb–Pb at $\sqrt{s_{NN}}$ = 5.02 TeV

New

ALICE

$$R_{AA} = \frac{1}{\langle N_{coll} \rangle} \frac{d^2\sigma_{AA} / (dp_T\, d\eta)}{d^2\sigma_{pp} / (dp_T\, d\eta)}$$

- **ALICE** & **CMS**: good agreement in the overlapping region 25 < p_T < 40–80 GeV/c

- 50-90%
  - ➡ Closer to 0.9 than 1 for both R likely due to centrality selection bias of Glauber model
  - ➡ Model by C. Loizides & A. Morsch (Phys. Lett. B773 (2017) 408-411) yields a value at 0.91
    - ✤ In agreement within the uncertainties

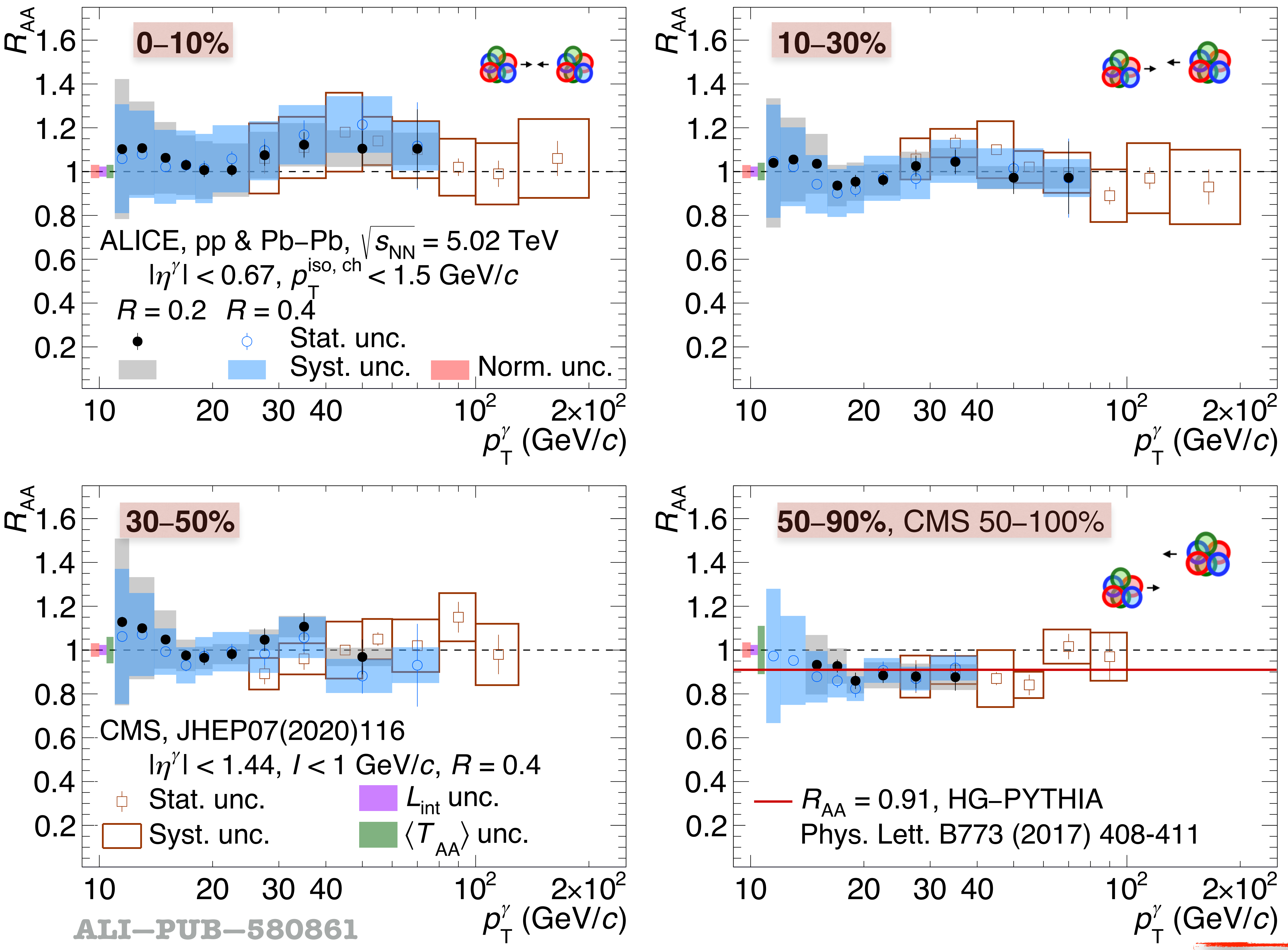

Data over theory, R = 0.4, pp & Pb–Pb at $\sqrt{s_{\mathrm{NN}}}$ = 5.02 TeV

ALICE

ALICE

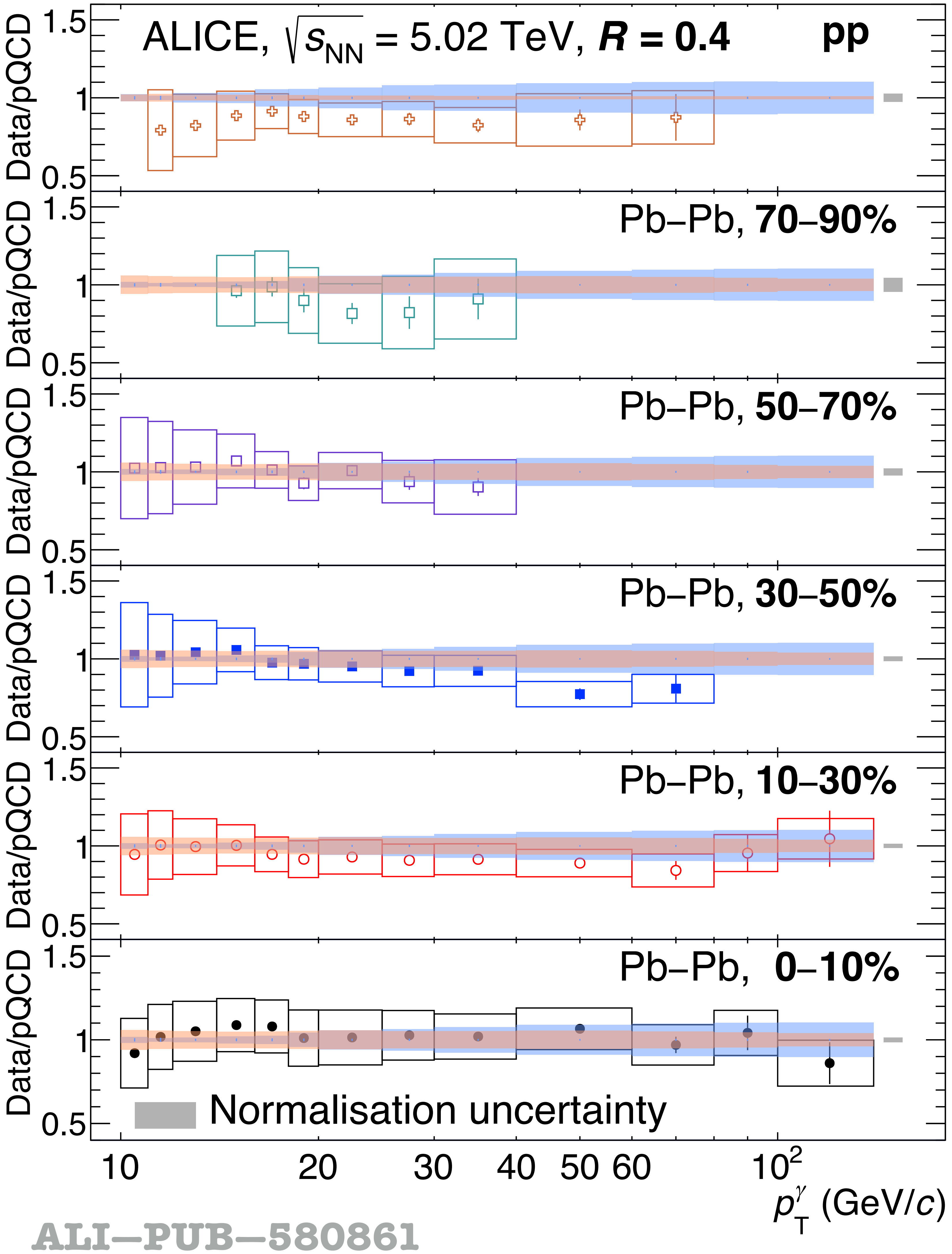

ALI–PUB–580861

CMS

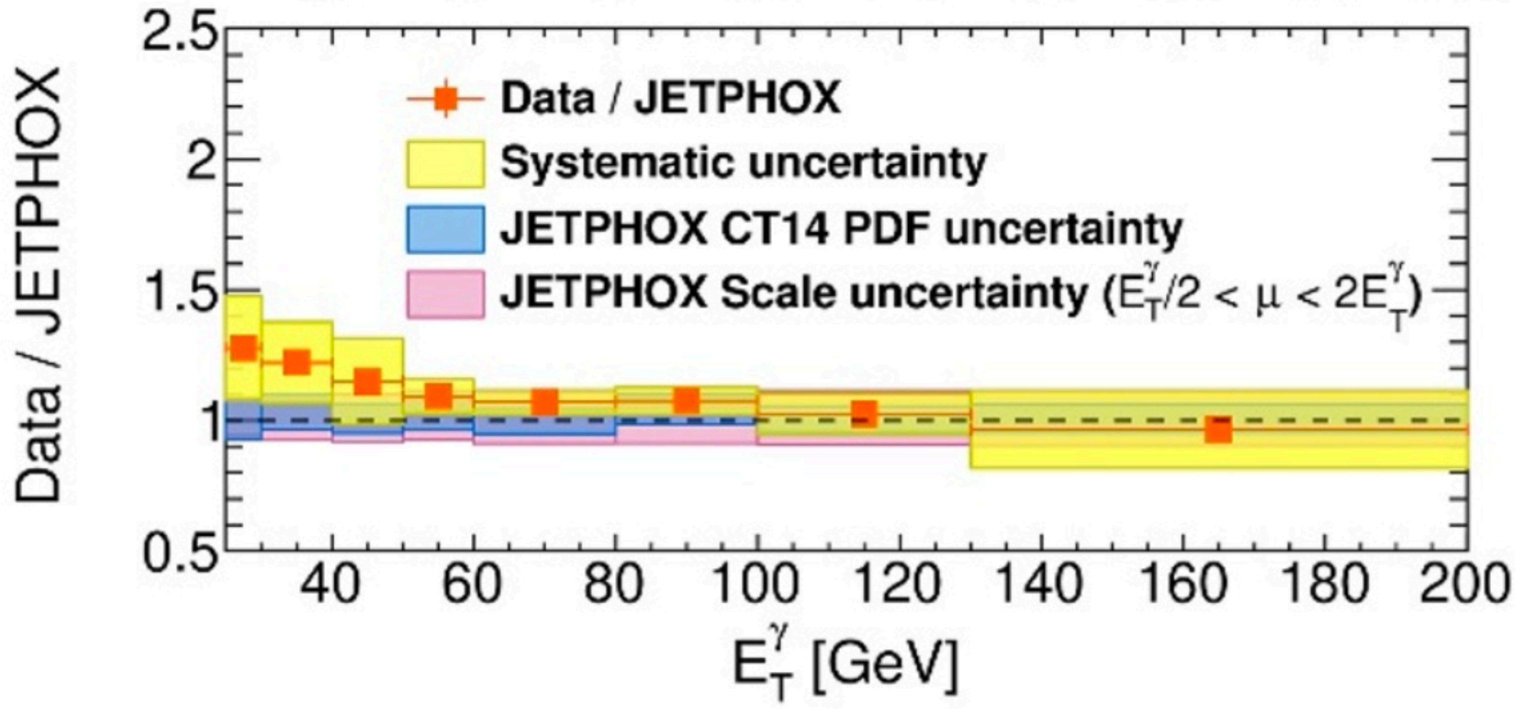

pp

CMS JHEP 07 (2020) 116
arXiv:2003.12797 [hep-ex]

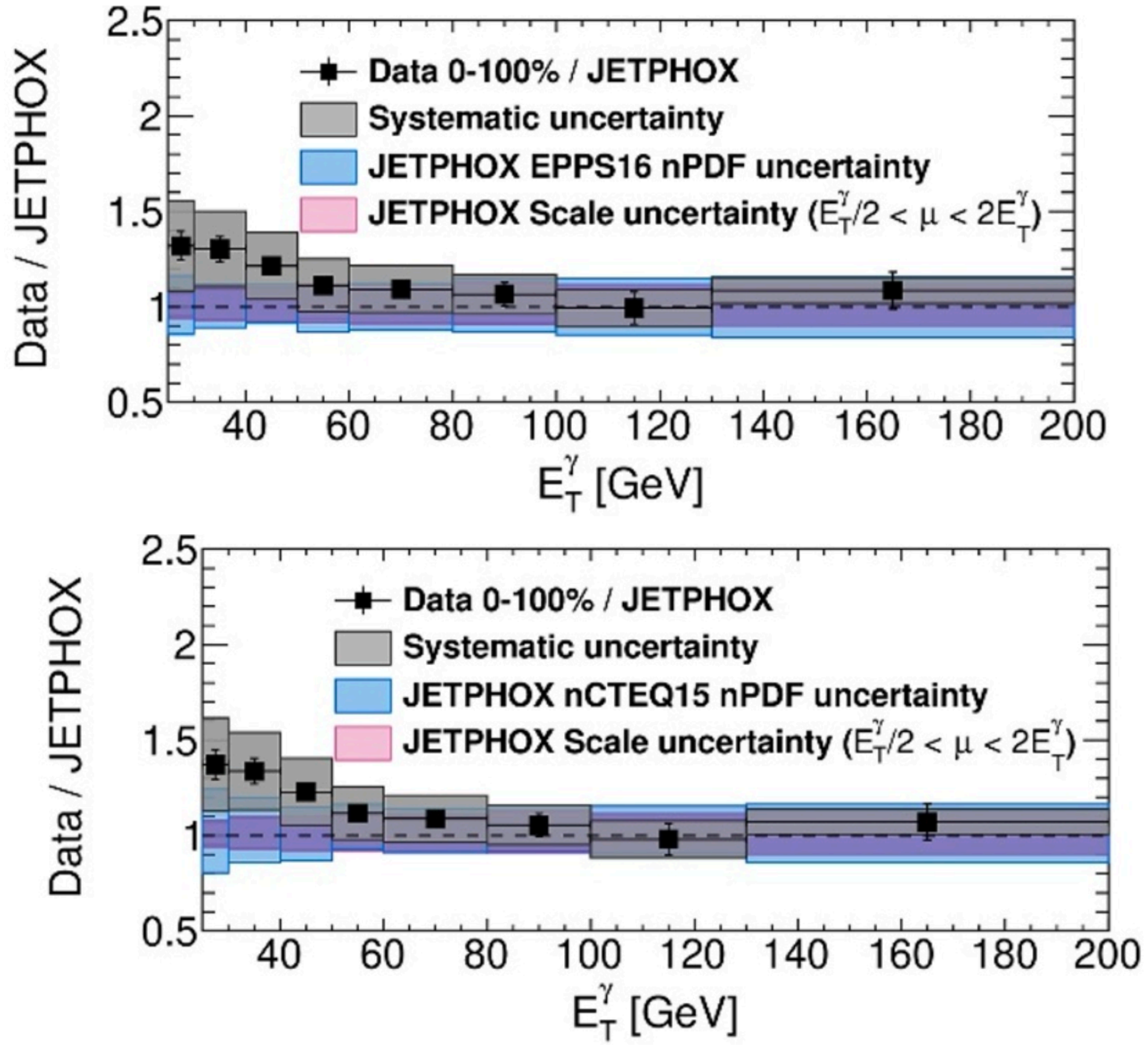

Pb–Pb 0–100%

Nuclear modification factor
pp data denominator replaced by pp NLO pQCD

ALICE-PUBLIC-2024-003

Pb–Pb cross section ratios

$$R_{CSP} = \frac{\langle N_{coll}\rangle^{50-70\%}}{\langle N_{coll}\rangle^{k}} \frac{d^2\sigma^{\gamma\,iso}_{Pb-Pb}/(dp_T\,d\eta)|_k}{d^2\sigma^{\gamma\,iso}_{Pb-Pb}/(dp_T\,d\eta)|_{50-70\%}}, \quad R_{CSC} = \frac{\langle N_{coll}\rangle^{30-50\%}}{\langle N_{coll}\rangle^{k}} \frac{d^2\sigma^{\gamma\,iso}_{Pb-Pb}/(dp_T\,d\eta)|_k}{d^2\sigma^{\gamma\,iso}_{Pb-Pb}/(dp_T\,d\eta)|_{30-50\%}}$$

New

ALICE

ALICE-PUBLIC-2024-003

Nuclear modification factor R_{AA}, pp & Pb–Pb at $\sqrt{s_{NN}}$ = 5.02 TeV

ALICE-PUBLIC-2024-003

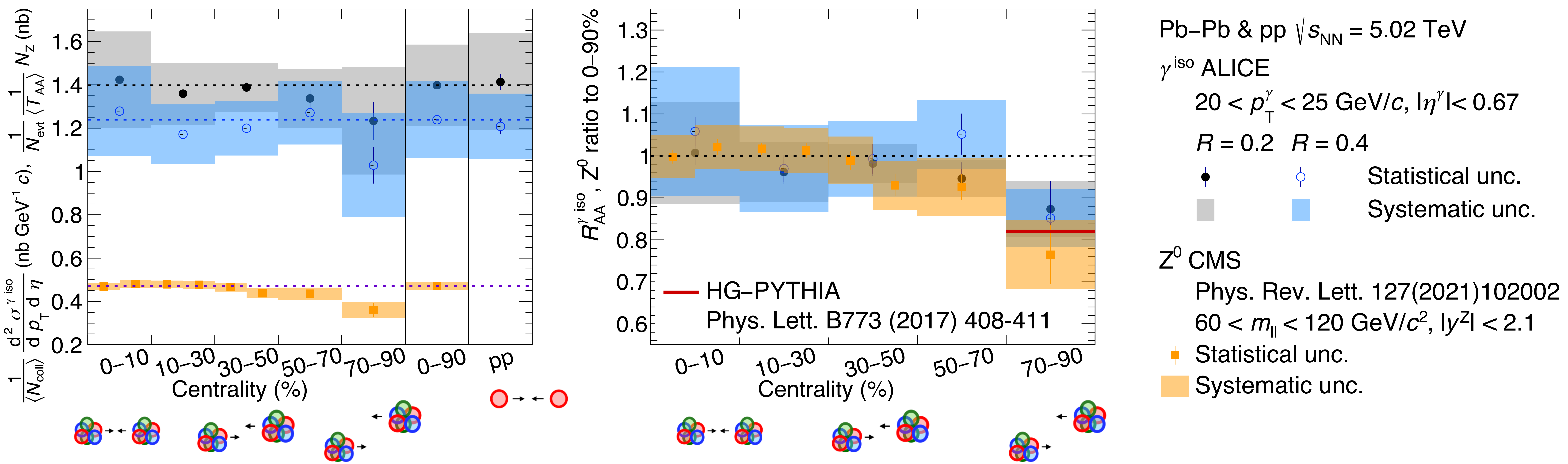

Cross section, p–Pb

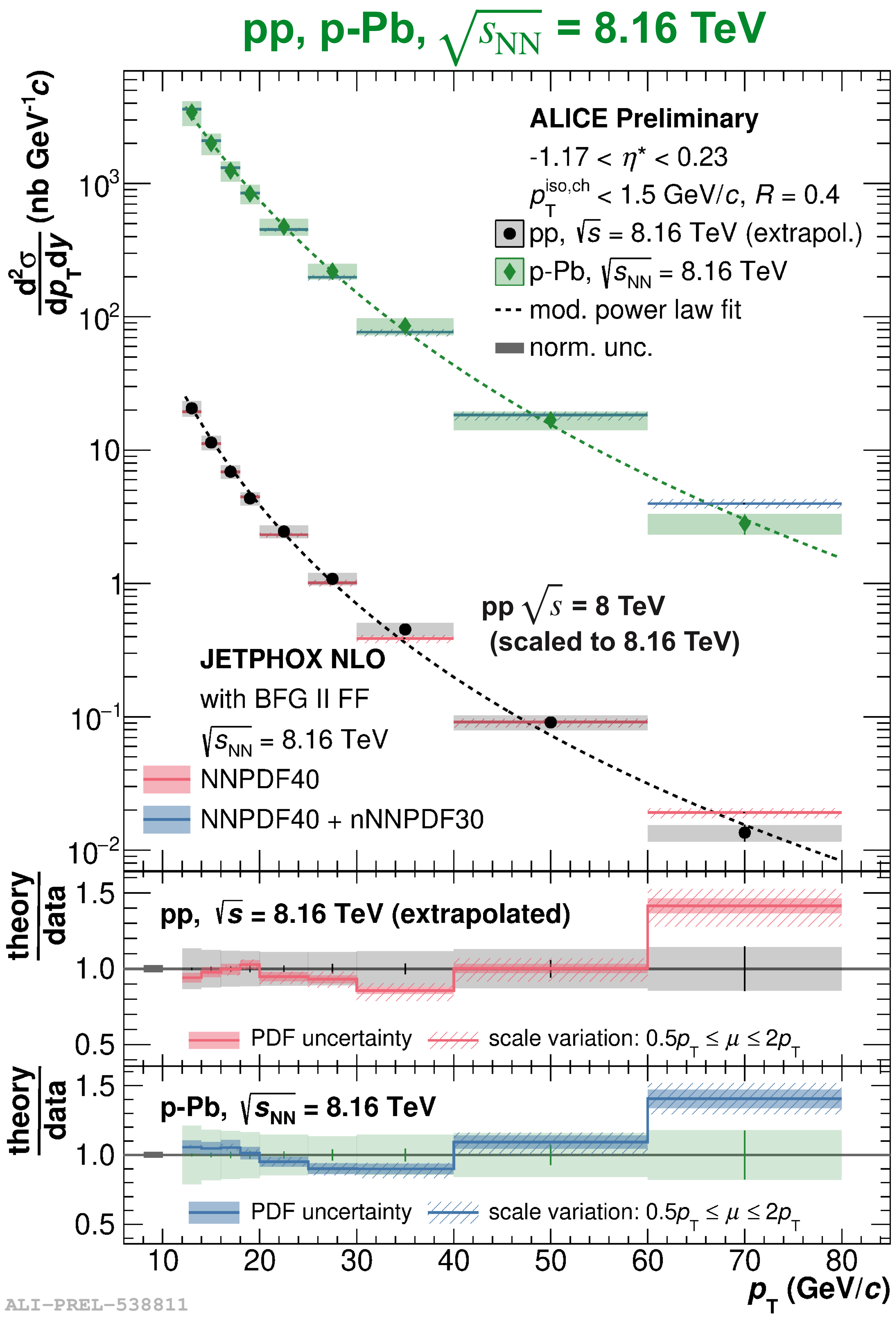

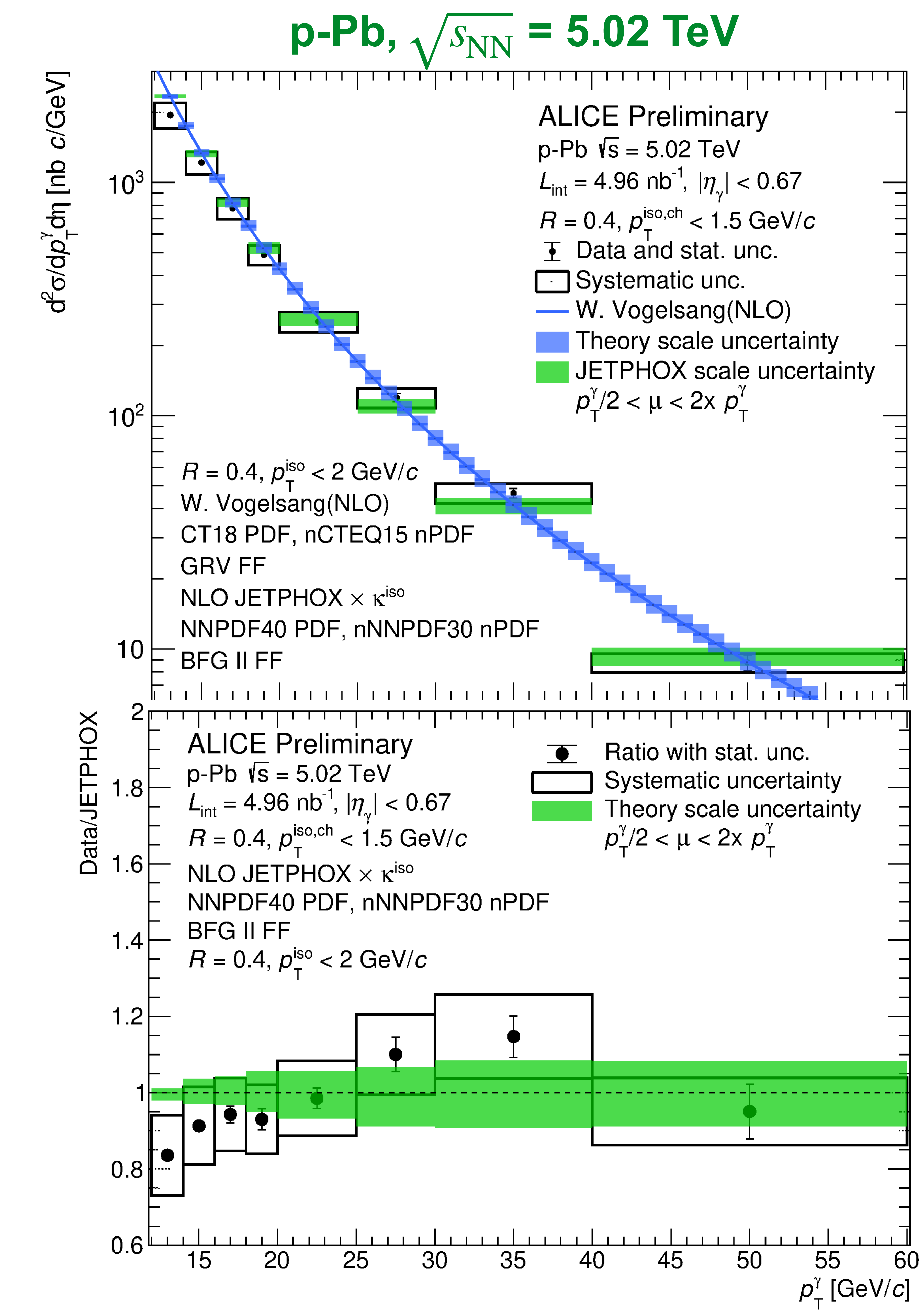

Cross section, pp $\sqrt{s}$ = 7 TeV

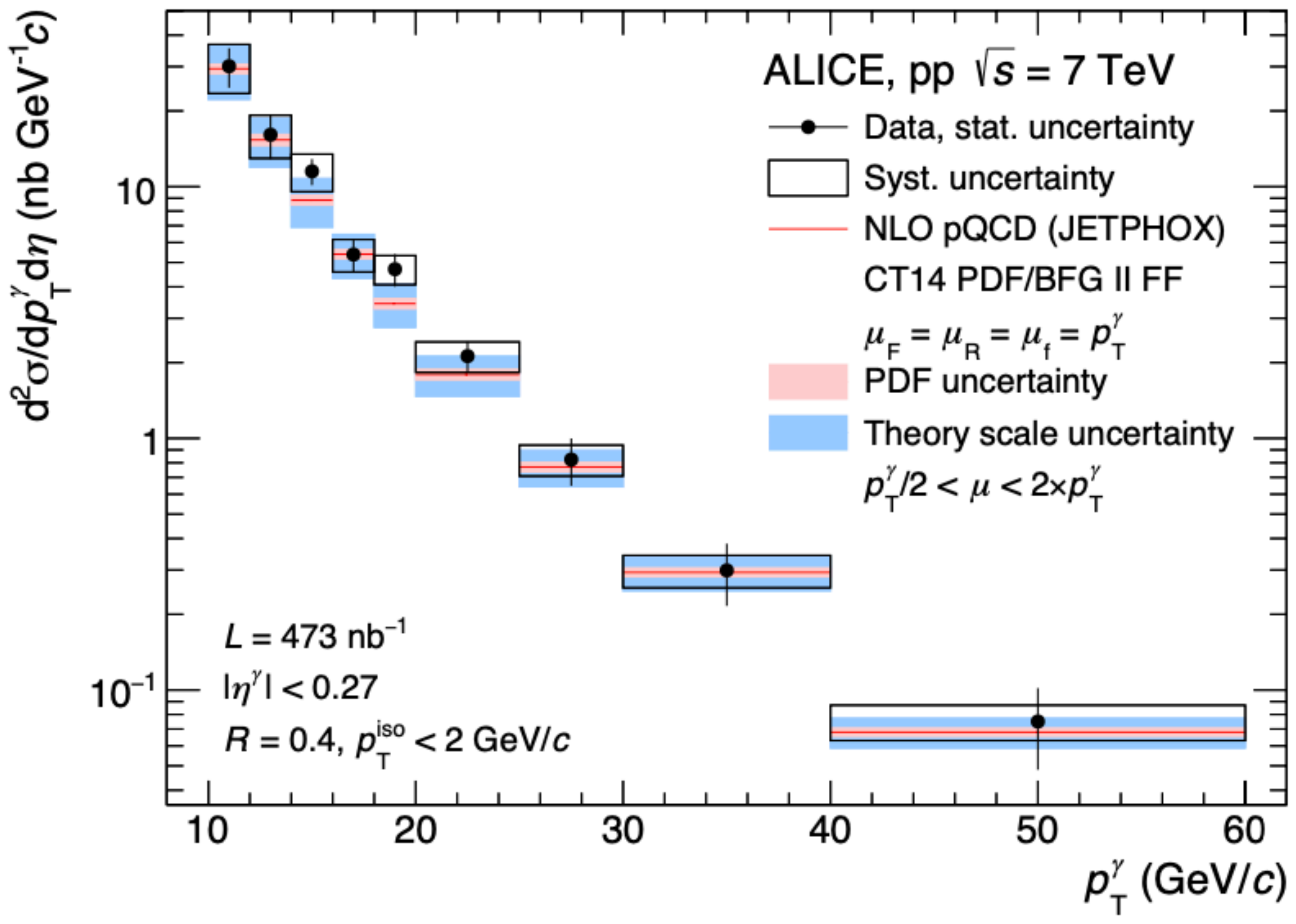

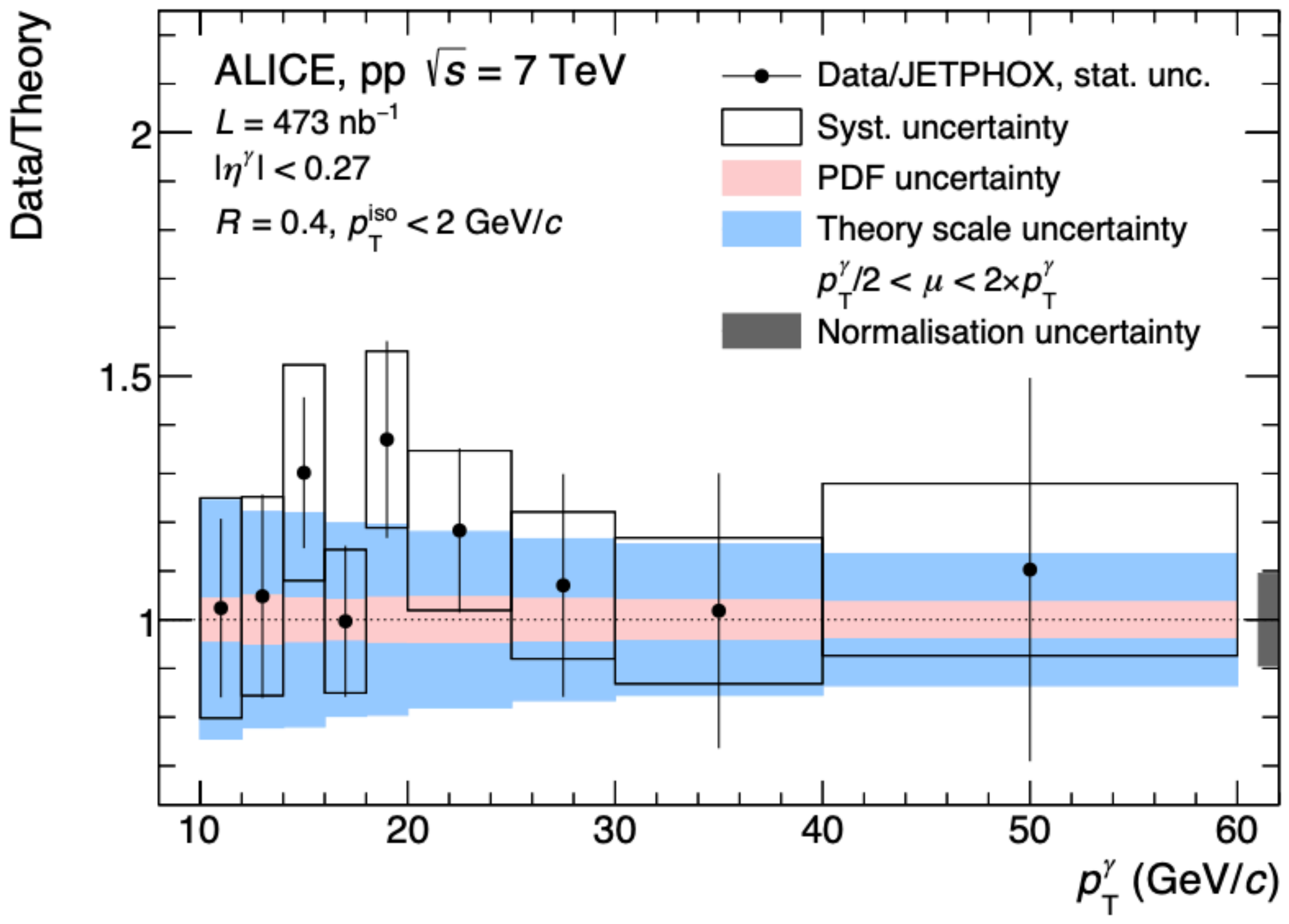

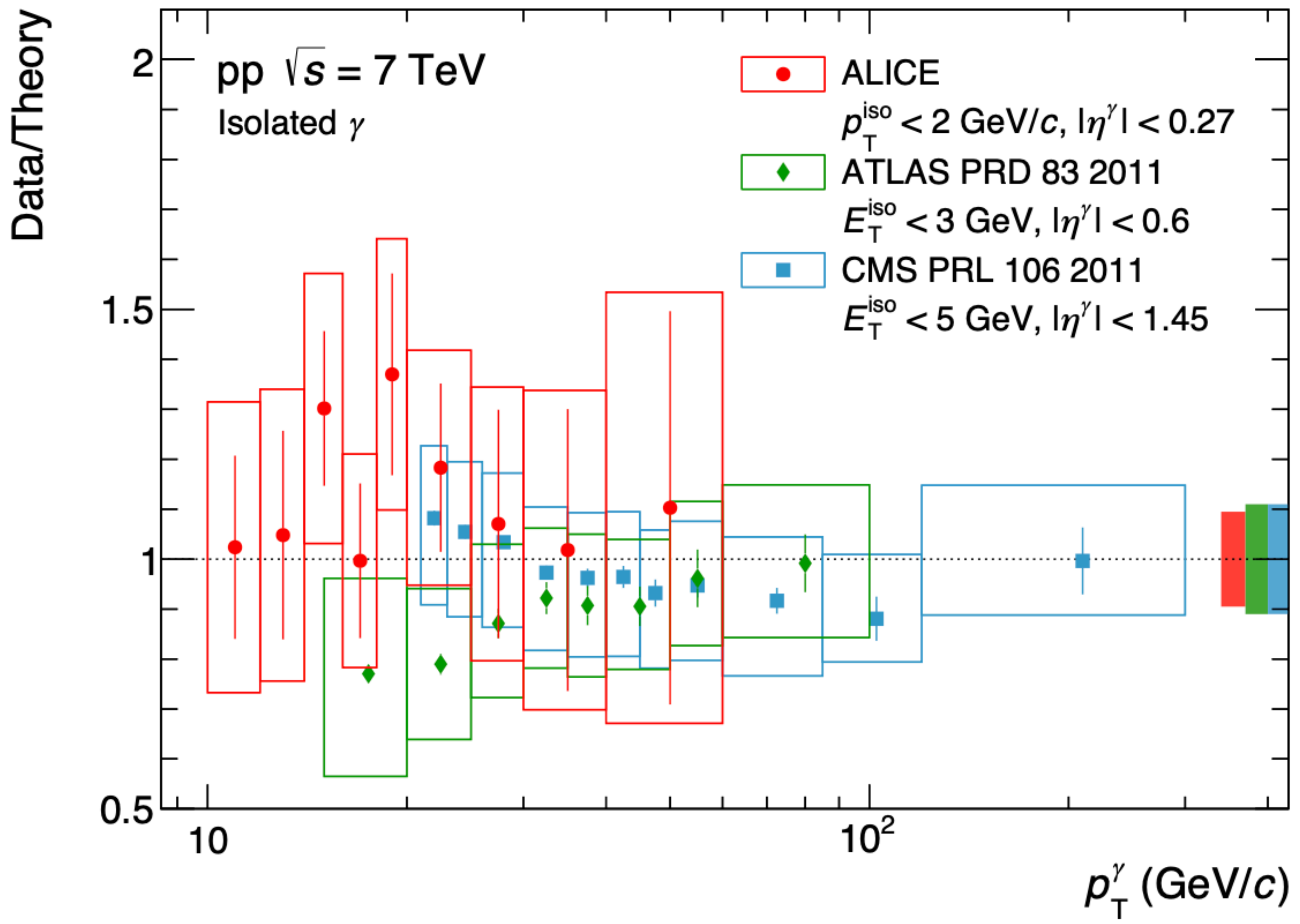

- arXiv:1906.01371
- Eur. Phys. J. C 79, 896 (2019)

Cross section ratios in pp collisions

New

ALICE

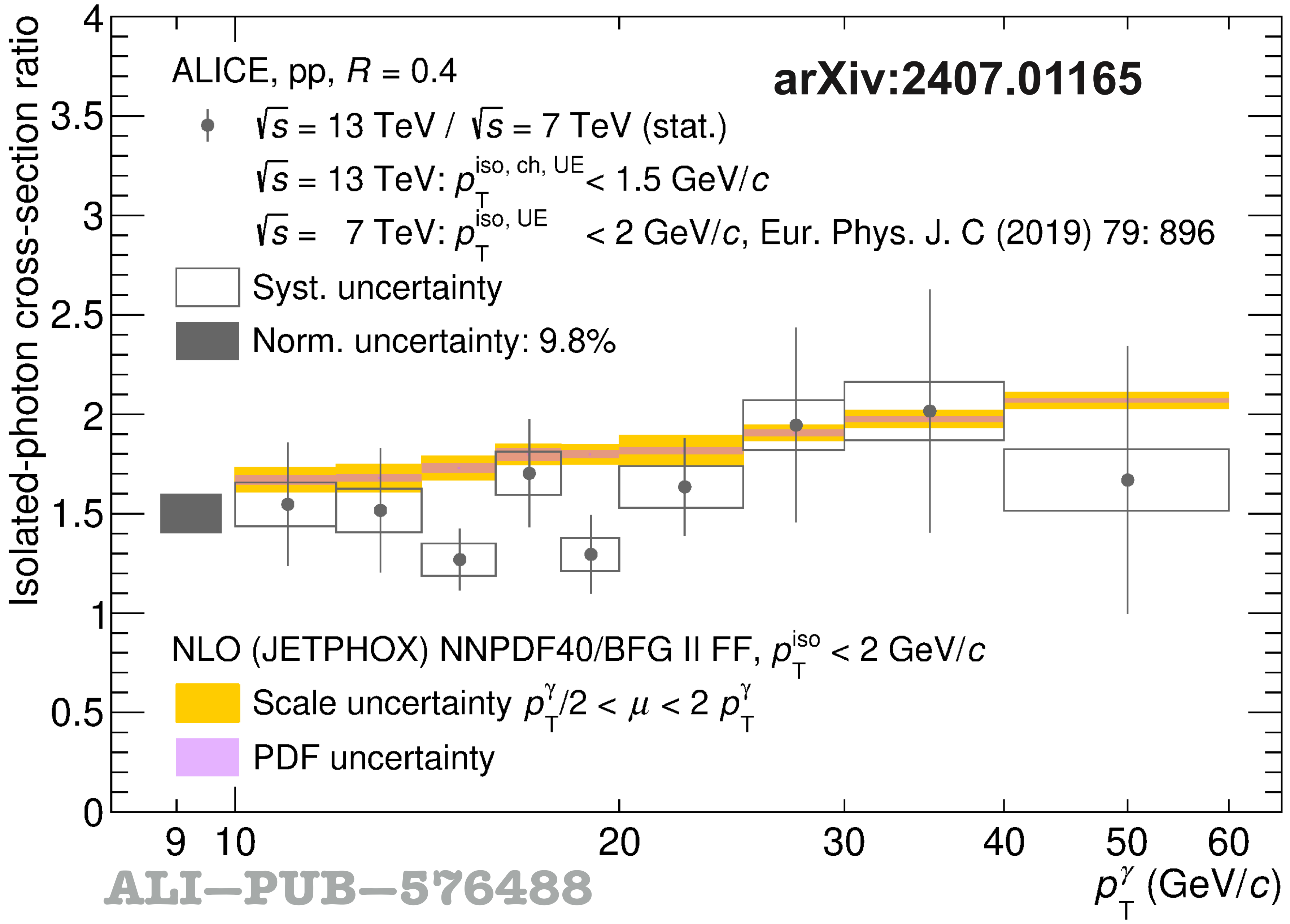

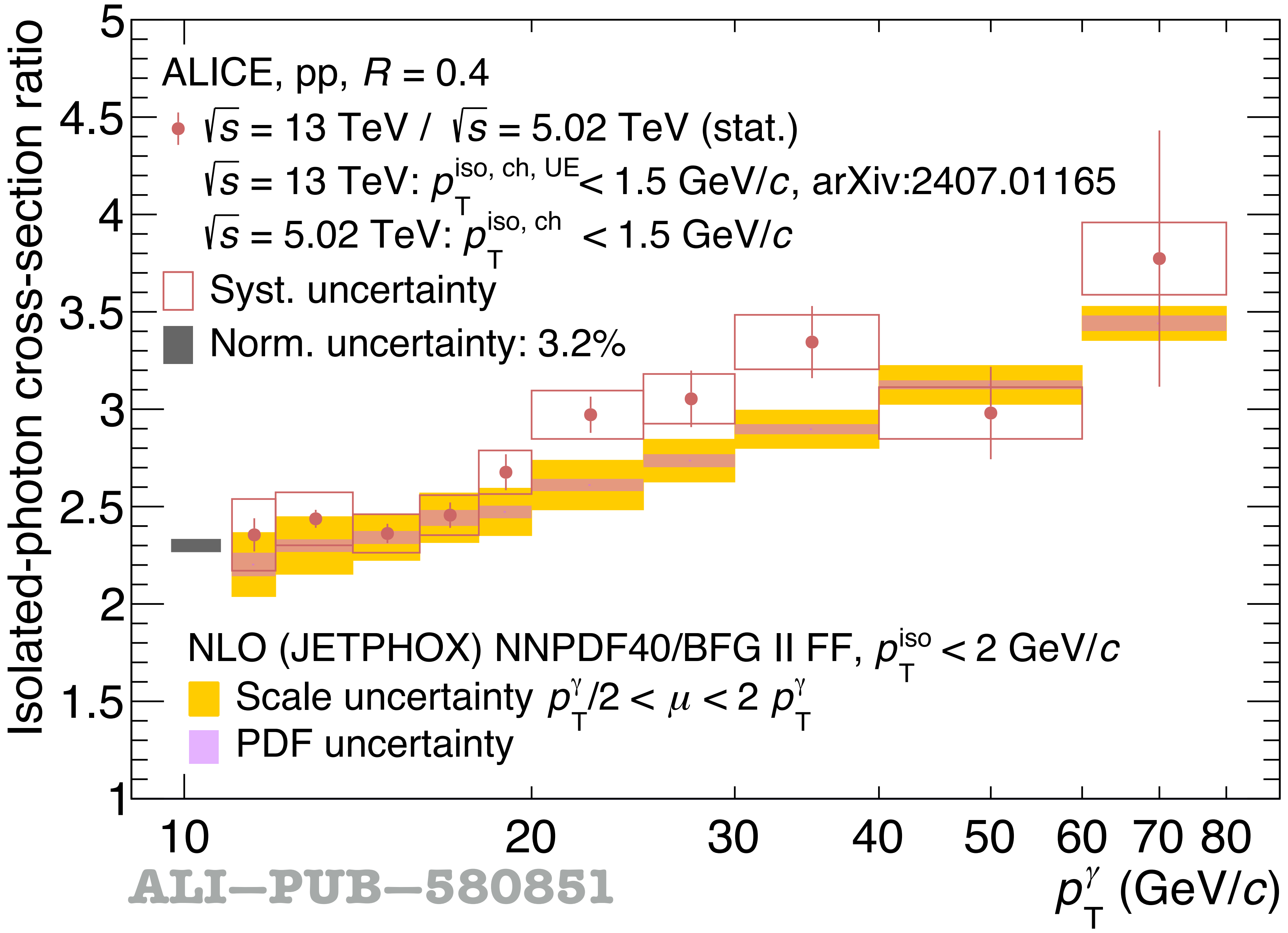

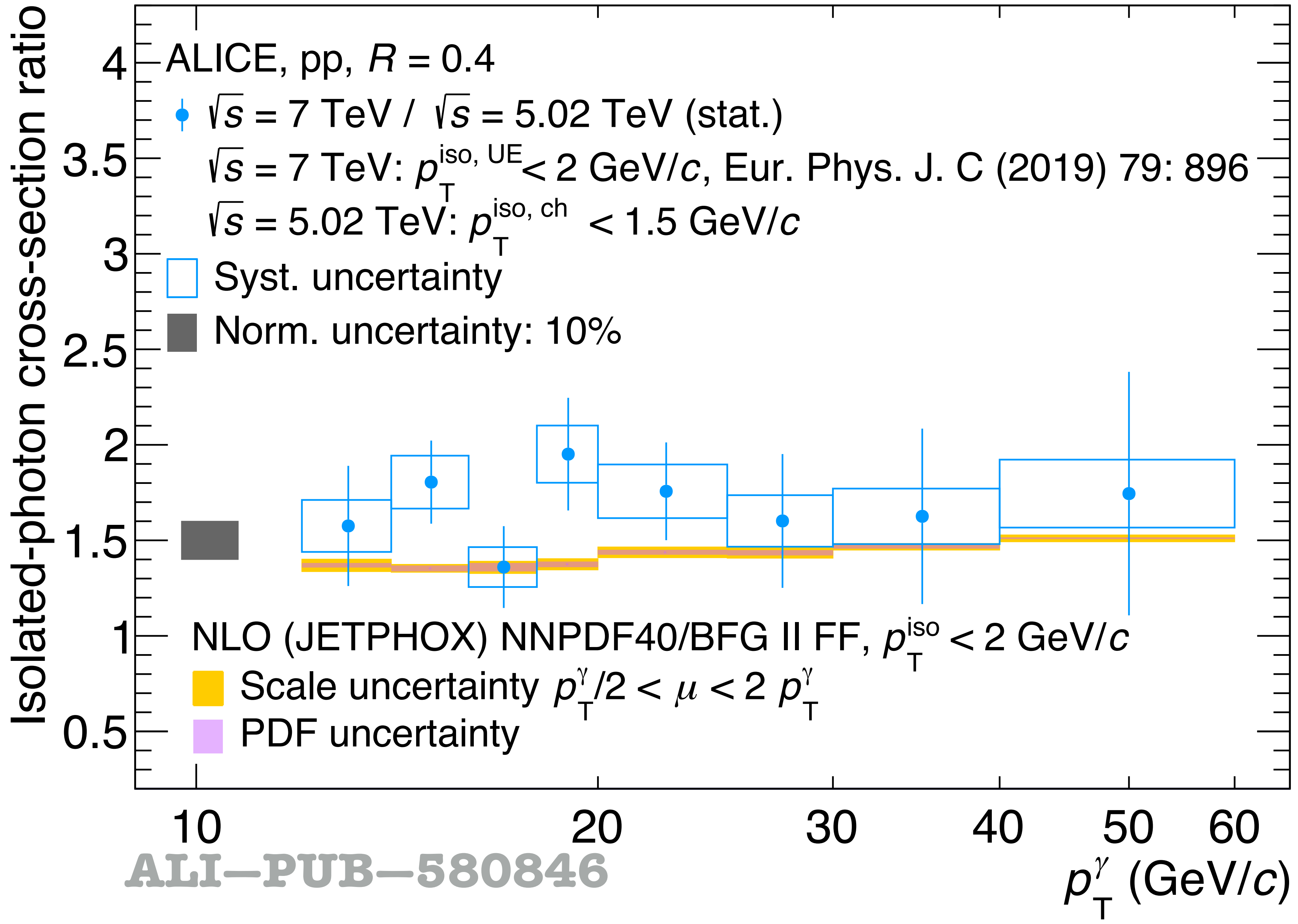

Nuclear modification factor R_{pA}

$$R_{pA} = \frac{d^2\sigma^{\gamma}_{pA}/dp_T\,dy^*}{A_{Pb} \times d^2\sigma^{\gamma}_{pp}/dp_T\,dy^*}$$

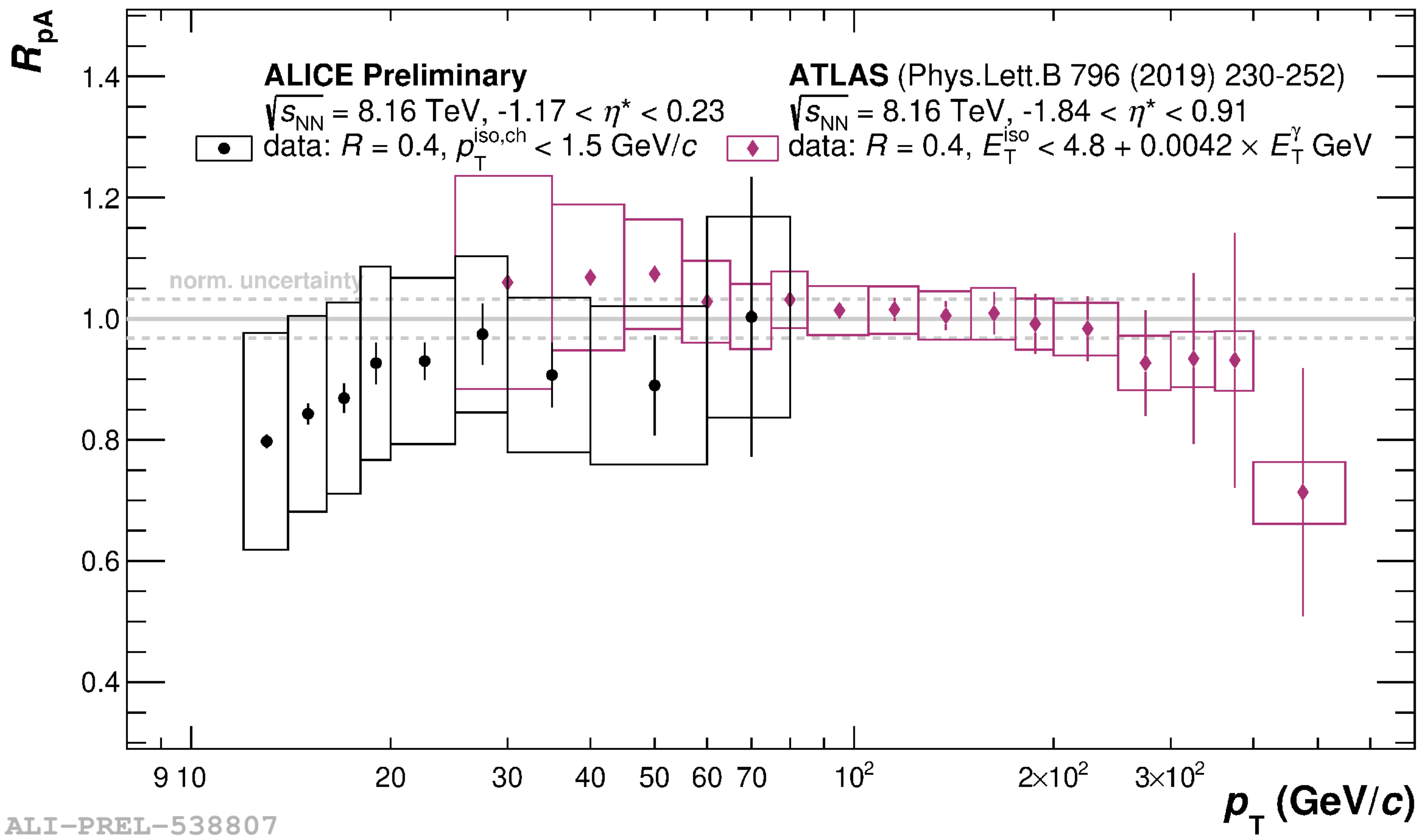

- $R_{p\text{-}Pb}$ in agreement with unity
  - Hints of lower than unity for $p_T < 20$ GeV/c, expected in theory, cold nuclear matter effects, shadowing
  - No suppression at high p_T, agreement with ATLAS

γ measurement in ALICE

- γ measurement
  - ➡ Calorimeters
    - EMCal: Pb/scintillator towers (6 × 6 cm)
      - 4.4 m from interaction point (IP)
      - $|\eta| < 0.67$ for $\Delta\varphi = 107^{\circ}$, $0.22 < |\eta| < 0.67$ for $\Delta\varphi = 60^{\circ}$ (DCal);
      - Identification via EM shower dispersion selection
      - E_{γ} > 700 MeV
    - PHOS: PWO_4 crystals (2.2 × 2.2 cm)
      - 4.6 m from IP
      - $|\eta| < 0.13$ for $\Delta\varphi = 70^{\circ}$
      - Identification via EM shower dispersion selection
      - E_{γ} > 200 MeV
  - ➡ Tracking, TPC & ITS
    - γ conversion method (PCM)
      - R < 180 cm
      - 8% conversion probability
      - $|\eta| < 0.9$ for $\Delta\varphi = 360^{\circ}$
      - E_{γ} > 100 MeV

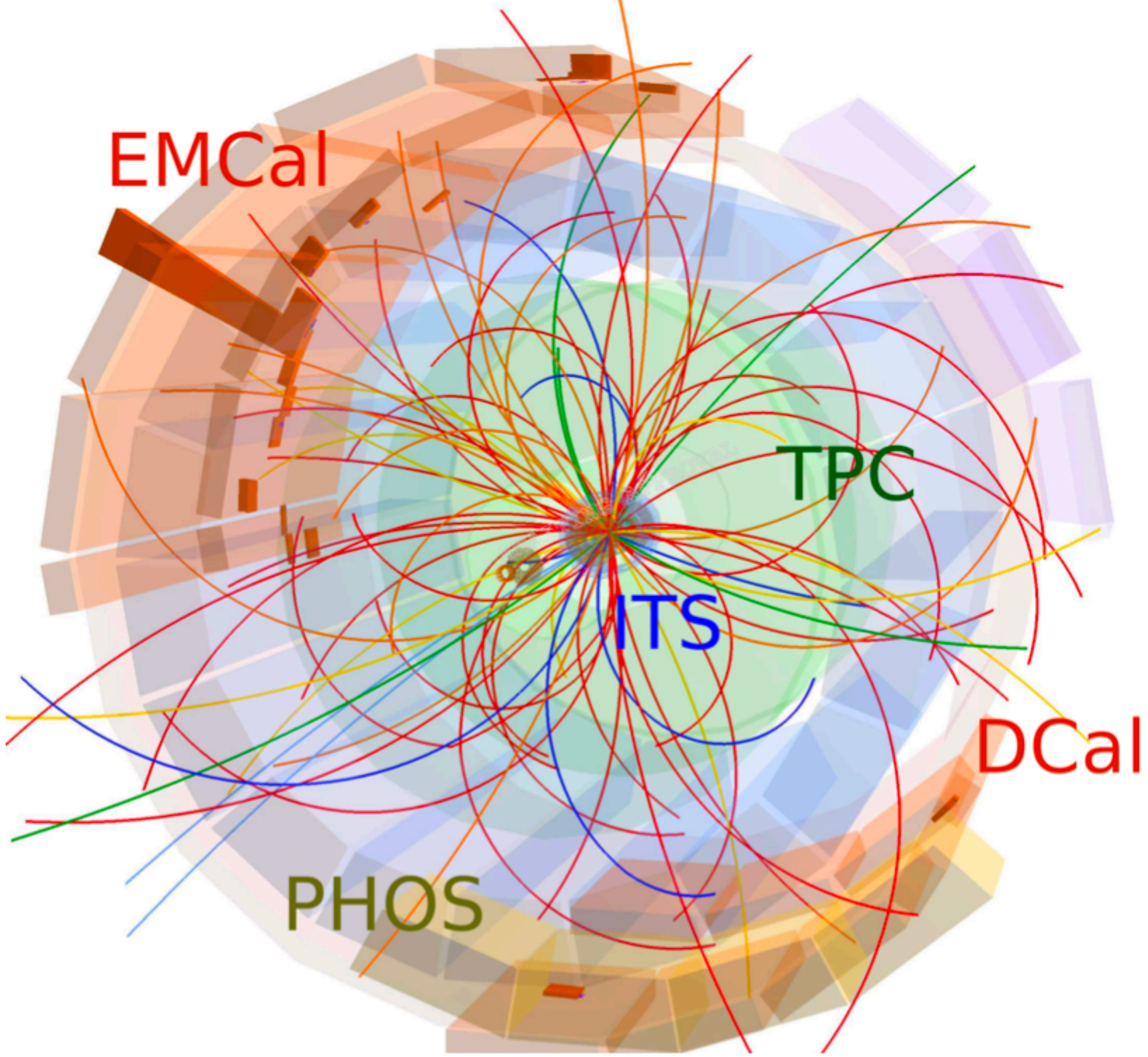

- γ identification combining tracking+calorimeter
  - ➡ Inclusive γ: Charged particle veto
  - ➡ Prompt γ: Isolation (next slides)

EMCal trigger performance, pp $\sqrt{s}$ = 13 TeV

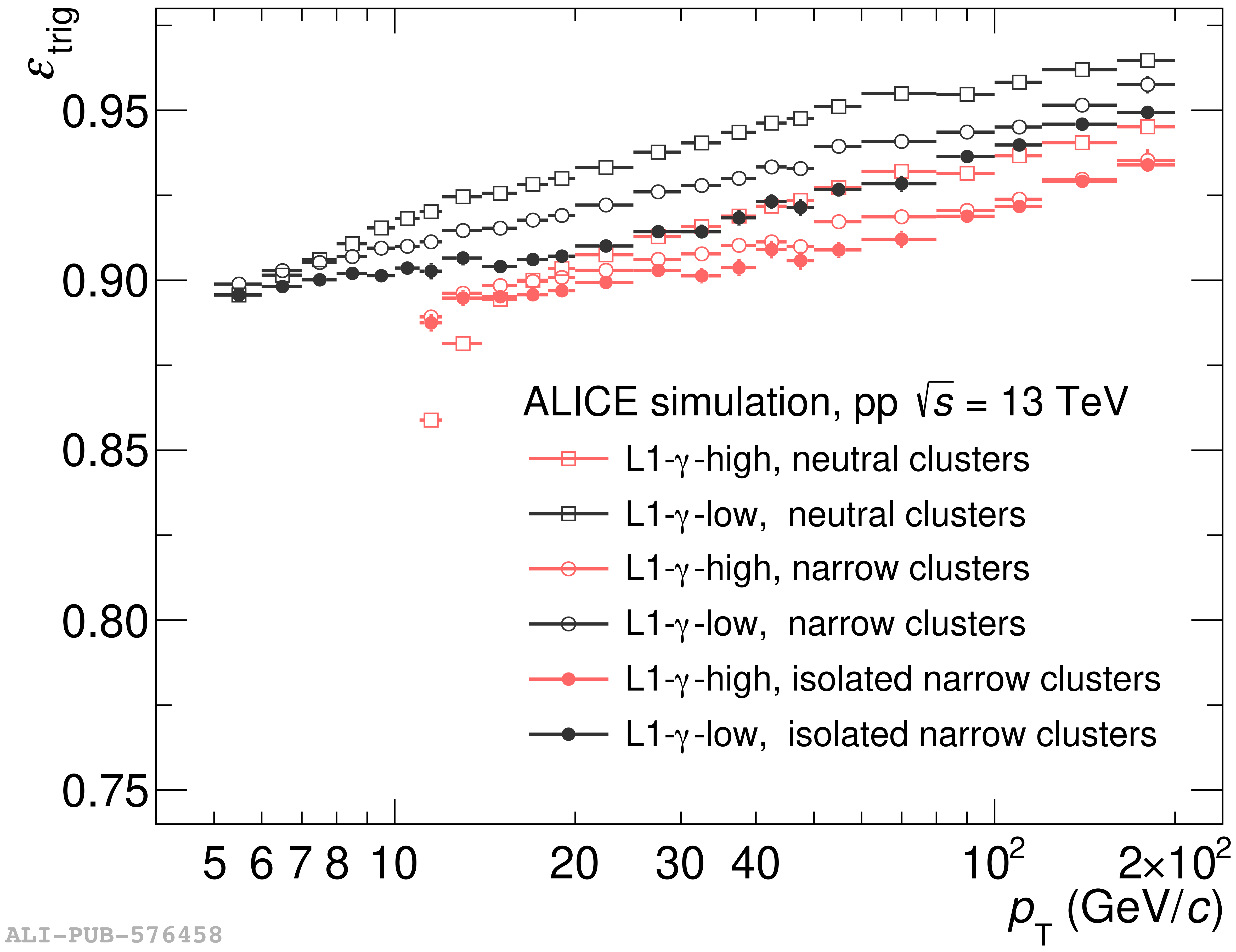

ALI-PUB-576458

$$RF^{trig}_{\varepsilon_{trig}} = \frac{1}{\varepsilon^{clus}_{trig}} \frac{1/N^{L1\text{-}\gamma}_{evt} \times dN^{L1\text{-}\gamma}/dp_T}{1/N^{MB}_{evt} \times dN^{MB}/dp_T}$$

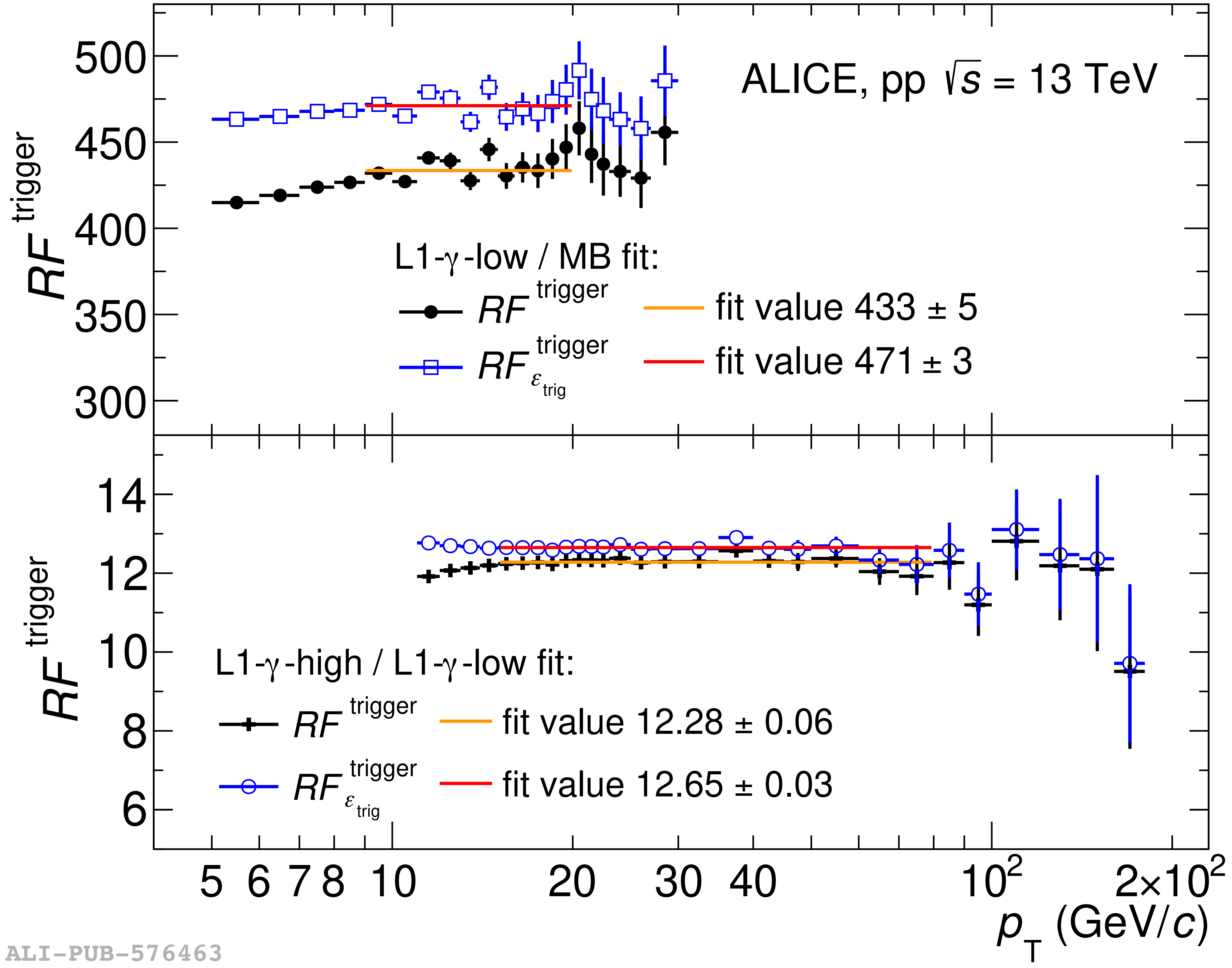

ALI-PUB-576463

EMCal trigger performance, pp & Pb–Pb $\sqrt{s_{NN}}$ = 5.02 TeV

New

ALICE

$$RF^{\rm trig}_{\varepsilon_{\rm trig}} = \frac{1}{\varepsilon^{\rm clus}_{\rm trig}} \frac{1/N^{\rm L1\text{-}\gamma}_{\rm evt} \times {\rm d}N^{\rm L1\text{-}\gamma}/{\rm d}p_T}{1/N^{\rm MB}_{\rm evt} \times {\rm d}N^{\rm MB}/{\rm d}p_T}$$

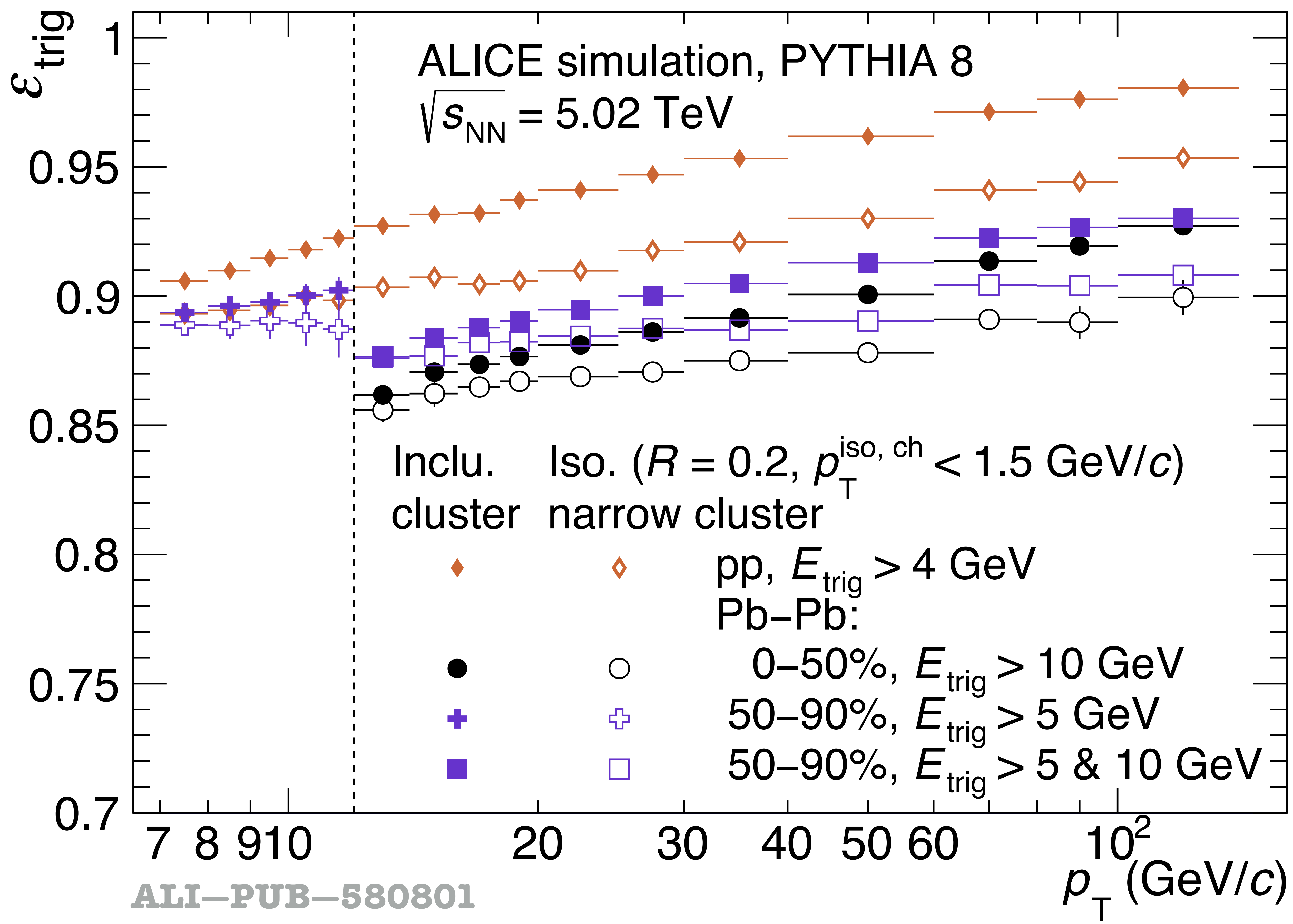

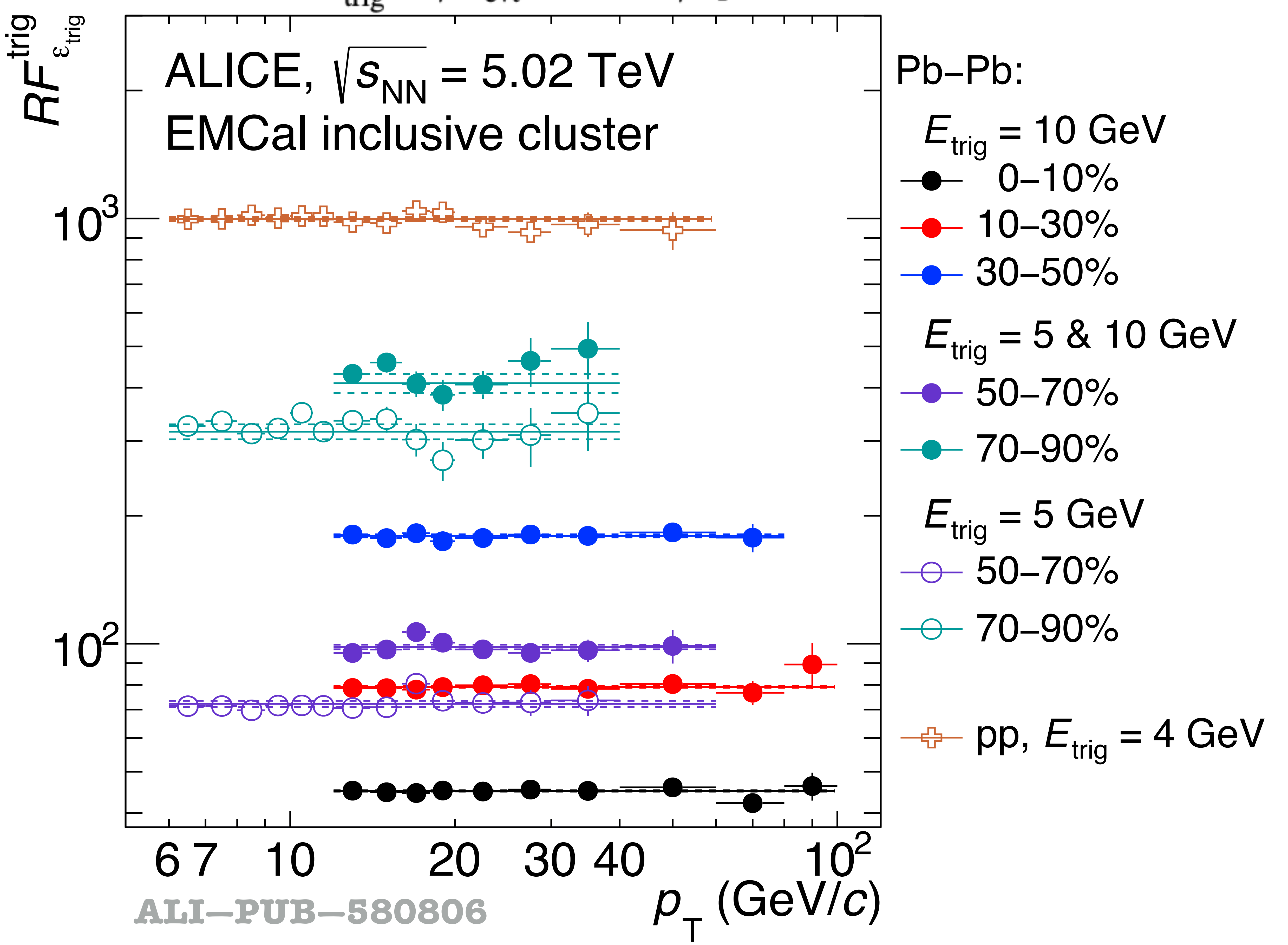

Prompt γ identification in ALICE: EM shower spread shape & isolation with tracks

Prompt γ at LO 2→2: *isolated*

- ➡ TPC+ITS charged tracks
  - ✱ ITS only for pp col. at $\sqrt{s}$ = 5.02 TeV
- ➡ Select γ with low hadronic activity in R, small $p_{\rm T}^{\rm iso,\,ch}$

$$\sqrt{(\eta_{\rm track}-\eta_{\gamma})^2+(\varphi_{\rm track}-\varphi_{\gamma})^2} < R = 0.4\ (0.2)$$

$$p_{\rm T}^{\rm iso,\,ch} = \sum p_{\rm T}^{\rm tracks\ in\ cone} - \rho_{\rm UE}\cdot\pi\cdot R^2 < 1.5\ {\rm GeV}/c$$

- ✱ Underlying event (UE) subtracted event-by-event, $\rho_{\rm UE}$ density estimation (back-up slide)

EM shower discrimination

- ➡ EMCal
- ➡ Shower elongation $\sigma^2_{\rm long}$
  - ✱ pp & Pb–Pb collisions at $\sqrt{s}$ = 5.02 TeV: Calculated in 5 × 5 cells around the highest energy cell → $\sigma^2_{\rm long,\,5\times5}$

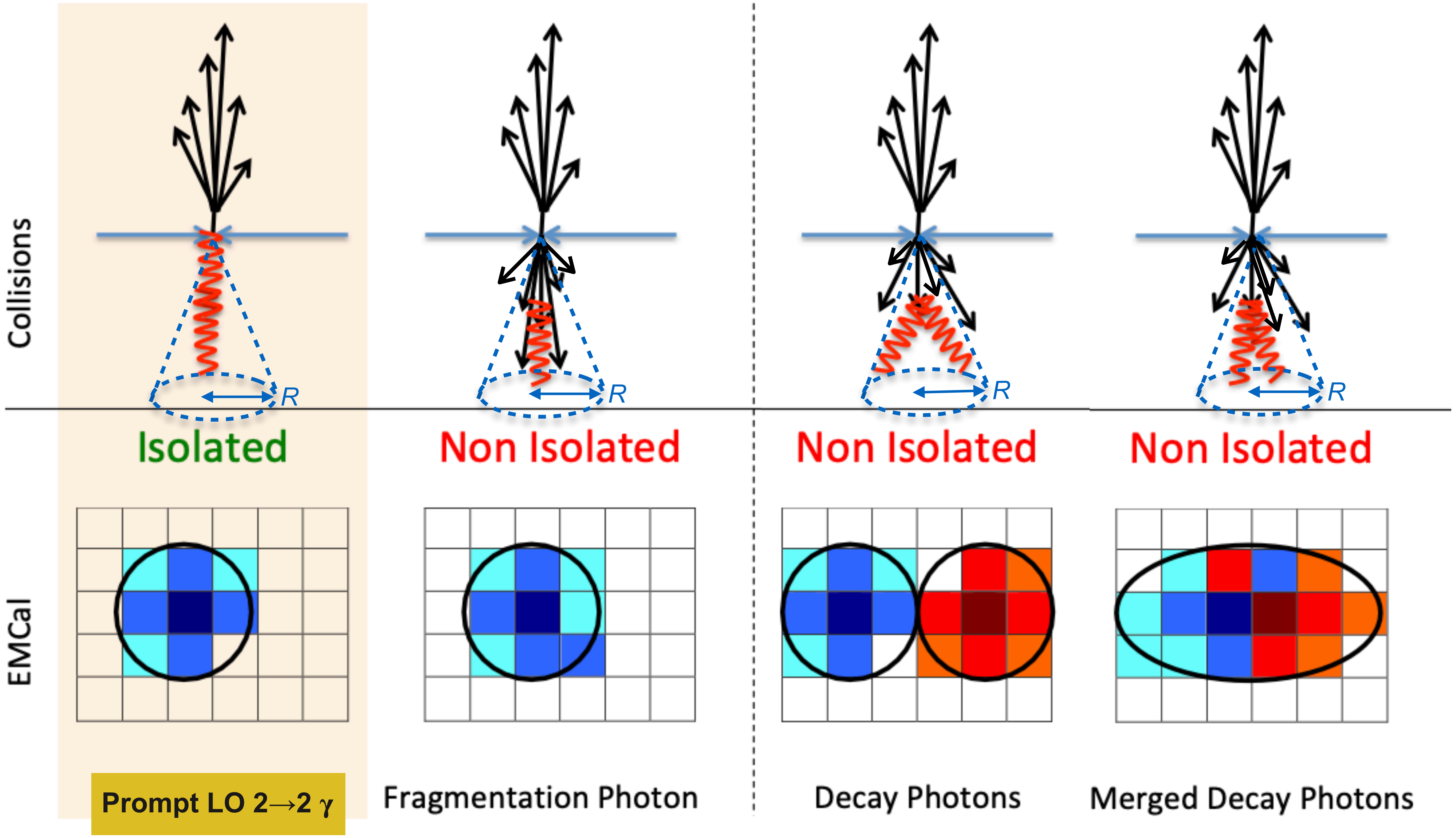

- ➡ **circular "narrow" cluster**
- ➡ circular narrow clusters, potentially wider due to jet particles nearby merging
- ➡ decay γ merge, E_{π^0} > 6 GeV **elliptical "wide" cluster**

EMCal cluster shower lateral dispersion parameter

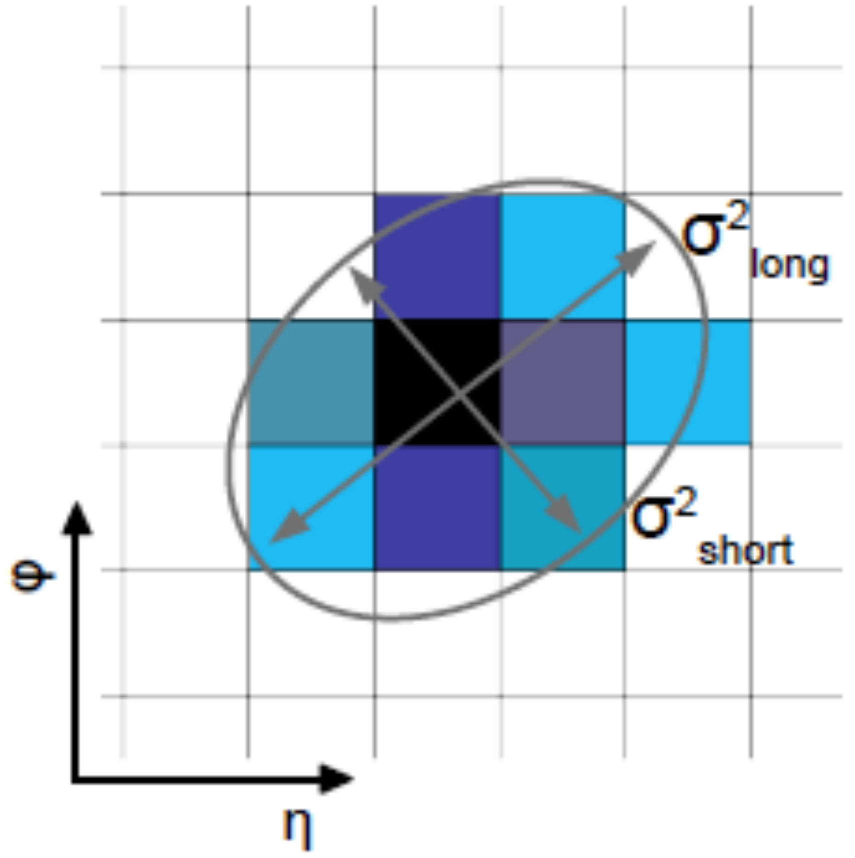

- Shower shape parameter $\sigma^2_{\rm long}$ is related to the longer axis of the cluster ellipse
- Parameter depends on cluster cells location and its energy

$$w_i = \text{Maximum}(0, w_0 + \ln(E_{\text{cell},\ i}/E))$$

$$\sigma^2_{\alpha\beta} = \sum_i \frac{w_i\alpha_i\beta_i}{w_{\rm tot}} - \sum_i \frac{w_i\alpha_i}{w_{\rm tot}} \sum_i \frac{w_i\beta_i}{w_{\rm tot}}$$

$$w_{\rm tot} = \sum_i w_i,$$

$$\sigma^2_{\rm long} = 0.5(\sigma^2_{\varphi\varphi} + \sigma^2_{\eta\eta}) + \sqrt{0.25(\sigma^2_{\varphi\varphi} - \sigma^2_{\eta\eta})^2 + \sigma^2_{\eta\varphi}},$$

$$\sigma^2_{\rm short} = 0.5(\sigma^2_{\varphi\varphi} + \sigma^2_{\eta\eta}) - \sqrt{0.25(\sigma^2_{\varphi\varphi} - \sigma^2_{\eta\eta})^2 + \sigma^2_{\eta\varphi}},$$

- V2 clusters: Used in pp & Pb–Pb at $\sqrt{s_{\rm NN}}$ = 5.02 TeV to get *E* and position
  - In other pp and p–Pb measurements V1 clusters are used
- For the $\sigma^2_{\rm long}$ calculation: consider the neighbour cells around the highest energy cell in a 5x5 fixed window
  - Increase meson decay merging but limiting UE merging

ALICE-PUBLIC-2024-003

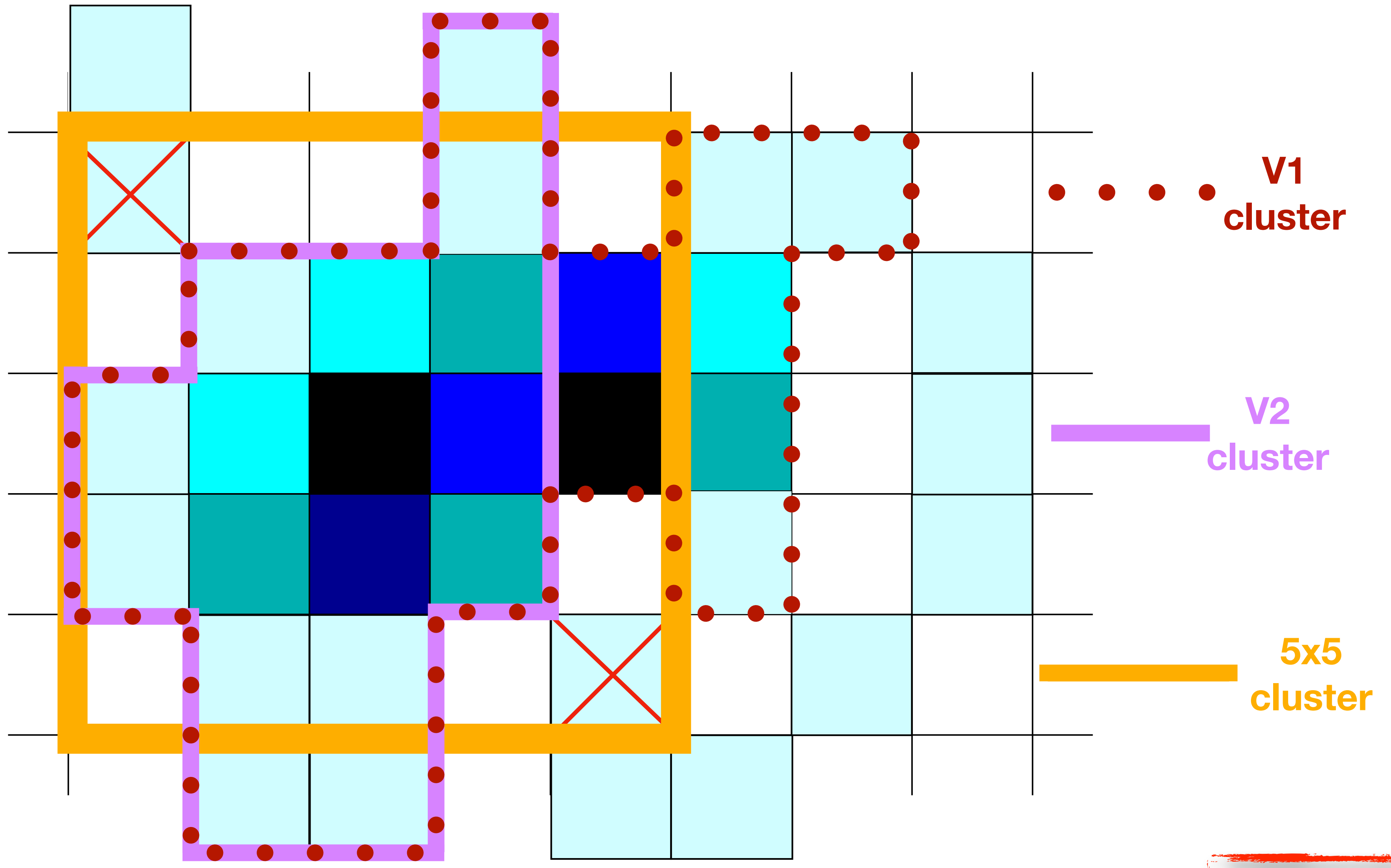

EMCal cluster shower shape, pp & Pb–Pb $\sqrt{s_{\mathrm{NN}}}$ = 5.02 TeV

New

ALICE

ALICE-PUBLIC-2024-003

EMCal cluster shower shape, pp & Pb–Pb $\sqrt{s_{NN}}$ = 5.02 TeV

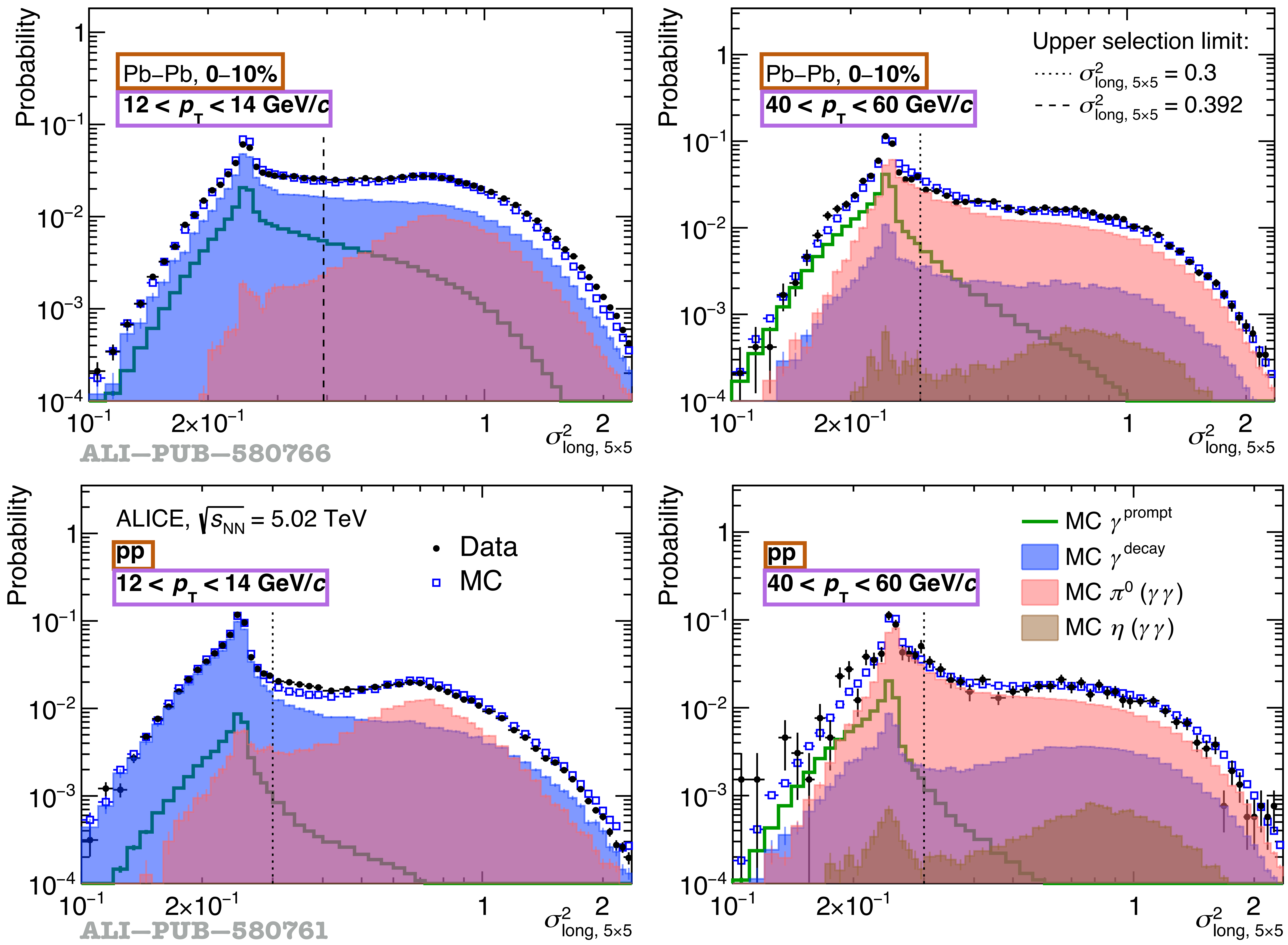

EMCal cluster shower shape, pp $\sqrt{s}$ = 13 TeV

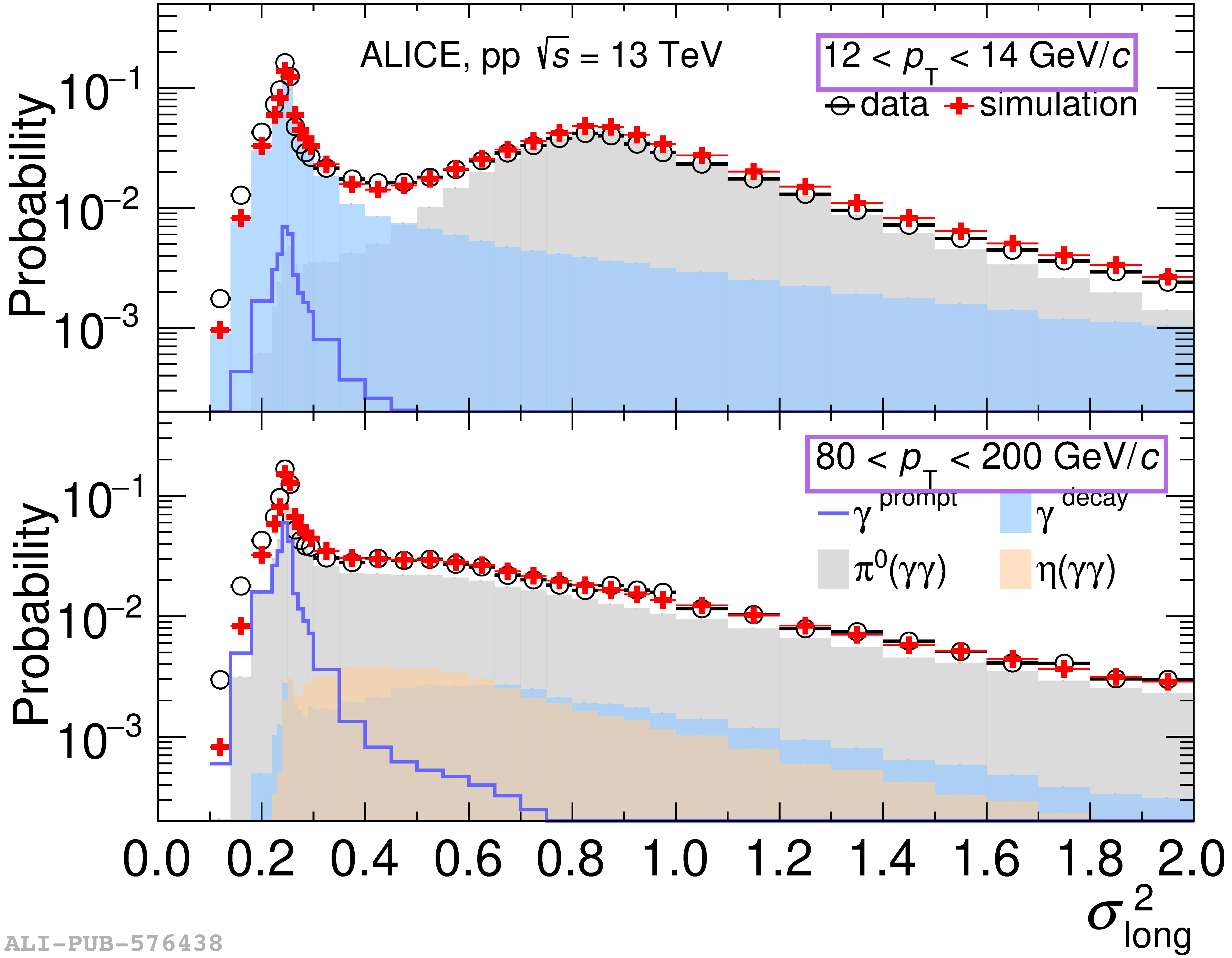

ALI-PUB-576438

Underlying event estimation

Track p_T UE density estimated on:

- Pb-Pb & pp at $\sqrt{s_{NN}}$ = 5.02 TeV:
  - ➡ Sum of tracks p_T normalised by **η-band** area
    → *Avoid flow effects*
  - ➡ Gap between cone and band of $\Delta R_{UE\ gap}$= 0.1
    → *Avoid jet remnants*
- p-Pb $\sqrt{s_{NN}}$ = 5.02, 8.16 TeV, pp $\sqrt{s}$ = 8 TeV
  - ➡ Perpendicular cone & jet-median

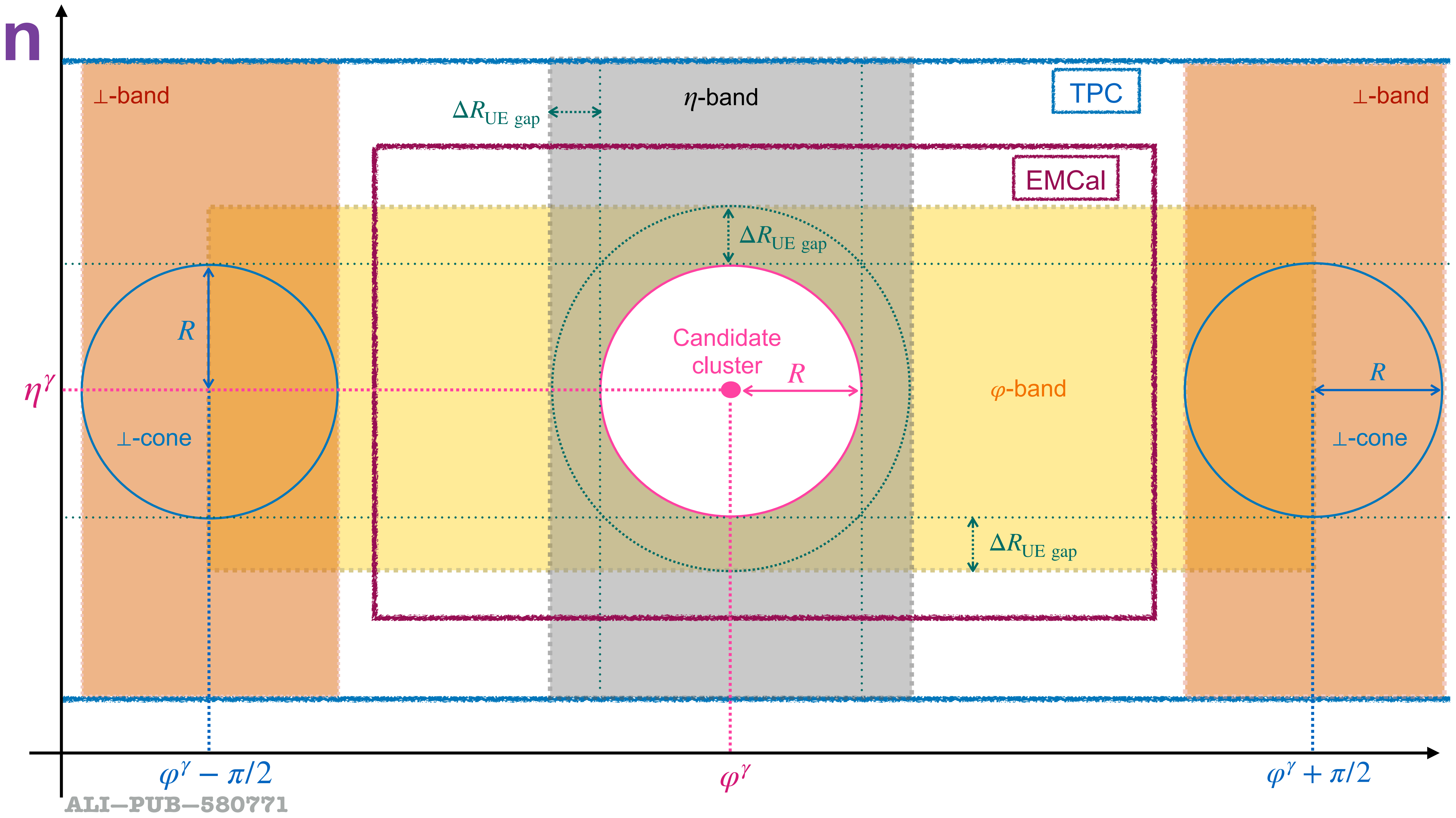

Remark: UE was not subtracted in $\sqrt{s}$ = 7 & 13 TeV measurements, UE small

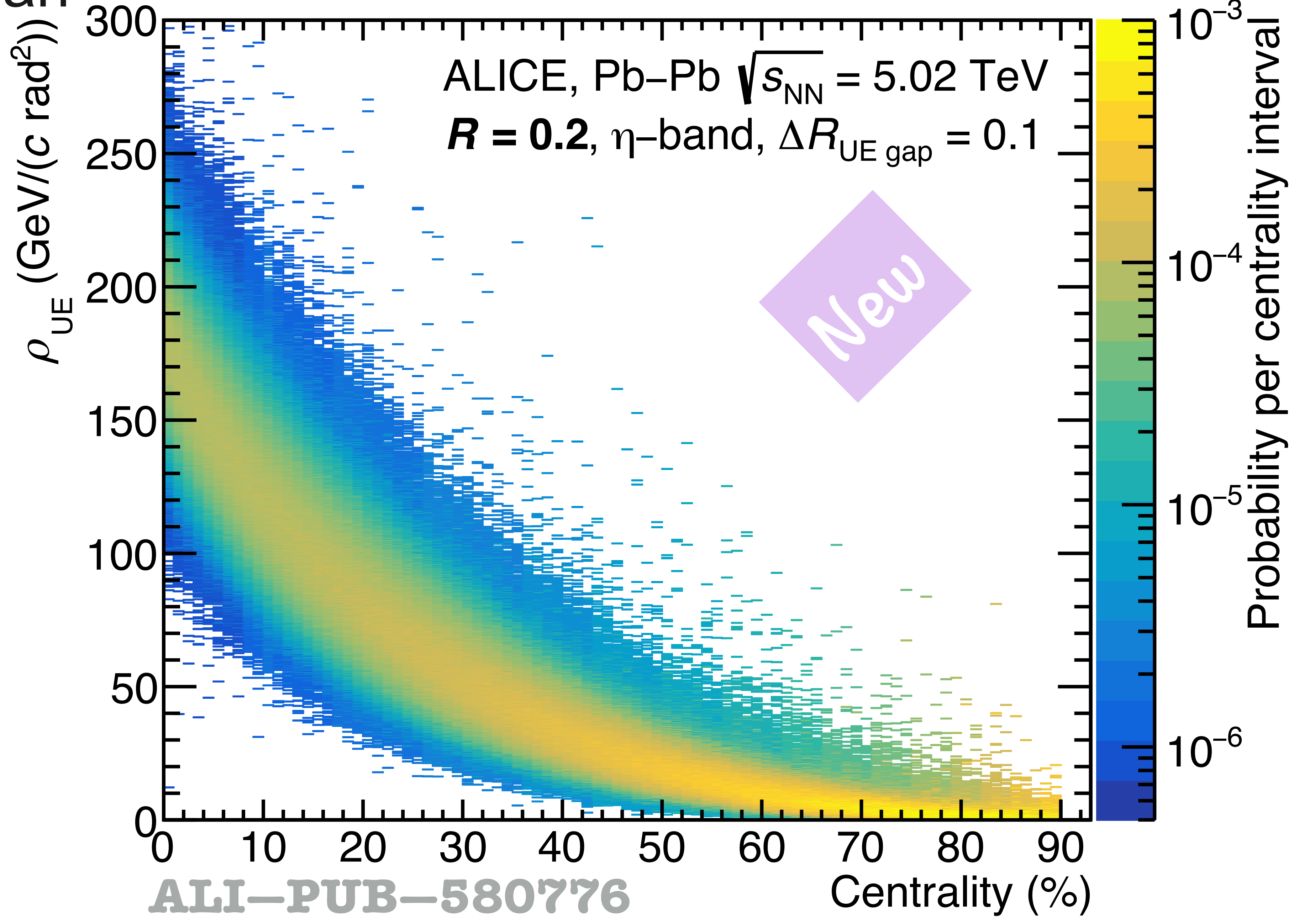

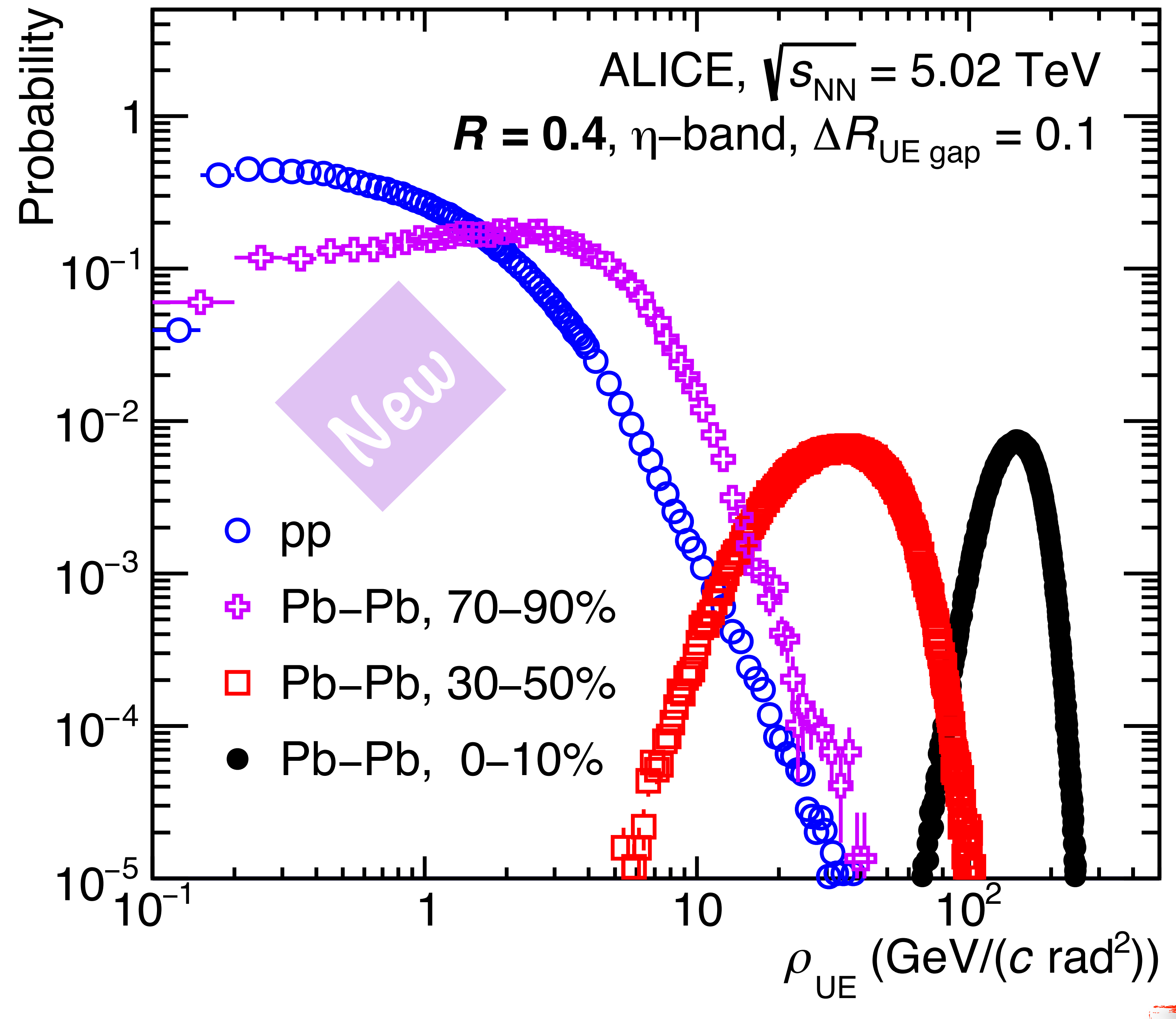

Isolation momentum in cone, pp & Pb–Pb $\sqrt{s_{NN}}$ = 5.02 TeV

ALICE-PUBLIC-2024-003

Prompt γ identification in ALICE: EM shape & isolation

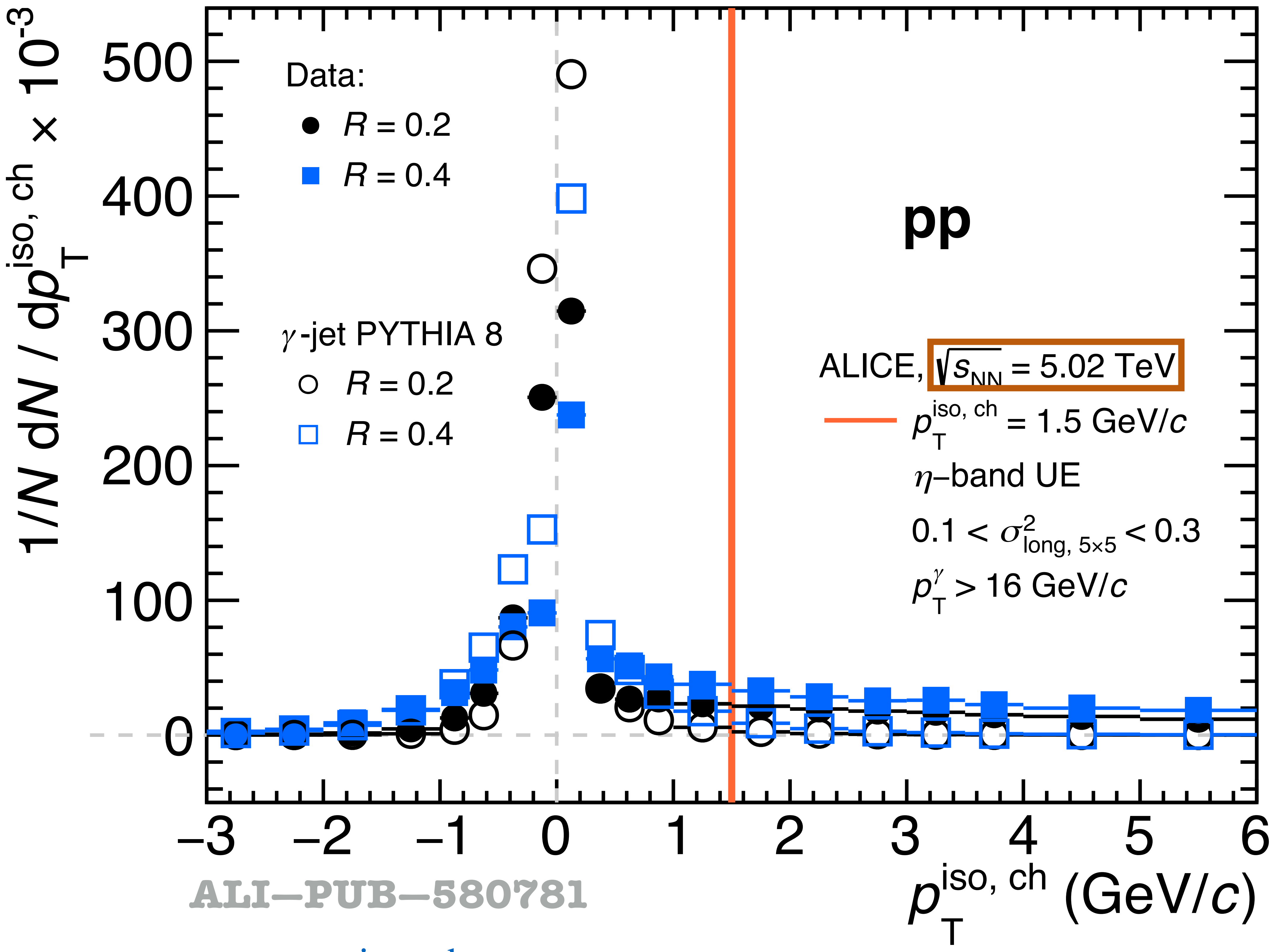

pp

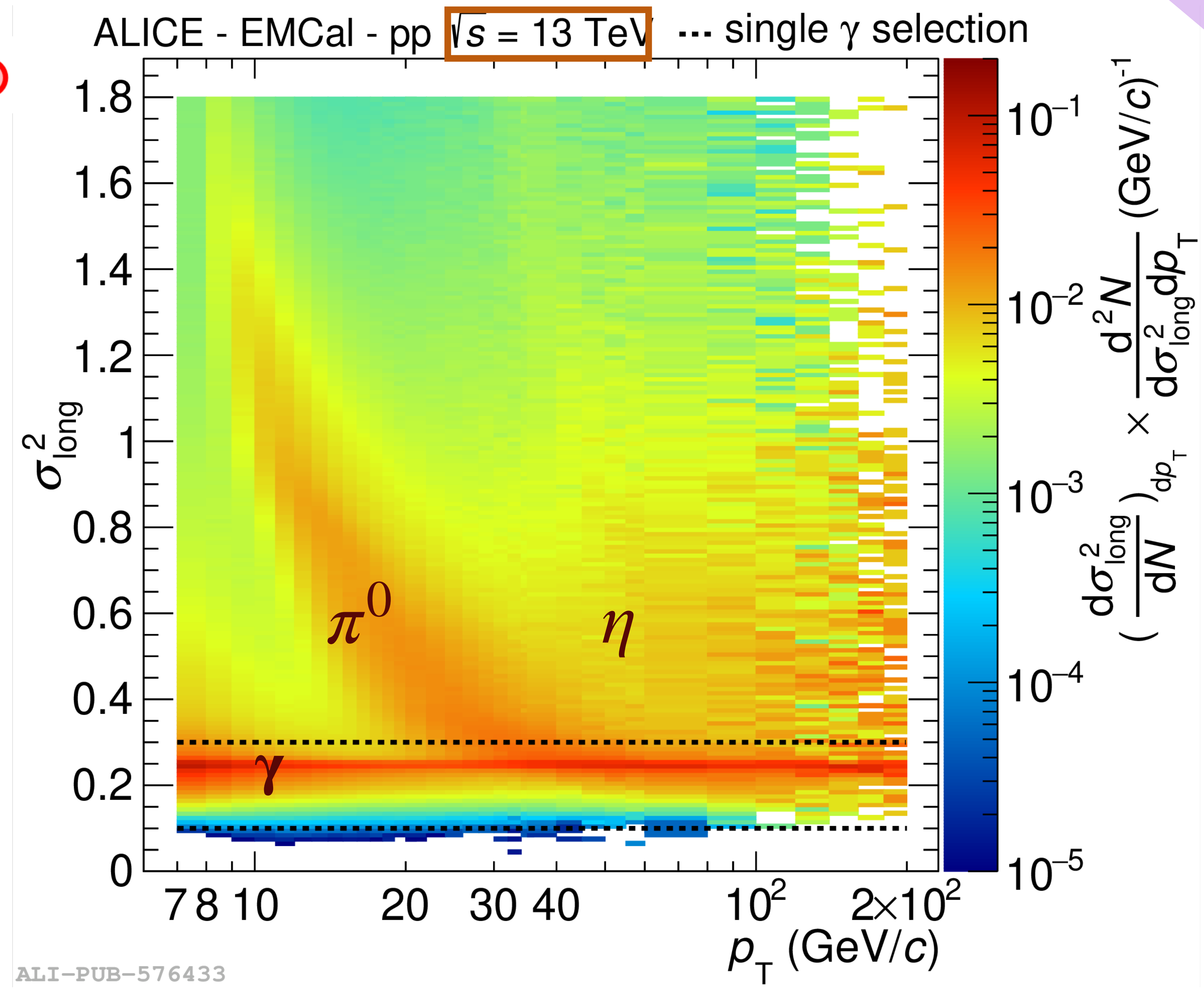

- Isolated if $p_{\mathrm{T}}^{\mathrm{iso,\,ch}}$ < 1.5 GeV/*c* (orange line) with *R* = 0.4 or 0.2
- Symmetric in PYTHIA 8 γ-jet process simulation, wider for *R* = 0.4 (UE)
- In data, more asymmetric and less peaked distribution due to jet contribution

- Visible bands for **γ** (narrow clusters) & π^0 (wide clusters)
- Select as **γ** clusters with $0.1 < \sigma^2_{\mathrm{long,\ 5\times5}} < 0.3$

Prompt γ identification in ALICE: EM shape & isolation

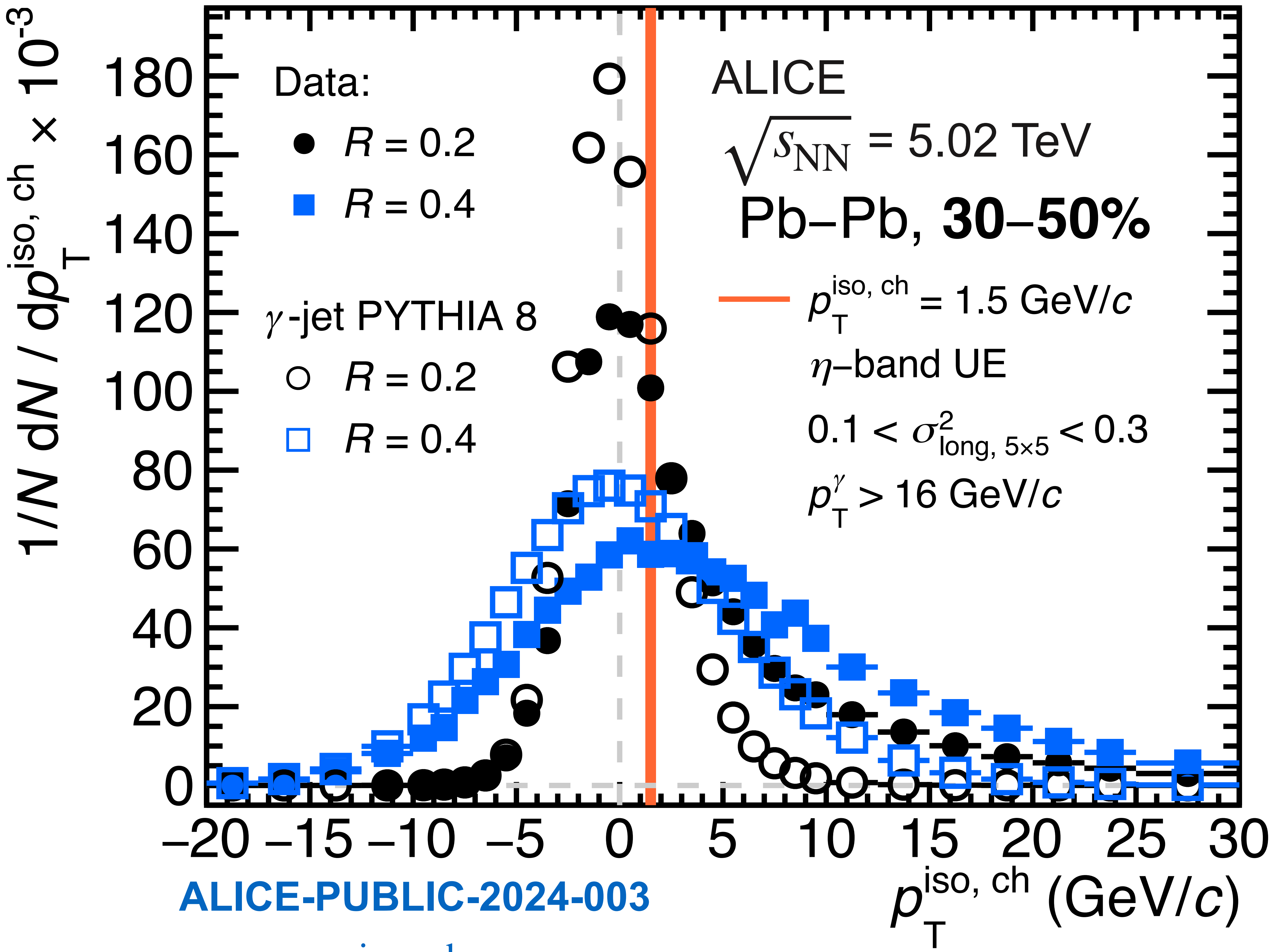

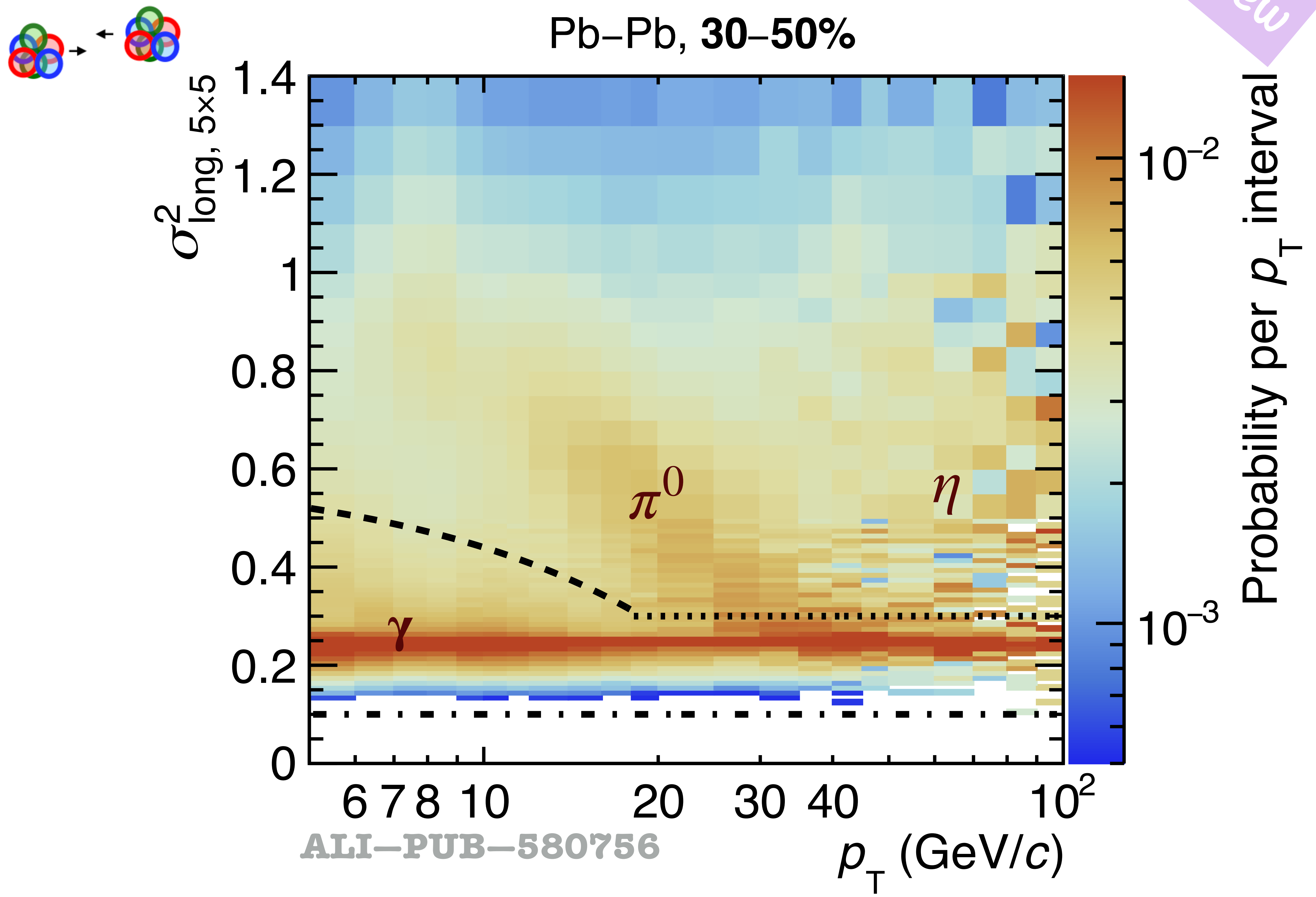

- Isolated if $p_{T}^{\text{iso, ch}}$ < 1.5 GeV/*c* (orange line) with *R* = 0.4 or 0.2
- Embedded pp PYTHIA 8 simulation into MB data, symmetric distribution
- In data, more asymmetric distribution due to jet contribution
- Significantly wider distributions for *R* = 0.4 due to UE fluctuations

- Visible bands for γ (narrow clusters) & π^0 (wide clusters)
- Select as γ clusters with
  - Pb–Pb:
    - $p_T < 18$ GeV/c: $0.1 < \sigma^2_{\text{long, }5\times5} < 0.6 - 0.016 \cdot p_T$
    - $p_T > 18$ GeV/c: $0.1 < \sigma^2_{\text{long, }5\times5} < 0.3$
  - pp & p–Pb:
    - $0.1 < \sigma^2_{\text{long, }5\times5} < 0.3$

Prompt γ identification in ALICE: EM shape & isolation

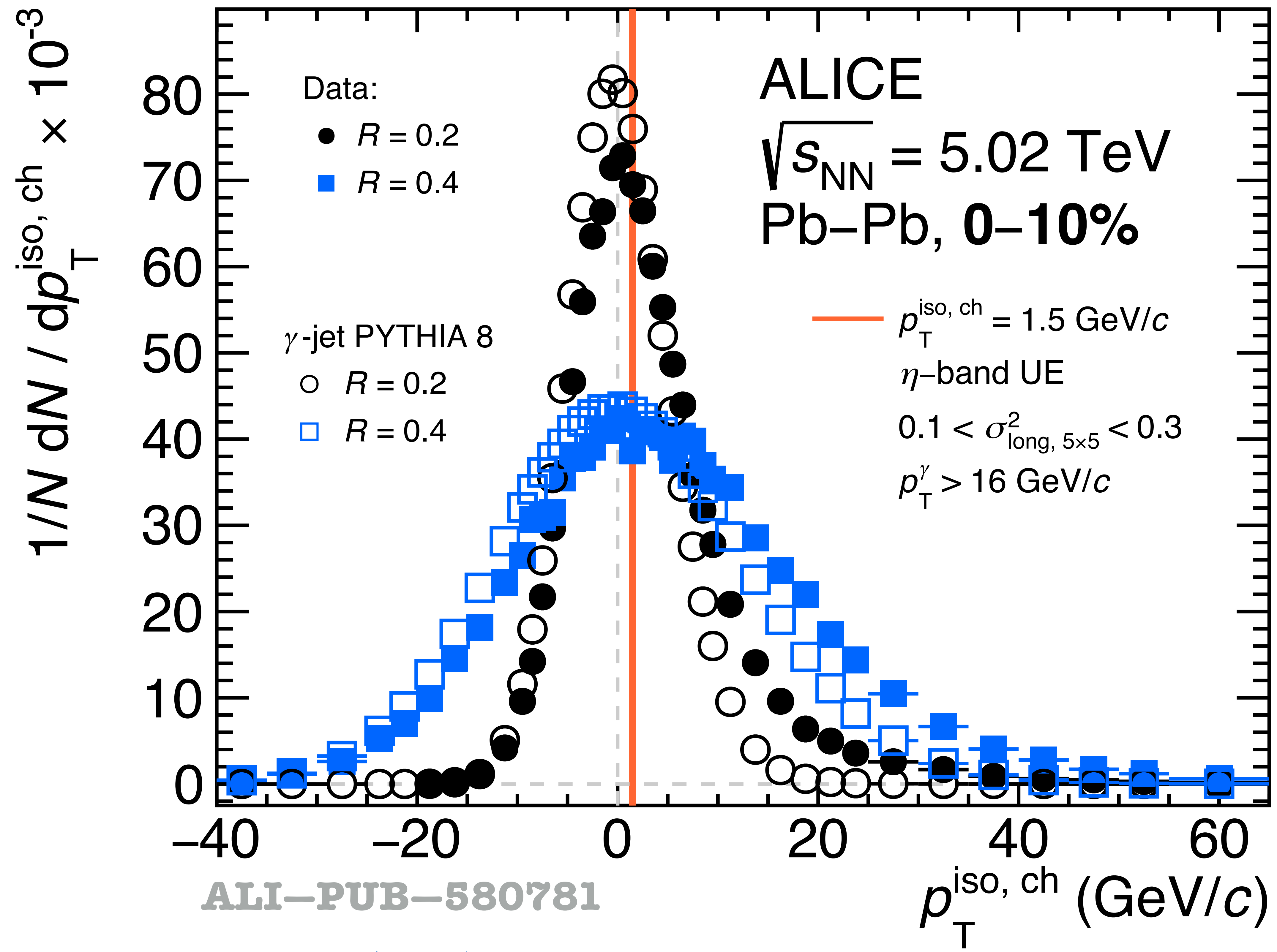

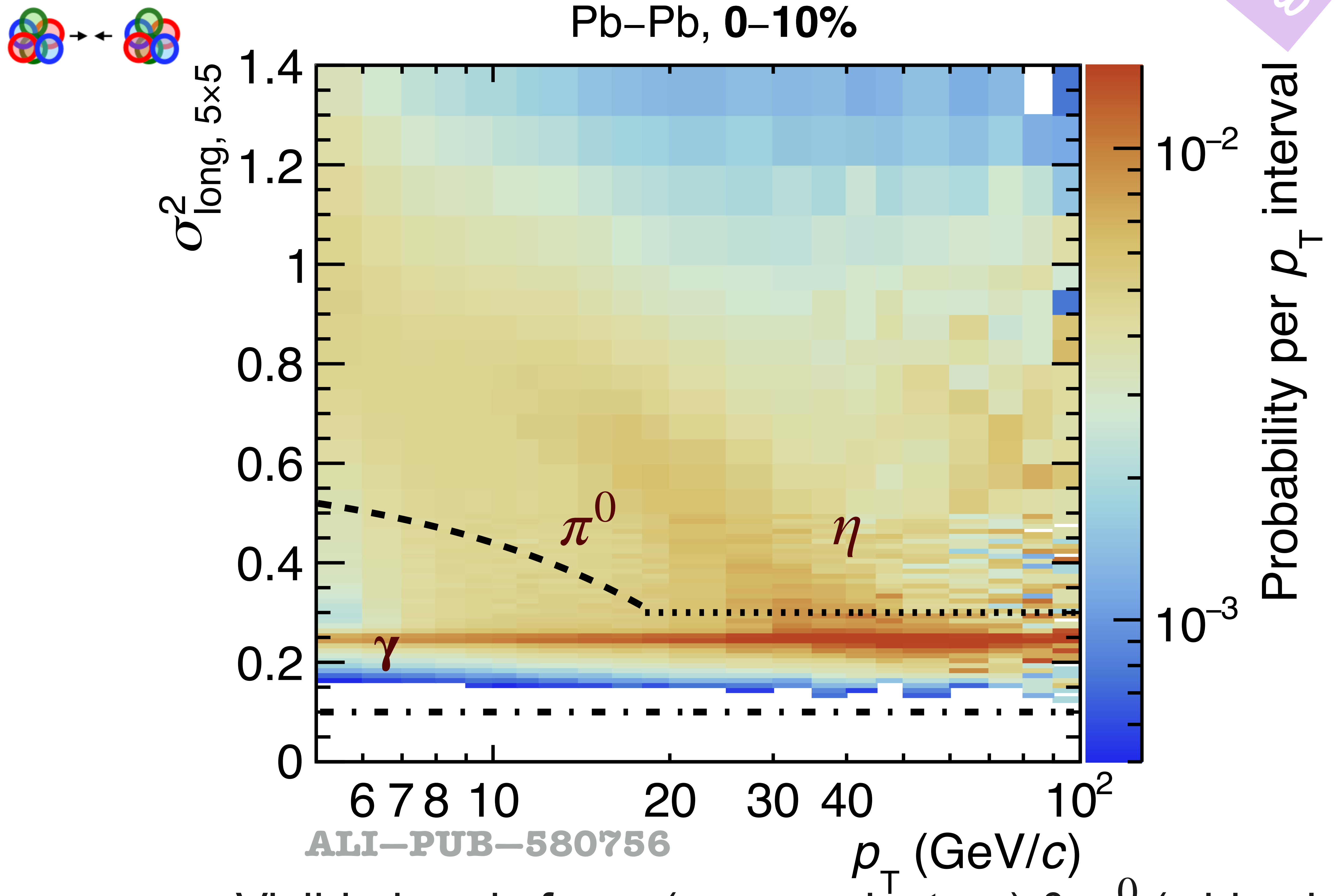

- Isolated if $p_T^{iso, ch} < 1.5$ GeV/c (orange line) with R = 0.4 or 0.2
- Embedded pp PYTHIA 8 simulation into MB data, symmetric distribution
- In data, more asymmetric distribution due to jet contribution
- Significantly **much** wider distributions for R = 0.4 due to UE fluctuations

- Visible bands for **γ** (narrow clusters) & π^0 (wide clusters)
- Select as **γ** clusters with
  - Pb–Pb:
    - $p_T < 18$ GeV/c: $0.1 < \sigma^2_{long, 5\times5} < 0.6 - 0.016 \cdot p_T$
    - $p_T > 18$ GeV/c: $0.1 < \sigma^2_{long, 5\times5} < 0.3$
  - pp & p–Pb:
    - $0.1 < \sigma^2_{long, 5\times5} < 0.3$
- **γ** increase their $\sigma^2_{long, 5\times5}$ due to the UE

Isolated γ purity in pp collisions, R = 0.4

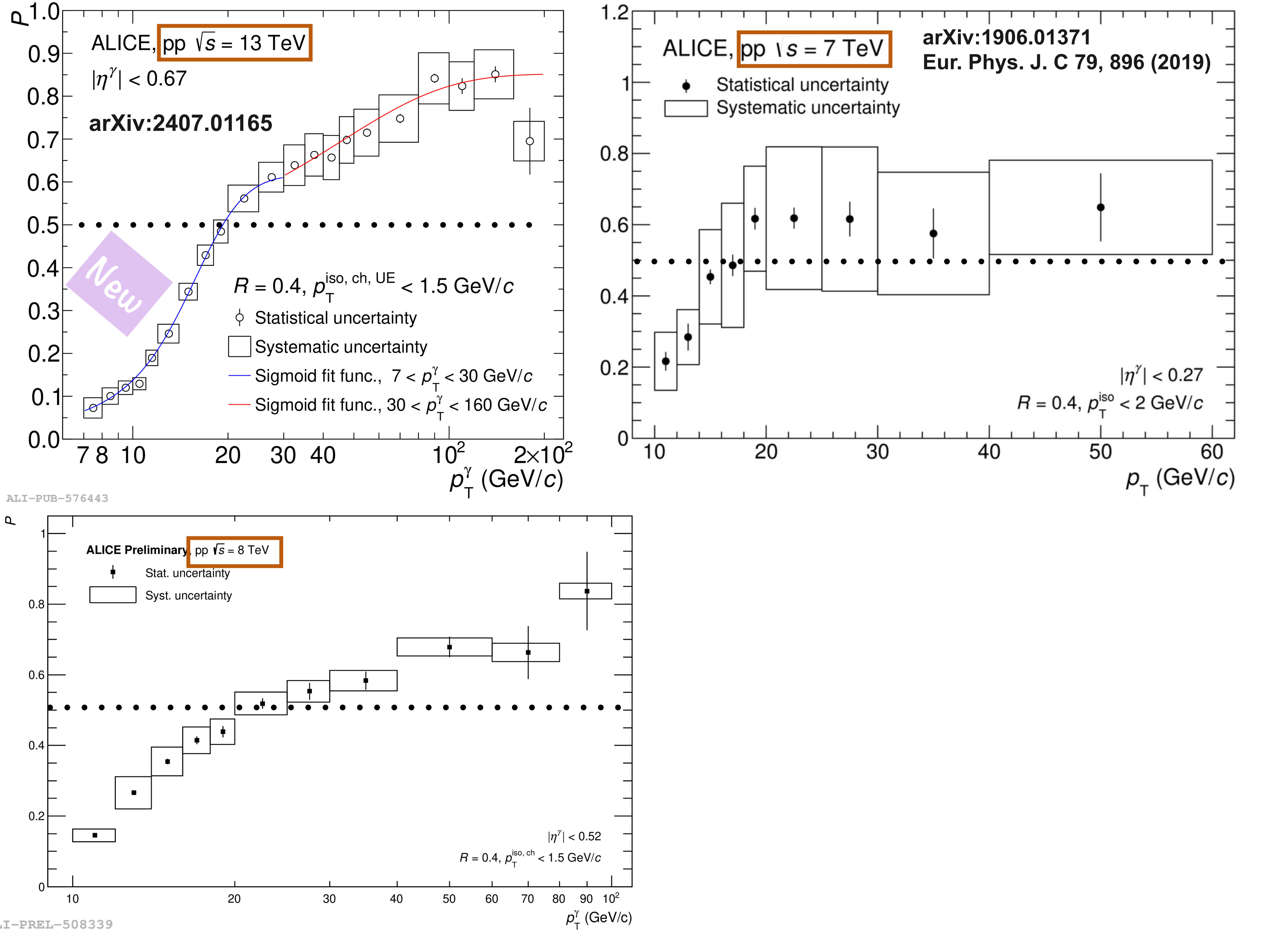

Isolated γ purity in p–Pb collisions, R = 0.4

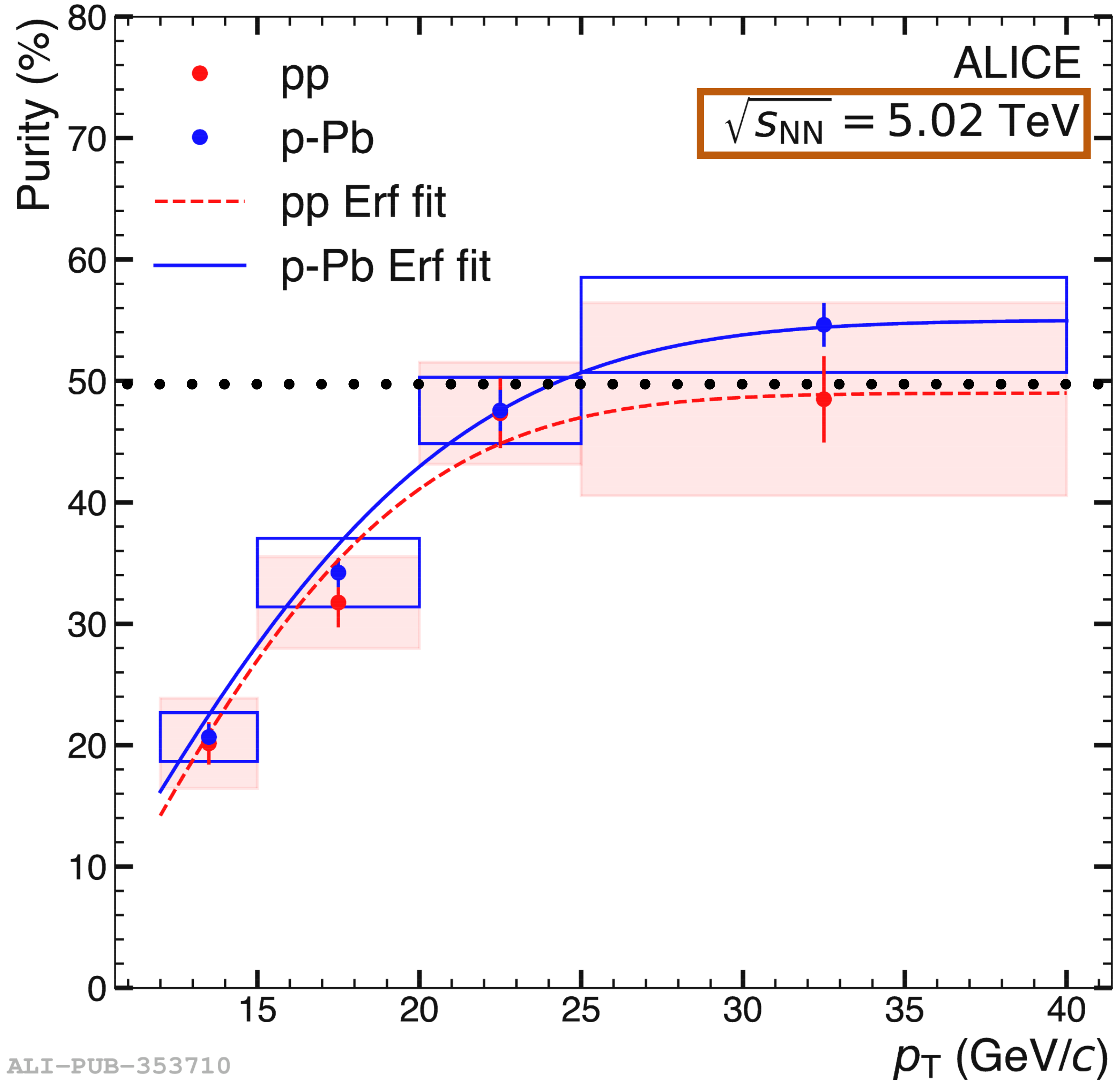

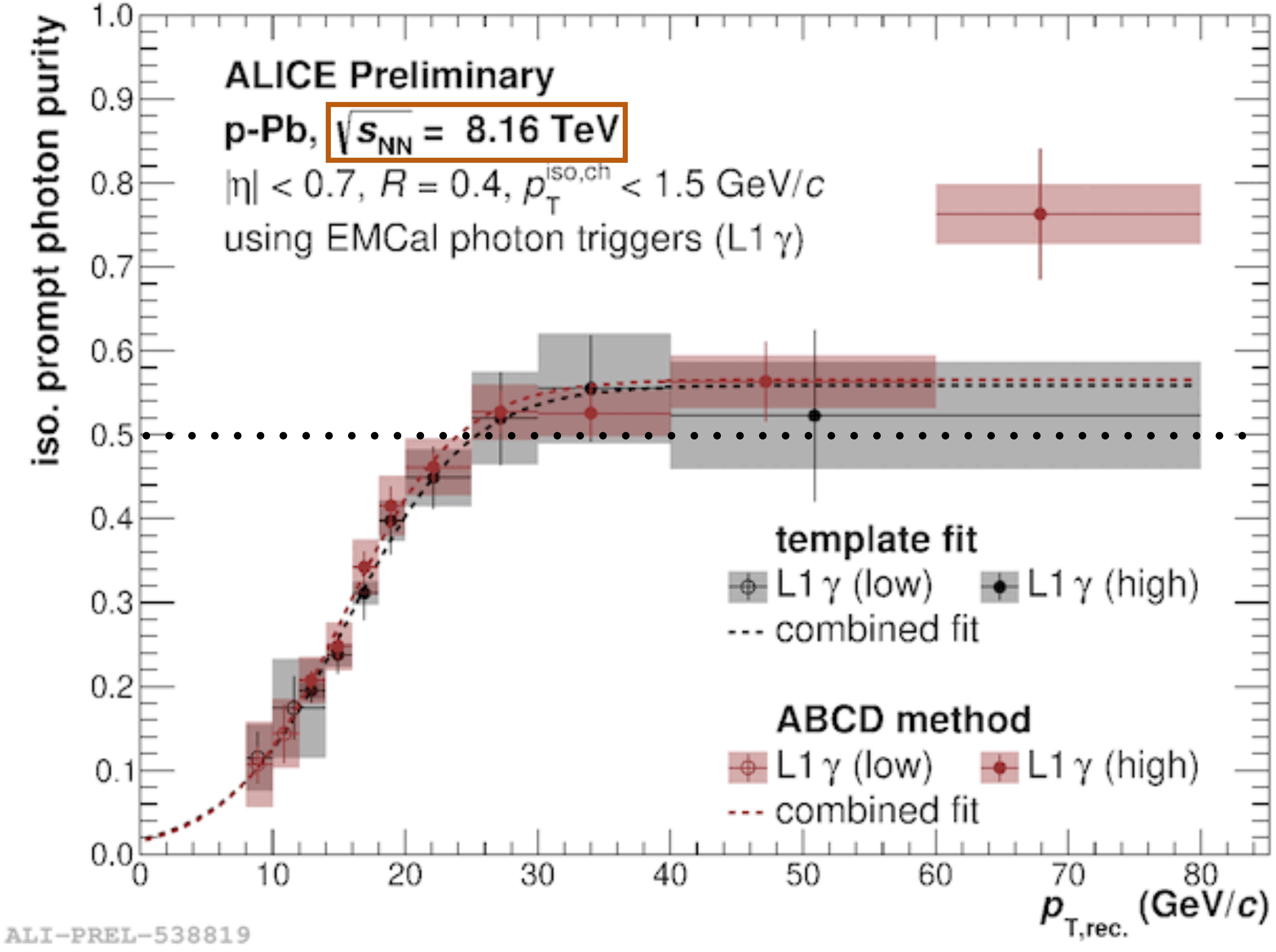

Purity for R = 0.2 & 0.4, pp & Pb–Pb $\sqrt{s_{NN}}$ = 5.02 TeV

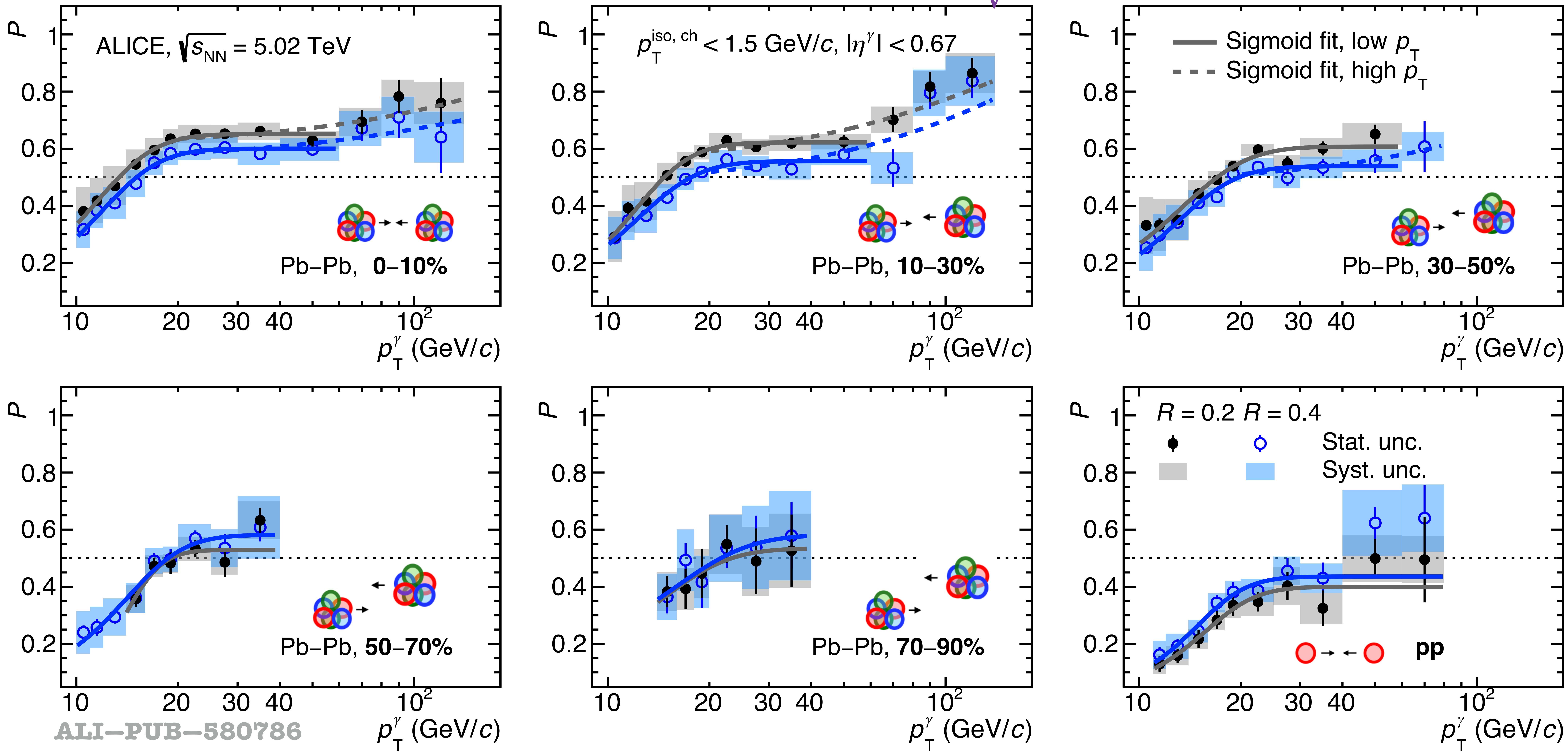

- Distributions fitted to sigmoid function to reduce influence of fluctuations, <u>fits used to correct the spectra</u>
- P (R = 0.4) > P (R = 0.2) in pp collisions, more jet particles in cone, but decreasing centrality P (R = 0.2) > P (R = 0.4), due to UE fluctuations, although not significantly different
- P (Pb–Pb) > P (pp) due to better tracking and higher $N(\gamma) / N(\pi^0)$ ratio $(R_{AA}(\pi^0) << 1)$

Isolated γ efficiency components, pp $\sqrt{s}$ = 13 TeV

$$\varepsilon^{\mathrm{sel}} = \frac{\mathrm{d}N^{\mathrm{cluster\ sel.}}_{\gamma_{\mathrm{prompt}}}/\mathrm{d}p_{\mathrm{T}}^{\mathrm{rec}}}{\mathrm{d}N^{\mathrm{gener.}}_{\gamma_{\mathrm{prompt}}}/\mathrm{d}p_{\mathrm{T}}^{\mathrm{gen}}}$$

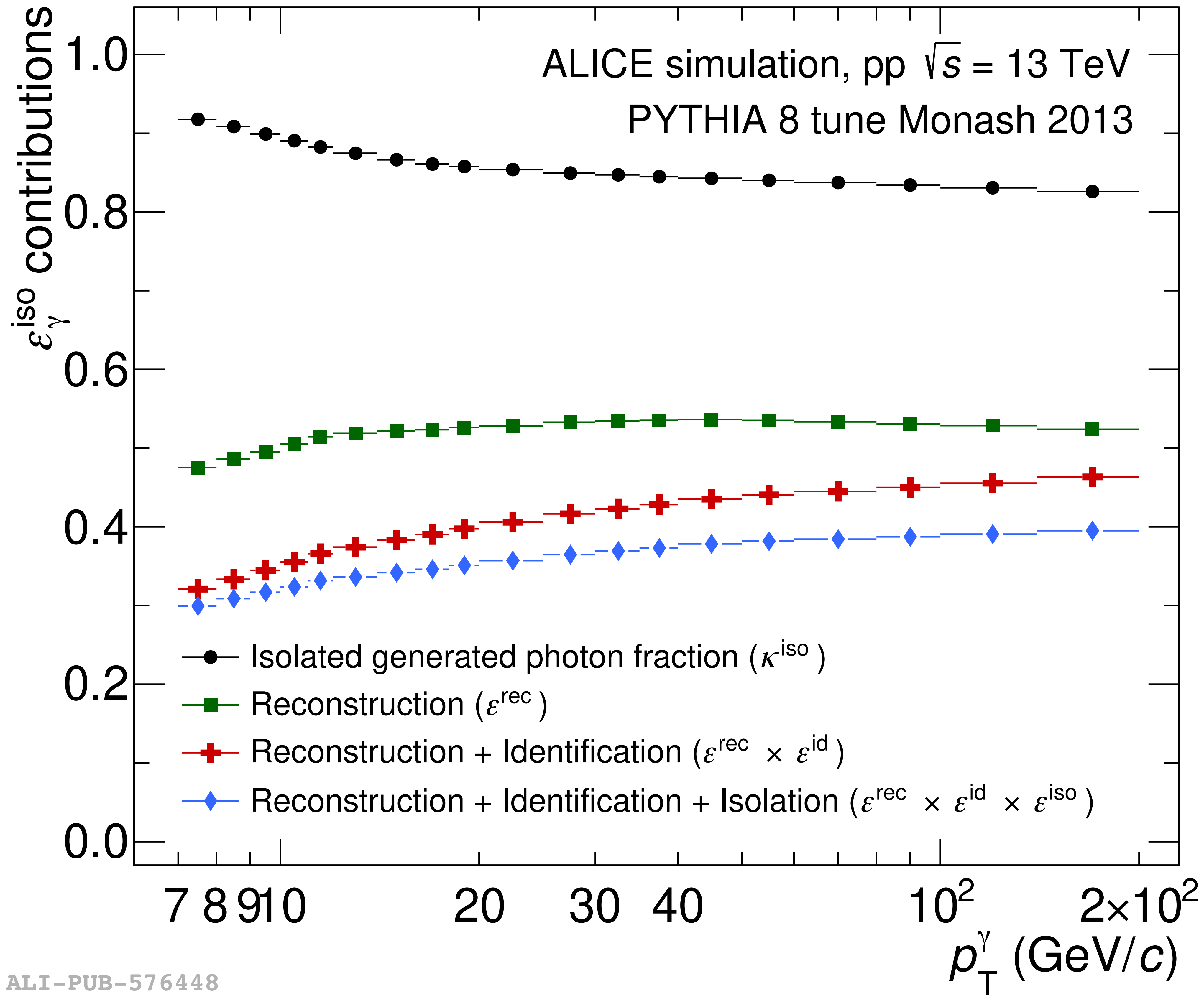

$$\varepsilon_{\gamma}^{\mathrm{iso}} = \frac{\mathrm{d}N^{\mathrm{cluster\ iso.\ narrow}}_{\gamma_{\mathrm{prompt}}}/\mathrm{d}p_{\mathrm{T}}^{\mathrm{rec}}}{\mathrm{d}N^{\mathrm{gener.\ iso.}}_{\gamma_{\mathrm{prompt}}}/\mathrm{d}p_{\mathrm{T}}^{\mathrm{gen}}}$$

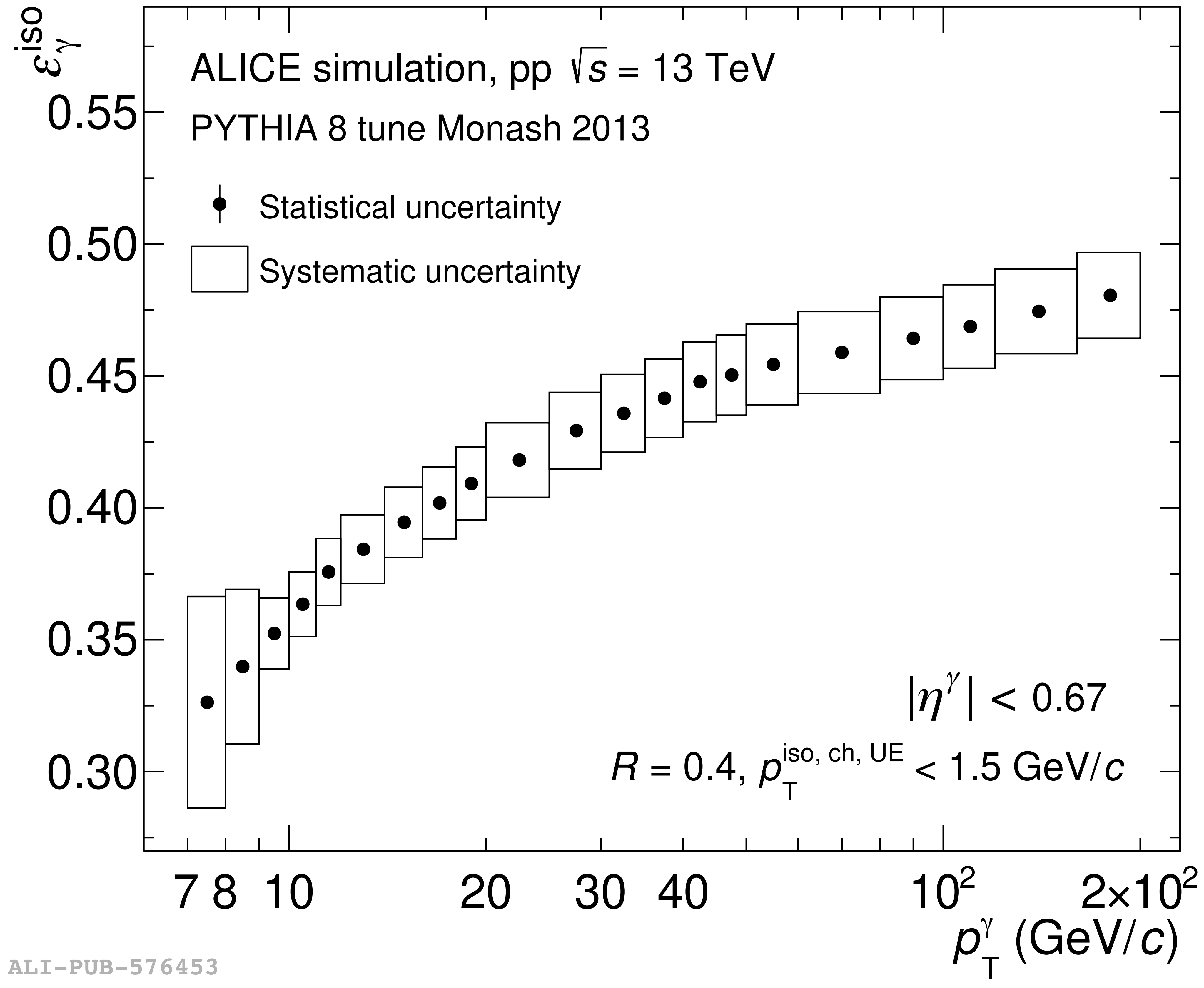

Isolated γ efficiency components, pp & Pb–Pb $\sqrt{s_{\mathrm{NN}}}$ = 5.02 TeV

New

$$\varepsilon^{\mathrm{sel}} = \frac{\mathrm{d}N^{\mathrm{cluster\ sel.}}_{\gamma_{\mathrm{prompt}}}/\mathrm{d}p_{\mathrm{T}}^{\mathrm{rec}}}{\mathrm{d}N^{\mathrm{gener.}}_{\gamma_{\mathrm{prompt}}}/\mathrm{d}p_{\mathrm{T}}^{\mathrm{gen}}}$$

ALICE-PUBLIC-2024-003

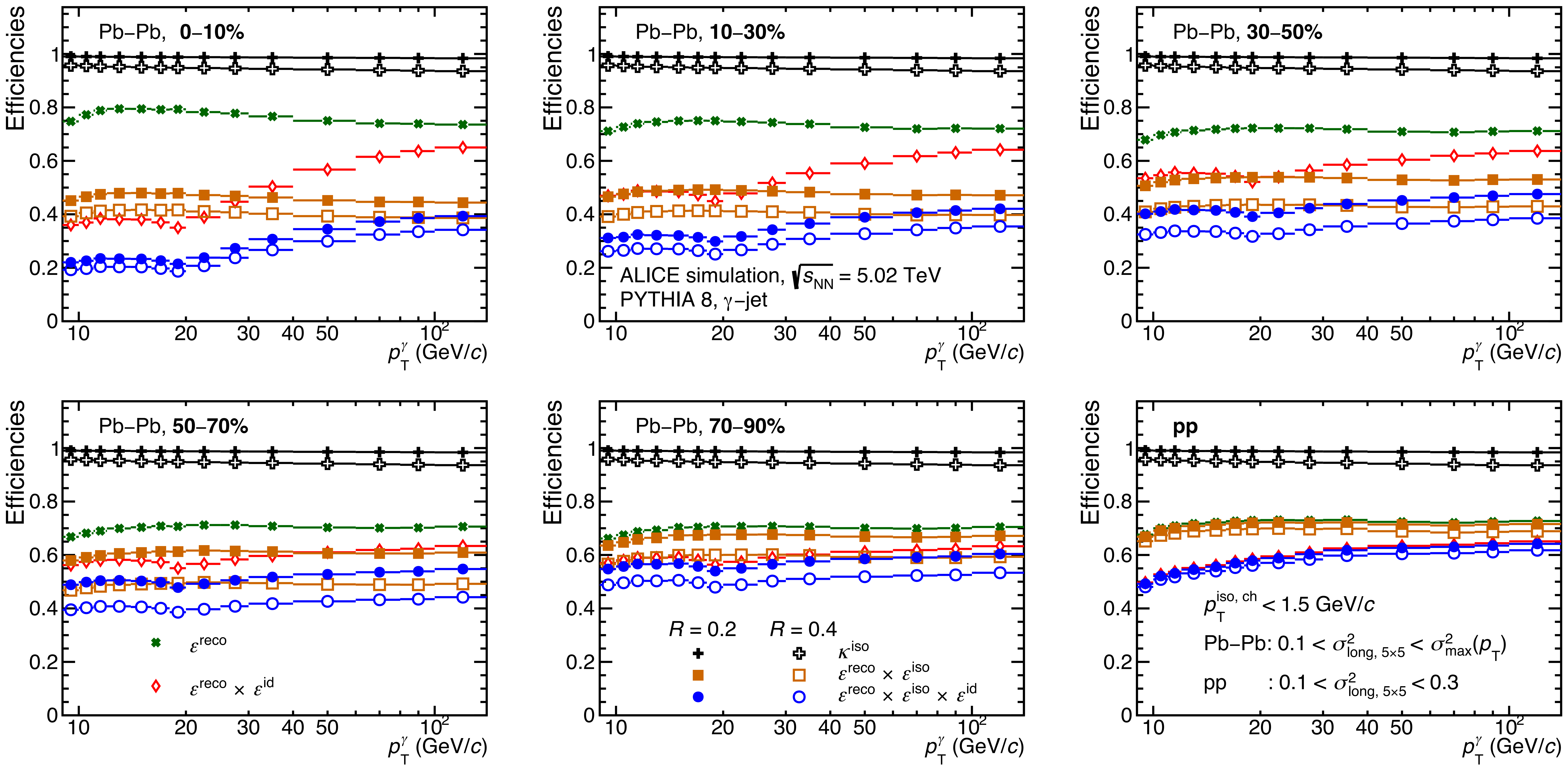

Efficiency, R = 0.2 & 0.4, pp & Pb–Pb $\sqrt{s_{NN}}$ = 5.02 TeV

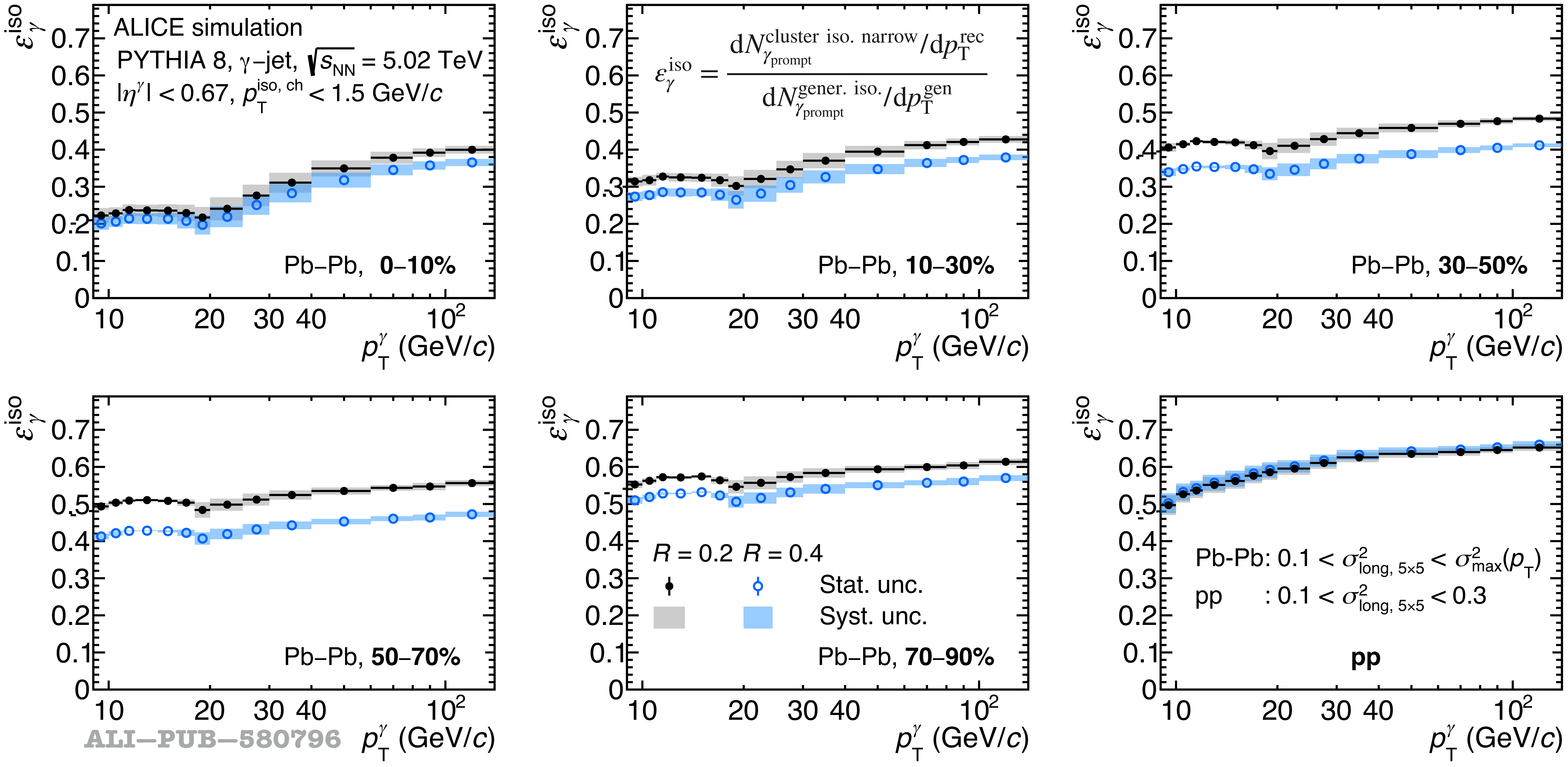

- $\varepsilon_{\gamma}^{iso}$ *(0-10%)* < $\varepsilon_{\gamma}^{iso}$ (50-90%*)*: UE increases cluster size in more central collisions
- In Pb–Pb, $\varepsilon_{\gamma}^{iso}$ (R = 0.2) > $\varepsilon_{\gamma}^{iso}$ (R = 0.4) a factor ~0.9 due to lower UE fluctuations
- In pp, $\varepsilon_{\gamma}^{iso}$ (R = 0.2) ≈ $\varepsilon_{\gamma}^{iso}$ (R = 0.4), due to the less performing ITS-only tracks

Pb–Pb 50-90%: efficiency and purity

ALICE-PUBLIC-2024-003

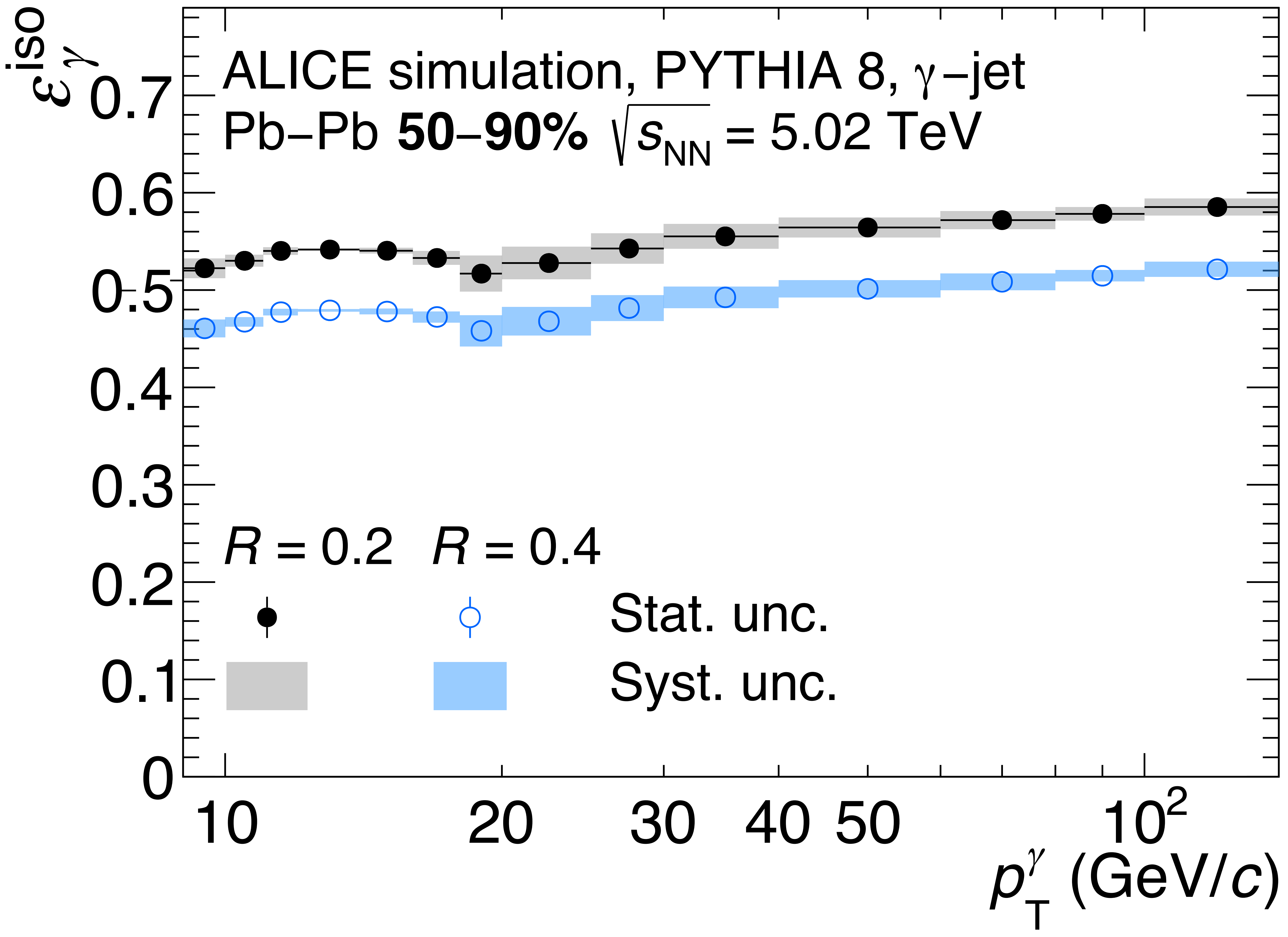

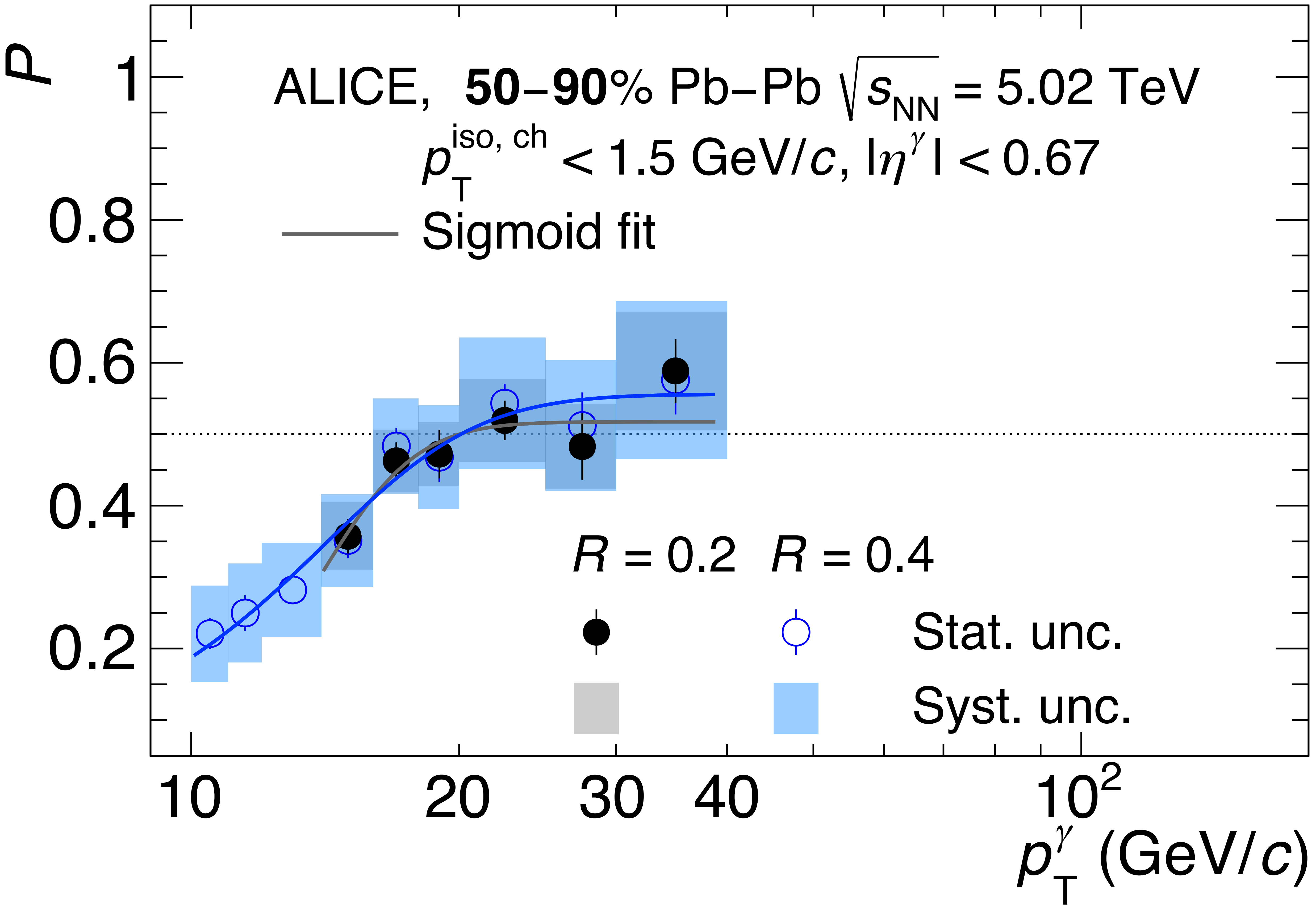

Uncertainties, pp $\sqrt{s}$ = 13 TeV

New

ALICE

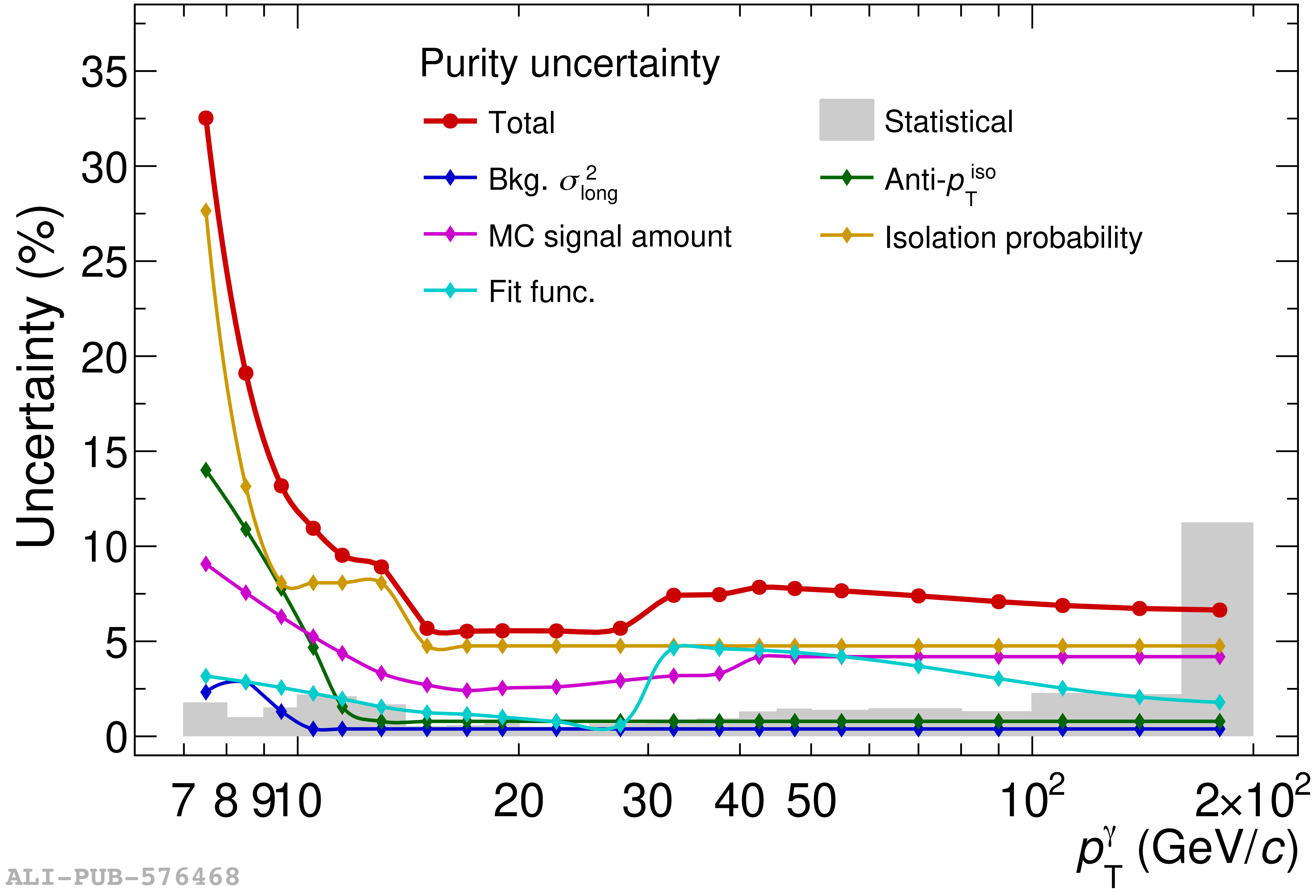

ALI-PUB-576468

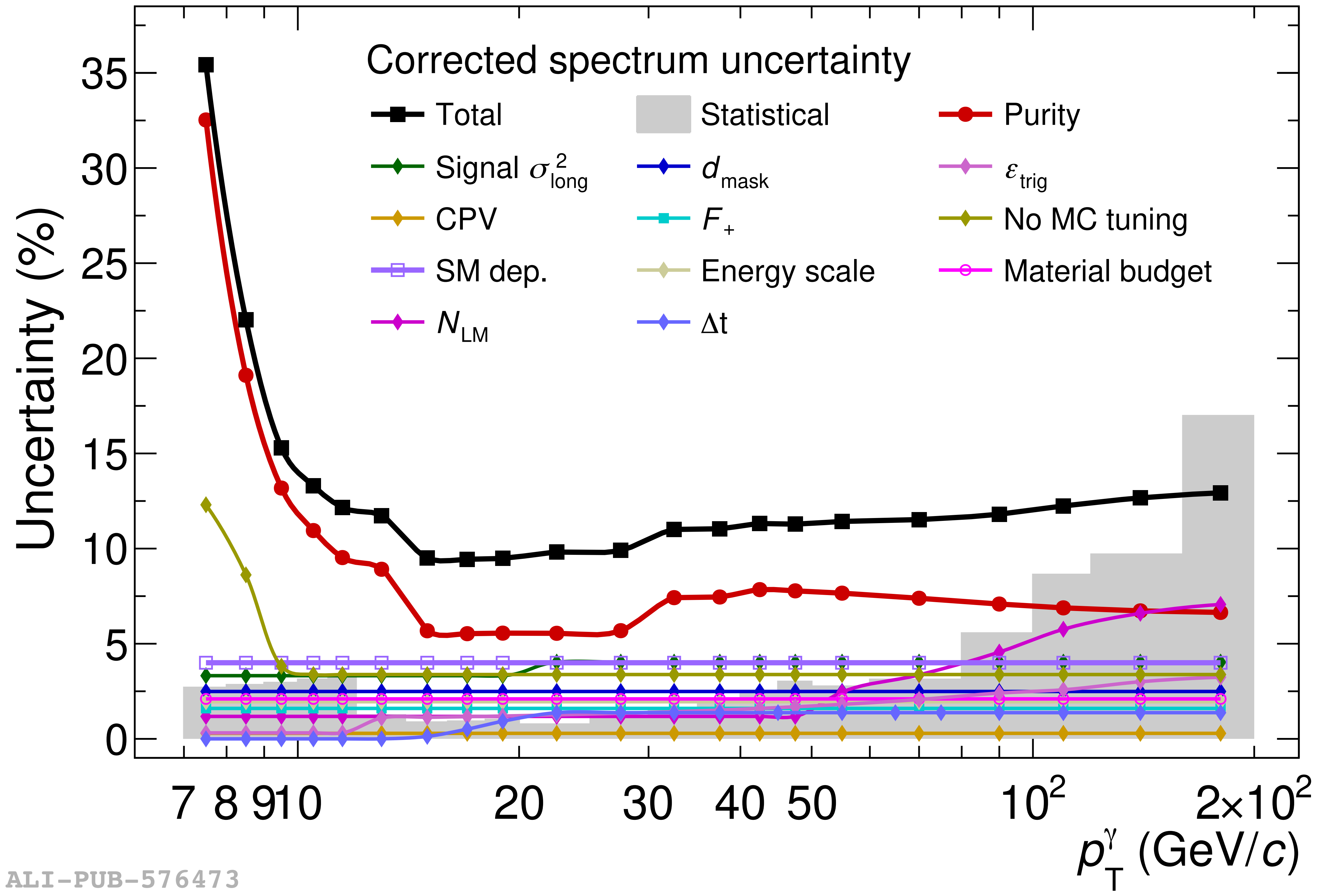

ALI-PUB-576473

Purity uncertainties, pp & Pb–Pb $\sqrt{s_{NN}}$ = 5.02 TeV, R = 0.2

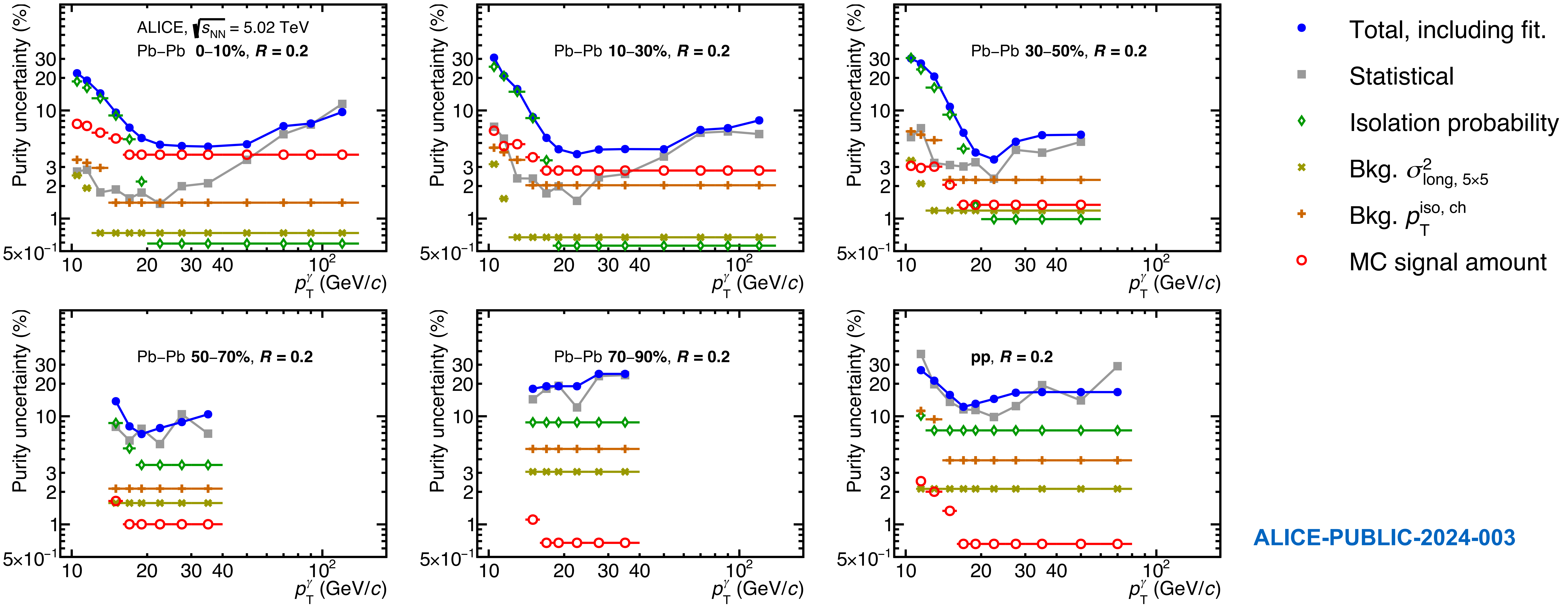

ALICE-PUBLIC-2024-003

Purity uncertainties, pp & Pb–Pb $\sqrt{s_{NN}}$ = 5.02 TeV, R = 0.4

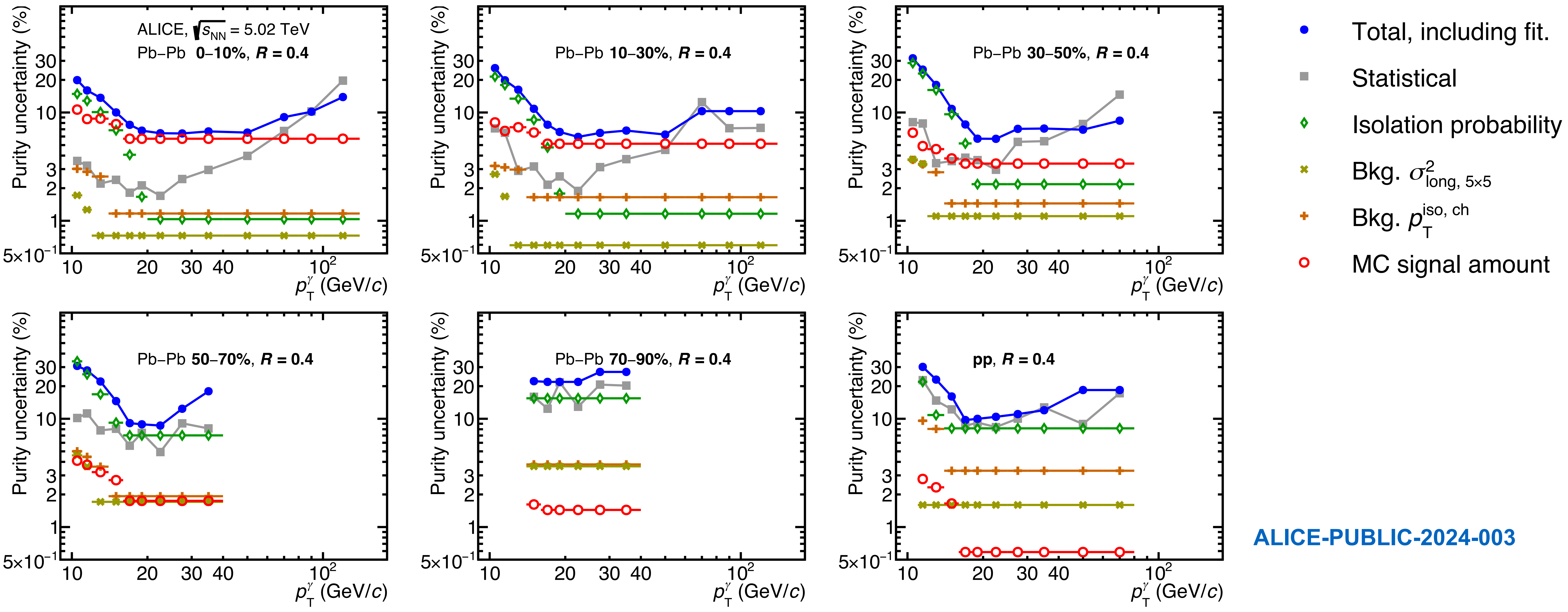

ALICE-PUBLIC-2024-003

Cross section uncertainties, pp & Pb–Pb $\sqrt{s_{NN}}$ = 5.02 TeV, R = 0.2

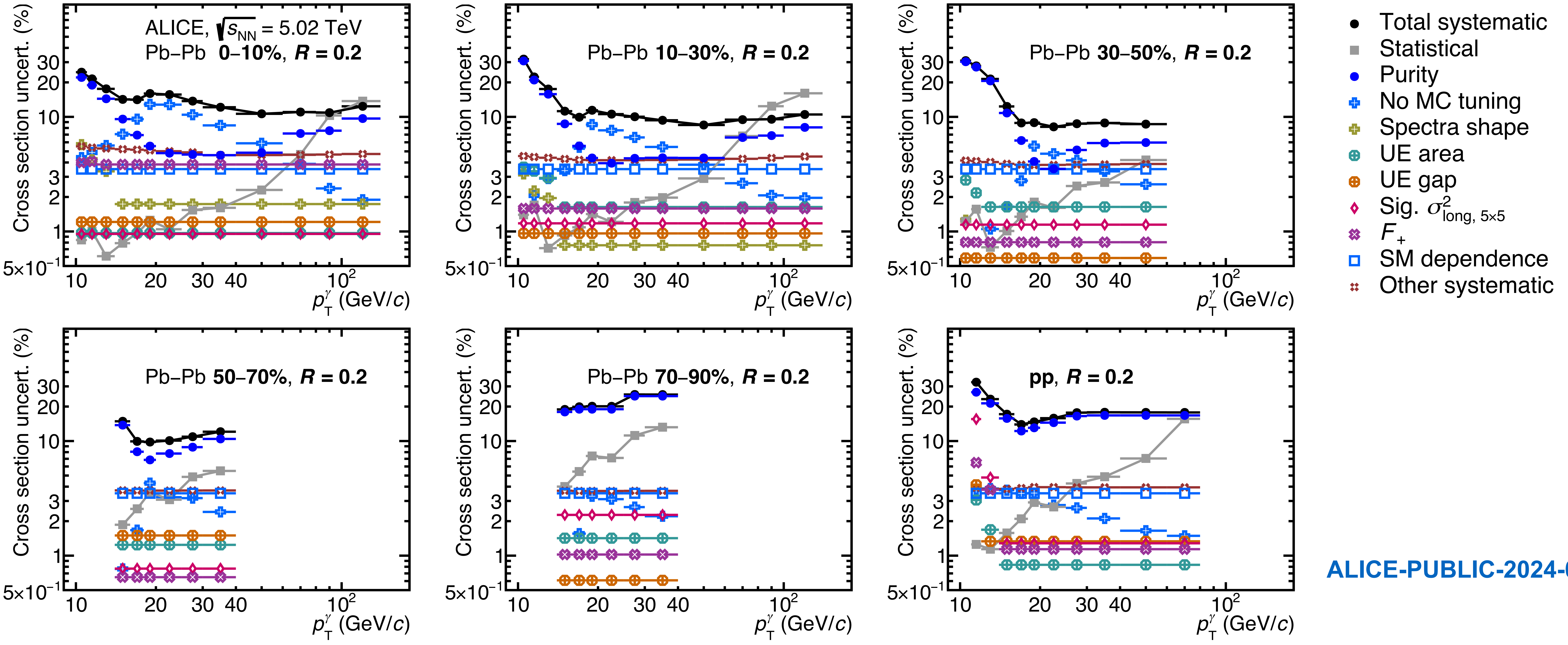

ALICE-PUBLIC-2024-003

Cross section uncertainties, pp & Pb–Pb $\sqrt{s_{NN}}$ = 5.02 TeV, R = 0.4

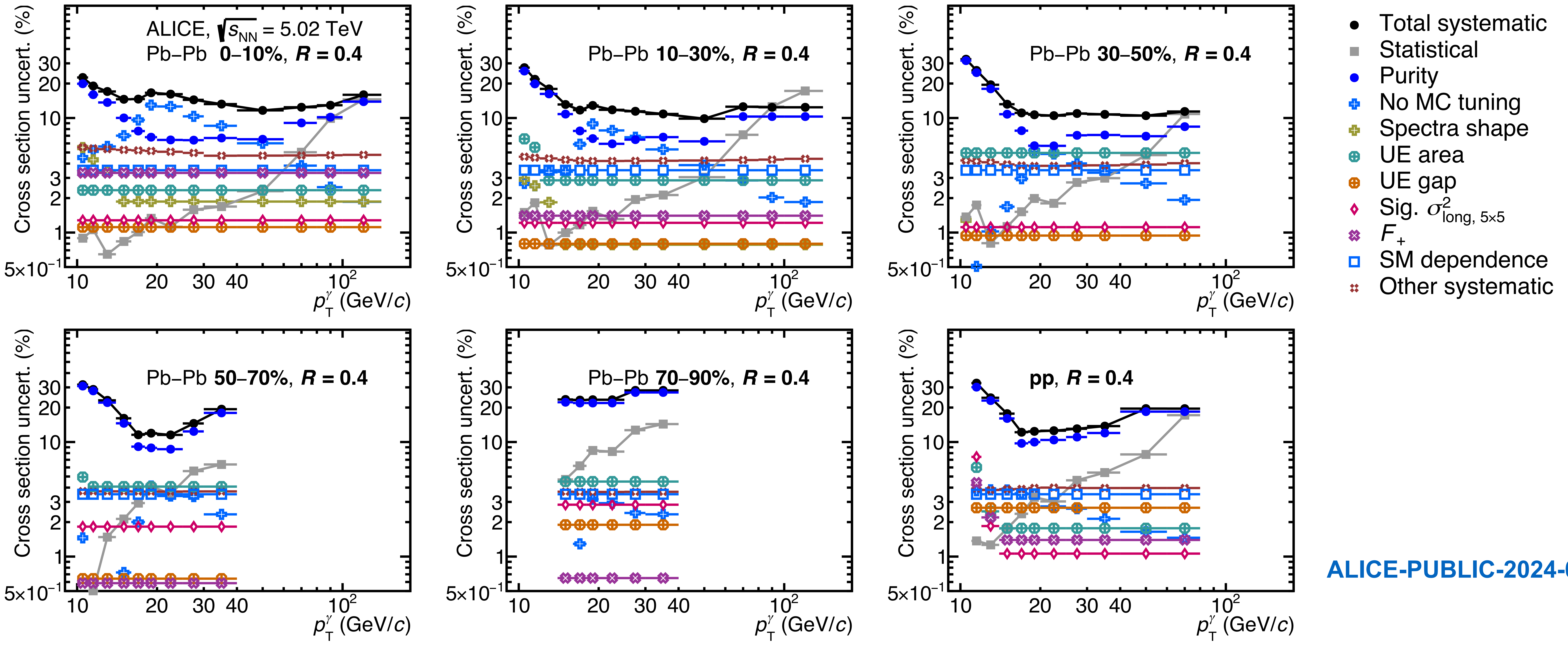

ALICE-PUBLIC-2024-003

R_{AA} uncertainties, R = 0.2

ALICE-PUBLIC-2024-003

R_{AA} uncertainties, R = 0.4

ALICE-PUBLIC-2024-003

R = 0.4 over R = 0.2 ratio uncertainties, pp & Pb–Pb $\sqrt{s_{NN}}$ = 5.02 TeV

ALICE-PUBLIC-2024-003

Isolated γ-hadron correlations in Pb–Pb: Azimuthal distribution

- UE in $\Delta\varphi$: uncorrelated tracks shift up the distribution
- *UE subtraction with mixed event*: artificial dataset created combining the trigger cluster with tracks on different collisions
- Purity < 1, considering $f(\Delta\varphi^{\mathrm{cls}^{\mathrm{iso}}_{\mathrm{narrow}}})$ bkg = $f(\Delta\varphi^{\mathrm{cls}^{\mathrm{iso}}_{\mathrm{wide}}})$:

$$f(\Delta\varphi^{\gamma^{\mathrm{iso}}}) = \frac{f(\Delta\varphi^{\mathrm{cls}^{\mathrm{iso}}_{\mathrm{narrow}}}) - (1-P)\cdot f(\Delta\varphi^{\mathrm{cls}^{\mathrm{iso}}_{\mathrm{wide}}})}{P}$$

➡ $D(z_T)$: Integrate $f(\Delta\varphi^{\gamma^{\mathrm{iso}}})$ in $3/5\pi < |\Delta\varphi| < \pi$ rad

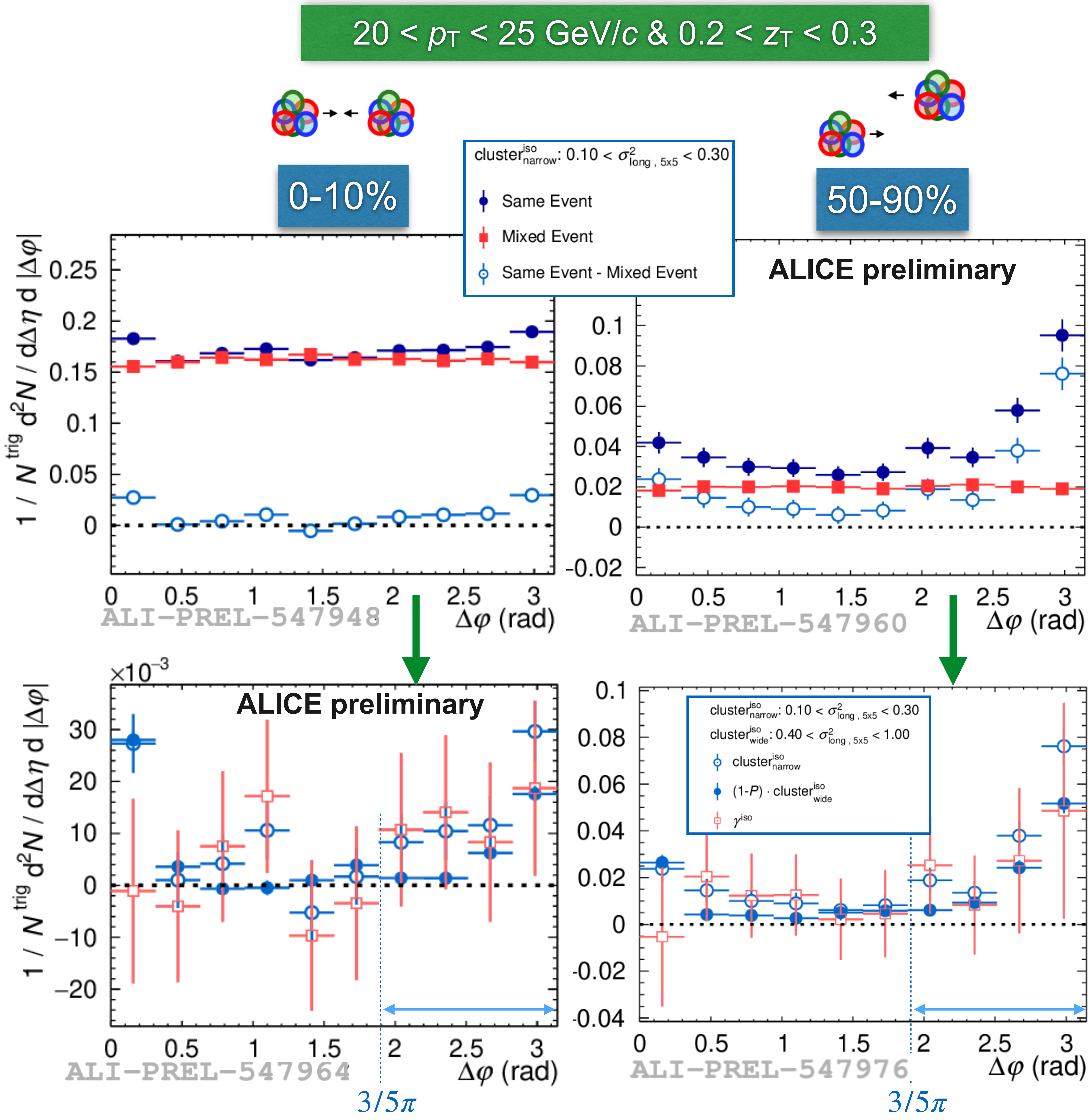

Isolated γ–hadron correlations in Pb–Pb: $D(z_T)$

I_{pQCD} = Pb–Pb Data / pp pQCD

I_{CP} = Pb–Pb (semi) central / peripheral

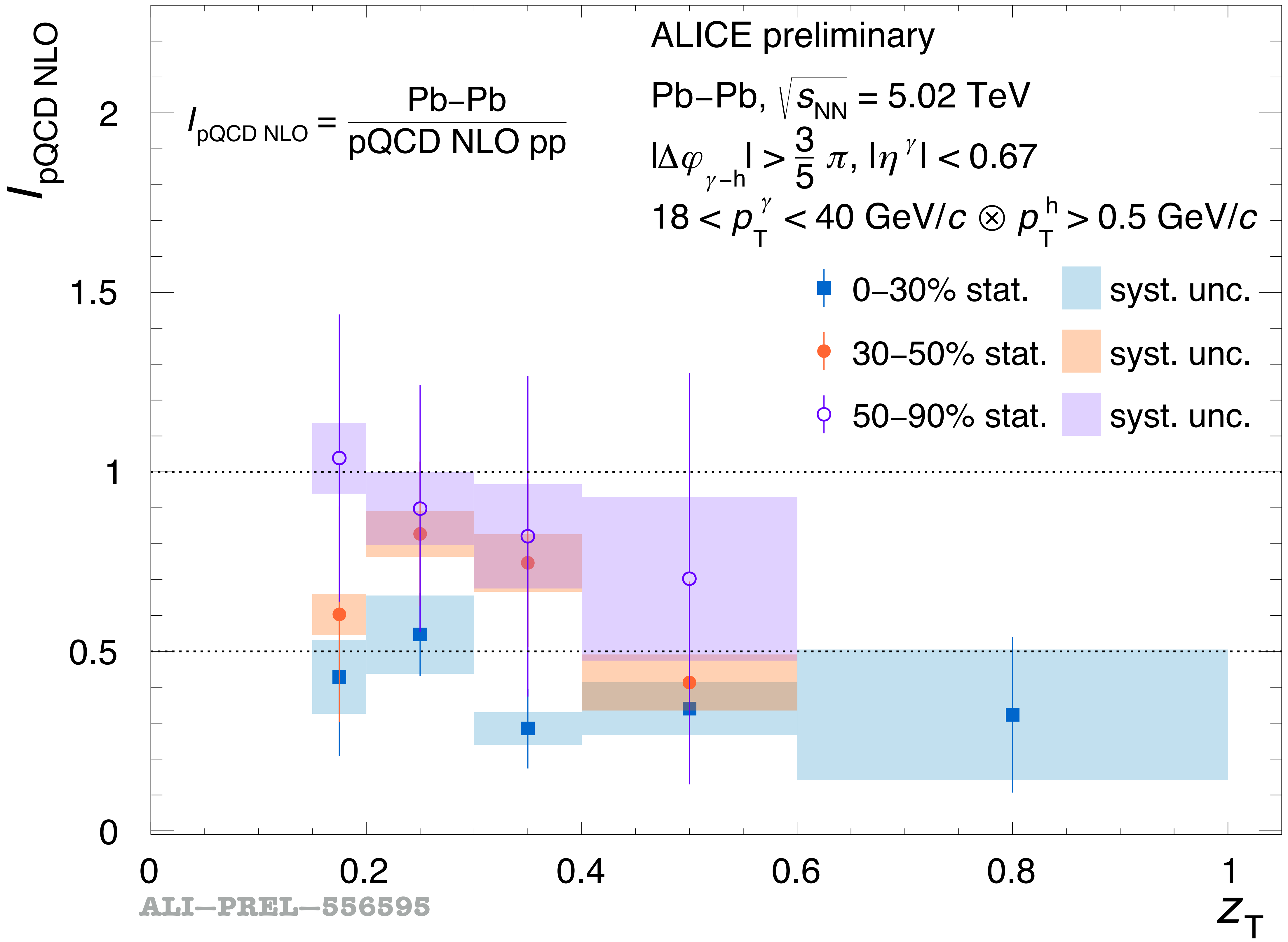

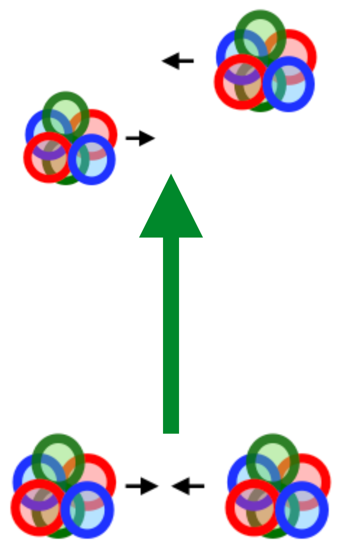

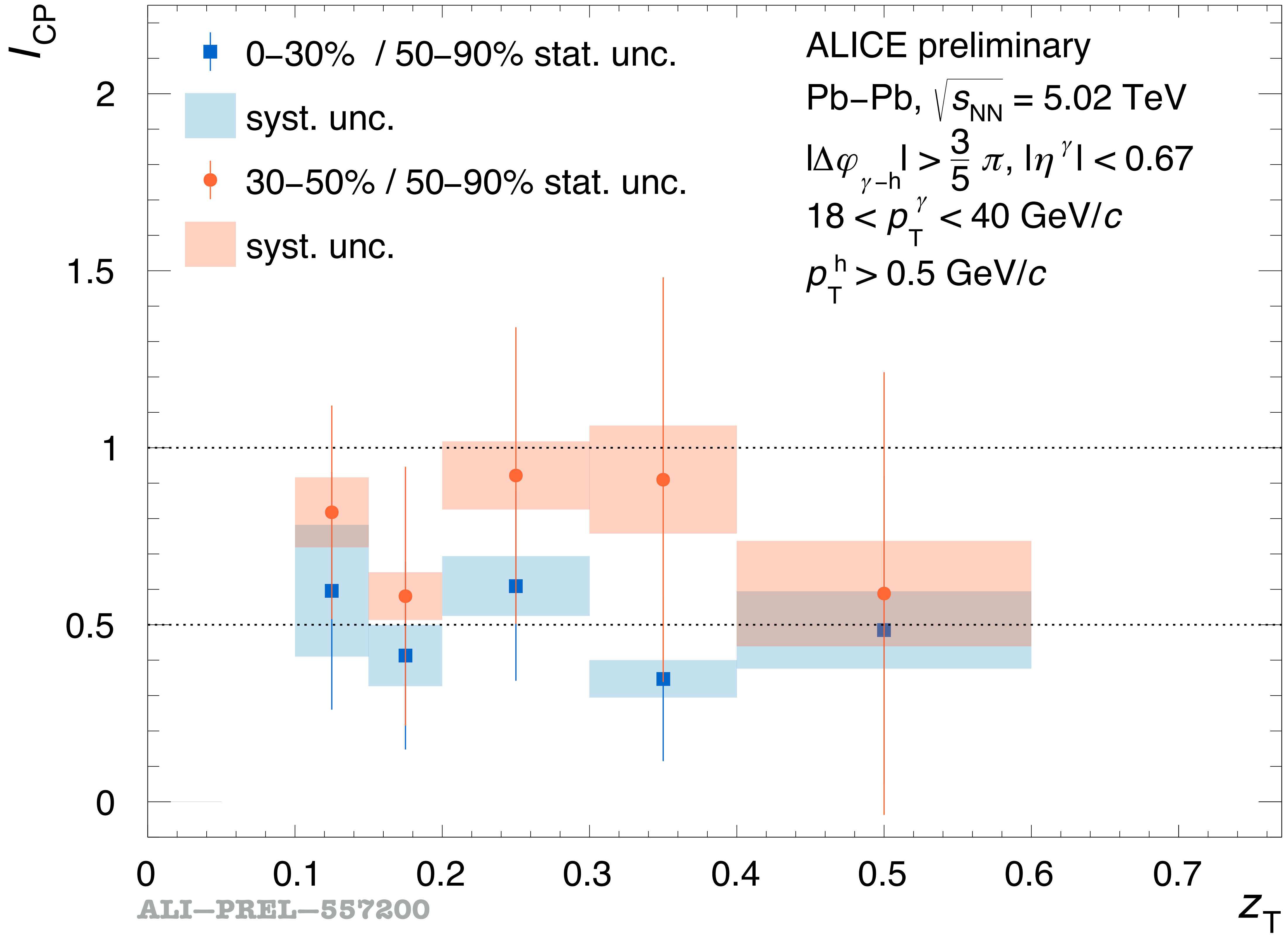

- Ordering between centralities, central more suppressed than peripheral
- Hints of less suppression at lower z_T in I_{pQCD}

Isolated γ-hadron correlations in Pb–Pb: RHIC & LHC

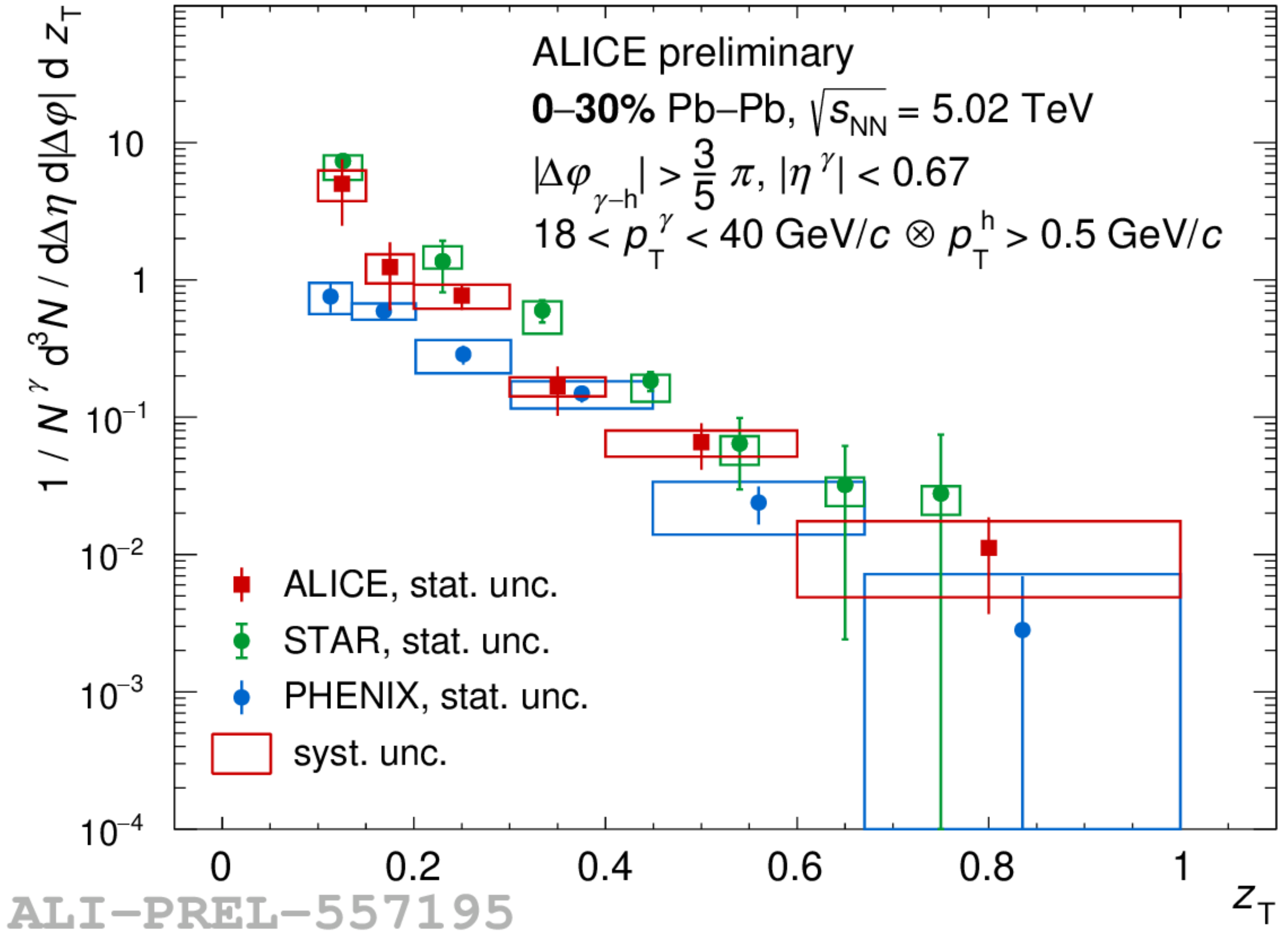

STAR, Phys.Lett.B 760 (2016) 689-696

0–12% Au–Au, $\sqrt{s_{NN}}$ = 200 GeV

$|\Delta\varphi_{\gamma-h} - \pi| \leq 1.4$

$12 < p_T^{\gamma} < 20$ GeV/c ⊗ $p_T^{h} > 1.2$ GeV/c

PHENIX, PRL 111, 032301 (2013)

0–40% Au–Au, $\sqrt{s_{NN}}$ = 200 GeV

$|\Delta\varphi_{\gamma-h} - \pi| < \pi/2$, $|y| < 0.35$

$5 < p_T^{\gamma} < 9$ GeV/c ⊗ $0.5 < p_T^{h} < 7$ GeV/c

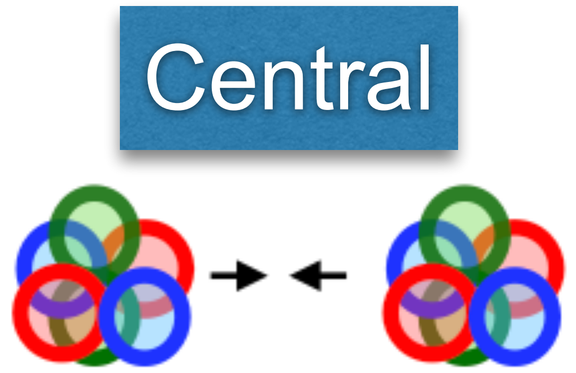

- Similar behaviour as observed at RHIC and LHC experiments

➡ Note: not completely apple-to-apple comparisons!

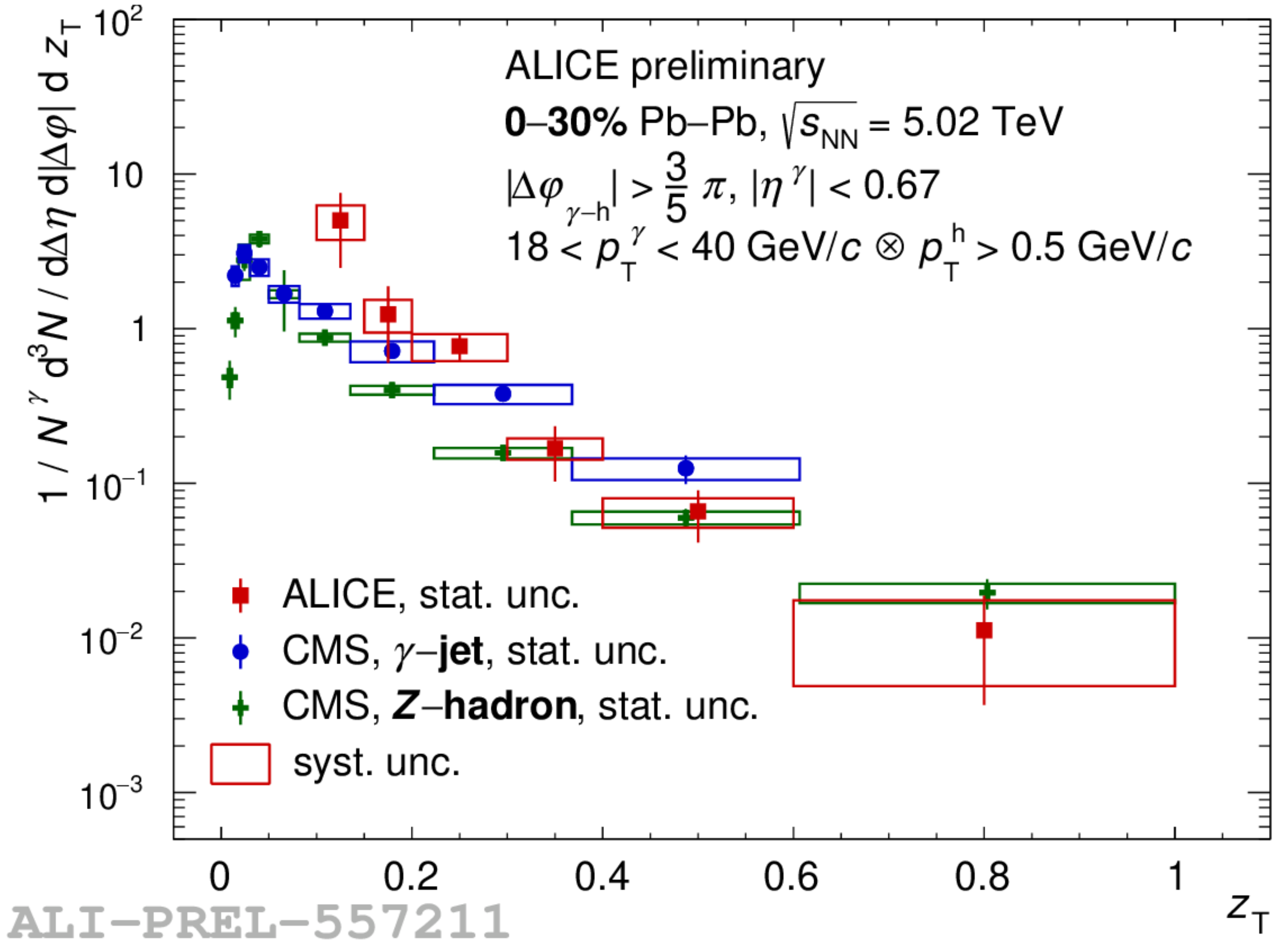

CMS, Phys.Rev.Lett. 121 (2018) 24, 242301, 2018

***γ*–jet, 0–10%**

anti-k_T jet R = 0.3, $p_T^{jet} > 30$ GeV/c, $|\eta^{jet}| < 1.6$

$|\Delta\varphi_{\gamma-jet}| > \frac{7}{8}\pi$, $|\eta^{\gamma}| < 1.44$, $p_T^{\gamma} > 60$ GeV/c ⊗ $p_T^{h} > 1$ GeV/c

CMS, Phys.Rev.Lett. 128 (2022) 12, 122301, 2022

***Z*–hadron, 0–30%**

$|\Delta\varphi_{Z-h}| > \frac{7}{8}\pi$, $p_T^{Z} > 30$ GeV/c ⊗ $p_T^{h} > 1$ GeV/c

Isolated γ-hadron correlations in Pb–Pb: RHIC & LHC

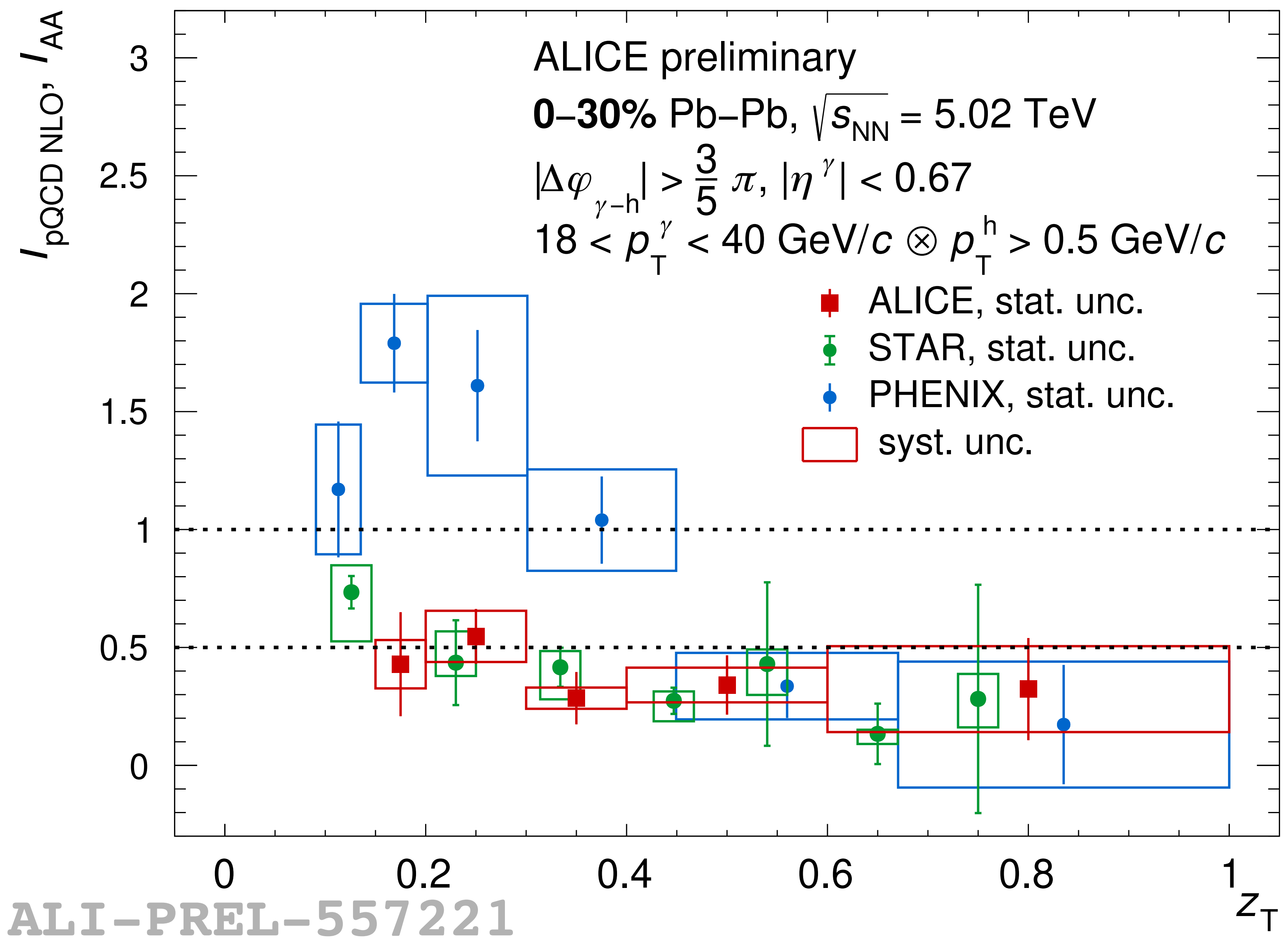

STAR, Phys.Lett.B 760 (2016) 689-696

0–12% Au–Au, $\sqrt{s_{NN}}$ = 200 GeV

$|\Delta\varphi_{\gamma-h} - \pi| \leq 1.4$

$12 < p_T^{\gamma} < 20$ GeV/c ⊗ $p_T^{h} > 1.2$ GeV/c

PHENIX, PRL 111, 032301 (2013)

0–40% Au–Au, $\sqrt{s_{NN}}$ = 200 GeV

$|\Delta\varphi_{\gamma-h} - \pi| < \pi/2$, $|y| < 0.35$

$5 < p_T^{\gamma} < 9$ GeV/c ⊗ $0.5 < p_T^{h} < 7$ GeV/c

Central

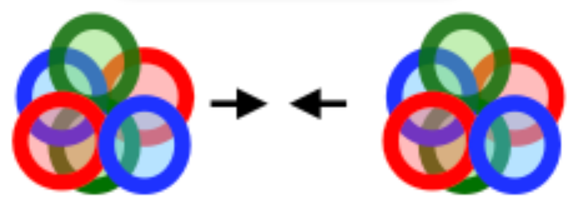

$$I_{AA}(z_T) = \frac{D(z_T, \mathrm{Pb-Pb})}{D(z_T, \mathrm{pp})}$$

- Similar behaviour as observed at RHIC and LHC experiments

➡ Note: <u>not completely apple-to-apple comparisons!</u>

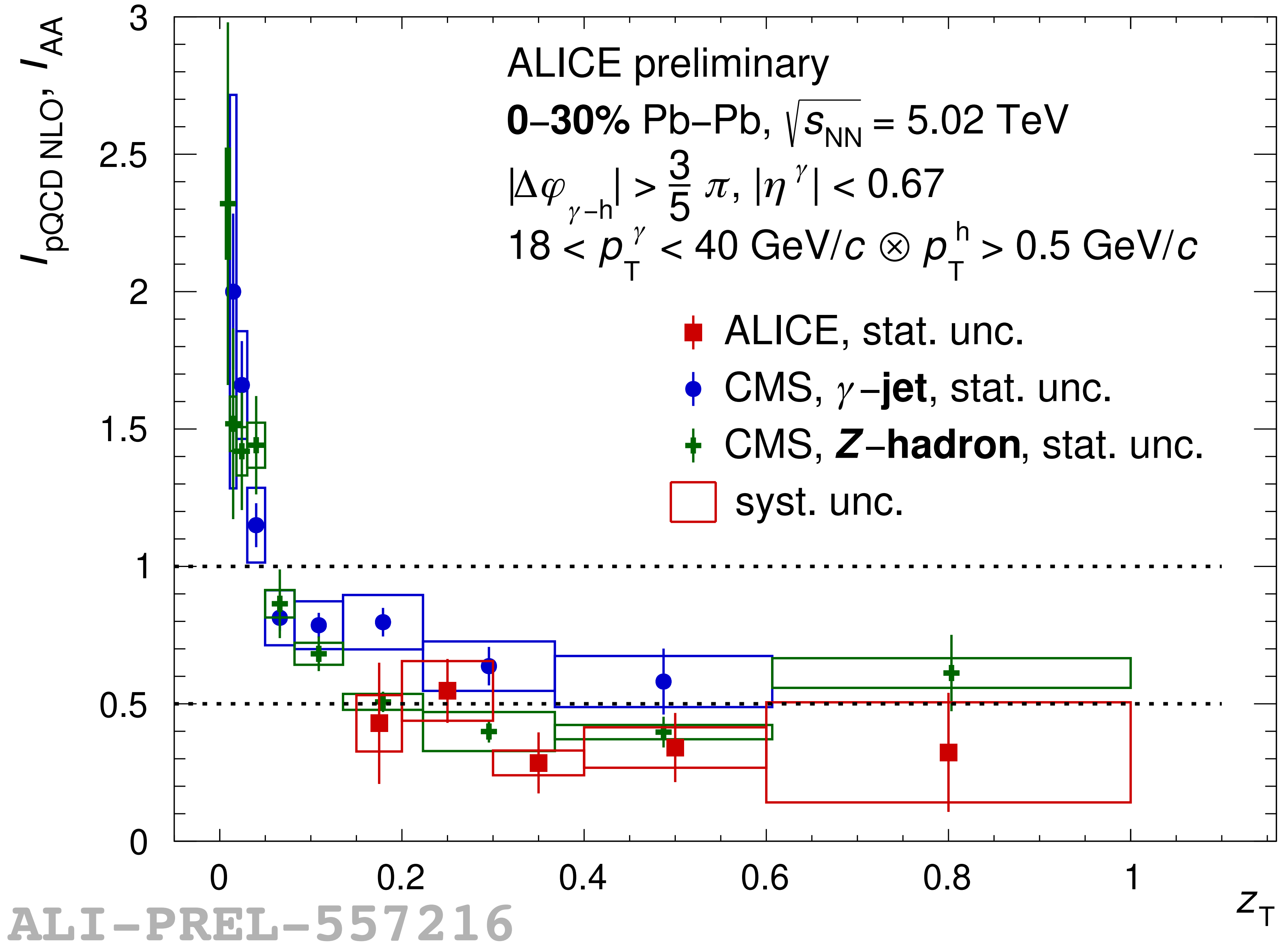

CMS, Phys.Rev.Lett. 121 (2018) 242301, 2018

γ–**jet**, **0–10%**

anti-k_T jet R = 0.3, $p_T^{jet} > 30$ GeV/c, $|\eta^{jet}| < 1.6$

$|\Delta\varphi_{\gamma-jet}| > \frac{7}{8}\pi$, $|\eta^{\gamma}| < 1.44$ $p_T^{\gamma} > 60$ GeV/c ⊗ $p_T^{h} > 1$ GeV/c

CMS, Phys.Rev.Lett. 128 (2022) 122301, 2022

***Z*–hadron**, **0–30%**

$|\Delta\varphi_{Z-h}| > \frac{7}{8}\pi$, $p_T^{Z} > 30$ GeV/c ⊗ $p_T^{h} > 1$ GeV/c

Isolated γ-hadron correlations in Pb–Pb: $D(z_T)$

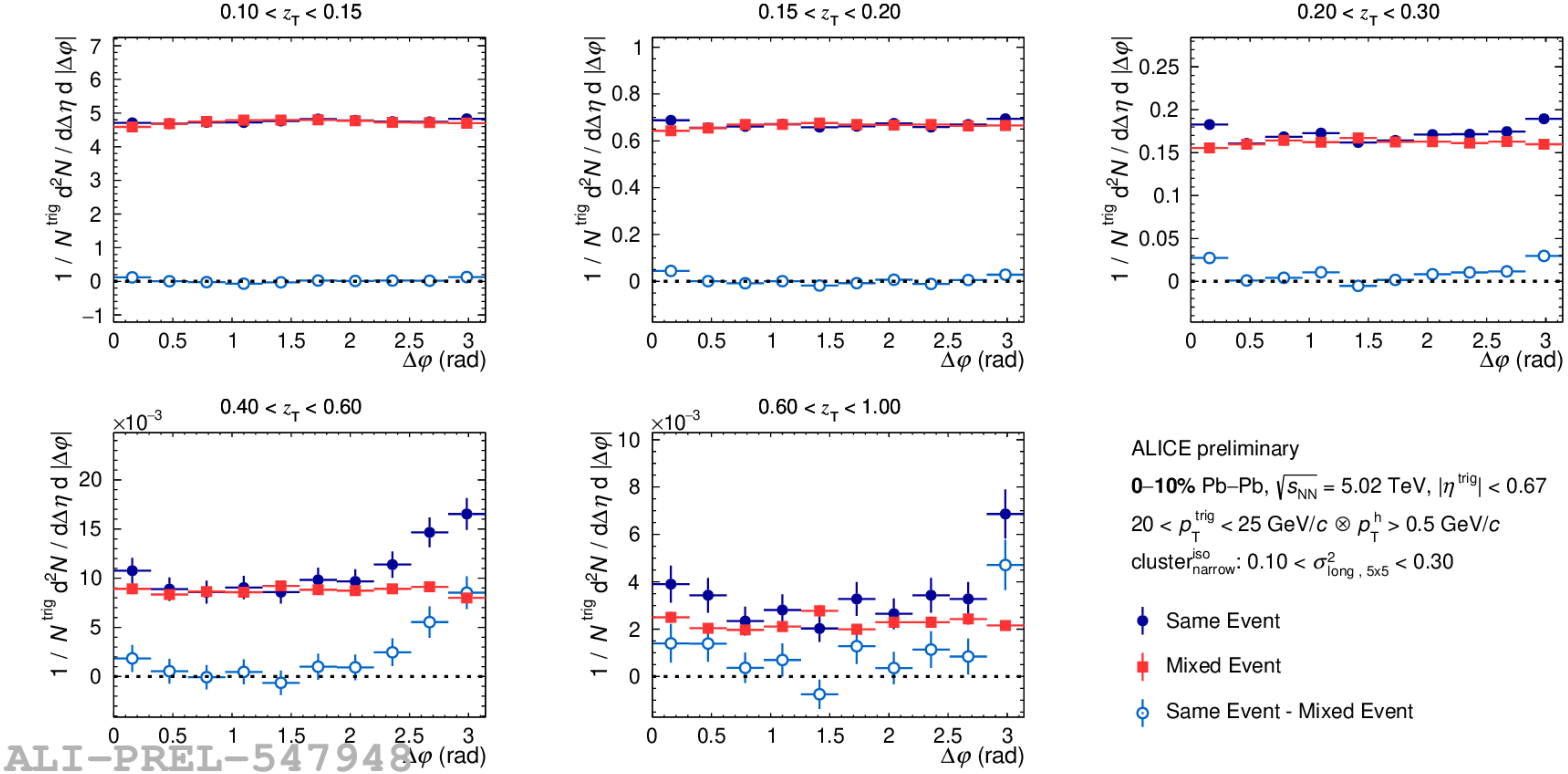

Isolated γ-hadron correlations in Pb–Pb: $D(z_T)$

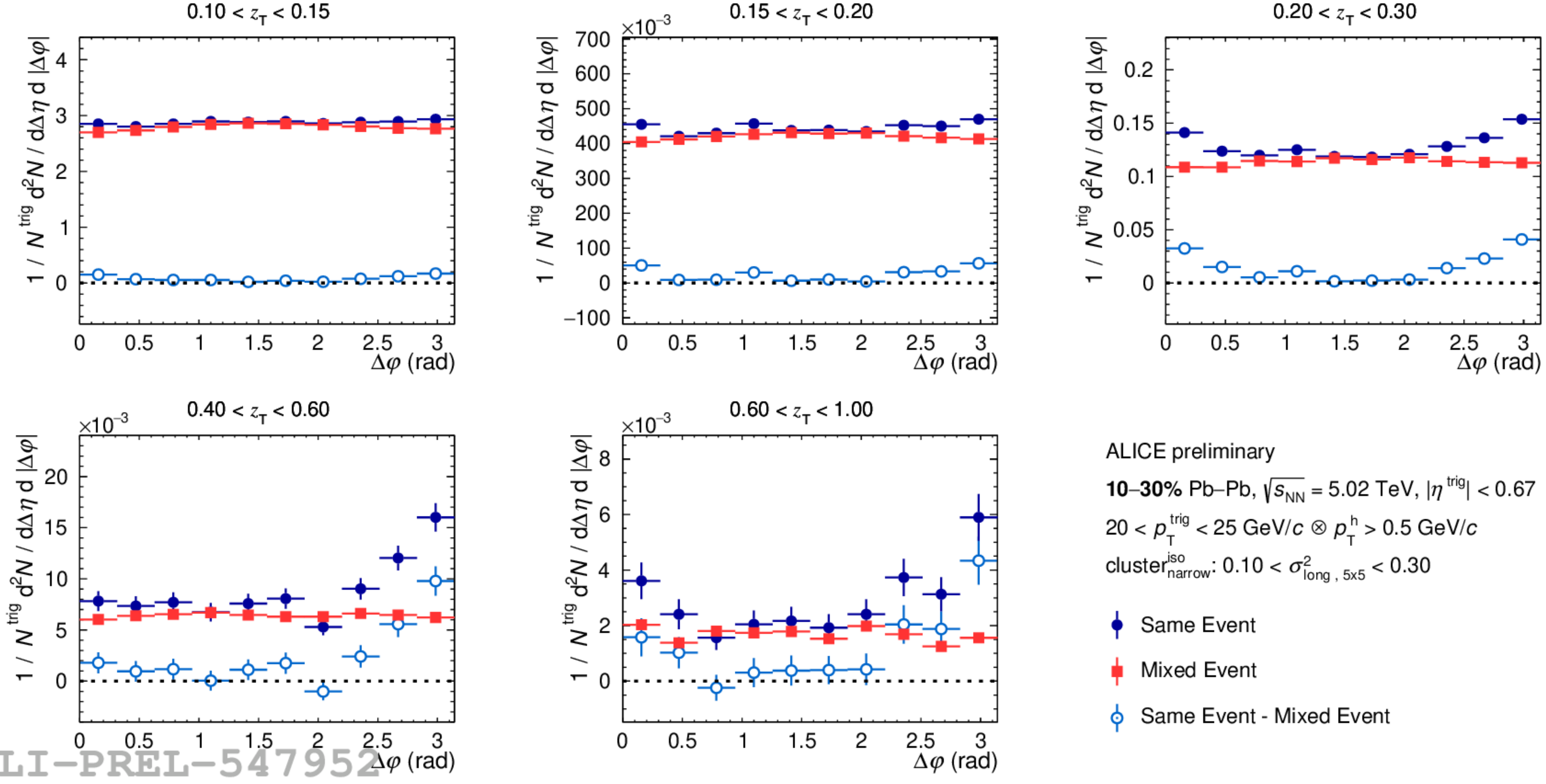

Isolated γ-hadron correlations in Pb–Pb: $D(z_T)$

Isolated γ-hadron correlations in Pb–Pb: $D(z_T)$

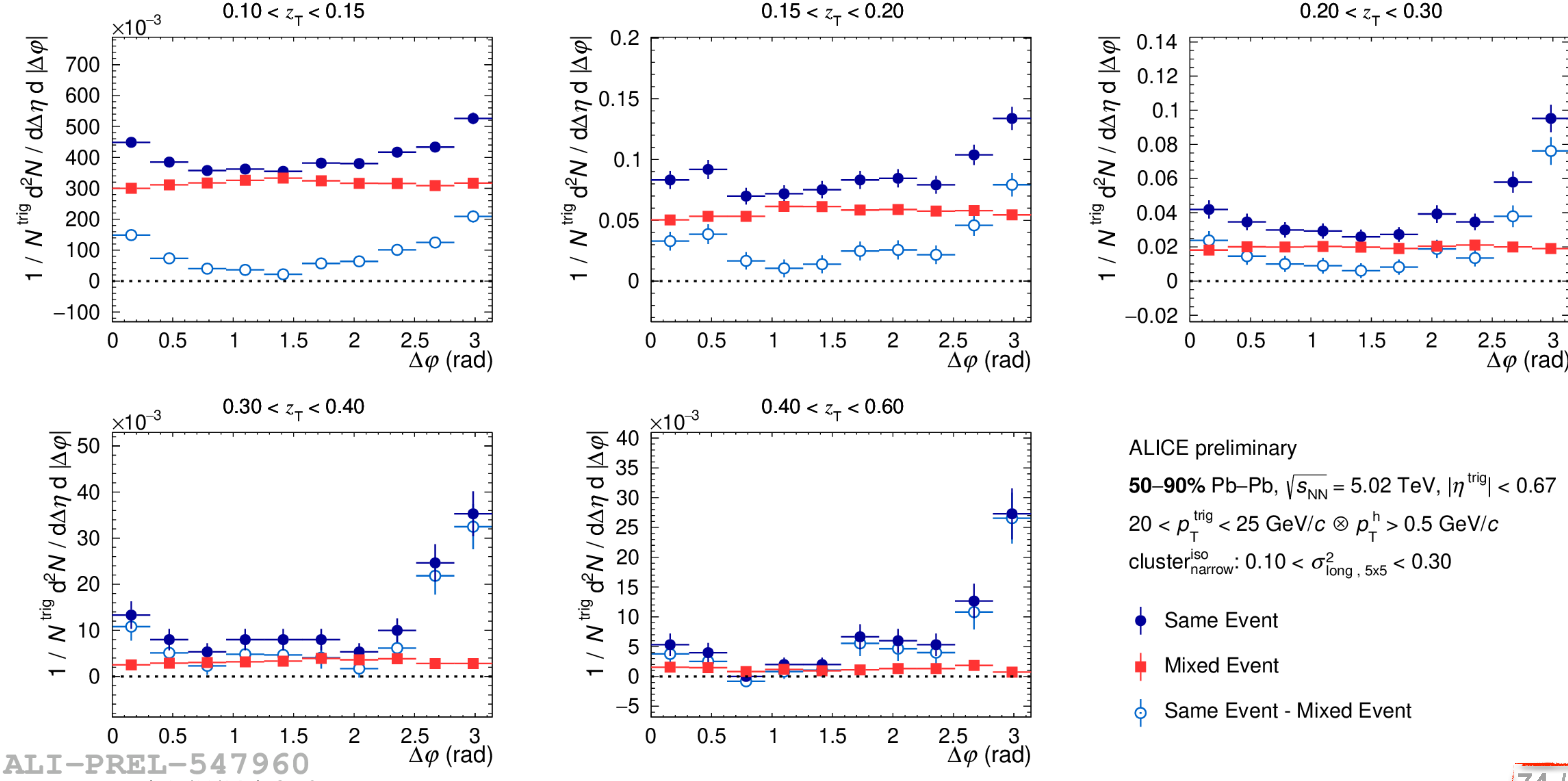

Isolated γ-hadron correlations in Pb–Pb: $D(z_T)$

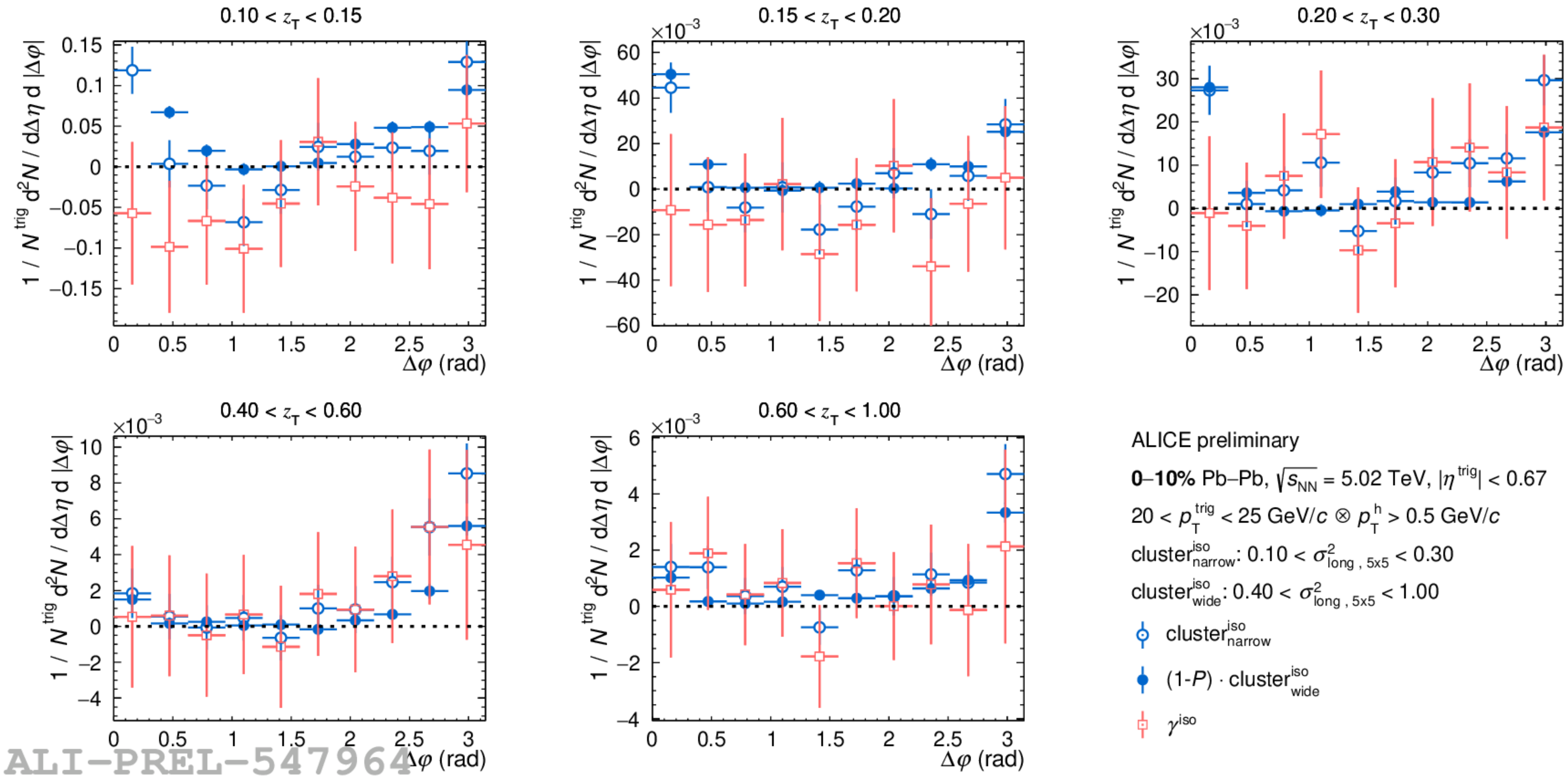

Isolated γ-hadron correlations in Pb–Pb: $D(z_T)$

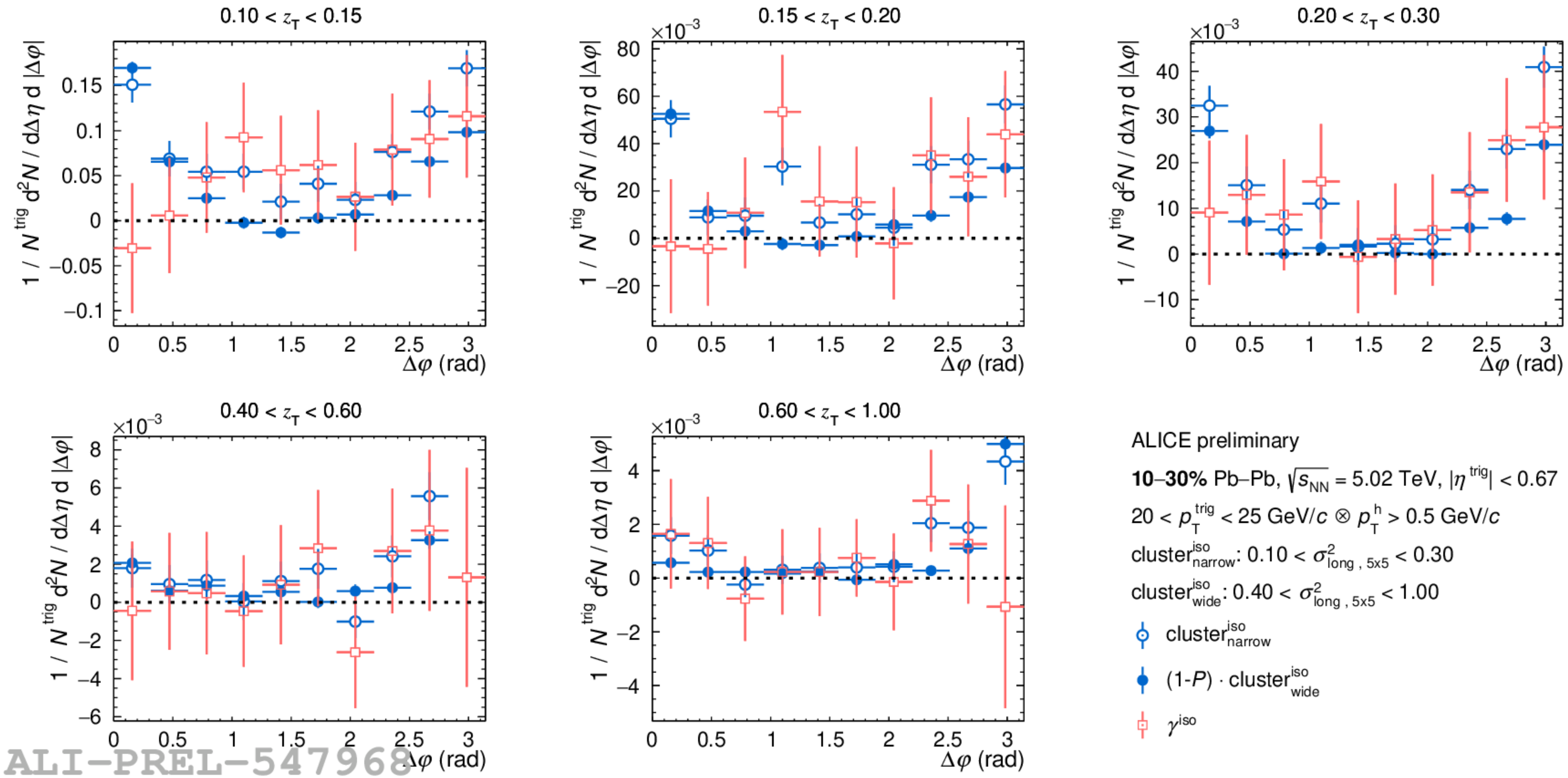

Isolated γ-hadron correlations in Pb–Pb: $D(z_T)$

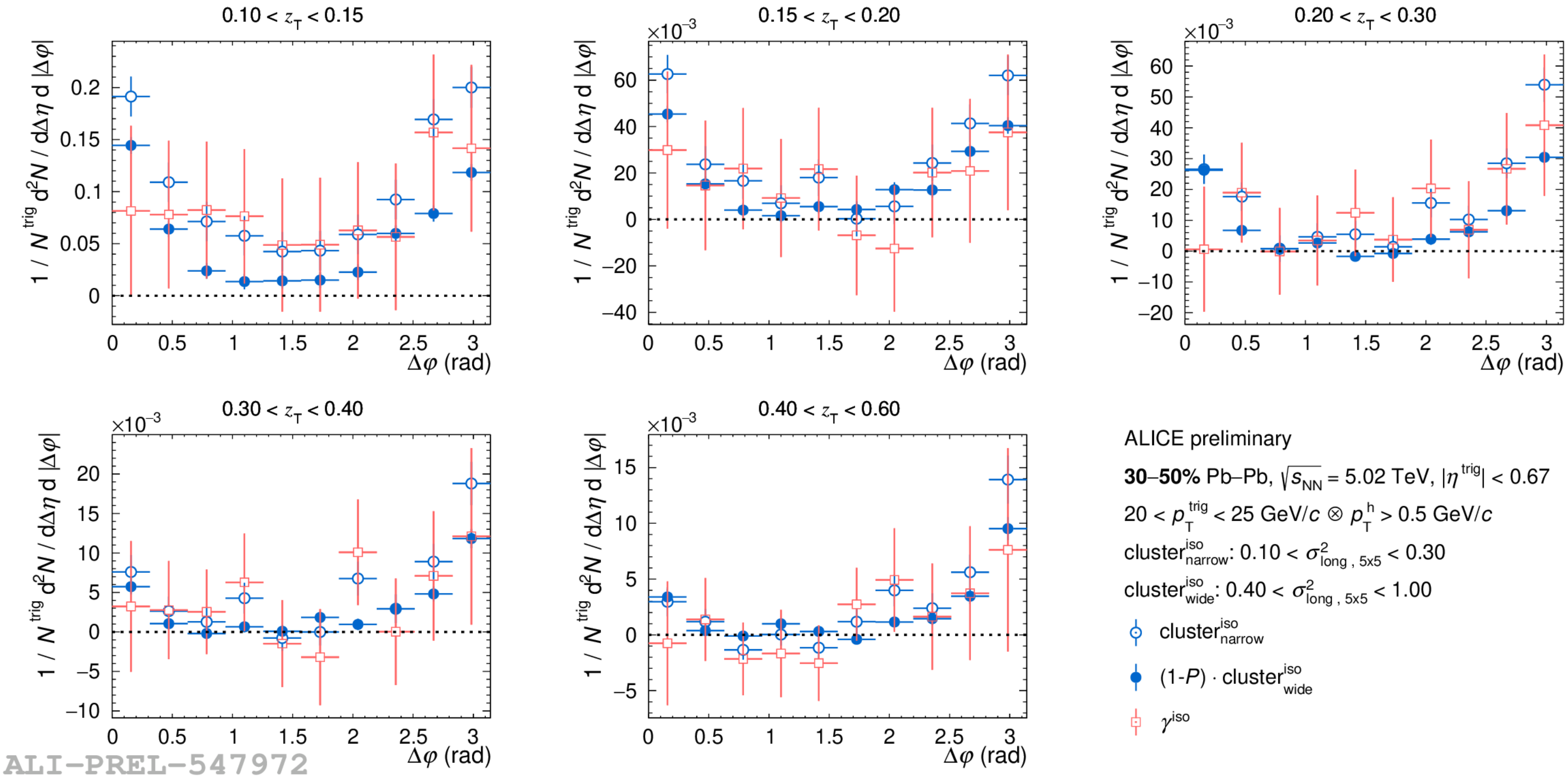

Isolated γ-hadron correlations in Pb–Pb: $D(z_T)$

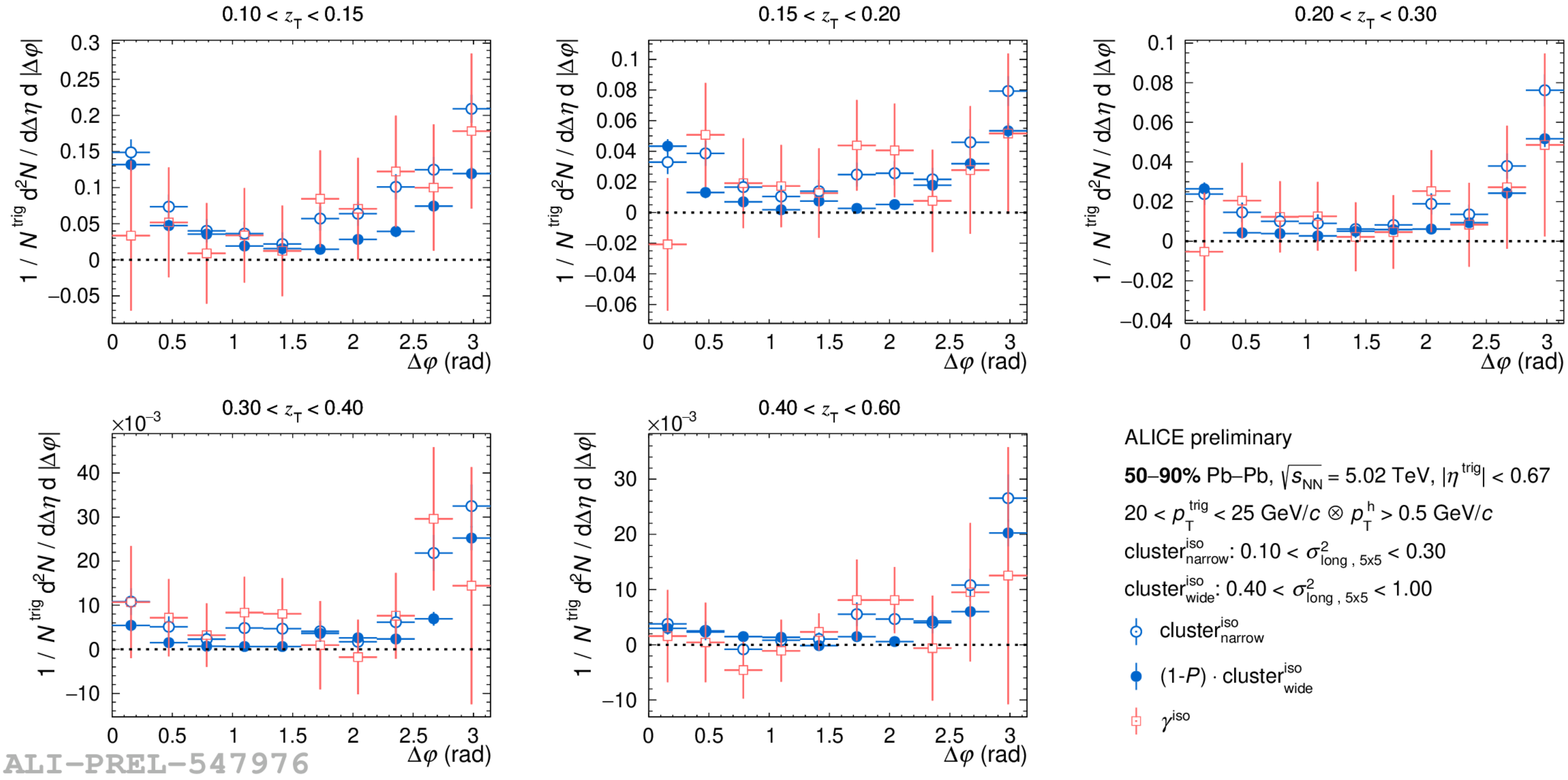

Isolated γ-hadron correlation uncertainty: $D(z_T)$

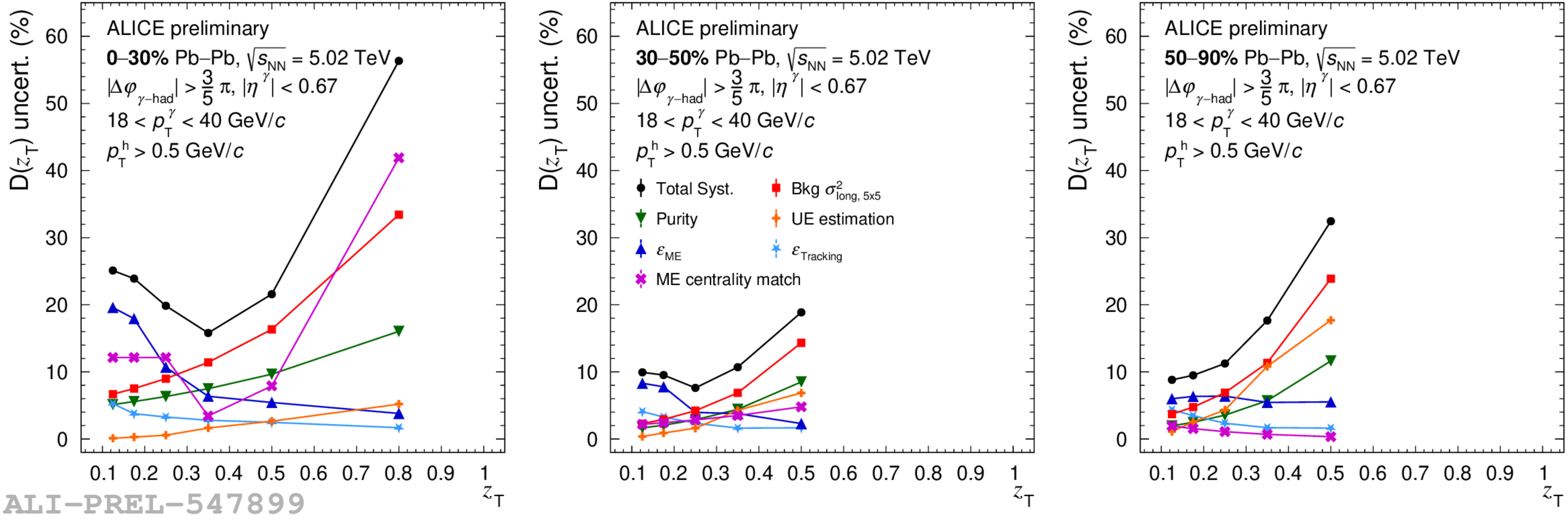

Isolated γ-hadron correlation uncertainty: I_{CP}

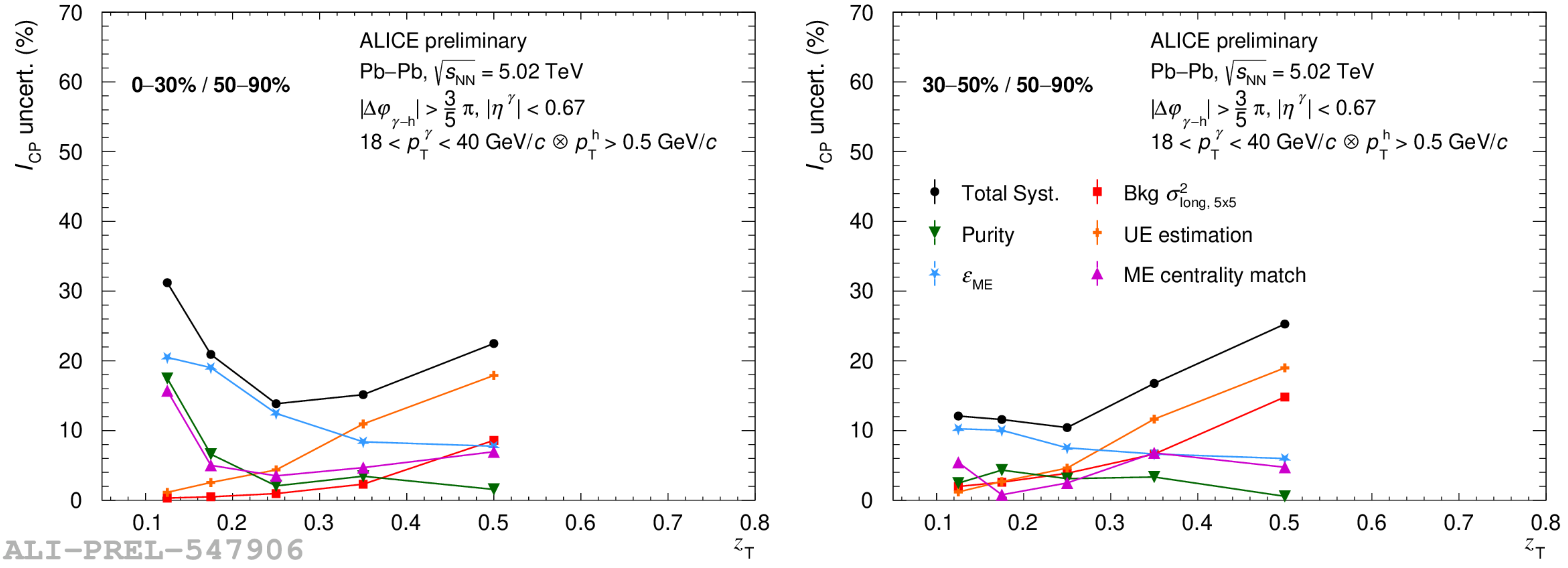

Isolated γ cross section *R* ratio in ATLAS, pp $\sqrt{s}$ = 13 TeV

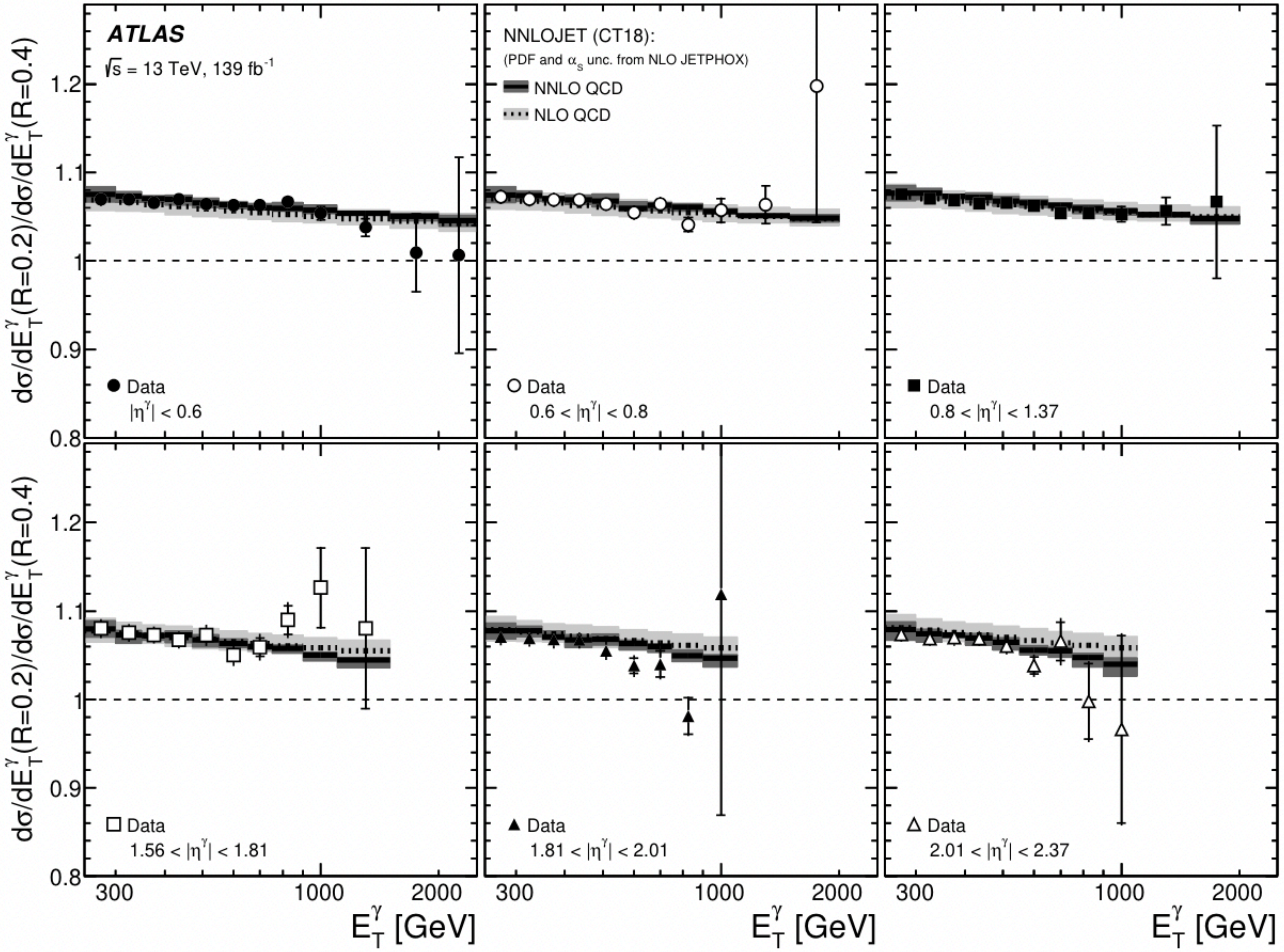

Figure 21: Measured ratios of the differential cross sections for inclusive isolated-photon production for $R = 0.2$ and $R = 0.4$ as functions of E_T^γ in different η^γ regions. The NLO (dotted lines) and NNLO (solid lines) pQCD predictions from NNLOJET based on the CT18 PDF set are also shown. The inner (outer) error bars represent the statistical uncertainties (statistical and systematic uncertainties added in quadrature) and the shaded bands represent the theoretical uncertainties. For some of the points, the inner and outer error bars are smaller than the marker size and, thus, not visible.

JHEP 07 (2023) 86

arXiv:2302.00510